



# Predisposition to domain-wide maladaptive changes in predictive coding in auditory phantom perception

Anusha Mohan<sup>a</sup>, Alison Luckey<sup>a</sup>, Nathan Weisz<sup>b</sup>, Sven Vanneste<sup>a,c,\*</sup>

<sup>a</sup> Global Brain Health Institute & Institute of Neuroscience, Trinity College Dublin, College Green 2, Dublin, Ireland

<sup>b</sup> Salzburg Brain Dynamics Lab, University of Salzburg, Austria

<sup>c</sup> Lab for Clinical & Integrative Neuroscience, School of Behavioral and Brain Sciences, The University of Texas at Dallas, United States

## ARTICLE INFO

### Keywords:

Functional connectivity  
Source localisation  
Neuropathology  
Gamma oscillations  
Event-related potentials

## ABSTRACT

Tinnitus is hypothesised to be a predictive coding problem. Previous research indicates lower sensitivity to prediction errors (PEs) in tinnitus patients while processing auditory deviants corresponding to tinnitus-specific stimuli. However, based on research with patients with hallucinations and no psychosis we hypothesise tinnitus patients may be more sensitive to PEs produced by auditory stimuli that are not related to tinnitus characteristics. Specifically in patients with minimal to no hearing loss, we hypothesise a more top-down subtype of tinnitus that may be driven by maladaptive changes in an auditory predictive coding network. To test this, we use an auditory oddball paradigm with omission of global deviants, a measure that is previously shown to empirically characterise hierarchical prediction errors (PEs).

We observe: (1) increased predictions characterised by increased pre-stimulus response and increased alpha connectivity between the parahippocampus, dorsal anterior cingulate cortex and parahippocampus, pregenual anterior cingulate cortex and posterior cingulate cortex; (2) increased PEs characterised by increased P300 amplitude and gamma activity and increased theta connectivity between auditory cortices, parahippocampus and dorsal anterior cingulate cortex in the tinnitus group; (3) increased overall feed-forward connectivity in theta from the auditory cortex and parahippocampus to the dorsal anterior cingulate cortex; (4) correlations of pre-stimulus theta activity to tinnitus loudness and alpha activity to tinnitus distress. These results provide empirical evidence of maladaptive changes in a hierarchical predictive coding network in a subgroup of tinnitus patients with minimal to no hearing loss. The changes in pre-stimulus activity and connectivity to non-tinnitus specific stimuli suggest that tinnitus patients not only produce strong predictions about upcoming stimuli but also may be predisposed to stimulus a-specific PEs in the auditory domain. Correlations with tinnitus-related characteristics may be a biomarker for maladaptive changes in auditory predictive coding.

## 1. Introduction

Tinnitus is the continuous perception of a ringing or buzzing in the ears in the absence of an external sound source (Baguley et al., 2013). There is no cure to tinnitus as of today and this is attributed to an immense heterogeneity in symptom characteristics amongst patients (Cederroth et al., 2019). A recent paper from our lab showed that there may be different subtypes of tinnitus based on the amount of hearing loss (Vanneste et al., 2019). Patients with moderate to severe hearing loss showed a more bottom-up tinnitus driven by the sensory deafferentation, whereas patients with minimal to no hearing loss presented a more top-down tinnitus driven by a failed noise-cancellation system.

Tinnitus is also theoretically explained under the predictive coding framework (De Ridder et al., 2014; Hullfish et al., 2019; Sedley et al.,

2016a). Prediction error (PE) is the weighted difference between the incoming stimulus and existing prediction about the external environment (Corlett et al., 2019; Knill and Pouget, 2004). These PEs are used to update the predicted model which is cyclically compared to new sensory information (Hullfish et al., 2019). This process is performed hierarchically where PEs are encoded by regions lower in the hierarchy and predictions by regions higher up and information is conveyed between them in specific frequency bands (Wacongne et al., 2011). Hierarchical predictive coding forms a theoretical basis of brain functioning explaining learning (Ylinen et al., 2017), conditioning (Powers et al., 2017), language (Lewis and Bastiaansen, 2015), perception (Mohan and Vanneste, 2017), neurophysiological (De Ridder et al., 2011; Moore, 2015; Van Boxtel and Lu, 2013) and psychiatric disorders (Corlett et al., 2019; Fletcher and Frith, 2009; Sterzer et al., 2018). Although a theoretical explanation to the canonical

\* Corresponding author.

E-mail address: [sven.vanneste@tcd.ie](mailto:sven.vanneste@tcd.ie) (S. Vanneste).

<https://doi.org/10.1016/j.neuroimage.2021.118813>.

Received 7 December 2020; Received in revised form 30 June 2021; Accepted 13 December 2021

Available online 17 December 2021.

1053-8119/© 2021 The Author(s). Published by Elsevier Inc. This is an open access article under the CC BY-NC-ND license

(<http://creativecommons.org/licenses/by-nc-nd/4.0/>)

microcircuits of hierarchical connections exists (Bastos et al., 2012; Bosman and Aboitiz, 2015), there is no system-level evidence for the same.

In theory, PEs can be produced in tinnitus patients either as a result of hearing loss (bottom-up subtype), as a result of an aberrant predictive coding system in the brain (top-down subtype) or a combination of both (Mohan and Vanneste, 2017). In the current study, we primarily aim to provide empirical evidence to a top-down problem in patients with tinnitus and minimal to no hearing loss mainly reflecting an aberrant predictive coding system in the brain thereby supporting the idea of the presences of subgroups of tinnitus. To do this, we recruit a patient and control group that is controlled for sex, age and hearing loss. Additionally, we also aim to use tinnitus as a predictive coding deficit model to provide empirical evidence for the system-level existence of an oscillation-specific hierarchical predictive coding network of brain regions that communicate predictions and PEs generated by the auditory system which displays maladaptive changes in the presence of a disorder. This way, we use a symbiotic approach to learn more about predictive coding and the mechanism of action in a subgroup of tinnitus patients.

Previous literature gives several insights to the existence of an auditory predictive coding network but has not empirically tested the existence of one. Sedley and colleagues (Sedley et al., 2016a) provide a comprehensive neurobiological model as to how the “tinnitus precursor signal” is perceived as ringing in the ears following a failure of the predictive coding network consisting of cortical and subcortical regions such as the basal forebrain (BF), dorsal anterior cingulate cortex (dACC), dorsal cochlear nucleus (DCN), primary auditory cortex (AC), inferior colliculus (IC), inferior parietal cortex (IPC), auditory thalamus, parahippocampal cortex (PHC), precuneus, thalamic reticular nucleus and ventromedial prefrontal cortex (vmPFC). The authors describe that the PE is encoded by the AC which is transmitted to regions higher up in the hierarchy and the predictions are encoded by the PHC which is also the auditory sensory memory (Munoz-Lopez et al., 2010; Sedley et al., 2016a).

Other studies from the past also account for the above regions to play a vital role in hierarchically encoding PEs. Along with the sensory cortex, the posterior cingulate cortex (PCC) has been shown to encode PEs at the lower level of the hierarchy (Kleckner et al., 2017; Pearson et al., 2011; Sterzer et al., 2018). The dACC is an integral part of the salience network and a well-established region of the error monitoring system that evaluates the valence or importance of PEs (Huang et al., 2018; Weiss et al., 2018). The pregenual anterior cingulate cortex/ventromedial prefrontal cortex (pgACC/vmPFC) provides top-down inhibitory connections to minimise the error signal to maintain homeostatic balance bringing the brain to a stable-energy state (De Ridder et al., 2014; Friston et al., 2016; Knill and Pouget, 2004; Mohan and Vanneste, 2017). If PE persists, the dACC would update the predictions in a top-down feedback fashion (Arnal and Giraud, 2012; O'Reilly et al., 2013).

Recent research suggests that PEs, encoded by gamma oscillations, are communicated from the lower to higher regions in the hierarchy by feedforward connections in theta oscillations and predictions, encoded by beta oscillations, are communicated from higher to lower regions by feedback connections in alpha oscillations (Alamia and VanRullen, 2019; Arnal and Giraud, 2012; Chao et al., 2018; Mejias et al., 2016; Recasens et al., 2018; Sedley et al., 2016b). Corticothalamic connections are known to modulate the gain of these oscillations by comparing top-down and bottom-up information increasing synchronicity of specifically gamma oscillations (Kanai et al., 2015).

In the current study we are interested in cortical regions involved in the predictive coding network. From the above literature, we propose that the cortical auditory predictive coding network would consist primarily of ACs and PCC at the lower levels and dACC, pgACC/vmPFC and parahippocampus at higher levels encoding PEs in gamma and predictions in beta frequency bands. We also propose that feedforward and

feedback connections will be facilitated in theta and alpha oscillations respectively.

To empirically describe this network and determine disorder related maladaptive changes, we compare the event-related potential (ERP) to an auditory oddball paradigm using omission of global deviants (Wacongne et al., 2011) between tinnitus patients and healthy controls. Auditory oddball paradigms use a train of frequent (standard) and infrequent (deviant) stimuli. Global deviants are generated based on changes in the pattern of stimulus presentation rather than changes in the characteristics of the stimulus (Chao et al., 2018). This requires more neural resources and is a more complex phenomenon thus eliciting a late positive potential (P300) even in a passive oddball task where participants are not performing a task but are attentively listening to the stimulus (Wacongne et al., 2011). The P300 to the omission of a global deviant is shown to be a system-level neural marker of the hierarchical predictive coding system of the brain that cannot be explained by stimulus adaptation (Chennu et al., 2013; Garrido et al., 2009; Wacongne et al., 2012). The P300 is also a neural marker of the change from the expected stimulus and thus is a neural marker of the PE itself. Changes in the signal calculated as the difference between standard and deviant responses, during the time prior to the onset of the first stimulus, known as the pre-stimulus timeframe, reflect the anticipation of the PE that occurs in the post-stimulus timeframe (Lazzaro et al., 2001; Partyka et al., 2019). Studying the differences in pre-stimulus neural markers between patients and controls can therefore inform us about differences in encoding of predictions of upcoming stimuli between the two groups.

Research done until now on empirically characterising changes in the predictive coding in tinnitus, shows that tinnitus patients' predictions of a stimulus is skewed when the stimulus characteristics match their tinnitus characteristics thereby affecting the resultant PE (Sedley et al., 2019). This is in line with the theory that chronically, the brain possibly learns that tinnitus is the new normal and updates its prediction (Hullfish et al., 2019; Sedley et al., 2016a). However, other research done in patients with hallucinations with/without psychosis and healthy controls suggests that patients with hallucinations but no psychosis encode stronger priors compared to controls (Powers et al., 2017) and thus, a novel stimulus would produce an increased deviation from their existing prediction. Per, this theory, we hypothesise that even if tinnitus were the new normal in the brain and they were less sensitive to PEs produced by tinnitus sounds, they would be more sensitive to PEs of stimuli produced by the rest of the auditory domain.

Thus, when we probe the tinnitus brain with omissions of global deviants in an auditory oddball paradigm with sounds that do not correspond to their tinnitus sound, we hypothesize that tinnitus patients will exhibit increased P300 establishing increased PEs reflecting their domain-wide predisposition. Corresponding increase in the amplitude of the pre-stimulus response would provide evidence for increased anticipation/stronger prediction of the PE in the post-stimulus timeframe. We also hypothesise changes in beta activity in the pre-stimulus timeframe and gamma activity during the P300 timeframe indicating oscillatory changes in encoding predictions and PEs, respectively. Crucially, we expect changes in functional connectivity within the hypothesized predictive coding network for the different time frames, with increased feedforward connectivity in theta in the pre-stimulus timeframe and feedback connectivity in alpha band in the P300 timeframe for the tinnitus group.

Choosing tinnitus as a predictive coding deficit model has its advantages. Tinnitus is a simple auditory percept where patients hear a ringing/buzzing rather than complex hallucinations which are musical or verbal (Vanneste et al., 2013b). Importantly, tinnitus is not tied to psychosis making it a much simpler model for simultaneously studying auditory perception and maladaptive changes in the brain. In this subgroup of tinnitus patients consisting of young adults with minimal to no hearing loss they very likely do not have severe cognitive deficits. Thus, we will be able to understand predictive coding at the systems level in a controlled way with a minimal number of confounding vari-

ables. Therefore, through this study, we aim to parallelly make a significant contribution to the dearth of evidence surrounding maladaptive changes in the spatio-spectro-temporal neural correlates of altered predictive coding in auditory phantom percepts, taking the field closer to fully understanding its mechanism of action and that of auditory perception in general.

## 2. Materials and methods

### 2.1. Ethical statement

The study was approved by the local ethical committee (The University of Texas at Dallas, IRB #15-06) and was in accordance with the Declaration of Helsinki. All participants gave written consent to participate.

### 2.2. Data and code availability statement

The data and code are present with the corresponding author and will be available on request. Those interested may contact him at sven.vanneste@tcd.ie. The data will be anonymised and will not contain personal identifying information. The code will also be made available offline upon request via email.

### 2.3. Participants

Participants with tinnitus ( $M = 25.9$  years;  $SD = 5.49$  years; 8 males and 2 females) and without tinnitus ( $M = 27$  years;  $SD = 4.71$  years; 4 males and 6 females) were enrolled in the study which was powered based on Wacongne and colleagues (Wacongne et al., 2011). The two groups were matched for age ( $t(18) = 0.48, p = .63, d = 0.21, 95\%CI = [-0.66, 1.09]$ ), gender ( $\chi^2 = 3.33, p = .06$ ), and hearing loss (supplementary section). Exclusion criteria included Meniere's disease, chronic ear infections, otosclerosis, tumours, mental disorders, chronic headache and pulsatile tinnitus. Only patients with continuous tinnitus present for at least a year were enrolled. Participants were asked to refrain from caffeine before the study due to its effect on EEG.

### 2.4. Audiological and behavioural assessments

All participants underwent a pure tone audiometry test where hearing thresholds at 250, 500, 1000, 2000, 3000, 4000, 6000, and 8000 Hz were obtained according to the procedures prescribed by the British Society of Audiology. Participants with hearing threshold  $>30$  dB HL at any frequency were excluded from the study. Furthermore, using two 10-cm visual analogue scales (VAS), tinnitus participants subjectively reported tinnitus loudness ( $M = 2.25, SD = 1.22$ ) and tinnitus-related distress ( $M = 1.13, SD = 1.2$ ); both the loudness and distress VAS were scored from 0 to 10 with 0 = "no tinnitus"/"no distress" and 10 = "as loud as imaginable"/"suicidal levels of distress". They also completed a set of questionnaires, including the Tinnitus Handicap Inventory (THI;  $M = 29, SD = 24.8$ ), Tinnitus Questionnaire (TQ;  $M = 24.67, SD = 12.88$ , one missing value), and Tinnitus Functional Index (TFI;  $M = 27.48, SD = 19.47$ ) which are also designed to assess tinnitus-related distress and impact on their lives (Hallam et al., 1988).

### 2.5. Event related potential (ERP) study

ERPs in response to auditory stimuli was collected from all participants following a procedure similar to (Wacongne et al., 2011). Participants were asked to always attend to the stimuli while keeping their eyes fixated on a point in front of them. No behavioural response was recorded. The stimuli had three sets of auditory sequences with a combination of tones and noise bursts. Sequence X had five 500 Hz tones; Sequence Y had four 500 Hz tones and one noise burst; Sequence Omission had four 500 Hz tones. The sequences were presented in three protocols

in an auditory oddball paradigm. The paradigm is visually represented in Fig. 1.

#### 2.5.1. Auditory oddball paradigm

Each protocol consisted of 7 blocks with 125 trials apiece. Every block started with 25 trials of the standard sequence to establish the global rule. Of the next 100 trials, the standard was presented with 75% probability, the deviant with 15% probability, and the omission sequence with 10% probability. In the omission-only condition, 125 trials of Sequence Omission were presented separately. Thus, in the 7 blocks, 700 standards, 105 deviants, and 70 omission sequences were presented for one protocol. The sequences were presented with a random inter-trial jitter of 700–1000 ms. The participants were randomly presented with the xxxxx or xxxxy protocol first and the omission-only protocol was presented towards the end to avoid any habituation to the omission sequence. The participants could take breaks between subsequent blocks and between subsequent protocols.

### 2.6. EEG data collection and pre-processing

The stimuli were presented through the Neuroscan Stim II system which triggered the Neuroscan Scan 4.5 Acquire software. The ERP data was collected using 64 channel Neuroscan Synamps<sup>2</sup> Quick Cap configured per the International 10–20 placement system with a reference close to Cz (impedance  $<5k\Omega$ ). The data was sampled using the Neuroscan Synamps<sup>2</sup> amplifier at 500 Hz and online band-pass filtered at 0.1–70 Hz. Data was pre-processed using Matlab, EEGLAB v13.6.5b and ERPLAB v5.1.1.0 and epoched between  $-600$  to  $+1950$  ms relative to the onset of the first stimulus in the sequence. Details regarding the pre-processing pipeline is given in the supplementary section.

#### 2.6.1. Comparing ERPs of the omission response between tinnitus and control groups

An omission response is the response to a missing stimulus in a sequence of stimuli. In the current study, standard omissions refer to the response of the brain to 4 identical tones with a gap for a possible 5th tone where the gap is expected (g, Fig. 1). Deviant omissions refer to the unexpected omission of a 5th stimulus (tone or noise burst) while presenting either 5 identical tones (c, Fig. 1) or 4 identical tones followed by a noise burst (f, Fig. 1) as the standard.

Given an imbalance between the number of standard and deviant omissions while comparing the ERPs of the omission responses, a random selection of standard omissions equal to the number of deviant omissions for each omission condition was drawn from the total number of standard omissions for each person. The average ERP for the standard and deviant omissions and the difference ERPs (omissionX (c – g, Fig. 1), and omissionY (f – g, Fig. 1)) were generated. This process was repeated 500 times to generate a set of difference ERPs for each person in each condition. The set of difference ERPs for each person in the control group was compared to each person in the tinnitus group using a 2-tailed independent sample *t*-test where the number of channel-time point pairs were corrected for multiple comparisons using a cluster correction. This process generated 100 (10 controls \* 10 tinnitus) individual *t*-test cluster maps. From this, only clusters that showed a  $p < .00025$  (after correcting for 100 contrasts and 2 conditions using Bonferroni correction) in more than 95 contrasts were considered significant. In addition, the pre-stimulus baseline activity of the difference ERPs was also compared between the control and tinnitus groups, using the same procedure for the two omission conditions. The standard error for the ERP for each group was calculated by pooling the standard error from the different contrasts.

#### 2.6.2. Topographical plots and source reconstruction

The topographical distribution of the significant differences in the time windows of interest (i.e. late positive potential (P300) 300–750 ms after the onset of the 5th stimulus and pre-stimulus baseline ( $-600$  to

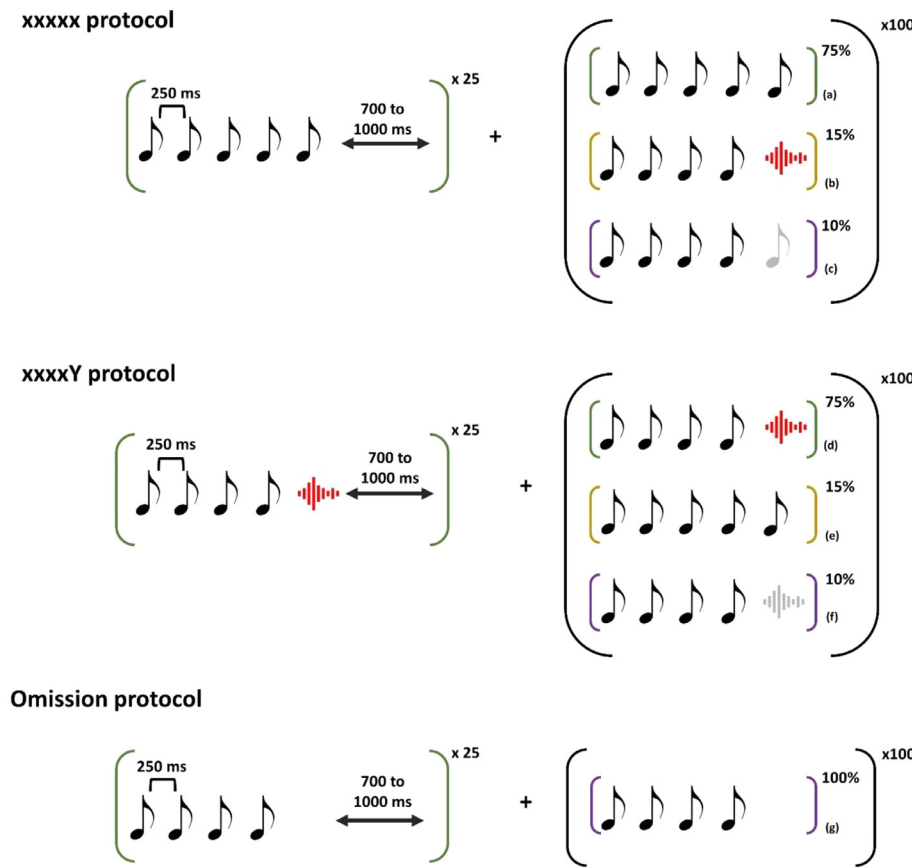


**Fig. 1.** Summary of the auditory oddball paradigm used in this study. Each black note represents the 500 Hz tone, the red burst represents the noise burst and the light grey sound represents the missing tone/noise burst as per the context. In the xxxxx condition the 5-tone sequence is presented with 75% probability, the 4 tones followed by a noise burst is presented with 15% probability and the 4 tones followed by a light grey note representing the omission to the 5th tone is presented with 10% probability. In the xxxxY condition, the 4 tones followed by a noise burst is presented with 75% probability, the 5-tone sequence is presented with 15% probability and the 4 tones followed by the light grey burst representing the omission to 5th noise burst is presented with 10% probability. A separate omission sequence consisting of 4 tones followed by a silence is presented with 100% probability.

0 ms) before the onset of the 1st stimulus) were computed as the mean amplitude across the significant time points for each comparison. These time windows are consistent with those used by (Wacongne et al., 2011). The mean of the difference ERP sets of all participants were source localized using a software called standardized low-resolution electromagnetic tomography (sLORETA) which is explained in detail in the supplementary section. The difference between the source signal of the two groups in the time windows of interest were compared in sLORETA using multiple voxel-by-voxel comparisons and an independent sample *t*-test whose distribution was drawn using a permutation test of 5000 iterations and was corrected for multiple comparisons using Bonferroni correction.

## 2.7. Time-frequency decomposition

To account for oscillatory changes happening during the two deviant omissions in terms of activity changes within a region and communication between regions, time-frequency analyses were carried out on the mean of the difference ERPs sets generated for all participants. A family of Morlet wavelets with a linearly increasing number of cycles between 2 cycles at 2 Hz and 15 cycles at 55 Hz sampled at 500 Hz was convolved with the ERP. A baseline normalization (−600 to −300 ms) was employed on the evoked power. The continuous frequency was divided into four frequency bands theta (4–7.5 Hz), alpha (8–12 Hz), beta (13–30 Hz) and gamma (30.5–50 Hz). The mean amplitude of the evoked beta and gamma frequency bands for the significant channel-time point clusters in the pre-stimulus and P300 time window respectively identified from the statistical analyses of the ERPs were averaged. Beta power in the pre-stimulus and gamma power in the P300 time frame were considered based on previous evidence that they encode predictions and PEs respectively. The beta evoked power in the pre-stimulus and gamma evoked power in the P300 time-frame was compared between the two

groups using a mixed model with group as fixed factor and channels as random factors and were corrected for multiple comparisons using Bonferroni correction. The *p*-value for the mixed model was thresholded at  $p < .025 (=0.05/2)$  for 2 omission conditions for the beta power in the pre-stimulus and gamma power in the P300 time frame.

## 2.8. Topological distribution and source reconstruction for time frequency analysis

The topological distribution of the group difference in evoked beta, and gamma amplitudes averaged across the significant time windows was plotted. The time series of the evoked beta and gamma amplitudes were localized on to the source space using sLORETA. The difference between the source signal of the two groups in the two frequency bands and the time windows of interest were compared in sLORETA using multiple voxel-by-voxel comparisons and an independent sample *t*-test whose distribution was drawn using a permutation test of 5000 iterations and was corrected for multiple comparisons using Bonferroni correction. Source reconstruction of these components was performed the same way as described previously.

### 2.8.1. Correlation of pre-stimulus frequency-specific activity with post-stimulus activity

Previous studies point out that the correlation between pre-stimulus and post-stimulus activity may be a reflection of anticipatory changes in the post stimulus period (Lazzaro et al., 2001). Thus, the average pre-stimulus beta evoked activity across the significant time points combined across groups and condition was correlated with the corresponding average evoked post-stimulus gamma activity in the P300 time frame. These correlations were thresholded at  $p < .025 (=0.05/2)$  correcting for the 2 omission conditions using Bonferroni correction.



### 2.8.2. Characterising the auditory predictive coding network

To empirically characterise the auditory predictive coding network, we delve into how the hypothesised regions of this network communicate with one another. To do so, we calculate the functional and effective connectivity between the regions of this network using the following methods and compare these measures between the two groups. Functional connectivity determines the amount of information shared between two regions and effective connectivity determines the directionality. Taken together, we will be able to characterise the changes in the oscillatory signature of feedforward and feedback connectivity in the hypothesised network.

### 2.8.3. Functional connectivity – pairwise-phase consistency (PPC)

Single trials of standard and deviant omissions were source localized on to regions of the hypothesised predictive coding network: left and right AC(BA 41), left and right parahippocampus(BA 27, 36), pgACC/vmPFC averaged between left and right(BA 32), dACC averaged between left and right(BA 24) and PCC averaged between left and right(BA 23, 31). The functional connectivity between the different areas was calculated using pairwise-phase consistency(PPC), the dot-product between the relative angular separation between pairwise combination of trials (El Karoui et al., 2015; Vinck et al., 2010). PPC is calculated using the following formula.

$$PPC_{kl}(t) = \frac{2}{N(N-1)} \sum_{i=1}^{N-1} \sum_{j=i+1}^N \cos(\Delta\phi_{kl}^i(t) - \Delta\phi_{kl}^j(t))$$

where  $PPC_{kl}$  is the functional connectivity between regions  $k$  and  $l$  at time point  $t$ ,  $\Delta\phi_{kl}^i(t)$  is the phase difference between regions  $k$  and  $l$  in trial  $i$  at time  $t$ .  $N$  is the total number of trials in that condition. PPC measures the rhythmic synchronization between the signals from two sources and is a population equivalent of the well-established phase-locking value(PLV) that is not biased by the number of trials in each condition. Further explanation of the PPC and the comparison between PPC and PLV are given in Vinck et al., 2010.

The functional connectivity network in the alpha frequency band in the pre-stimulus and theta frequency band in the P300 time frames were calculated as the arithmetic mean of the PPC across the specific frequency bands and significant time points. This is based on the literature stating that predictions are communicated in a feedforward way in the alpha frequency band and PEs are communicated in a feedback way in the theta frequency band. The difference PPC between the deviant and standard omissions for the omissionX and omissionY conditions were calculated. Group comparisons between the difference PPC was performed using independent  $t$ -tests for each connection in the network. The  $t$ -tests were corrected for multiple comparisons for the number of connections in the network(21), and number of conditions(2) using a Benjamini-Hochberg False Discovery Rate of  $\alpha=0.30$  in each time frame.

### 2.8.4. Effective connectivity – Granger causality

The effective connectivity between connections that showed significant changes in PPC was calculated using Granger Causality(GC) in the pre-stimulus and post-stimulus time frames. GC reflects the strength of causal interactions(i.e. extracted activity of one area of causal influences of one neural element over another) from one region to another by quantifying how much the signal in the seed region is able to predict the signal in the target region (Granger, 1969). GC is based on formulating a multivariate autoregressive model and calculating the corresponding partial coherences after setting all irrelevant connections to zero. It is defined as the log-ratio between the error variance of a reduced model, which predicts one time series based only on its own past values, and that of the full model, which in addition includes the past values of another time series. It is important to note that GC does not imply anatomical connectivity between regions but causal functional connectivity between two sources giving a direction of flow of information

in time. The effective connectivity of the evoked response was calculated from the mean of the difference ERP sets calculated above. The GC between pairs of regions of interest mentioned in the section above was calculated using sLORETA (Pascual-Marqui et al., 2014) where the full technical details can be found. The GC was compared between the two groups using independent  $t$ -tests that were corrected for number of connections (to-and-fro), and number of conditions in each time frame using a Benjamini-Hochberg False Discovery Rate of  $\alpha=0.30$ .

### 2.8.5. Correlations with behavioural data

A post-hoc analysis was performed correlating the significant mean evoked pre-stimulus activity with the THI scores controlling for subjective loudness and with the VAS for loudness controlling for THI, TQ, and mean hearing loss scores using a Pearson correlation. The correlation with THI scores was done with pre-stimulus activity in alpha and that with loudness in the theta band based on previous literature showing correlations of resting state alpha activity with tinnitus-related distress (Vanneste et al., 2013a, 2010) and theta activity with tinnitus loudness (De Ridder et al., 2015). These correlations were corrected for multiple comparison using a Bonferroni correction for the 2 conditions( $p < .05/2 = 0.025$ ). Missing data were excluded from the analyses.

## 3. Results

The primary outcome measure of the study was change in ERP amplitude. Secondary outcome measures include changes in time-frequency component, functional and effective connectivity.

### 3.1. Comparing group difference between deviants and standards in the omission conditions in the P300 time frame

In Fig. 2, we observe significantly greater ERP amplitude in the tinnitus than in the control group, following a positive polarity between 300 and 750ms(omissionX) and 340–700ms(omissionY) in the frontal and central electrodes. These localise to decreased ERP amplitude over pgACC/vmPFC, dACC, PCC, primary AC, and parahippocampus and increased ERP amplitude in the frontal and temporal pole in the tinnitus group. In both conditions, we observe a wide-spread increase in the topographical gamma activity. The omissionX condition showed no significant change in gamma( $F(1, 378)=1.89, p=.17, \text{partial}\eta^2=0.005, 95\%CI=[0, .02]$ ) activity between the two groups. However, the omissionY condition showed a significant increase in and gamma( $F(1318)=11.62, p=.001, \text{partial}\eta^2=0.04, 95\%CI=[.01, .07]$ ) activity in the tinnitus group.

At the source level this is reflected in increased gamma activity over widespread frontal regions, primary and secondary ACs, parahippocampus, dACC, PCC, and temporal-parietal junction; and decreased gamma activity over the pgACC/vmPFC region in the tinnitus group in the omissionY condition.

### 3.2. Pre-stimulus activity in the two omission conditions

From Fig. 3, we observe greater ERP amplitude in the tinnitus than in the control group following a positive polarity between –480 and –70ms(omissionX) and –510 and –70ms(omissionY) in the frontal-central electrodes. This is localised to increased ERP amplitude over the frontal and temporal pole, DLPFC and decreased ERP amplitude over the secondary ACs, superior parietal regions, pgACC/vmPFC region, and the parahippocampus in both conditions, including dACC and PCC in the omissionY condition in the tinnitus group.

Topographically, beta activity was observed in the central and parietal sites in the tinnitus group, however, no significant difference between the two groups was observed in the omissionX( $F(1338)=0.37, p=.54, \text{partial}\eta^2=0.001, 95\%CI=[0, .01]$ ) or omissionY( $F(1378)=3.76, p=.053, \text{partial}\eta^2=0.01, 95\%CI=[0, .03]$ ) condition.

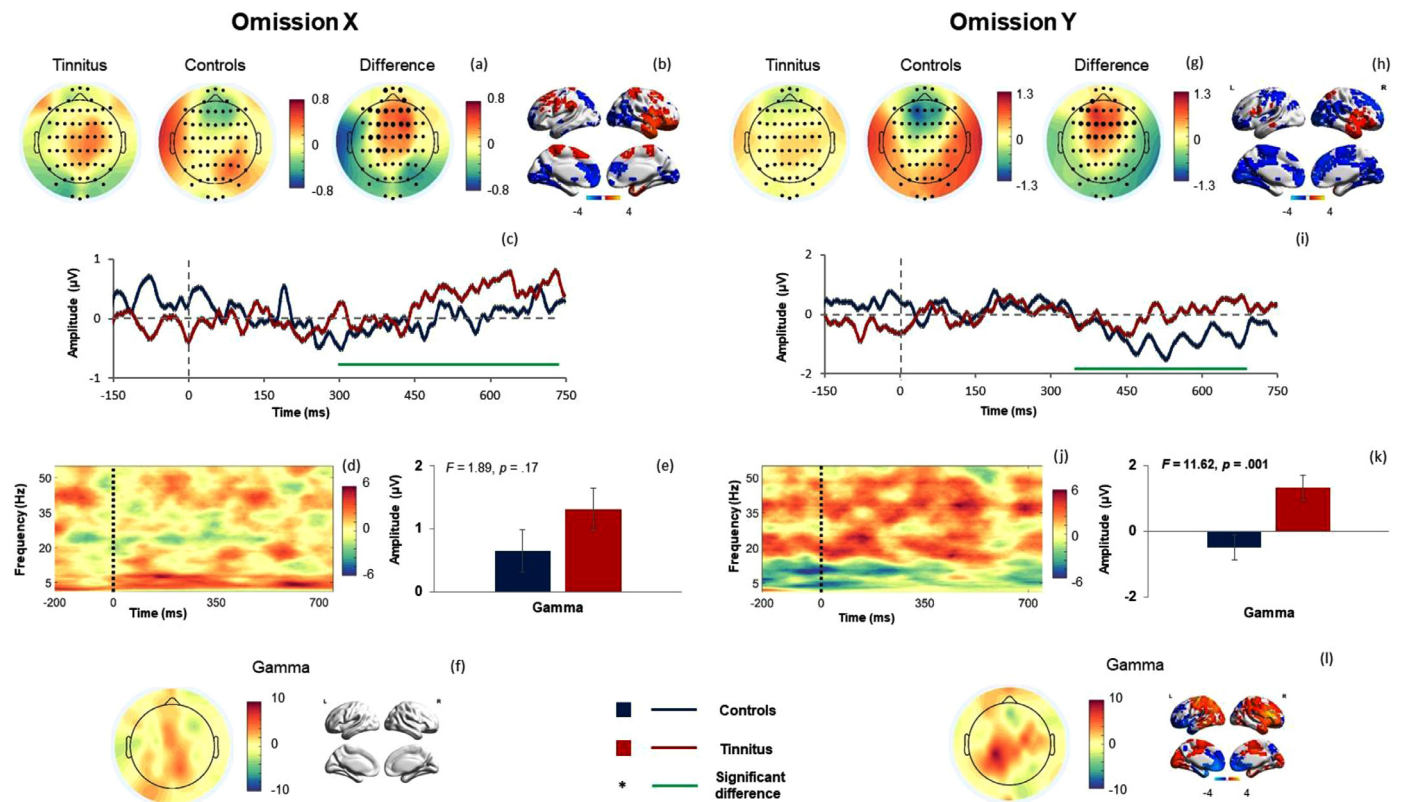


**Fig. 2.** Summary results of the comparison of the difference ERP (deviant – standard) for the omissionX and omissionY conditions between the controls and tinnitus group during the P300 time frame. Row 1 shows the topographical distribution (a, g) of the P300 amplitude for the significant time points from the ERP analysis for the tinnitus, controls, and the difference between the two groups (significant electrodes shown in bold) and the corresponding source localizations (b, h). Row 2 shows the difference ERP of the control (blue line) and tinnitus (red line) group at the C2 electrode for the omissionX (c) and FCz electrode for the omissionY (i) and the significant time points (green line). Row 3 shows the difference between the time-frequency decomposition (d, j) averaged over the significant electrodes shown in bold between the tinnitus and control group and the mean gamma amplitude averaged also over the significant time points from the ERP analysis in the controls (blue rectangle) and tinnitus (red rectangle) group (e, k). Row 4 shows the topographical and source localization of the difference in average gamma amplitude over the significant time points from the ERP analysis between the controls and tinnitus group (f, l). Error bars show 95%CI calculated using the pooled standard error.

### 3.3. Correlation of pre-stimulus frequency band activity with post-stimulus

In Fig. 4, we observe that the pre-stimulus beta activity is significantly correlated with the post-stimulus (P300) gamma activity in the omissionY ( $r = 0.61, p = .004$ ) but not in the omissionX ( $r = 0.48, p = .034$ ) condition after Bonferroni correction.

#### 3.3.1. Characterising the auditory predictive coding network

##### 1 Functional connectivity

In the pre-stimulus time frame, there is increased alpha functional connectivity between the pgACC/vmPFC and PCC ( $t(18) = 3.16, p = .005, d = 1.40, 95\%CI = [.4, 2.38]$ ), and pgACC/vmPFC and left parahippocampus ( $t(18) = 2.58, p = .019, d = 1.56, 95\%CI = [.21, 2.10]$ ) in the omissionX condition and between left parahippocampus and dACC ( $t(18) = 3.04, p = .007, d = 1.37, 95\%CI = [.37, 2.33]$ ) for the omissionY condition.

In the P300 time frame, increased theta functional connectivity between the left and right AC ( $t(18) = 2.73, p = .010, d = 1.22, 95\%CI = [.26, 2.17]$ ), dACC and left AC ( $t(18) = 2.39, p = .030, d = 1.07, 95\%CI = [.13, 2.01]$ ) and dACC and left parahippocampus ( $t(18) = 3.34, p = .003, d = 1.50, 95\%CI = [.50, 2.49]$ ) in the omissionX condition; and between left and right AC ( $t(18) = 2.25, p = .038, d = 1.01, 95\%CI = [.08, 1.94]$ ), dACC and left AC ( $t(18) = 2.66, p = .016, d = 1.19, 95\%CI = [.24, 2.14]$ ), dACC and left parahippocampus ( $t(18) = 2.47, p = .023, d = 1.11, 95\%CI = [.17, 2.05]$ ) and left parahippocampus and right AC ( $t(18) = 2.17, p = .043, d = 0.97, 95\%CI = [.04, 1.90]$ ) in the omissionY condition. These results are shown in Fig. 5.

##### 1 Effective connectivity

In the pre-stimulus time frame there is no significant difference in the effective connectivity between the two groups. In the post-stimulus timeframe an increase in theta connectivity from the left AC to dACC ( $t(18) = 2.73, p = .014, d = 1.21, 95\%CI = [.26, 2.16]$ ) and from left parahippocampus to dACC ( $t(18) = 4.40, p < .001, d = 1.96, 95\%CI = [.89, 3.03]$ ) in the omissionY condition was observed for the tinnitus group. This is illustrated in Fig. 5.

#### 3.3.2. Correlation of behavioural variables with pre-stimulus activity

From our post-hoc analysis ( $N = 8$ ) we observe a strong, significant, positive correlation of the overall THI score with the evoked pre-stimulus alpha activity in the omissionX condition ( $r = 0.74, p = .024$ ) but not in the omissionY condition ( $r = 0.34, p = .37$ ). Similarly, a strong significant positive correlation was observed between the mean evoked pre-stimulus theta activity and the VAS for loudness in the omissionX ( $r = 0.89, p = .041$ ) before Bonferroni correction but not in the omissionY ( $r = -0.48, p = .42$ ) condition.

### 4. Discussion

We show condition-related increase in pre-stimulus, and late attention-modulated (P300) components of ERPs to omissions of global deviants relative to their predicted counterparts in the tinnitus group. The response to omission of global deviants is an absolute empirical explanation to hierarchical predictive coding that cannot be explained by

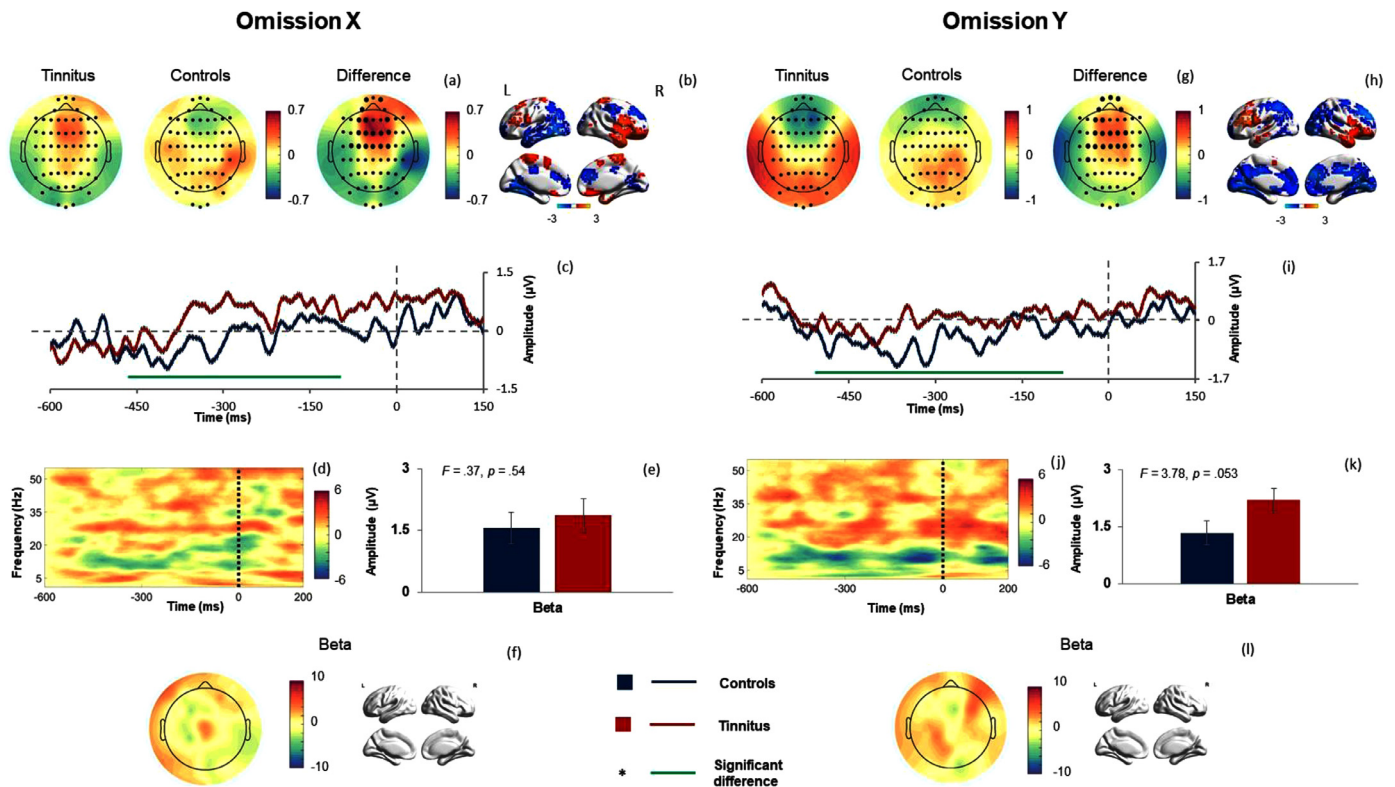


**Fig. 3.** Summary results of the comparison of the difference ERP (deviant – standard) for the pre-stimulus baseline time frame between the controls and tinnitus group for the omissionX and omissionY conditions. Row 1 shows the topographical distribution (a, g) of the pre-stimulus baseline amplitude for the significant time points from the ERP analysis for the tinnitus, controls, and the difference between the two groups (significant electrodes shown in bold) and the corresponding source localizations for the omissionX (b) and omissionY (h) conditions. Row 2 shows the difference ERP of the control (blue line) and tinnitus (red line) group for the FCZ electrode and the significant time points (green line) for the two omission conditions (c, i). Row 3 shows the difference between the time-frequency decomposition (d, j) averaged over the significant electrodes shown in bold between the tinnitus and control group and the mean beta amplitude averaged also over the significant time points from the ERP analysis in the controls (blue rectangle) and tinnitus (red rectangle) group for the two omission conditions (e, k). Row 4 shows the topographical and source localization of the difference in average beta amplitude over the significant time points from the ERP analysis between the controls and tinnitus group for the two omission conditions (f, l). Error bars show 95%CI calculated using the pooled standard error.

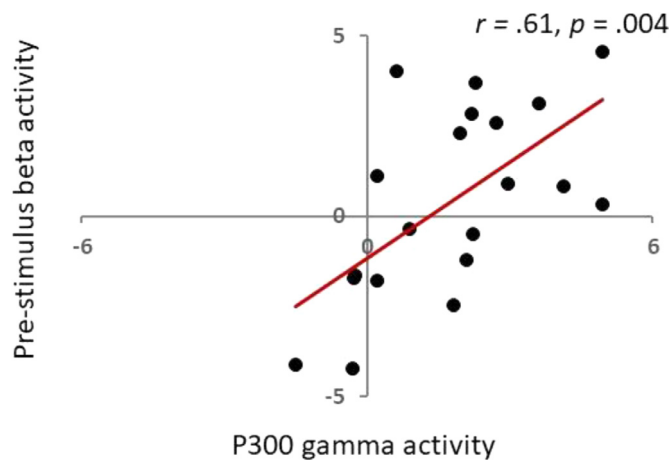


**Fig. 4.** Correlation of pre-stimulus beta activity (deviant – standard) of both the controls and tinnitus group with corresponding post-stimulus (P300) gamma activity for the omissionY condition.

stimulus adaptation (Wacongne et al., 2011) and is a signature of involuntary attention to unexpected irregularities in input (Polich, 2007). From the current study, we understand that these are neural markers of increased hierarchical PEs produced by external non-tinnitus related auditory stimuli during the chronic perception of a phantom sound.

PEs generated by omissions to global deviants show increased evoked gamma activity in lower and higher regions of the hierarchy in the P300 time frame in tinnitus. Increase of gamma band activity in auditory oddball and omission responses have been previously shown (Başar-Eroglu and Başar, 1991; Başar et al., 1992) however, the precise role of gamma oscillations associated with late potentials is still under debate. There is a broad range of literature that explains the role of gamma oscillations in sensory processing. Gamma oscillations have been associated with feature linking and binding sensory inputs into a unitary sensation that we perceive (Jefferys et al., 1996). Specifically, gamma band responses related to late auditory potentials correlate with attention to auditory targets (Marshall et al., 1996). Particularly from the predictive coding framework, increase in gamma band activity has been associated with increased PEs in both lower and higher regions of the hierarchy (Arnal and Giraud, 2012; Chao et al., 2018; Mejias et al., 2016; Sedley et al., 2016b). Increase in gamma band activity in tinnitus patients in response to omission of global deviants in different levels of the hierarchy indicates increased PEs in tinnitus patients. Furthermore, it may also indicate that tinnitus patients may have increased attention orientated to omission of global deviants compared to controls.

The other explanation for increased PEs in tinnitus may be increased precision of prediction of repetitive stimuli (Cassidy et al., 2018). Increased pre-stimulus response is characteristic of creating strong predictions (Partyka et al., 2019) suggesting tinnitus patients make a stronger memory trace of standards than healthy controls. Such a strong-prior hypothesis to auditory hallucinations is also proposed by other authors (Corlett et al., 2019; Powers et al., 2017). Thus, tinnitus patients may



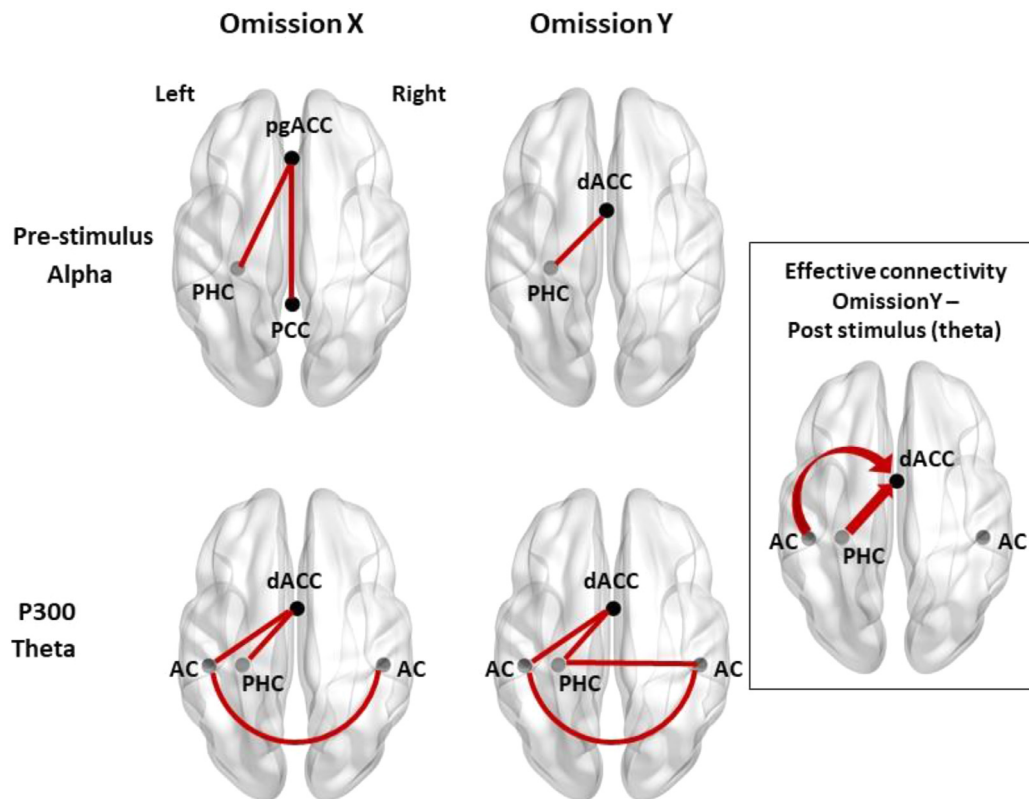


**Fig. 5.** Summary of functional connectivity changes of the deviant-standard responses in for the two omission conditions in the pre-stimulus (top-row) and P300 (bottom-row) time frames. The figure shows the significantly increased functional connectivity in the tinnitus group. It also shows the direction of significantly increased flow of information in the tinnitus group highlighted by the boxed image.

be making stronger associations creating a stronger memory trace of repetitive stimuli and thus, when it is violated, they create larger PEs. Furthermore, post-stimulus gamma activity that is a signature of PEs is significantly correlated with pre-stimulus beta activity that encodes predictions. This correlation of anticipation in the pre-stimulus time frame with the PE in the post-stimulus time frames agree with the strong-prior hypothesis (Arnal and Giraud, 2012; Engel and Fries, 2010).

#### 4.1. Hierarchical predictive coding network

Although gamma activity is the widely recognized oscillatory signature for PEs, recent studies show that PEs are fed forward in theta and predictions are fed back in alpha bands (Alamia and VanRullen, 2019; Recasens et al., 2018). During the P300 time frame, we observe increased theta functional connectivity between the ACs, parahippocampus and the dACC. Increased gamma activity together with increased theta functional connectivity between these regions suggest an increased feedforward communication of PEs through the predictive coding network.

During the pre-stimulus time frame, where we hypothesise prediction about the change is being encoded, we observe increased alpha functional connectivity between the pgACC/vmPFC, parahippocampus and PCC in the omission X condition, between the dACC and PHC in the omission Y condition. The pgACC/vmPFC is associated with top-down inhibition of unnecessary signals forming a “noise-cancellation system” (Rauschecker et al., 2010). The alpha frequency band is also well established in inhibiting unnecessary information (Klimesch, 2012). Thus, the increase in alpha connectivity between these regions, could suggest an anticipation of a compensation of increased PE generated in the post-stimulus time frame. Furthermore, the pgACC/vmPFC, parahippocampus and PCC are part of the default mode network that is active in the absence of a stimulus and encodes prior beliefs (Yeshurun et al., 2021).

Thus, increased alpha activity between these regions in the pre-stimulus time frame may also be an indicator for strong priors in tinnitus patients.

Effectively we observe that increased information is passed from AC and the parahippocampus (auditory memory) to dACC (error monitoring system) in the theta band providing concrete evidence for increased feedforward communication of PEs in tinnitus.

#### 4.2. Predisposition to auditory domain-wide PEs and its possible biomarker

We observe that tinnitus patients show increased PEs by stimuli that do not possess the audiological characteristics of the phantom sound. This suggests a predisposition of these patients to PEs generated throughout the auditory domain. This idea expands on recent evidence showing neural changes to tinnitus-related stimuli and the theory that chronically the brain updates tinnitus as the new prediction (Hullfish et al., 2019; Sedley et al., 2019, 2016a). The current study and a recent unpublished study (Partyka et al., 2019), suggest that changes in predictive coding may not be tinnitus-specific but a systemic change in auditory predictive coding.

The post-hoc correlations of evoked theta activity with tinnitus loudness and alpha activity with tinnitus-related distress go together with previous resting-state findings (De Ridder et al., 2015; Vanneste et al., 2013a, 2010) and have the potential to serve as a biomarker for this domain-wide systemic maladaptive predictive coding. In a recently published study, we showed a positive correlation between the intensity of a transient auditory illusion and evoked theta activity (Mohan et al., 2020). This activity was localised to the pgACC/vmPFC and parahippocampus potentially reflecting premature maladaptive changes in the “noise-cancellation” system. Based on these congruent results, we propose that changes in scalp-level theta activity may be a biomarker for maladaptive changes in auditory predictive coding. Further hypothesis-driven analysis with a larger sample size is required to confirm this.



Thus, the current study is the first to our knowledge to provide empirical evidence for the presence of a maladaptive predictive coding network showing predisposition of tinnitus patients with minimal to no hearing loss with phantom percepts to domain-wide stimulus a-specific PEs. It is important to note that the source-level analyses in the study are restricted by spatial resolution and should be confirmed by other techniques. Findings about the strong-prior hypothesis, maladaptive changes in the predictive coding network and its potential biomarkers are key in the early diagnosis of any disorder.

It is also important to note that tinnitus is a highly heterogeneous disorder and we are only looking at one subgroup of tinnitus patients with minimal to no hearing loss. Consistent with previous studies from our lab, we propose that this subgroup of patients pose a type of tinnitus that is probably driven by a more top-down problem – aberration of the auditory predictive coding network that predisposes them to PEs throughout the auditory domain. However, this is not to rule out any heterogeneity that may be brought about by other tinnitus symptoms such as tinnitus loudness and distress, for example. Controlling for these factors, future studies can investigate the aberration of the auditory predictive coding network in tinnitus from different perspectives, thereby contributing to understanding the mechanism of action in different tinnitus subtypes.

The current study uses a paradigm to specifically test PEs, however, this network can also be probed to test how predictions and precisions of predictions are encoded in different pathologies to get deeper insight of the working of the brain. Characterising the auditory predictive coding network also sets the stage to identifying treatment targets for neuro-modulation. Importantly, if tinnitus patients are predisposed to prediction errors in the auditory domain, the next question is to determine whether this predisposition generalises to other sensory domains. This would also mean that aberrant predictive coding is a more fundamental problem and presents the possibility of generalising to other disorders. Through this, future longitudinal studies can also focus on the possibility of finding early markers of aberrant predictive coding with the vision of developing preventative medicine.

## Conclusion

The tinnitus group produces increased PEs to omission of global deviants compared to a matched control group. This is accompanied by changes in gamma activity in lower and higher levels of the hierarchy. Importantly there is increased theta functional connectivity between the AC parahippocampus and dACC in the post-stimulus time frame and increased alpha functional connectivity between the pgACC/vmPFC, parahippocampus and PCC in the pre-stimulus time frame and increased overall feed forward connectivity in theta from the AC and parahippocampus to the dACC in the tinnitus group. The changes to non-tinnitus specific stimuli suggest that patients not only produce strong predictions about upcoming stimuli but may also be predisposed to stimulus a-specific PEs in the auditory domain. Furthermore, post-hoc correlations of pre-stimulus theta activity to tinnitus loudness and alpha activity to tinnitus distress propose a possible biomarker of maladaptive changes in the hierarchical predictive coding system.

## Declaration of Competing Interest

The authors declare no competing interests

## Acknowledgements

We thank S. Lauren McLeod for her valuable comments on the manuscript.

## Supplementary materials

Supplementary material associated with this article can be found, in the online version, at [doi:10.1016/j.neuroimage.2021.118813](https://doi.org/10.1016/j.neuroimage.2021.118813).

## References

- Alamia, A., VanRullen, R., 2019. Alpha oscillations and traveling waves: signatures of predictive coding? *PLoS Biol.* 17.
- Arnal, L.H., Giraud, A.-L., 2012. Cortical oscillations and sensory predictions. *Trends Cogn. Sci. (Regul. Ed.)* 16, 390–398.
- Baguley, D., McFerran, D., Hall, D., 2013. Tinnitus. *Lancet* 382, 1600–1607.
- Başar-Eroglu, C., Başar, E., 1991. A compound P300-40Hz response of the cat hippocampus. *Int. J. Neurosci.* 60, 227–237.
- Başar, E., Başar-Eroglu, C., Parneffjord, R., Rahn, E., Schürmann, M., 1992. Evoked Potentials: Ensembles of Brain Induced Rhythmicities in the Alpha, Theta and Gamma Ranges. *Induced Rhythms in the Brain*. Springer, pp. 155–181.
- Bastos, A.M., Uusitalo, W.M., Adams, R.A., Mangun, G.R., Fries, P., Friston, K.J., 2012. Canonical microcircuits for predictive coding. *Neuron* 76, 695–711.
- Bosman, C.A., Aboitiz, F., 2015. Functional constraints in the evolution of brain circuits. *Front. Neurosci.* 9, 303–303.
- Cassidy, C.M., Balsam, P.D., Weinstein, J.J., Rosengard, R.J., Slifstein, M., Daw, N.D., Abi-Dargham, A., Horga, G., 2018. A perceptual inference mechanism for hallucinations linked to striatal dopamine. *Curr. Biol.* 28, 503–514 e504.
- Cederroth, C.R., Gallus, S., Hall, D.A., Kleinjung, T., Langguth, B., Maruotti, A., Meyer, M., Norena, A., Probst, T., Pryss, R., Searchfield, G., Shekawat, G., Spiliopoulou, M., Vanneste, S., Schlee, W., 2019. Editorial: towards an understanding of tinnitus heterogeneity. *Front. Aging Neurosci.* 11, 53–53.
- Chao, Z.C., Takaura, K., Wang, L., Fujii, N., Dehaene, S., 2018. Large-scale cortical networks for hierarchical prediction and prediction error in the primate brain. *Neuron* 100, 1252–1266 e1253.
- Chennu, S., Noreika, V., Gueorguiev, D., Blenkmann, A., Kochen, S., Ibáñez, A., Owen, A.M., Bekinschtein, T.A., 2013. Expectation and attention in hierarchical auditory prediction. *J. Neurosci.* 33, 11194.
- Corlett, P.R., Horga, G., Fletcher, P.C., Alderson-Day, B., Schmack, K., Powers, A.R., 2019. Hallucinations and strong priors. *Trends Cogn. Sci. (Regul. Ed.)* 23, 114–127.
- De Ridder, D., Congedo, M., Vanneste, S., 2015. The neural correlates of subjectively perceived and passively matched loudness perception in auditory phantom perception. *Brain Behav.* 5.
- De Ridder, D., Elgoyhen, A.B., Romo, R., Langguth, B., 2011. Phantom percepts: tinnitus and pain as persisting aversive memory networks. *Proc. Natl. Acad. Sci.* 108, 8075–8080.
- De Ridder, D., Vanneste, S., Freeman, W., 2014. The Bayesian brain: phantom percepts resolve sensory uncertainty. *Neurosci. Biobehav. Rev.* 44, 4–15.
- El Karoui, I., King, J.-R., Sitt, J., Meyniel, F., Van Gaal, S., Hasboun, D., Adam, C., Navarro, V., Baulac, M., Dehaene, S., Cohen, L., Naccache, L., 2015. Event-related potential, time-frequency, and functional connectivity facets of local and global auditory novelty processing: an intracranial study in humans. *Cereb. Cortex* 25, 4203–4212.
- Engel, A.K., Fries, P., 2010. Beta-band oscillations—signalling the status quo? *Curr. Opin. Neurobiol.* 20, 156–165.
- Fletcher, P.C., Frith, C.D., 2009. Perceiving is believing: a Bayesian approach to explaining the positive symptoms of schizophrenia. *Nat. Rev. Neurosci.* 10, 48–58.
- Friston, K., FitzGerald, T., Rigoli, F., Schwartenbeck, P., O'Doherty, J., Pezzulo, G., 2016. Active inference and learning. *Neurosci. Biobehav. Rev.* 68, 862–879.
- Garrido, M.I., Kilner, J.M., Stephan, K.E., Friston, K.J., 2009. The mismatch negativity: a review of underlying mechanisms. *Clin. Neurophysiol.* 120, 453–463.
- Granger, C.W., 1969. Investigating causal relations by econometric models and cross-spectral methods. *Econometrica*. *J. Econometric Soc.* 424–438.
- Hallam, R., Jakes, S., Hinchcliffe, R., 1988. Cognitive variables in tinnitus annoyance. *Br. J. Clin. Psychol.* 27, 213–222.
- Huang, Y., Mohan, A., De Ridder, D., Sunaert, S., Vanneste, S., 2018. The neural correlates of the unified percept of alcohol-related craving: a fMRI and EEG study. *Sci. Rep.* 8, 923.
- Hullfish, J., Sedley, W., Vanneste, S., 2019. Prediction and perception: insights for (and from) tinnitus. *Neurosci. Biobehav. Rev.*
- Jefferys, J.G., Traub, R.D., Whittington, M.A., 1996. Neuronal networks for induced '40 Hz' rhythms. *Trends Neurosci.* 19, 202–208.
- Kanai, R., Komura, Y., Shipp, S., Friston, K., 2015. Cerebral hierarchies: predictive processing, precision and the pulvinar. *Philos. Trans. R. Soc. Lond., B, Biol. Sci.* 370, 20140169.
- Kleckner, I.R., Zhang, J., Touroutoglou, A., Chanes, L., Xia, C., Simmons, W.K., Quigley, K.S., Dickerson, B.C., Barrett, L.F., 2017. Evidence for a large-scale brain system supporting allostasis and interoception in humans. *Nature Hum. Behav.* 1, 0069.
- Klimesch, W., 2012. Alpha-band oscillations, attention, and controlled access to stored information. *Trends Cogn. Sci. (Regul. Ed.)* 16, 606–617.
- Knill, D.C., Pouget, A., 2004. The Bayesian brain: the role of uncertainty in neural coding and computation. *Trends Neurosci.* 27, 712–719.
- Lazzaro, L., Gordon, E., Whitmont, S., Meares, R., Clarke, S., 2001. The modulation of late component event related potentials by pre-stimulus EEG theta activity in ADHD. *Int. J. Neurosci.* 107, 247–264.
- Lewis, A.G., Bastiaansen, M., 2015. A predictive coding framework for rapid neural dynamics during sentence-level language comprehension. *Cortex* 68, 155–168.
- Marshall, L., Mölle, M., Bartsch, P., 1996. Event-related gamma band activity during passive and active oddball tasks. *Neuroreport* 7, 1517–1520.
- Mejias, J.F., Murray, J.D., Kennedy, H., Wang, X.-J., 2016. Feedforward and feedback frequency-dependent interactions in a large-scale laminar network of the primate cortex. *Sci. Adv.* 2, e1601335.
- Mohan, A., Bhamoo, N., Riquelme, J.S., Long, S., Norena, A., Vanneste, S., 2020. Investigating functional changes in the brain to intermittently induced auditory illusions and its relevance to chronic tinnitus. *Hum. Brain Mapp.*

- Mohan, A., Vanneste, S., 2017. Adaptive and maladaptive neural compensatory consequences of sensory deprivation—from a phantom percept perspective. *Prog. Neurobiol.* 153, 1–17.
- Moore, P., 2015. A predictive coding account of OCD. *arXiv preprint arXiv:1504.06732*.
- Munoz-Lopez, M., MohedanoMorian, A., Insausti, R., 2010. Anatomical pathways for auditory memory in primates. *Front. Neuroanat.* 4.
- O'Reilly, J.X., Schüfflgen, U., Cuell, S.F., Behrens, T.E.J., Mars, R.B., Rushworth, M.F.S., 2013. Dissociable effects of surprise and model update in parietal and anterior cingulate cortex. *Proc. Natl. Acad. Sci. U.S.A.* 110, E3660–E3669.
- Partyka, M., Demarchi, G., Roesch, S., Suess, N., Sedley, W., Schlee, W., Weisz, N., 2019. Phantom auditory perception (tinnitus) is characterised by stronger anticipatory auditory predictions. *bioRxiv*, 869842.
- Pascual-Marqui, R., Biscay, R., Bosch-Bayard, J., Lehmann, D., Kochi, K., Yamada, N., Kinoshita, T., Sadato, N., 2014. Isolated effective coherence (iCoh): causal information flow excluding indirect paths. *arXiv preprint arXiv:1402.4887*.
- Pearson, J.M., Heilbronner, S.R., Barack, D.L., Hayden, B.Y., Platt, M.L., 2011. Posterior cingulate cortex: adapting behavior to a changing world. *Trends Cogn. Sci. (Regul. Ed.)* 15, 143–151.
- Polich, J., 2007. Updating P300: an integrative theory of P3a and P3b. *Clin. Neurophysiol.* 118, 2128–2148.
- Powers, A.R., Mathys, C., Corlett, P.R., 2017. Pavlovian conditioning-induced hallucinations result from overweighting of perceptual priors. *Science* 357, 596.
- Rauschecker, J.P., Leaver, A.M., Mühlau, M., 2010. Tuning out the noise: limbic-auditory interactions in tinnitus. *Neuron* 66, 819–826.
- Recasens, M., Gross, J., Uhlhaas, P.J., 2018. Low-frequency oscillatory correlates of auditory predictive processing in cortical-subcortical networks: a MEG-study. *Sci. Rep.* 8, 14007.
- Sedley, W., Alter, K., Gander, P.E., Berger, J., Griffiths, T.D., 2019. Exposing pathological sensory predictions in tinnitus using auditory intensity deviant evoked responses. *J. Neurosci.* 39, 10096–10103.
- Sedley, W., Friston, K.J., Gander, P.E., Kumar, S., Griffiths, T.D., 2016a. An integrative tinnitus model based on sensory precision. *Trends Neurosci.* 39, 799–812.
- Sedley, W., Gander, P.E., Kumar, S., Kovach, C.K., Oya, H., Kawasaki, H., Howard III, M.A., Griffiths, T.D., 2016b. Neural signatures of perceptual inference. *Elife* 5, e11476.
- Sterzer, P., Adams, R.A., Fletcher, P., Frith, C., Lawrie, S.M., Muckli, L., Petrovic, P., Uhlhaas, P., Voss, M., Corlett, P.R., 2018. The predictive coding account of psychosis. *Biol. Psychiatry* 84, 634–643.
- Van Boxtel, J., Lu, H., 2013. A predictive coding perspective on autism spectrum disorders. *Front. Psychol.* 4.
- Vanneste, S., Alsalman, O., De Ridder, D., 2019. Top-down and bottom-up regulated auditory phantom perception. *J. Neurosci.* 39, 364.
- Vanneste, S., Congedo, M., De Ridder, D., 2013a. Pinpointing a highly specific pathological functional connection that turns phantom sound into distress. *Cereb. Cortex* bht068.
- Vanneste, S., Plazier, M., Van Der Loo, E., Van de Heyning, P., Congedo, M., De Ridder, D., 2010. The neural correlates of tinnitus-related distress. *Neuroimage* 52, 470–480.
- Vanneste, S., Song, J.-J., De Ridder, D., 2013b. Tinnitus and musical hallucinosis: the same but more. *Neuroimage* 82, 373–383.
- Vinck, M., van Wingerden, M., Womelsdorf, T., Fries, P., Pennartz, C.M., 2010. The pairwise phase consistency: a bias-free measure of rhythmic neuronal synchronization. *Neuroimage* 51, 112–122.
- Wacongne, C., Changeux, J.-P., Dehaene, S., 2012. A neuronal model of predictive coding accounting for the mismatch negativity. *J. Neurosci.* 32, 3665–3678.
- Wacongne, C., Labyt, E., van Wassenhove, V., Bekinschtein, T., Naccache, L., Dehaene, S., 2011. Evidence for a hierarchy of predictions and prediction errors in human cortex. *Proc. Natl. Acad. Sci.* 108, 20754–20759.
- Weiss, A.R., Gillies, M.J., Philastides, M.G., Apps, M.A., Whittington, M.A., FitzGerald, J.J., Boccard, S.G., Aziz, T.Z., Green, A.L., 2018. Dorsal anterior cingulate cortices differentially lateralize prediction errors and outcome valence in a decision-making task. *Front. Hum. Neurosci.* 12, 203.
- Yeshurun, Y., Nguyen, M., Hasson, U., 2021. The default mode network: where the idiosyncratic self meets the shared social world. *Nat. Rev. Neurosci.* 22, 181–192.
- Ylinen, S., Bosseler, A., Junttila, K., Huotilainen, M., 2017. Predictive coding accelerates word recognition and learning in the early stages of language development. *Dev. Sci.* 20, e12472.

## Further reading

- Brett, M., Johnsrude, I.S., Owen, A.M., 2002. The problem of functional localization in the human brain. *Nat. Rev. Neurosci.* 3, 243.
- Jung, T.-P., Makeig, S., Bell, A.J., Sejnowski, T.J., 1998. Independent Component Analysis of Electroencephalographic and Event-Related Potential Data. *Central auditory Processing and Neural Modeling*. Springer, pp. 189–197.
- Lancaster, J.L., Woldorff, M.G., Parsons, L.M., Liotti, M., Freitas, C.S., Rainey, L., Kochunov, P.V., Nickerson, D., Mikiten, S.A., Fox, P.T., 2000. Automated Talairach Atlas labels for functional brain mapping. *Hum. Brain Mapp.* 10, 120–131.
- Mazziotta, J., Toga, A., Evans, A., Fox, P., Lancaster, J., Zilles, K., Woods, R., Paus, T., Simpson, G., Pike, B., Holmes, C., Collins, L., Thompson, P., MacDonald, D., Iacoboni, M., Schormann, T., Amunts, K., Palomero-Gallagher, N., Geyer, S., Parsons, L., Narr, K., Kabani, N., Le Goualher, G., Boomsma, D., Cannon, T., Kawashima, R., Mazoyer, B., 2001. A probabilistic atlas and reference system for the human brain: International Consortium for Brain Mapping (ICBM). *Philos. Trans. R. Soc. London. Series B* 356, 1293–1322.
- Pascual-Marqui, R.D., 2002. Standardized low-resolution brain electromagnetic tomography (sLORETA): technical details. *Methods Find. Exp. Clin. Pharmacol.* 24, 5–12.



# Symptom dimensions to address heterogeneity in tinnitus

Anusha Mohan<sup>a</sup>, Sook Ling Leong<sup>a</sup>, Dirk De Ridder<sup>b</sup>, Sven Vanneste<sup>a,\*,1</sup>

<sup>a</sup> Global Brain Health Institute, Institute of Neuroscience, Trinity College Dublin, Dublin, Ireland

<sup>b</sup> Department of Surgical Sciences, Section of Neurosurgery, Dunedin School of Medicine, University of Otago, New Zealand

## ARTICLE INFO

### Keywords:

Tinnitus dimensions  
Tinnitus heterogeneity  
Tinnitus frameworks  
Hearing loss and tinnitus  
Auditory cortex  
Parahippocampus  
Tinnitus networks

## ABSTRACT

Tinnitus, the auditory phantom percept, is a well-known heterogeneous disorder with multiple subtypes. Researchers and clinicians have tried to classify these subtypes according to clinical profiles, aetiologies, and response to treatment with little success. The occurrence of overlapping tinnitus subtypes suggests that the disorder exists along a continuum of severity, with no clear distinct boundaries. In this perspective, we propose a neuro-mechanical framework, viewing tinnitus as a dimensional disorder which is a complex interplay of its behavioural, biological and neurophysiological phenotypes. Moreover, we explore the potential of these dimensions as interacting networks without a common existing cause, giving rise to tinnitus. Considering tinnitus as partially overlapping, dynamically changing, interacting networks, each representing a different aspect of the unified tinnitus percept, suggests that the interaction of these networks determines the phenomenology of the tinnitus, ultimately leading to a dimensional spectrum, rather than a categorical subtyping. A combination of a robust theoretical framework and strong empirical evidence can advance our understanding of the functional mechanisms underlying tinnitus and ultimately, improve treatment strategies.

## 1. Introduction

Tinnitus is defined as the occurrence of a phantom sound perception in the absence of a corresponding external acoustic source, and tinnitus disorder is defined as tinnitus with associated suffering (De Ridder et al., 2021). Worldwide, tinnitus is a common condition affecting 12%–30% of the general adult population (Shargorodsky et al., 2010). Tinnitus is a well-known heterogeneous disorder (De Ridder et al., 2021). The experience of tinnitus can be intermittent, constant, or pulsatile, varying in perceived intensity in one or both ears (Langguth et al., 2013). It has often been described as ringing, hissing, or buzzing (Langguth et al., 2013). It is associated with a range of co-morbidities such as hyperlipidaemia, osteoarthritis and both hypo- and hyperthyroidism (Kim et al., 2015; Nondahl et al., 2012). Tinnitus has also been related to a wide range of causal risk factors; age, stress/anxiety, hearing loss and temporomandibular joint disorder being the most common (Langguth et al., 2013). To add on to its complexity, the adverse psychological reaction to tinnitus, termed tinnitus-related distress or simply distress, substantially vary among sufferers (Langguth et al., 2013). It has been estimated that approximately 20 % of all tinnitus cases are severely

debilitating, making it a challenge for an individual to carry out daily activities (McCormack et al., 2016). Tinnitus sufferers also often report concentration difficulties, negative emotions, work hindrance, interference with social interaction as well as sleep, depression, anxiety, problems with speech perception and reduced overall health (McCormack et al., 2016). Also, patients seem to respond differently to the diverse treatment options (Langguth et al., 2013).

One viable explanation of the observed heterogeneity is the existence of multiple tinnitus subtypes (Cederroth et al., 2019; Hall et al., 2016). Over the years, researchers and clinicians have with modest consensus tried to classify the different tinnitus subtypes according to their clinical profiles, aetiologies, response to treatment and from neurological markers (Cederroth et al., 2019; Hall et al., 2016). In practice, tinnitus typologies are to an extent inflexible, leading a patient to be classified into an 'all-or-nothing' group, with no in-betweens. In other words, the patient either has a specific tinnitus entity or does not. The presence of overlapping tinnitus subtypes suggests a limitation to the categorical approach, leaving many cases ambiguous, borderline, and unaccounted for.

Alternatively, a dimensional framework would allow the flexibility

\* Corresponding author at: Lab for Clinical & Integrative Neuroscience, Global Brain Health Institute and Institute of Neuroscience, Trinity College Dublin, College Green 2, Dublin, Ireland.

E-mail address: [sven.vanneste@tcd.ie](mailto:sven.vanneste@tcd.ie) (S. Vanneste).

<sup>1</sup> website: <http://www.lab-clint.org>.

<https://doi.org/10.1016/j.neubiorev.2022.104542>

Received 1 July 2021; Received in revised form 11 January 2022; Accepted 14 January 2022

Available online 17 January 2022

0149-7634/© 2022 The Authors. Published by Elsevier Ltd. This is an open access article under the CC BY license (<http://creativecommons.org/licenses/by/4.0/>).

for this disorder to exist along a continuum of severity, with no clear distinct boundaries. It would explain the co-occurrence and heterogeneity among individuals sharing the same diagnosis, trait, or treatment response. The proposition for tinnitus to lie on a continuity rather than have distinct subtypes has been previously suggested by van den Berge and colleagues and Santacruz and colleagues (Santacruz et al., 2021; van den Berge et al., 2017). In the former, the authors showed that a cluster analysis on 1783 tinnitus patients, revealed “no substantial” cluster structure and a low silhouette value indicating that tinnitus may not have distinct subtypes but may lie on a continuous spectrum (van den Berge et al., 2017). The latter study also showed a low silhouette value for the clustering solution when a group of 336 tinnitus patients were analysed according to hearing thresholds and minimum masking level of the tinnitus, suggesting tinnitus heterogeneity to lie on a continuum rather than be categorical (Santacruz et al., 2021). Therefore, numerous causal factors, perception, as well as genetic factors, would make small but important contributions to the severity of tinnitus, a patient’s psychological reaction and ultimately their response to treatment.

In their editorial, Cederroth and colleagues talk about the heterogeneity of tinnitus varying in these four dimensions – perception of tinnitus (laterality, pitch, type and other acoustic aspects), causal risk factors (hearing loss, temporal mandibular joint disorder, age, etc), distress and psychological comorbidities and treatment response (Cederroth et al., 2019). Here, they attribute dimensions to group tinnitus characteristics and discuss how these phenotypical attributes contribute to tinnitus heterogeneity. However, in this perspective, we take a more neural and bio-marker approach and propose tinnitus as a multidimensional disorder wherein increasing symptom severity ties together with increasing complexity of neural networks. This combined with genetic markers could better explain the heterogeneity in tinnitus patients on a continuum rather than classify them into categorical subtypes. This approach thus has the potential for improved assessment and clinical implications. The advancement in theoretical approaches in combination with robust empirical evidence can only bring upon a thorough understanding of the functional mechanisms underlying tinnitus and ultimately, improved treatment approaches.

## 2. Early classification in tinnitus – moving from categorical to dimensional models

Tinnitus was broadly classified as objective and subjective tinnitus depending on the presence/absence of a source. Subjective tinnitus was further classified as conductive, senso-neural and central tinnitus based on the aetiology of damage (Zenner, 1998). Senso-neural tinnitus had sub-classifications depending on where the damage was located in the auditory pathways – (i) motor or Type I tinnitus was associated with damage to the outer hair cells, (ii) transduction or Type II tinnitus was associated with damage of transduction in the inner hair cells, (iii) transformation or Type III tinnitus was associated with damaged auditory nerve affecting transformation of chemical signals to neural signals and (iv) extrasensory tinnitus was associated with damage to extrasensory elements via the stria vascularis. Central tinnitus also had sub-classifications – (i) Primary central tinnitus associated with damage to brain regions owing to tumors and multiple sclerosis, (ii) Secondary central tinnitus or phantom tinnitus, wherein the tinnitus is produced in the brain irrespective to the origin of damage. This is illustrated in Fig. 1.

More recent studies have tried to objectively identify tinnitus subtypes through hypothesis-driven, data-driven and treatment response clustering and machine learning algorithms. A recent review showed that many of these studies used a hypothesis-driven approach to subtype tinnitus phenotypes (Genitsaridi et al., 2020). Overall, 94 different tinnitus and non-tinnitus related variables were used across the different studies, the most important being age, hearing ability and tinnitus severity in terms of intensity of the sound and distress because of it. Although the attempt to classify tinnitus phenotypes has gained popularity in the last 5 years, there is still no success. Furthermore, only very few studies have considered objective neural and biomarkers of tinnitus in data-driven classification techniques (Genitsaridi et al., 2020).

In 2008, the United States National Institute of Mental Health initiated the Research Domain Criteria (RDoC) which is a programmatic initiative that aspires to build research literature to inform future psychiatric nosologies based on neuroscience and behavioural science rather than descriptive phenomenology (Cuthbert, 2014). It aims to move away from categorical descriptions of psychiatric disorders and

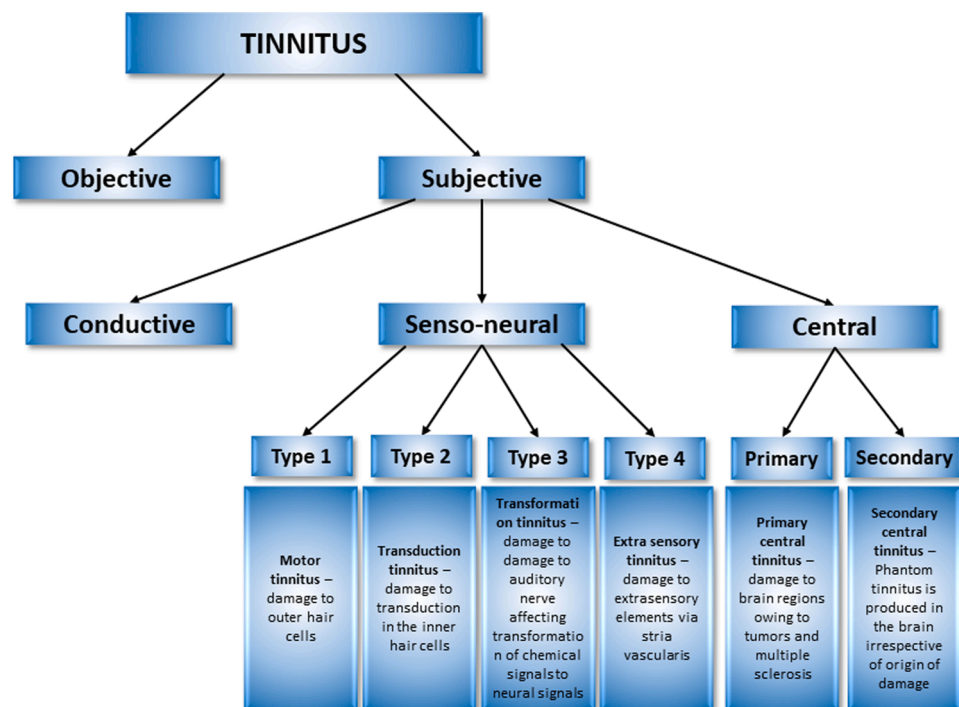


**Fig. 1.** Pictorial representation of early tinnitus classification. The figure goes through how tinnitus was initially classified based on the origin of sensory damage.



validate dimensions that are eventually useful for clinical work. This way it provides information and experience on how to conceive and implement such an alternative approach to future diagnostic practices that harness genetics and neuroscience in the service of more effective treatment and prevention (Kozak and Cuthbert, 2016). Particularly, the RDoC matrix seeks to build a dimensional framework integrating biological (i.e. genetic, neurocircuitry) and psychological constructs (i.e. cognition, negative valence) (Yee et al., 2015).

Like the discipline of psychiatry, tinnitus research is well positioned for the promising view that the auditory phantom percept reflects dysfunction in neural circuitry leading to the manifestation of comorbid symptoms. A dimensional matrix that integrates the relationships between the domains of neuroscience, psychology, and genetics that contribute to tinnitus will allow a rigorous explanatory account of this disorder as a multifaceted whole.

Thus, in the current perspective, we argue that tinnitus is a dimensional disorder whose classification may be better described by using the RDoC approach of examining neural and genetic markers in addition to its phenotypes. Here we review the literature around the neural and biomarkers of the most important factors of tinnitus – age, hearing ability and tinnitus severity (loudness, distress) which may form the multidimensional framework of tinnitus. We also suggest how future research could use hypothesis-driven, data-driven and treatment response to empirically test the different tinnitus dimensions. Considering tinnitus as a consequence of partially overlapping, dynamically changing, interacting networks, each representing a different aspect (loudness, distress, lateralization, mood, type etc.) of the unified tinnitus percept (De Ridder et al., 2014b), suggests that the interaction of these networks determines the phenomenology of the tinnitus, ultimately leading to a dimensional spectrum, rather than a categorical subtyping.

### 3. Describing tinnitus dimensions

#### 3.1. Age, duration and onset of tinnitus

Although tinnitus affects about 10–15 % of the general adult population these numbers rise to 30 % among those 50 years or older (Shargorodsky et al., 2010) showing an increased prevalence of tinnitus amongst the older population. In a retrospective review of 470 patients, those of ages 40–60 years were seen most frequently in the clinic (Al-Swiahb and Park, 2016). Patients > 60 years were more likely females (Al-Swiahb and Park, 2016). Although there was no difference in location, type, time of onset or severity of distress among different age groups, the percentage of people affected seem to lie in the 40–60 years age group. Only hearing loss seemed to be significantly different with age. There is also a potential gender bias in the way older patients cope with different tinnitus symptoms. In a study including 607 females and 573 males with tinnitus >3 months and between ages 17–81 years, middle-aged men and women (45–59 years) were more annoyed by their tinnitus than their younger peers (Seydel et al., 2013). This decreased in older males (> = 60 years) but not in older females. Females also had cognitive distress that progressed with age, where older women reported more sleep disturbances and were unable to cope with their tinnitus than older men.

Other factors that are highly correlated with age are hearing loss, tinnitus duration and age of tinnitus onset. Hearing loss is a very important confounding variable for age-related effects and will be discussed in the next section. Tinnitus duration affects the auditory pathways beginning from the brainstem to the auditory cortex. Patients with sub-acute tinnitus (< 3 months) show decreased Wave V amplitude and increased Wave V latency compared to the acute tinnitus (< 1 month) group. In addition, the chronic group exhibit a trend of decreased Wave V amplitude and increased Wave V latency compared to the acute group. This suggests a possible decrease in compensatory neural firing observed after 1 month of tinnitus (Joo et al., 2020). However, from a behavioural perspective, tinnitus symptoms such as tinnitus annoyance, severity,

unpleasantness seem to stabilize over 6 months (Vielsmeier et al., 2020). At the cortical level, longer tinnitus duration is associated with increased metabolic activity in the right inferior frontal gyrus (IFG), right ventro-medial prefrontal cortex (vmPFC) and right posterior cingulate cortex (PCC) (Schecklmann et al., 2013). These regions were also identified as a part of a network using magnetoencephalography (MEG) showing increased functional connectivity with increased tinnitus duration (Schlee et al., 2009a, b). Furthermore, results from a resting-state functional magnetic resonance imaging (rsfMRI) study show that fronto-striatal connections between the nucleus accumbens (NAc) and vmPFC is negatively correlated with age and positively correlated with tinnitus duration after controlling for age and mean hearing loss (Hullfish et al., 2019). Additionally, functional connectivity between the NAc and parahippocampal cortex (PHC) is positively correlated with duration after controlling for age and mean hearing loss (Hullfish et al., 2019). The PHC is recognised as one of the primary players in generating tinnitus (De Ridder and Vanneste, 2014; Sedley et al., 2015; Vanneste et al., 2010a) and fronto-striatal connections play a significant role in assigning an emotional value to the tinnitus signal (Rauschecker et al., 2015). Increased connectivity between NAc-PHC and NAc-vmPFC with duration shows a possible neural correlate for the chronification of the disorder.

In addition to duration, the age of onset of tinnitus also differently affects the tinnitus phenotype and the neural dimensionality. After controlling for hearing loss and tinnitus duration, researchers report that patients who develop tinnitus earlier in their life suffer less (Schlee et al., 2011). From a brain perspective, after controlling for hearing loss at the tinnitus frequency, patients with later onset of tinnitus show increased beta activity in the prefrontal and dorsal anterior cingulate cortex (dACC), increased gamma activity in the orbital frontal cortex (OFC) and decreased delta activity in the PCC compared to an early onset group (Song et al., 2013). The late onset group also show increased functional connectivity between bilateral auditory cortices and insulae and right insula and subgenual anterior cingulate cortex (sgACC) in the theta band, and between the right secondary auditory cortex and bilateral precuneus in the alpha frequency band (Song et al., 2013). The dACC, OFC, sgACC and insulae are part of a distress network explained in tinnitus (De Ridder et al., 2011; Vanneste et al., 2010a) and pain (Peyron et al., 2000; Vermetten et al., 2007). Increase in activity and functional connectivity between these regions depending on the age of tinnitus onset may corroborate the findings of more distress in late onset tinnitus as proposed from the behavioural study (Schlee et al., 2011).

#### 3.2. Hearing ability

The health of the auditory pathways is objectively measured using ABRs, tympanometry, pure tone air/bone conduction audiometry, speech in noise tests, and subjectively using hearing questionnaires. Today 466 million people worldwide have disabling hearing loss which can rise to >900 million in 2050 (WHO). More than 80 % of patients with bilateral profound hearing loss have tinnitus (Baguley et al., 2013). Since hearing is degenerative, age-related hearing loss or presbycusis remains one of the primary co-morbidities of tinnitus. Tinnitus is not just passively associated with hearing loss, but also predicts the occurrence of further hearing loss (Curhan et al., 2021).

Deafferentation-based neural models of tinnitus are popularly discussed at the cellular and systems levels. At the cellular level, when the deafferentation is minimal, merely exceeding the auditory receptive fields, information is attained from the surrounding auditory cortical area, through the process of decreasing lateral inhibition via the unmasking of silent inputs of overlapping tuning curves of the neighbouring cortical cells (Rajan, 1998). If this information is insufficient, dendritic, and axonal rewiring of tonotopic map follows. Initially map plasticity was related to tinnitus, given that larger reorganization was associated with increased tinnitus severity (Muhlnickel et al., 1998), and the occurrence of a reversal process following clinical improvements

(Bartels et al., 2007). However, later studies suggest that reorganization is more related to hearing loss than tinnitus (Langers et al., 2012). At the system-level, the brain is said to contain an internal prediction model of the external environment (Knill and Pouget, 2004). The deafferentation creates a prediction error and an uncertainty since it deviates from this internal model and tinnitus is perceived as a maladaptive compensation to this uncertainty (Mohan and Vanneste, 2017). When the deafferentation is minimal, the information is provided by the neighbouring cortical area. However if the deafferentation is severe, information is drawn from the PHC auditory memory as a way of “filling in” the missing sensory information of the brain and creating tinnitus thereby compensating the increased uncertainty (De Ridder et al., 2014a).

On the other hand, tinnitus is also viewed as a failure of top-down inhibitory mechanisms. Hearing loss increases spontaneous neural activity at the level of the auditory nerve and the cortex changing tonotopic map organisation to over-represent the deafferented frequency. One of the theories is that this over-representation increases noise at the level of the thalamus (Rauschecker et al., 2010). This noise is theoretically reduced by fronto-striatal connections between the cortico-limbic regions such as the auditory cortex, pregenual anterior cingulate cortex/ventromedial prefrontal cortex (pgACC/vmPFC), prefrontal cortex (PFC) and NAc which is relayed through the thalamus back to the auditory cortex through inhibitory connections (Rauschecker et al., 2015). When this noise cancelling system malfunctions, there is tinnitus, and the more dysfunction the more the tinnitus is perceived (Song et al., 2015). Earlier studies did not take hearing loss into account while investigating neural correlates of tinnitus. Specifically, changes in map plasticity, changes in gray matter or white matter integrity in the auditory regions are now debated to be more of a neural correlate to hearing loss than to tinnitus itself (Boyen et al., 2013; Husain et al., 2011; Vanneste et al., 2015). With cortical thickness, the effects of age seem to be more pronounced than hearing loss and tinnitus (Profant et al., 2020).

This has sparked the interest to study hearing loss as a separate dimension. In patients with tinnitus and hearing loss, the gray matter volume in the lingual gyrus is greater than their peers with hearing loss but no tinnitus (Koops et al., 2020). Based on the amount of hearing loss, the complexity of the neural networks that are engaged in generating tinnitus is increased suggesting a multiphase compensation of hearing loss. Particularly, in patients with no tinnitus, those with hearing loss show increased alpha activity in the pgACC/vmPFC region compared to those with minimal to no hearing loss (Vanneste et al., 2019). Alpha activity is associated with increased lateral inhibition and inhibitory control (Klimesch, 2012). This possibly reflects a healthy top-down inhibitory system that “silences” the noise generated by the deafferentation at the level of the thalamus. In patients with minimal to no hearing loss, those with tinnitus show increased theta activity in the pgACC/vmPFC region compared to those without tinnitus (Vanneste et al., 2019). Theta activity is associated with pathological activity characterising decreased inhibition (Llinás et al., 2001). In tinnitus patients with hearing loss, we observe increased theta activity not only in the pgACC/vmPFC but also in the PHC, indicating a more complex neural signature combining reduced inhibition and possibly pulling out the missing information from the auditory memory (Vanneste et al., 2019). It has been theorized that the PHC plays a central role in memory recollection, retrieving information from the hippocampus, and sending it to associated areas (Tulving and Markowitsch, 1997). Neuroimaging studies using EEG (Lan et al., 2021; Moazami-Goudarzi et al., 2010), PET (Schecklmann et al., 2013) and resting state fMRI (Maudoux et al., 2012a, b) have provided evidence that the PHC is involved in tinnitus. Also, neurophysiological (Schlee et al., 2009b), and neuroimaging (Maudoux et al., 2012a, b) studies have consistently reported a PHC-auditory cortex functional connectivity in tinnitus.

The multiphase compensation mechanism is not simply theoretical. Results from an EEG study report that patients with no or little hearing loss showed increased activity over the auditory cortex while those with

severe hearing loss had increased activity over the PHC (Vanneste and De Ridder, 2016). Also, findings show that there is a stronger correlation between tinnitus loudness and auditory cortex activity in mild hearing loss and a stronger association between loudness and PHC activity in severe hearing loss patients (Vanneste and De Ridder, 2016).

Furthermore, mean and range of hearing loss at the tinnitus frequency is correlated with functional connectivity between the left auditory cortex and the left PHC in the theta and alpha frequency bands (Vanneste and De Ridder, 2016). This finding is in line with research demonstrating that slower theta and alpha oscillations are key for long-range communications and fits with the thalamocortical dysrhythmia (TCD) model that will be discussed in a subsequent section (Llinás et al., 1999; Weisz et al., 2007). In terms of directionality, while communication from the left PHC to the left auditory cortex is mediated by the mean and range of hearing loss, the transmission of information from the left auditory cortex to the left PHC is associated with the tinnitus frequency.

### 3.3. Tinnitus severity (emotional component – distress)

The next major variable in the tinnitus dimensional symptomatology is tinnitus-related distress or simply distress. About 2–3 % of the tinnitus population are severely impaired by their tinnitus. Tinnitus is partly interpreted in a vulnerability-stress framework where emotional exhaustion and low emotional well-being predict the risk of developing tinnitus (Trevis et al., 2018). Other studies show that existing emotional distress predict higher tinnitus-related distress (Hébert et al., 2012), and higher emotional well-being and psychological resilience show lower tinnitus-related distress (Wallhäusser-Franke et al., 2014). Similar to chronic pain (Boecking et al., 2020; Linton, 2000; Moller, 2000), tinnitus is conceptualised as a function of an interaction of pre-existing psychological vulnerability and life stressors including but not limited to tinnitus itself. These pre-existing psychological stressors may be reflected in certain personality traits which are associated with higher perceived tinnitus-related distress (Biehl et al., 2020; Durai and Searchfield, 2016; Strumila et al., 2017). Tinnitus-related distress is also very strongly predicted by general stress, depression and hearing loss as a co-morbidity. Particularly depression is highly correlated with tinnitus-distress subscales such as “emotional stress”, “intrusiveness” and “sleep” (Brüggemann et al., 2016).

From a neural-correlates perspective, depression and tinnitus-related distress (or simply distress) are encoded by slightly different areas. Depression and distress are encoded by similar regions as changes in alpha and beta activity in frontopolar, orbitofrontal cortex (OFC) and sgACC (Joos et al., 2012). However, after controlling for the other variable, depression and distress show a lateralisation where depression is characterised by increased alpha activity in the left frontopolar cortex and OFC and distress in the right frontopolar cortex and OFC (Joos et al., 2012). These are then hypothesised to communicate with the sgACC and parahippocampus which are common to both symptoms. Another study confirmed similarities of the neural underpinnings of depression and distress in tinnitus patients using a principal component analysis (Meyer et al., 2017).

Distress is extremely variable among tinnitus patients and is one of the key sources of heterogeneity. One of the earliest studies to lay the groundwork for the neural correlates of distress show increased alpha and beta activity in the dACC, sgACC, OFC, insula and PHC and decreased alpha activity in the PCC and precuneus in the high distress group compared to the low distress group (Vanneste et al., 2010a). Of these patients, those who were unable to cope with their distress show increased alpha activity in the sgACC, insula and PHC and decreased activity in the precuneus. The core tinnitus distress network consists of the PHC, hippocampus, sgACC, temporal pole, inferior frontal gyrus, ventrolateral prefrontal cortex in the alpha frequency band (Mohan et al., 2020). These results have been replicated by other groups confirming the regions of the tinnitus distress network (Golm et al., 2013;

Ueyama et al., 2013). These regions are also implicated in chronic pain (Moisset and Bouhassira, 2007), somatic distress (Landgrebe et al., 2008) and social rejection distress (Kross et al., 2007). rsfMRI in both tinnitus patients show that compared to healthy controls, patients exhibit increased functional connectivity between the right anterior insula and left inferior frontal gyrus which positively correlates with the activity in the auditory cortex (Burton et al., 2012). A resting state MEG study shows that the strength of the inflow of information from the prefrontal cortices, precuneus and PCC to the temporal cortices is correlated with tinnitus annoyance (Schlee et al., 2009b).

Distress is also hypothesised as a behavioural manifestation of a paradoxical salience or increased attention to the tinnitus sound (Kandepan et al., 2019). This is supported by the increase in activity in the salience network consisting mainly of the dACC and anterior insula. Furthermore, studies show that depending on the amount of distress, there is increased connectivity between the auditory regions and regions of the distress network (Chen et al., 2017). This suggests that patients who are highly distressed may be making an association between the loudness component and the emotional component of tinnitus thereby creating a negative reward network that favours the paradoxical salience and one that can be difficult to modify. We also see this in the role of the PHC. The PHC, as mentioned above, is key in pulling out the missing information from memory using connections in the theta frequency band (Vanneste and De Ridder, 2016). However, we see that in patients with high distress, the stability of connectivity of the PHC in the alpha frequency band becomes more hardwired thereby indicating a less flexible brain network for neuromodulation (Mohan et al., 2018). In high distress, brain networks are paradoxically more efficiently wired and probably more difficult to modify (Yoo et al., 2021).

### 3.4. Tinnitus severity (acoustic component – loudness)

The unified framework of tinnitus is consistent with the expression of a global workspace integrating the deafferentation and noise-cancelling models. The global workspace serves as an interface for the integration of multiple processing modules into a single percept with internally consistent content (Baars, 1993). When applied to the communication between brain regions, it proposes that the emergence of a unified percept such as tinnitus relies on the coordination of scattered mosaics of functionally specialized brain regions into the global workspace (Schlee et al., 2008). Although the mechanisms behind these large-scale integrations are unknown, the most plausible candidate is the formation of dynamic links mediated by the synchrony of multiple frequency bands. There is evidence from invasive human recordings (Canolty et al., 2006), MEG (Weisz et al., 2007) as well as EEG (van der Loo et al., 2009) that cross-frequency coupling through phase-amplitude (nested oscillations) or phase-phase interactions are related to sensory awareness (Monto et al., 2008).

At a more intricate level, it has been advocated that the emergence of a coherent auditory percept requires the synchronization and binding of separate gamma-band activities, present in different thalamocortical columns (Crone et al., 2001; Tiitinen et al., 1993). Research has also shown that sound intensity is reflected by the amount of gamma-band activity (Crone et al., 2001; Tiitinen et al., 1993; van der Loo et al., 2009). As interpreted from a predictive coding perspective, it could be postulated that gamma oscillations reflect the prediction error and could be important in optimizing the extraction of relevant sensory input in time. Indeed, beta activity is associated with auditory predictions and gamma to prediction errors (Arnal and Giraud, 2012; Arnal et al., 2011). When applied to tinnitus, gamma band activity thus, may not relate to the conscious perception of the sound but a prerequisite for the presence of the auditory perception.

Subsequently, it is proposed that tinnitus, as a conscious percept, should be associated with persistent gamma-band activity in the auditory cortex. Research has shown that the amount of gamma activity is positively related to subjective perception of tinnitus and worsening in

tinnitus loudness (Ashton et al., 2007; Mukamel et al., 2005; van der Loo et al., 2009). However, gamma oscillations are confined to small neural spaces and are responsible for encoding tinnitus intensity (Ashton et al., 2007; Mukamel et al., 2005; van der Loo et al., 2009). The nesting of gamma onto theta oscillations allows tinnitus to be experienced or reach consciousness as theta bands are carrier waves that synchronizes with the larger network (aka global workspace) (Agarwal et al., 2014). Indeed, EEG (van der Loo et al., 2009), MEG (Weisz et al., 2007) and intracranial recording (Sedley et al., 2015) demonstrate that tinnitus is related to gamma-band activity that is nested on theta activity in the auditory cortex.

Both the bottom-up deafferentation and the top-down noise-cancelling deficit can be argued to alter the auditory thalamocortical signal transmission, resulting in TCD (Llinás et al., 1999). In the presence of deafferentation, thalamocortical resting state alpha activity slows down to theta, resulting in decreased surrounding inhibition (Weisz et al., 2007). This allows missing auditory information to be retrieved from the neighbouring cortical area or the PHC according to the multiphase compensation mechanism (Vanneste and De Ridder, 2016). Changes in input, because of a deficient top-down inhibitory pathway (Rauschecker et al., 2010), results in a reduction of GABA<sub>A</sub>-mediated lateral inhibition, inducing gamma band activity surrounding the deafferented thalamocortical columns. The increased surrounding gamma activity couples with theta, and in due course, becomes the pathological signature of tinnitus loudness (Sedley et al., 2015; Vanneste et al., 2018b).

### 3.5. Using neuromodulation to target tinnitus loudness and distress

Different researchers have tried to modify tinnitus loudness and distress by targeting its neural correlates using different neuromodulation techniques. Transcranial magnetic stimulation (TMS) is a non-invasive stimulation that delivers bursts of magnetic pulses to a targeted region. Transcranial electrical stimulation is a non-invasive stimulation technique that delivers low amplitude direct, alternating or random noise (between 0.1–640 Hz) current to a targeted region (tDCS/tACS/tRNS). High frequency (5–20 Hz) repetitive TMS (rTMS) and anodal tDCS increase cortical excitability and low frequency (1 Hz) rTMS and cathodal tDCS reduce cortical excitability. Low and high frequency rTMS over the temporoparietal cortex, dorsomedial prefrontal cortex and temporoparietal cortex modifies cortical excitability, resulting in temporary suppression of tinnitus (Chung et al., 2012; Kleijung et al., 2005; Kreuzer et al., 2019; Lee et al., 2013; Mennemeier et al., 2011; Rossi et al., 2007). Anodal tDCS over the left temporoparietal cortex (Garin et al., 2011; Shekhawat et al., 2013), bifrontal (Vanneste and De Ridder, 2011; Vanneste et al., 2010b) and bilateral tDCS over the auditory cortex (Joos et al., 2014) suppresses tinnitus loudness and distress. Adding frontal cortex stimulation before auditory cortex stimulation or combining high-frequency rTMS of the dorsolateral prefrontal cortex with low-frequency of the temporoparietal cortices suppresses tinnitus more effectively by attacking both loudness and distress components (Langguth et al., 2014; Lefaucheur et al., 2014). To increase the depth and specificity of the target and avoid current spread to other regions, researchers apply high definition tDCS with multiple small electrodes. Multiple sessions of high definition tDCS over the left temporoparietal area (Shekhawat et al., 2016) and dorsolateral prefrontal cortex (Shekhawat and Vanneste, 2018) show a lasting effect of tinnitus suppression. Other stimulation techniques such as burst rTMS (De Ridder et al., 2007) and tRNS (Van Doren et al., 2014) of the auditory cortex also suppress tinnitus. While high (100–640 Hz) and low (0.1–100 Hz) frequency tRNS suppress tinnitus loudness, only low frequency tRNS suppress tinnitus distress (Joos et al., 2015).

More invasive procedures such as deep brain stimulation are also used to target the auditory cortex and PHC to suppress tinnitus (De Ridder and Vanneste, 2014; De Ridder et al., 2010). Here responders show increased theta connectivity between the auditory cortex and PHC. Similarly deep brain stimulation of the anterior cingulate shows a



significant suppression of tinnitus distress (De Ridder et al., 2016). Other techniques include bi-modal stimulation which combines electrical stimulation of the vagus nerve (VNS), trigeminal nerve or the greater occipital nerve in combination with sound stimulation (Marks et al., 2018; Tyler et al., 2017). VNS targets the maladaptive map plasticity which is proposed to be the source of tinnitus generation. Combining VNS with stimulation of all sounds except the tinnitus sound is proposed to remap the tonotopic organisation by increasing the activity of all the frequencies except the tinnitus frequency there by rendering the tinnitus frequency “unimportant” (Engineer et al., 2011). In trigeminal and occipital nerve stimulation, authors argue that combining this stimulation with the tinnitus tone, they induce inhibition of the tinnitus tone at the level of the dorsal cochlear nucleus where there is an interaction between somatosensory and auditory pathways (Koehler and Shore, 2013). A recent study shows that trigeminal nerve accessed through tongue stimulation combined with sound stimulation could improve tinnitus distress up to one year (Conlon et al., 2020). In addition to stimulating peripheral nerves, direct stimulation of the ear through hydrotransmissive stimulation of the auditory meatus was also shown to considerably decrease tinnitus perception (Mielczarek and Olszewski, 2014).

Residual inhibition, a technique proposed to reduce cortical excitability by improving lateral inhibition, intermittently suppresses tinnitus following the presentation of a proper masking stimulus (Roberts, 2007). This reduces gamma activity, increases alpha activity over the right temporal cortex (Schoiswohl et al., 2021) and reduces theta-gamma coupling in the PHC and the amount of reduction is correlated with decrease in tinnitus intensity (Sedley et al., 2015). Neurofeedback is a brain re-training therapy that targets the TCD model of tinnitus (Güntensperger et al., 2019, 2017). Participants' brains are trained to produce more alpha activity and lower delta activity by targeting to increase the alpha/delta ratio in the auditory cortex. This is successful in suppressing tinnitus loudness after repeated sessions of neurofeedback training (Güntensperger et al., 2019). This has also been attempted using fMRI by trying to reduce the increased BOLD activity in the auditory cortex (Güntensperger et al., 2017).

### 3.6. Gene polymorphisms in tinnitus

A further domain of this tinnitus framework that is gaining momentum involves the investigation of the enzyme catechol-O-methyltransferase (COMT). The, COMT Val<sup>158</sup>Met polymorphism is linked to inadequate auditory gating through the prefrontal cortex – auditory cortex mechanism (Majic et al., 2011). A recent study reported that the interaction between the severity of hearing loss and the COMT Val<sup>158</sup>Met polymorphism can increase an individual's susceptibility to the clinical manifestation of tinnitus (Vanneste et al., 2018a). Among participants with hearing loss that are Met carriers, the PHC increasingly delivers tinnitus related information (loudness perception) to the pgACC and the auditory cortex (Vanneste et al., 2018a). Concurrently, the gatekeeping mechanism of the pgACC is found to perform at a poorer level, giving rise to an increased perception of tinnitus loudness (Vanneste et al., 2018a).

Another important research avenue is the study of potential associations between brain-derived neurotrophic factor (BDNF) gene polymorphisms and tinnitus (Coskunoglu et al., 2017; Orenay-Boyacioglu et al., 2019). BDNF is important in the regulation of neural plasticity and Val<sup>66</sup>Met polymorphism may have adverse effects on the anatomy and functions of the prefrontal cortex and hippocampus (Bhang et al., 2011). Indeed, in tinnitus patients, results from MRI scans revealed significant gray matter decrease in the right inferior colliculus and left hippocampus (Landgrebe et al., 2009). Recent studies show that the relationship between BDNF polymorphism and tinnitus severity is mediated by distress (Jeong et al., 2021; Vanneste et al., 2021). Specifically patients who are Met carriers of Val<sup>66</sup>Met polymorphism show increased alpha activity in the sgACC, and increased functional connectivity from sgACC

to PHC (Vanneste et al., 2021). Both these neural markers mediate the relationship between BDNF Val<sup>66</sup>Met polymorphism and tinnitus distress.

In addition, among Met-allele carriers, there appears to be decreased functional connectivity between hippocampus and PHC with areas of the default-mode, executive and paralimbic networks at resting state (Thomason et al., 2009), particularly in situations involving behavioral adaptation (Fregni et al., 2006). In a complementary fashion, one could speculate that given the influence of BDNF polymorphism on functional connectivity between large-scale networks, Val<sup>66</sup>Met polymorphism carriers and non-carriers would respond differently to tinnitus treatments.

Although still in its infancy, genetics parameters have the potential of linking tinnitus subtypes to certain brain regions and their functions. These specifications could in the future permit a more thorough understanding of the different dimensions of tinnitus as well as the refinement of tinnitus therapies beyond what current treatment approaches can achieve, paving a path for the advancement of personalized and targeted tinnitus therapies.

## 4. Reconceptualising tinnitus subtypes – moving towards a dimensional network model of tinnitus

From the above literature and the neural markers of tinnitus dimensions summarised in Table 1, it is evident that tinnitus heterogeneity is a much more complex interplay of behavioural, neurophysiological and biological markers. Thus, carrying out tinnitus research in an ununified way, with different researchers independently seeking to identify ‘the mechanism’, ‘the biomarker’, or ‘the psychological factor’ to explain a subtype of tinnitus limits us from embracing this complexity. As in the field of psychiatry (Kapur et al., 2012), there are two main limitations at play when researching tinnitus in a categorical manner. Firstly, a categorical approach assumes that a certain disease or disorder has discrete entities, shared by homogenous subgroups. Indeed, it is a well-known fact that tinnitus is a heterogenous condition with patients presenting a variety of overlapping symptoms (Cederroth et al., 2019). Secondly, compared to other fields such as cardiovascular disease or diabetes, there is a lack of a biological test to diagnose this disorder (Cederroth et al., 2019). This limits a researcher's ability to make a clear segregation between what entails a control or an intervention group. A major consequence of unclear boundaries in diagnosis is a great number of publications suggesting various biomarkers of tinnitus that are not replicable.

Thus, a less reductionist and a more holistic method that acknowledges that the generation and progression of tinnitus, from slight to severe, exists along a continuum and including multiple signatures as factors explaining the occurrence of tinnitus may possibly be a way forward in understanding this complex disorder (Fig. 2). This dimensional approach allows the focus of the degree to which a particular trait of tinnitus in a domain is present (e.g., non-hearing loss to hearing loss). A detailed understanding of the relations and differentiations among the traits would be of great importance, given that a certain trait in a domain (e.g., hearing-loss) may be associated with other traits (e.g., distress). One could argue the possibility of various tinnitus traits belonging to certain domains mutually reinforcing the severity of tinnitus.

Based on previous research there is compelling evidence to hypothesise the presence of overlapping subnetworks in tinnitus that encode different tinnitus symptoms (Fig. 3) providing an explanation for changes in clinical aspects of tinnitus, such as age, duration, loudness, distress, lateralization, or sound characteristics (De Ridder et al., 2014c; Mohan et al., 2017; Schlee et al., 2009b). Moreover, from the literature reviewed above, it is quite clear that the complexity of the network involved in encoding a behavioural phenotype of tinnitus increases with the severity of the symptom. Thus, it is logical to conclude that these subnetworks may represent the various tinnitus dimensions and can be hypothesised to be causally responsible for the presence of tinnitus



**Table 1**  
Summary of neural markers of tinnitus dimensions.

Tinnitus dimension	Neural markers
Age, duration, age of onset	<ul style="list-style-type: none"> <li>- Decreased Wave V amplitude and increase in Wave V latency with increased tinnitus duration showing possible decrease in compensatory firing</li> <li>- Longer tinnitus duration corresponds increased metabolic activity and functional connectivity (FC) between right inferior frontal gyrus (IFG), right ventromedial prefrontal cortex (vmPFC), right posterior cingulate cortex (PCC)</li> <li>- Increasing FC between nucleus accumbens (NAc) – vmPFC and NAc – parahippocampus (PHC) with duration after controlling for age and hearing loss</li> <li>- Increased beta activity in the prefrontal cortex (PFC), dorsal anterior cingulate cortex (dACC), increased gamma activity in orbital frontal cortex (OFC) and decreased delta activity in PCC in late onset compared to early onset</li> <li>- Increased theta FC between subgenual anterior cingulate cortex (sgACC) and insula, increased alpha FC between right secondary auditory cortex and bilateral precuneus.</li> </ul>
Hearing ability	<ul style="list-style-type: none"> <li>- Hearing loss is related to increased spontaneous neural activity and tonotopic map re-organisation to over-represent the missing sensory input</li> <li>- Increased gray matter volume of the lingual gyrus</li> <li>- Increased alpha activity in the vmPFC in patients with hearing loss and no tinnitus; increased theta activity in vmPFC in patients with tinnitus and no hearing loss; increased theta activity in vmPFC and PHC in patients with tinnitus and hearing loss compared to healthy subjects controlled for hearing loss.</li> <li>- Mean range of hearing loss is correlated with theta and alpha FC between left auditory cortex (AC) and left PHC.</li> <li>- FC from left AC to left PHC correlates with tinnitus frequency</li> </ul>
Tinnitus-related distress	<ul style="list-style-type: none"> <li>- Increase in alpha and beta activity in sgACC, insula, dACC, PHC, frontopolar cortex (FPC) and OFC</li> <li>- Decreased alpha activity in PCC and precuneus</li> <li>- Both are related to coping with distress</li> <li>- In patients with high distress there is increased alpha FC between sgACC and AC</li> <li>- In patients with high distress, connection of other brain regions with PHC becomes more chaotic with increasing loudness, and more stable and hardwired with increasing distress</li> </ul>
Tinnitus loudness	<ul style="list-style-type: none"> <li>- Related to aberrant thalamocortical rhythms a.k.a slowing of alpha to theta activity and increasing gamma activity in AC</li> <li>- Long distance integration between regions of global workspace through cross-frequency theta-gamma coupling</li> </ul>
Suppression of tinnitus loudness and distress through neuromodulation	<ul style="list-style-type: none"> <li>- Low frequency repetitive transcranial magnetic stimulation (rTMS) and anodal transcranial direct current stimulation (tDCS) over temporoparietal regions</li> <li>- Bifrontal and bilateral tDCS over AC, independently and in succession</li> <li>- High-definition tDCS over temporoparietal areas and dorsolateral prefrontal cortex</li> <li>- Burst rTMS and transcranial random noise stimulation over AC</li> </ul>

**Table 1 (continued)**

Tinnitus dimension	Neural markers
	<ul style="list-style-type: none"> <li>- Deep brain stimulation of AC and PHC</li> <li>- Bimodal electrical and sound stimulation of vagus nerve, trigeminal nerve and greater occipital nerve</li> <li>- Residual inhibition using tonal auditory stimulation</li> <li>- Neurofeedback therapy to re-train brain oscillations</li> </ul>
Genetic polymorphisms	<ul style="list-style-type: none"> <li>- Catechol-O-methyltransferase Val<sup>158</sup>Met polymorphism – Met carriers show increased FC from PHC to vmPFC and AC – increased loudness</li> <li>- BDNF Val<sup>66</sup>Met polymorphism – Met carriers show increased activity in sgACC and increased FC from sgACC to PHC – relationship between loudness and the polymorphism is mediated by distress, and these markers mediate the relationship between the polymorphism and tinnitus distress.</li> </ul>

symptoms. Diverging and expanding on that framework, the interactions between these domains or subnetworks could be regarded as mereological instead of causal (Jones et al., 2017).

When applying the network approach, the terms ‘nodes’ would represent the different dimensions (sensory, salience, default and control) while ‘edges’ constitute the associations between the nodes (Fig. 4). For instance, the sensory network could be directly associated with the salience network as well as the default mode network, creating an interconnected structure. Consider the example of tinnitus distress; the distress trait (salience network) could be causally related to decreased attention (control network), a symptom of hearing loss (sensory network) or a mediator between hearing loss and attention. A network structure will allow us to visualize the relations among these tinnitus traits, thus a better understanding of the patient’s condition.

Among the nodes, a central trait or ‘centrality’ (e.g., hearing loss) could display a more prominent role among other traits in the node. The identification of a central trait in a network structure of the pathology of tinnitus could be useful for clinicians and researchers to examine typical tendencies that tinnitus patients share. The use of network theory to unravel the nature of tinnitus considers the occurrence of tinnitus as an emergent property (De Ridder et al., 2014b). It advocates that the current way we study tinnitus; independently selecting clinical traits and subsequently endeavour to find an explanatory circumscribed brain mechanism, may not be the best approach. Instead, brain networks of healthy individuals and tinnitus patients should be mapped and compared to identify differences that could lead to certain clinical traits.

Indeed, recently, there has been a discussion of the need to reconstruct the way we study the relationship between brain and cognition. It was argued that cognitive neuroscientists should focus on an ‘inside-out’ approach, in which the research of neurobiology should have priority over psychological concepts (Buzsáki, 2020). According to Buzsáki, we should focus on how the interactions between neurobiological mechanisms give rise to clinical symptoms (Buzsáki, 2020). Although this is an interesting and alluring proposition, as pointed out by Poeppel and Adolfi (Poeppel and Adolfi, 2020), a hierarchical ‘inside-out’ method is at present, a radical idea, given that ‘background’ information (i.e., clinical characteristics, behaviours) is always required for neurobiological exploration. To an extent, explaining neural mechanisms in terms of observational (e.g., behavioural, clinical) data will always be of interest.

## 5. Testing the dimensional network model of tinnitus and clinical implications

Researchers could employ hypothesis-driven, data-driven or

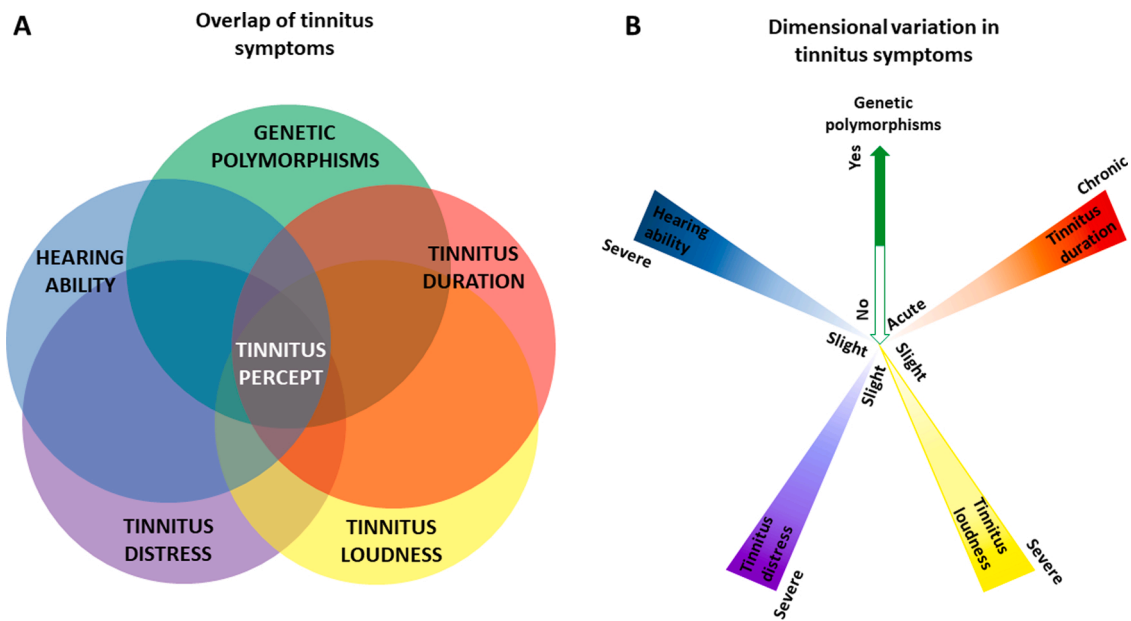


**Fig. 2.** A graphical representation of tinnitus dimensions. (A) Shows the overlapping nature of different tinnitus symptoms to form the complex tinnitus percept. (B) the variations of these symptoms on a continuum thereby forming tinnitus dimensions.

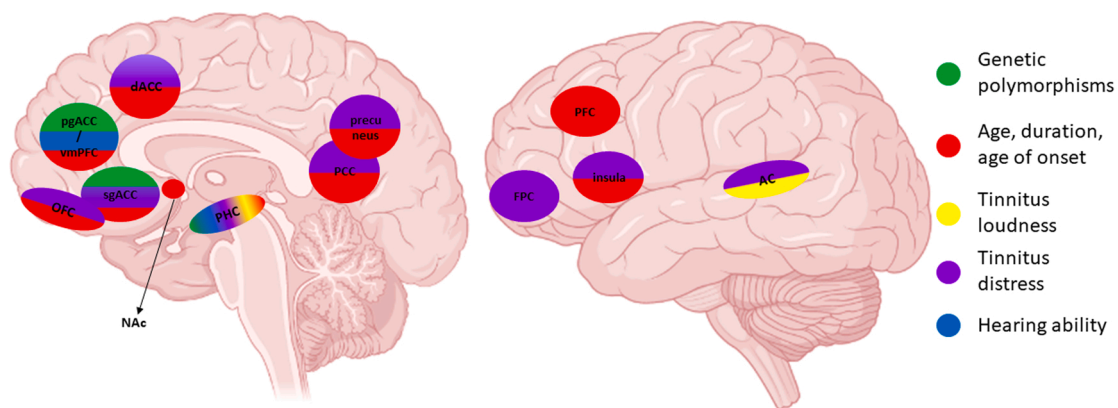


**Fig. 3.** The different regions that form overlapping subnetworks that encode the different tinnitus dimensions.

dACC: dorsal anterior cingulate cortex; pgACC/vmPFC: pregenual anterior cingulate/ventromedial prefrontal cortex; sgACC: subgenual anterior cingulate cortex; OFC: orbital frontal cortex; NAc: nucleus accumbens; PHC: parahippocampus; PCC: posterior cingulate cortex; PFC: prefrontal cortex; FPC: frontopolar cortex; AC: auditory cortex.

treatment response measures to test the dimensional network model of tinnitus. To effectively and rigorously perform this, one needs to unpack each dimension along its continuum while keeping the other factors constant as much as possible. If you take the hearing loss dimension for example, we observe that tinnitus patients with no hearing loss show increased theta activity in the pgACC compared to their peers with no tinnitus, and tinnitus patients with hearing loss show increased theta activity in the pgACC and PHC compared to their peers with tinnitus. From this, we can hypothesise that if tinnitus patients were on a hearing loss continuum where the complexity of the neural network increased with increasing in hearing loss, then targeting regions with neuro-modulation based on the amount of hearing loss must relieve tinnitus symptoms – a.k.a tinnitus patients with no hearing loss would respond better to frontal stimulation and those with hearing loss may respond better to a combination of frontal and temporo-parietal stimulation. This

would be both a hypothesis-driven and treatment response way to empirically confirming the dimensional network model of tinnitus along hearing loss. Similar methods could be applied for other dimensions.

Another way would be to longitudinally follow up patients from an acute stage to a chronic stage and combining different neuroimaging techniques to look at how structural, functional and genetic factors have an impact on tinnitus progression along different dimensions. Here, data-driven approaches could be used to determine how hearing loss, environmental and genetic factors affect one or more dimensions and if there are specific risk factors for each dimension. This can also help predict a tinnitus profile based on a given medical history. Although this is a very ambitious aim given the heterogeneity in the behavioural and neurophysiological phenotypes, with a collaborative effort to meticulously collect longitudinal data at different research sites along with the support of funding agencies promoting Big Data and Open Science, it

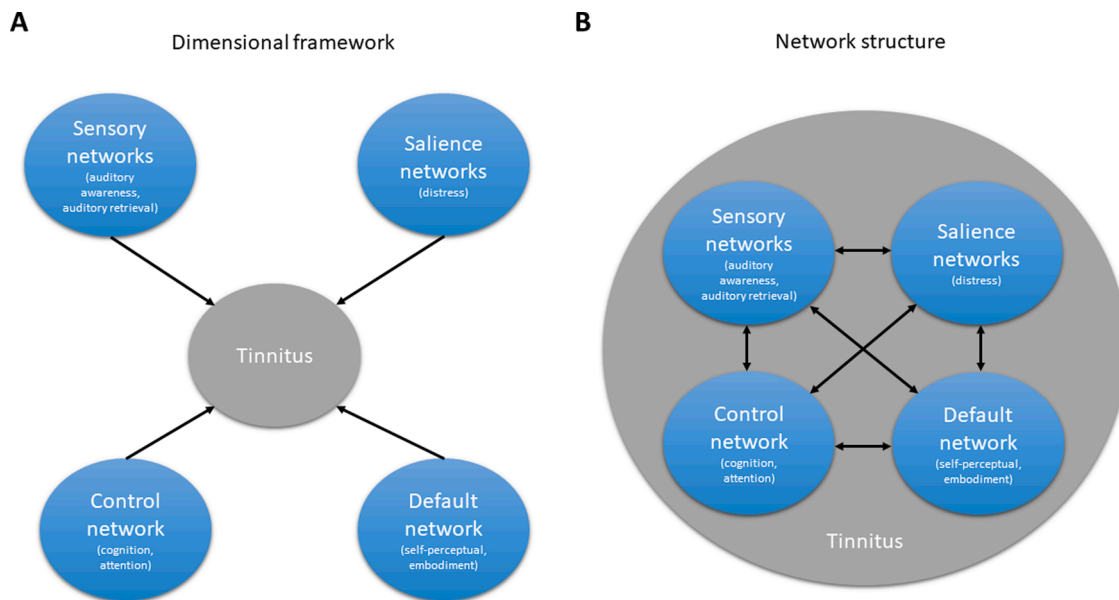


**Fig. 4.** The graphical representation of the RDoC concept for tinnitus. (A) The different neural networks that encode the different tinnitus dimensions. (B) How they can interact with one another to in the complex tinnitus percept showing how tinnitus is a dimensional disorder.

would be an effort worth the benefits.

If results are repeatable, the described model would make it possible for clinicians to establish a patient's risk of developing tinnitus with greater gradation. For example, a patient who has hearing loss and is a COMT Val<sup>158</sup>Met polymorphism carrier would be at greater risk of developing tinnitus than a non-Met carrier with hearing loss. This would allow clinicians to assess the patient in relation to the degree of risk in developing tinnitus instead of categorising based on 'at risk' or 'not at risk'. A dimensional approach therefore increases diagnostic precision and represents the disorder in a more clinically realistic manner.

Another relevant advantage of a dimensional model versus a categorical model is that an integrated framework with multiple domains provides the clinician an upper hand when assessing the problem of comorbidities occurring in conjunction with tinnitus. It is common that patients with tinnitus present not only with a phantom sound perception but a wide range of associated clinical comorbidities (i.e. anxiety, depression), and this has been defined as tinnitus (sound component) and tinnitus disorder (phantom sound + suffering) (De Ridder et al., 2021). Dimensional assessments can allow the evaluation of changes in associated comorbidities that are directly related to tinnitus (e.g. tinnitus loudness may not change but permits the documentation of changes in depression and anxiety).

## 6. Conclusion

In this perspective, we propose that tinnitus should be considered as a dimensional disorder that varies in severity of the symptoms and complexity of neural networks on a continuous spectrum rather than be forced into categorical subtypes. We propose a dimensional network model of overlapping subnetworks whose role depends on the severity of the symptom. We also propose empirical ways of testing the dimensional network model by piecing out each individual dimension by applying hypothesis-driven, data-driven, treatment-response driven or a combination of ways. Thereby we propose to think about tinnitus as a complex matrix of behavioural, biological and neurophysiological phenotypes.

## Data availability

Data will be made available on request.

## Author contributions

**Vanneste S:** Conceptualization, Writing- Reviewing and Editing. **De Ridder D:** Conceptualization, Writing- Reviewing and Editing. **Leong SL:** Writing- Original draft, **Mohan A:** Writing original draft, Reviewing and Editing.

## Funding

Mohan A is funded by the Government of Ireland Postdoctoral Fellowship 2020-2022. Project ID: GOIPD/2020/663.

## Declaration of Competing Interest

The authors report no declarations of interest.

## Acknowledgements

We want to thank Katherine Adcock for her valuable comments in manuscript.

## References

- Agarwal, G., Stevenson, I.H., Berényi, A., Mizuseki, K., Buzsáki, G., Sommer, F.T., 2014. Spatially distributed local fields in the hippocampus encode rat position. *Science* 344, 626–630.
- Al-Swiahb, J., Park, S.N., 2016. Characterization of tinnitus in different age groups: a retrospective review. *Noise Health* 18, 214–219.
- Arnal, L.H., Giraud, A.L., 2012. Cortical oscillations and sensory predictions. *Trends Cogn. Sci.* 16, 390–398.
- Arnal, L.H., Wyart, V., Giraud, A.L., 2011. Transitions in neural oscillations reflect prediction errors generated in audiovisual speech. *Nat. Neurosci.* 14, 797–801.
- Ashton, H., Reid, K., Marsh, R., Johnson, I., Alter, K., Griffiths, T., 2007. High frequency localised "hot spots" in temporal lobes of patients with intractable tinnitus: a quantitative electroencephalographic (QEEG) study. *Neurosci. Lett.* 426, 23–28.
- Baars, B.J., 1993. *A Cognitive Theory of Consciousness*. Cambridge University Press.
- Baguley, D., McFerran, D., Hall, D., 2013. Tinnitus. *Lancet* 382, 1600–1607.
- Bartels, H., Staal, M.J., Albers, F.W., 2007. Tinnitus and neural plasticity of the brain. *Otol. Neurotol.* 28, 178–184.
- Bhang, S., Ahn, J.-H., Choi, S.-W., 2011. Brain-derived neurotrophic factor and serotonin transporter gene-linked promoter region genes alter serum levels of brain-derived neurotrophic factor in humans. *J. Affect. Disord.* 128, 299–304.
- Biehl, R., Boecking, B., Brueggemann, P., Grosse, R., Mazurek, B., 2020. Personality traits, perceived stress, and tinnitus-related distress in patients with chronic tinnitus: support for a vulnerability-stress model. *Front. Psychol.* 10, 3093.

- Boecking, B., von Sass, J., Sieveking, A., Schaefer, C., Brueggemann, P., Rose, M., Mazurek, B., 2020. Tinnitus-related distress and pain perceptions in patients with chronic tinnitus—Do psychological factors constitute a link? *PLoS One* 15, e0234807.
- Boyen, K., Langers, D.R., de Kleine, E., van Dijk, P., 2013. Gray matter in the brain: differences associated with tinnitus and hearing loss. *Hear. Res.* 295, 67–78.
- Brüggemann, P., Szczepek, A.J., Rose, M., McKenna, L., Olze, H., Mazurek, B., 2016. Impact of multiple factors on the degree of tinnitus distress. *Front. Hum. Neurosci.* 10, 341.
- Burton, H., Wineland, A., Bhattacharya, M., Nicklaus, J., Garcia, K.S., Piccirillo, J.F., 2012. Altered networks in bothersome tinnitus: a functional connectivity study. *BMC Neurosci.* 13, 1–15.
- Buzsáki, G., 2020. The brain–cognitive behavior problem: a retrospective. *Eneuro* 7.
- Canolty, R.T., Edwards, E., Dalal, S.S., Soltani, M., Nagarajan, S.S., Kirsch, H.E., Berger, M.S., Barbaro, N.M., Knight, R.T., 2006. High gamma power is phase-locked to theta oscillations in human neocortex. *Science* 313, 1626–1628.
- Cederroth, C.R., Gallus, S., Hall, D.A., Kleijnung, T., Langguth, B., Maruotti, A., Meyer, M., Norena, A., Probst, T., Pryss, R., 2019. Towards an understanding of tinnitus heterogeneity. *Front. Aging Neurosci.* 11, 53.
- Chen, Y.C., Xia, W., Chen, H., Feng, Y., Xu, J.J., Gu, J.P., Salvi, R., Yin, X., 2017. Tinnitus distress is linked to enhanced resting-state functional connectivity from the limbic system to the auditory cortex. *Hum. Brain Mapp.* 38, 2384–2397.
- Chung, H.-K., Tsai, C.-H., Lin, Y.-C., Chen, J.-M., Tsou, Y.-A., Wang, C.-Y., Lin, C.-D., Jeng, F.-C., Chung, J.-G., Tsai, M.-H., 2012. Effectiveness of theta-burst repetitive transcranial magnetic stimulation for treating chronic tinnitus. *Audiol. Neurotol.* 17, 112–120.
- Conlon, B., Langguth, B., Hamilton, C., Hughes, S., Meade, E., Connor, C.O., Schecklmann, M., Hall, D.A., Vanneste, S., Leong, S.L., 2020. Bimodal neuromodulation combining sound and tongue stimulation reduces tinnitus symptoms in a large randomized clinical study. *Sci. Transl. Med.* 12.
- Coskunoglu, A., Orenay-Boyacioglu, S., Deveci, A., Bayam, M., Onur, E., Onan, A., Cam, F.S., 2017. Evidence of associations between brain-derived neurotrophic factor (BDNF) serum levels and gene polymorphisms with tinnitus. *Noise Health* 19, 140.
- Crone, N.E., Boatman, D., Gordon, B., Hao, L., 2001. Induced electrocorticographic gamma activity during auditory perception. *Clin. Neurophysiol.* 112, 565–582.
- Curhan, S.G., Halpin, C., Wang, M., Eavey, R.D., Curhan, G.C., 2021. Tinnitus and 3-year change in audiometric hearing thresholds. *Ear Hear.* 42 (4), 886.
- Cuthbert, B.N., 2014. The RDoC framework: facilitating transition from ICD/DSM to dimensional approaches that integrate neuroscience and psychopathology. *World Psychiatry* 13, 28–35.
- De Ridder, D., Vanneste, S., 2014. Targeting the parahippocampal area by auditory cortex stimulation in tinnitus. *Brain Stimul.* 7, 709–717.
- De Ridder, D., van der Loo, E., Van der Kelen, K., Menovsky, T., van de Heyning, P., Moller, A., 2007. Theta, alpha and beta burst transcranial magnetic stimulation: brain modulation in tinnitus. *Int. J. Med. Sci.* 4, 237.
- De Ridder, D., Vanneste, S., van der Loo, E., Plazier, M., Menovsky, T., van de Heyning, P., 2010. Burst stimulation of the auditory cortex: a new form of neurostimulation for noise-like tinnitus suppression. *J. Neurosurg.* 112, 1289–1294.
- De Ridder, D., Vanneste, S., Congedo, M., 2011. The distressed brain: a group blind source separation analysis on tinnitus. *PLoS One* 6, e24273.
- De Ridder, D., Vanneste, S., Freeman, W., 2014a. The Bayesian brain: phantom percepts resolve sensory uncertainty. *Neurosci. Biobehav. Rev.* 44, 4–15.
- De Ridder, D., Vanneste, S., Weisz, N., Londero, A., Schlee, W., Elgoyhen, A.B., Langguth, B., 2014b. An integrative model of auditory phantom perception: tinnitus as a unified percept of interacting separable subnetworks. *Neurosci. Biobehav. Rev.* 44, 16–32.
- De Ridder, D., Vanneste, S., Weisz, N., Londero, A., Schlee, W., Elgoyhen, A.B., Langguth, B., 2014c. An integrative model of auditory phantom perception: tinnitus as a unified percept of interacting separable subnetworks. *Neurosci. Biobehav. Rev.* 44, 16–32.
- De Ridder, D., Joos, K., Vanneste, S., 2016. Anterior cingulate implants for tinnitus: report of 2 cases. *J. Neurosurg.* 124, 893–901.
- De Ridder, D., Schlee, W., Vanneste, S., Londero, A., Weisz, N., Kleijnung, T., Shekawat, G.S., Elgoyhen, A.B., Song, J.J., Andersson, G., Adhia, D., de Azevedo, A. A., Baguley, D.M., Biesinger, E., Binetti, A.C., Del Bo, L., Cederroth, C.R., Cima, R., Eggermont, J.J., Figueiredo, R., Fuller, T.E., Gallus, S., Gilles, A., Hall, D.A., Van de Heyning, P., Hoare, D.J., Khedr, E.M., Kikidis, D., Kleinstaeuber, M., Kreuzer, P.M., Lai, J.T., Lainez, J.M., Landgrebe, M., Li, L.P., Lim, H.H., Liu, T.C., Lopez-Escamez, J. A., Mazurek, B., Moller, A.R., Neff, P., Pantev, C., Park, S.N., Piccirillo, J.F., Poepl, T.B., Rauschecker, J.P., Salvi, R., Sanchez, T.G., Schecklmann, M., Schiller, A., Searchfield, G.D., Tyler, R., Vielsmeier, V., Vlaeyen, J.W.S., Zhang, J., Zheng, Y., de Nora, M., Langguth, B., 2021. Tinnitus and tinnitus disorder: theoretical and operational definitions (an international multidisciplinary proposal). *Prog. Brain Res.* 260, 1–25.
- Durai, M., Searchfield, G., 2016. Anxiety and depression, personality traits relevant to tinnitus: a scoping review. *Int. J. Audiol.* 55, 605–615.
- Engineer, N.D., Riley, J.R., Seale, J.D., Vrana, W.A., Shetake, J.A., Sudanagunta, S.P., Borland, M.S., Kilgard, M.P., 2011. Reversing pathological neural activity using targeted plasticity. *Nature* 470, 101–104.
- Fregni, F., Boggio, P.S., Nitsche, M.A., Rigonatti, S.P., Pascual-Leone, A., 2006. Cognitive effects of repeated sessions of transcranial direct current stimulation in patients with depression. *Depress. Anxiety* 23, 482–484.
- Garin, P., Gilain, C., Van Damme, J.-P., De Fays, K., Jamart, J., Osseman, M., Vandermereen, Y., 2011. Short- and long-lasting tinnitus relief induced by transcranial direct current stimulation. *J. Neurol.* 258, 1940–1948.
- Genitsaridi, E., Hoare, D.J., Kypraios, T., Hall, D.A., 2020. A review and a framework of variables for defining and characterizing tinnitus subphenotypes. *Brain Sci.* 10, 938.
- Golm, D., Schmidt-Samoa, C., Dechent, P., Kröner-Herwig, B., 2013. Neural correlates of tinnitus related distress: an fMRI-study. *Hear. Res.* 295, 87–99.
- Güntensperger, D., Thüning, C., Meyer, M., Neff, P., Kleijnung, T., 2017. Neurofeedback for tinnitus treatment—review and current concepts. *Front. Aging Neurosci.* 9, 386.
- Güntensperger, D., Thüning, C., Kleijnung, T., Neff, P., Meyer, M., 2019. Investigating the efficacy of an individualized alpha/delta neurofeedback protocol in the treatment of chronic tinnitus. *Neural Plast.* 2019, 3540898.
- Hall, D.A., Haider, H., Szczepek, A.J., Lau, P., Rabau, S., Jones-Diette, J., Londero, A., Edvall, N.K., Cederroth, C.R., Mielczarek, M., 2016. Systematic review of outcome domains and instruments used in clinical trials of tinnitus treatments in adults. *Trials* 17, 270.
- Hébert, S., Canlon, B., Hasson, D., 2012. Emotional exhaustion as a predictor of tinnitus. *Psychother. Psychosom.* 81, 324–326.
- Hullfish, J., Abenes, I., Yoo, H.B., De Ridder, D., Vanneste, S., 2019. Frontostriatal network dysfunction as a domain-general mechanism underlying phantom perception. *Hum. Brain Mapp.* 40, 2241–2251.
- Husain, F.T., Medina, R.E., Davis, C.W., Szymko-Bennett, Y., Simonyan, K., Pajor, N.M., Horwitz, B., 2011. Neuroanatomical changes due to hearing loss and chronic tinnitus: a combined VBM and DTI study. *Brain Res.* 1369, 74–88.
- Jeong, J.-E., Jeon, S., Han, J.S., Cho, E.Y., Hong, K.S., Park, S.N., Kim, J.J., 2021. The mediating effect of psychological distress on the association between BDNF, 5-HTTLPR, and tinnitus severity. *Psychiatry Investig.* 18, 187.
- Jones, P.J., Heeren, A., McNally, R.J., 2017. Commentary: a network theory of mental disorders. *Front. Psychol.* 8, 1305.
- Joo, J.W., Jeong, Y.J., Han, M.S., Chang, Y.-S., Rah, Y.C., Choi, J., 2020. Analysis of auditory brainstem response change, according to tinnitus duration, in patients with tinnitus with normal hearing. *J. Int. Adv. Otol.* 16, 190–196.
- Joos, K., Vanneste, S., De Ridder, D., 2012. Disentangling depression and distress networks in the tinnitus brain. *PLoS One* 7, e40544.
- Joos, K., De Ridder, D., Van de Heyning, P., Vanneste, S., 2014. Polarity specific suppression effects of transcranial direct current stimulation for tinnitus. *Neural Plast.* 2014.
- Joos, K., De Ridder, D., Vanneste, S., 2015. The differential effect of low-versus high-frequency random noise stimulation in the treatment of tinnitus. *Exp. Brain Res.* 233, 1433–1440.
- Kandeeppan, S., Maudoux, A., de Paula, D.R., Zheng, J., Cabay, J., Gómez, F., Chronik, B., Ridder, D., Vanneste, S., Soddu, A., 2019. Tinnitus distress: a paradoxical attention to the sound? *J. Neurol.* 266, 2197–2207.
- Kapur, S., Phillips, A.G., Insel, T.R., 2012. Why has it taken so long for biological psychiatry to develop clinical tests and what to do about it? *Mol. Psychiatry* 17, 1174–1179.
- Kim, H.-J., Lee, H.-J., An, S.-Y., Sim, S., Park, B., Kim, S.W., Lee, J.S., Hong, S.K., Choi, H. G., 2015. Analysis of the prevalence and associated risk factors of tinnitus in adults. *PLoS One* 10.
- Kleijnung, T., Eichhammer, P., Langguth, B., Jacob, P., Marienhagen, J., Hajak, G., Wolf, S.R., Strutz, J., 2005. Long-term effects of repetitive transcranial magnetic stimulation (rTMS) in patients with chronic tinnitus. *Otolaryngol. Head. Neck Surg.* 132, 566–569.
- Klimesch, W., 2012. Alpha-band oscillations, attention, and controlled access to stored information. *Trends Cogn. Sci.* 16, 606–617.
- Knill, D.C., Pouget, A., 2004. The Bayesian brain: the role of uncertainty in neural coding and computation. *Trends Neurosci.* 27, 712–719.
- Koehler, S.D., Shore, S.E., 2013. Stimulus timing-dependent plasticity in dorsal cochlear nucleus is altered in tinnitus. *J. Neurosci.* 33, 19647–19656.
- Koops, E.A., de Kleine, E., van Dijk, P., 2020. Gray matter declines with age and hearing loss, but is partially maintained in tinnitus. *Sci. Rep.* 10, 1–12.
- Kozak, M.J., Cuthbert, B.N., 2016. The NIMH research domain criteria initiative: background, issues, and pragmatics. *Psychophysiology* 53, 286–297.
- Kreuzer, P.M., Downar, J., de Ridder, D., Schwarzbach, J., Schecklmann, M., Langguth, B., 2019. A comprehensive review of dorsomedial prefrontal cortex rTMS utilizing a double cone coil. *Neuromodul.: Technol. Neural Interface* 22, 851–866.
- Kross, E., Egner, T., Ochsner, K., Hirsch, J., Downey, G., 2007. Neural dynamics of rejection sensitivity. *J. Cogn. Neurosci.* 19, 945–956.
- Lan, L., Li, J., Chen, Y., Chen, W., Li, W., Zhao, F., Chen, G., Liu, J., Chen, Y., Li, Y., 2021. Alterations of brain activity and functional connectivity in transition from acute to chronic tinnitus. *Hum. Brain Mapp.* 42, 485–494.
- Landgrebe, M., Barta, W., Rosengarth, K., Frick, U., Hauser, S., Langguth, B., Rutschmann, R., Greenlee, M.W., Hajak, G., Eichhammer, P., 2008. Neuronal correlates of symptom formation in functional somatic syndromes: a fMRI study. *NeuroImage* 41, 1336–1344.
- Landgrebe, M., Langguth, B., Rosengarth, K., Braun, S., Koch, A., Kleijnung, T., May, A., De Ridder, D., Hajak, G., 2009. Structural brain changes in tinnitus: grey matter decrease in auditory and non-auditory brain areas. *NeuroImage* 46, 213–218.
- Langers, D.R., de Kleine, E., van Dijk, P., 2012. Tinnitus does not require macroscopic tonotopic map reorganization. *Front. Syst. Neurosci.* 6, 2.
- Langguth, B., Kreuzer, P.M., Kleijnung, T., De Ridder, D., 2013. Tinnitus: causes and clinical management. *Lancet Neurol.* 12, 920–930.
- Langguth, B., Landgrebe, M., Frank, E., Schecklmann, M., Sand, P., Vielsmeier, V., Hajak, G., Kleijnung, T., 2014. Efficacy of different protocols of transcranial magnetic stimulation for the treatment of tinnitus: pooled analysis of two randomized controlled studies. *World J. Biol. Psychiatry* 15, 276–285.
- Lee, H.Y., Yoo, S.D., Ryu, E.W., Byun, J.Y., Yeo, S.G., Park, M.S., 2013. Short term effects of repetitive transcranial magnetic stimulation in patients with catastrophic intractable tinnitus: preliminary report. *Clin. Exp. Otorhinolaryngol.* 6, 63.
- Lefaucheur, J.-P., André-Obadia, N., Antal, A., Ayache, S.S., Baeken, C., Benninger, D.H., Cantello, R.M., Cincotta, M., de Carvalho, M., De Ridder, D., 2014. Evidence-based



- guidelines on the therapeutic use of repetitive transcranial magnetic stimulation (rTMS). *Clin. Neurophysiol.* 125, 2150–2206.
- Linton, S.J., 2000. A review of psychological risk factors in back and neck pain. *Spine* 25, 1148–1156.
- Llinás, R.R., Ribary, U., Jeanmonod, D., Kronberg, E., Mitra, P.P., 1999. Thalamocortical dysrhythmia: a neurological and neuropsychiatric syndrome characterized by magnetoencephalography. *Proc. Natl. Acad. Sci.* 96, 15222.
- Llinás, R., Ribary, U., Jeanmonod, D., Cancro, R., Kronberg, E., Schulman, J., Zonenshayn, M., Magnin, M., Morel, A., Siegmund, M., 2001. Thalamocortical dysrhythmia I: functional and imaging aspects. *Thalamus Relat. Syst.* 1, 237–244.
- Majic, T., Rentzsch, J., Gudowski, Y., Ehrlich, S., Juckel, G., Sander, T., Lang, U.E., Winterer, G., Gallinat, J., 2011. COMT Val108/158Met genotype modulates human sensory gating. *NeuroImage* 55, 818–824.
- Marks, K.L., Martel, D.T., Wu, C., Basura, G.J., Roberts, L.E., Schwartz-Leyzac, K.C., Shore, S.E., 2018. Auditory-somatosensory bimodal stimulation desynchronizes brain circuitry to reduce tinnitus in guinea pigs and humans. *Sci. Transl. Med.* 10, Maudoux, A., Lefebvre, P., Cabay, J.-E., Demertzi, A., Vanhaudenhuyse, A., Laureys, S., Sodu, A., 2012a. Auditory resting-state network connectivity in tinnitus: a functional MRI study. *PLoS One* 7, e36222.
- Maudoux, A., Lefebvre, P., Cabay, J.-E., Demertzi, A., Vanhaudenhuyse, A., Laureys, S., Sodu, A., 2012b. Connectivity graph analysis of the auditory resting state network in tinnitus. *Brain Res.* 1485, 10–21.
- McCormack, A., Edmondson-Jones, M., Somerset, S., Hall, D., 2016. A systematic review of the reporting of tinnitus prevalence and severity. *Hear. Res.* 337, 70–79.
- Mennemeier, M., Chelette, K.C., Allen, S., Bartel, T.B., Triggs, W., Kimbrell, T., Crew, J., Munn, T., Brown, G.J., Dornhoffer, J., 2011. Variable changes in PET activity before and after rTMS treatment for tinnitus. *Laryngoscope* 121, 815–822.
- Meyer, M., Neff, P., Grest, A., Hemsley, C., Weidt, S., Kleinjung, T., 2017. EEG oscillatory power dissociates between distress-and depression-related psychopathology in subjective tinnitus. *Brain Res.* 1663, 194–204.
- Mielczarek, M., Olszewski, J., 2014. Direct current stimulation of the ear in tinnitus treatment: a double-blind placebo-controlled study. *Eur. Arch. Oto-Rhino-Laryngol.* 271, 1815–1822.
- Moazami-Goudarzi, M., Michels, L., Weisz, N., Jeanmonod, D., 2010. Temporo-insular enhancement of EEG low and high frequencies in patients with chronic tinnitus. *QEEG study of chronic tinnitus patients.* *BMC Neurosci.* 11, 1–12.
- Mohan, A., Vanneste, S., 2017. Adaptive and maladaptive neural compensatory consequences of sensory deprivation—from a phantom percept perspective. *Prog. Neurobiol.* 153, 1–17.
- Mohan, A., Moreno, N., Song, J.-J., De Ridder, D., Vanneste, S., 2017. Evidence for behaviorally segregated, spatiotemporally overlapping subnetworks in phantom sound perception. *Brain Connect.* 7, 197–210.
- Mohan, A., De Ridder, D., Idiculla, R., DSouza, C., Vanneste, S., 2018. Distress-dependent temporal variability of regions encoding domain-specific and domain-general behavioral manifestations of phantom percepts. *Eur. J. Neurosci.* 48, 1743–1764.
- Mohan, A., Davidson, C., De Ridder, D., Vanneste, S., 2020. Effective connectivity analysis of inter- and intramodular hubs in phantom sound perception—identifying the core distress network. *Brain Imaging Behav.* 14, 289–307.
- Moisset, X., Bouhassira, D., 2007. Brain imaging of neuropathic pain. *NeuroImage* 37, S80–S88.
- Moller, A.R., 2000. Similarities between severe. *J. Am. Acad. Audiol.* 11, 115–124.
- Monto, S., Palva, S., Voipio, J., Palva, J.M., 2008. Very slow EEG fluctuations predict the dynamics of stimulus detection and oscillation amplitudes in humans. *J. Neurosci.* 28, 8268–8272.
- Muhlneckel, W., Elbert, T., Taub, E., Flor, H., 1998. Reorganization of auditory cortex in tinnitus. *Proc. Natl. Acad. Sci. U. S. A.* 95, 10340–10343.
- Mukamel, R., Gelbard, H., Arieli, A., Hasson, U., Fried, I., Malach, R., 2005. Coupling between neuronal firing, field potentials, and fMRI in human auditory cortex. *Science* 309, 951–954.
- Nondahl, D.M., Cruickshanks, K.J., Huang, G.-H., Klein, B.E., Klein, R., Tweed, T.S., Zhan, W., 2012. Generational differences in the reporting of tinnitus. *Ear Hear.* 33, 640.
- Orenay-Boyacioglu, S., Caliskan, M., Boyacioglu, O., Coskunoglu, A., Bozkurt, G., Cam, F. S., 2019. Chronic tinnitus and BDNF/GDNF CpG promoter methylations: a case-control study. *Mol. Biol. Rep.* 46, 3929–3936.
- Peyron, R., Laurent, B., Garcia-Larrea, L., 2000. Functional imaging of brain responses to pain. A review and meta-analysis (2000). *Neurophysiol. Clin. Neurophysiol.* 30, 263–288.
- Poeppel, D., Adolfs, F., 2020. Against the epistemological primacy of the hardware: the brain from inside out, turned upside down. *Eneuro* 7.
- Profant, O., Škoch, A., Tintera, J., Svobodová, V., Kuchárová, D., Burianová, J.S., Syka, J., 2020. The influence of aging, hearing, and tinnitus on the morphology of cortical gray matter, Amygdala, and Hippocampus. *Front. Aging Neurosci.* 12.
- Rajan, R., 1998. Receptor organ damage causes loss of cortical surround inhibition without topographic map plasticity. *Nat. Neurosci.* 1, 138–143.
- Rauschecker, J.P., Leaver, A.M., Mühlau, M., 2010. Tuning out the noise: limbic-auditory interactions in tinnitus. *Neuron* 66, 819–826.
- Rauschecker, J.P., May, E.S., Maudoux, A., Ploner, M., 2015. Frontostriatal gating of tinnitus and chronic pain. *Trends Cogn. Sci.* 19, 567–578.
- Roberts, L.E., 2007. Residual inhibition. *Prog. Brain Res.* 166, 487–495.
- Rossi, S., De Capua, A., Ulivelli, M., Bartalini, S., Falzarano, V., Filippone, G., Passero, S., 2007. Effects of repetitive transcranial magnetic stimulation on chronic tinnitus: a randomised, crossover, double blind, placebo controlled study. *J. Neurol. Neurosurg. Psychiatr.* 78, 857–863.
- Santacruz, J.L., de Kleine, E., van Dijk, P., 2021. Investigating the Relation between Minimum Masking Levels and Hearing Thresholds for Tinnitus Subtyping.
- Scheckmann, M., Landgrebe, M., Poepl, T.B., Kreuzer, P., Männer, P., Marienhagen, J., Wack, D.S., Kleinjung, T., Hajak, G., Langguth, B., 2013. Neural correlates of tinnitus duration and distress: a positron emission tomography study. *Hum. Brain Mapp.* 34, 233–240.
- Schlee, W., Weisz, N., Bertrand, O., Hartmann, T., Elbert, T., 2008. Using auditory steady state responses to outline the functional connectivity in the tinnitus brain. *PLoS One* 3, e3720.
- Schlee, W., Hartmann, T., Langguth, B., Weisz, N., 2009a. Abnormal resting-state cortical coupling in chronic tinnitus. *BMC Neurosci.* 10, 1–11.
- Schlee, W., Mueller, N., Hartmann, T., Keil, J., Lorenz, I., Weisz, N., 2009b. Mapping cortical hubs in tinnitus. *BMC Biol.* 7, 1–14.
- Schlee, W., Kleinjung, T., Hiller, W., Goebel, G., Kolassa, I.-T., Langguth, B., 2011. Does tinnitus distress depend on age of onset? *PLoS One* 6, e27379.
- Schoiswohl, S., Scheckmann, M., Langguth, B., Schlee, W., Neff, P., 2021. Neurophysiological correlates of residual inhibition in tinnitus: hints for trait-like EEG power spectra. *Clin. Neurophysiol.* 132, 1694–1707.
- Sedley, W., Gander, P.E., Kumar, S., Oya, H., Kovach, C.K., Nourski, K.V., Kawasaki, H., Howard III, M.A., Griffiths, T.D., 2015. Intracranial mapping of a cortical tinnitus system using residual inhibition. *Curr. Biol.* 25, 1208–1214.
- Seydel, C., Haupt, H., Olze, H., Szczeppek, A.J., Mazurek, B., 2013. Gender and chronic tinnitus: differences in tinnitus-related distress depend on age and duration of tinnitus. *Ear Hear.* 34, 661–672.
- Shargorodsky, J., Curhan, G.C., Farwell, W.R., 2010. Prevalence and characteristics of tinnitus among US adults. *Am. J. Med.* 123, 711–718.
- Shekawat, G.S., Vanneste, S., 2018. Optimization of transcranial direct current stimulation of dorsolateral prefrontal cortex for tinnitus: a non-linear dose-response effect. *Sci. Rep.* 8, 1–8.
- Shekawat, G.S., Stinear, C.M., Searchfield, G.D., 2013. Transcranial direct current stimulation intensity and duration effects on tinnitus suppression. *Neurorehabil. Neural Repair* 27, 164–172.
- Shekawat, G.S., Sundram, F., Bikson, M., Truong, D., De Ridder, D., Stinear, C.M., Welch, D., Searchfield, G.D., 2016. Intensity, duration, and location of high-definition transcranial direct current stimulation for tinnitus relief. *Neurorehabil. Neural Repair* 30, 349–359.
- Song, J.-J., De Ridder, D., Schlee, W., Van de Heyning, P., Vanneste, S., 2013. “Distressed aging”: the differences in brain activity between early- and late-onset tinnitus. *Neurobiol. Aging* 34, 1853–1863.
- Song, J.J., Vanneste, S., De Ridder, D., 2015. Dysfunctional noise cancelling of the rostral anterior cingulate cortex in tinnitus patients. *PLoS One* 10, e0123538.
- Strumila, R., Lengvenytė, A., Vainutienė, V., Lesinskas, E., 2017. The role of questioning environment, personality traits, depressive and anxiety symptoms in tinnitus severity perception. *Psychiatr. Q.* 88, 865–877.
- Thomason, M.E., Yoo, D.J., Glover, G.H., Gotlib, I.H., 2009. BDNF genotype modulates resting functional connectivity in children. *Front. Hum. Neurosci.* 3, 55.
- Tiitinen, H., Sinkkonen, J., Reinikainen, K., Alho, K., Lavikainen, J., Näätänen, R., 1993. Selective attention enhances the auditory 40-Hz transient response in humans. *Nature* 364, 59–60.
- Trevis, K.J., McLachlan, N.M., Wilson, S.J., 2018. A systematic review and meta-analysis of psychological functioning in chronic tinnitus. *Clin. Psychol. Rev.* 60, 62–86.
- Tulving, E., Markowitsch, H.J., 1997. Memory beyond the hippocampus. *Curr. Opin. Neurobiol.* 7, 209–216.
- Tyler, R., Cacace, A., Stocking, C., Tarver, B., Engineer, N., Martin, J., Deshpande, A., Stecker, N., Pereira, M., Kilgard, M., 2017. Vagus nerve stimulation paired with tones for the treatment of tinnitus: a prospective randomized double-blind controlled pilot study in humans. *Sci. Rep.* 7, 1–11.
- Ueyama, T., Donishi, T., Ukai, S., Ikeda, Y., Hotomi, M., Yamanaka, N., Shinosaki, K., Terada, M., Kaneoke, Y., 2013. Brain regions responsible for tinnitus distress and loudness: a resting-state fMRI study. *PLoS One* 8, e67778.
- van den Berge, M.J., Free, R.H., Arnold, R., de Kleine, E., Hofman, R., van Dijk, J.M.C., van Dijk, P., 2017. Cluster analysis to identify possible subgroups in tinnitus patients. *Front. Neurol.* 8, 115.
- van der Loo, E., Gais, S., Congedo, M., Vanneste, S., Plazier, M., Menovsky, T., Van de Heyning, P., De Ridder, D., 2009. Tinnitus intensity dependent gamma oscillations of the contralateral auditory cortex. *PLoS One* 4, e7396: 7391–7395.
- Van Doren, J., Langguth, B., Scheckmann, M., 2014. Electroencephalographic effects of transcranial random noise stimulation in the auditory cortex. *Brain Stimul.* 7, 807–812.
- Vanneste, S., De Ridder, D., 2011. Bifrontal transcranial direct current stimulation modulates tinnitus intensity and tinnitus-distress-related brain activity. *Eur. J. Neurosci.* 34, 605–614.
- Vanneste, S., De Ridder, D., 2016. Deafferentation-based pathophysiological differences in phantom sound: tinnitus with and without hearing loss. *NeuroImage* 129, 80–94.
- Vanneste, S., Plazier, M., der Loo, E., de Heyning, P.V., Congedo, M., De Ridder, D., 2010a. The neural correlates of tinnitus-related distress. *Neuroimage* 52, 470–480.
- Vanneste, S., Plazier, M., Ost, J., van der Loo, E., Van de Heyning, P., De Ridder, D., 2010b. Bilateral dorsolateral prefrontal cortex modulation for tinnitus by transcranial direct current stimulation: a preliminary clinical study. *Exp. Brain Res.* 202, 779–785.
- Vanneste, S., Van De Heyning, P., De Ridder, D., 2015. Tinnitus: a large VBM-EEG correlational study. *PLoS One* 10, e0115122.
- Vanneste, S., Alsaman, O., De Ridder, D., 2018a. COMT and the neurogenetic architecture of hearing loss induced tinnitus. *Hear. Res.* 365, 1–15.
- Vanneste, S., Song, J.-J., De Ridder, D., 2018b. Thalamocortical dysrhythmia detected by machine learning. *Nat. Commun.* 9, 1103–1103.
- Vanneste, S., Alsaman, O., De Ridder, D., 2019. Top-down and bottom-up regulated auditory phantom perception. *J. Neurosci.* 39, 364.

- Vanneste, S., Mohan, A., De Ridder, D., To, W.T., 2021. The BDNF Val 66 Met polymorphism regulates vulnerability to chronic stress and phantom perception. *Prog. Brain Res.* 260, 301–326.
- Vermetten, E., Schmahl, C., Southwick, S.M., Bremner, J.D., 2007. A positron tomographic emission study of olfactory induced emotional recall in veterans with and without combat-related posttraumatic stress disorder. *Psychopharmacol. Bull.* 40, 8.
- Vielsmeier, V., Santiago Stiel, R., Kwok, P., Langguth, B., Schecklmann, M., 2020. From acute to chronic tinnitus: pilot data on predictors and progression. *Front. Neurol.* 11, 1–6.
- Wallhäuser-Franke, E., Delb, W., Balkenhol, T., Hiller, W., Hörmann, K., 2014. Tinnitus-related distress and the personality characteristic resilience. *Neural Plast.* 2014.
- Weisz, N., Müller, S., Schlee, W., Dohrmann, K., Hartmann, T., Elbert, T., 2007. The neural code of auditory phantom perception. *J. Neurosci.* 27, 1479–1484.
- Yee, C.M., Javitt, D.C., Miller, G.A., 2015. Replacing DSM categorical analyses with dimensional analyses in psychiatry research: the research domain criteria initiative. *JAMA Psychiatry* 72, 1159–1160.
- Yoo, H.B., Mohan, A., De Ridder, D., Vanneste, S., 2021. Paradoxical relationship between distress and functional network topology in phantom sound perception. *Prog. Brain Res.* 260, 367–395.
- Zenner, H.-P., 1998. Generator. *Mechanisms. Int. Tinnitus J.* 4.

# Phantom perception as a Bayesian Inference problem

<sup>+</sup>Anusha Yasoda-Mohan<sup>1</sup>, <sup>+</sup>Feifan Chen<sup>2</sup>, Colum Ó Sé<sup>2</sup>, Remy Allard<sup>3</sup>, Jan Ost<sup>4</sup>, & Sven Vanneste<sup>1,2,4\*</sup>

1. Global Brain Health Institute, Trinity College Dublin, Ireland.
2. Lab for Clinical and Integrative Neuroscience, Trinity College Institute for Neuroscience, School of Psychology, Trinity College Dublin, Ireland
3. School of Optometry, University of Montreal, Montreal, Canada
4. Brain Research Center for Advanced, International, Innovative and Interdisciplinary Neuromodulation, Ghent, Belgium.

## Author Contributions

A.Y.M.: Experimental design, data collection, data analysis and writing manuscript

F.C: Data collection, data analysis

C.O.S: Data analysis, making figures, writing manuscript

R.A.: Stimulus preparation, experimental design, review manuscript

J.O.: Data collection

S.V.: Ideation, supervision, writing manuscript

<sup>+</sup> both authors contributed equally

**\*Correspondence to:** Sven Vanneste, Lab for Clinical and Integrative Neuroscience, Institute for Neuroscience, School of Psychology, Trinity College Dublin, College Green, Dublin 2, Ireland. Email: [sven.vanneste@tcd.ie](mailto:sven.vanneste@tcd.ie). Website: [www.lab-clint.org](http://www.lab-clint.org).

## 24    **Abstract**

25            Our brains constantly make decisions on how to make sense of the uncertain sensory  
26 information it receives from the environment. One way this information is processed is  
27 through the Bayesian Perceptual Inference model. Per the model, we In the current study, we  
28 empirically test this hypothesis. First we train the brain to associate a cue with an uncertain  
29 target signal. In the test phase, we present only the cue to see if the person perceives an  
30 illusion of the signal. We observe that in both the clinical and non-clinical populations, the  
31 perception of a phantom is more likely in a group that perceives the cue and signal to come  
32 from the same source. This is seen with an increase in the event related potential to the  
33 training and testing stimuli and increase in alpha desynchronisation and phase locking with  
34 for the phantom perception. Furthermore, the clinical group with a chronic phantom auditory  
35 percept also exhibited increased reliability on the visual information when the auditory  
36 information was reliable. This study shows that (i) the ability to make strong associations  
37 from the environment may be a predisposing factor to chronic phantom perception and (ii)  
38 chronic phantom perception in one sensory domain possibly increases the reliability on  
39 another sensory domain that is more peripherally intact.

40    **Keywords:** tinnitus, predictive coding, strong priors, multisensory integration, audio-visual  
41 perception

42    **New and noteworthy:** Tinnitus, the continuous perception of a ringing in the ears. The  
43 reasons for why some people develop tinnitus without a hearing deficiency or why not all  
44 people with hearing deficiency don't develop tinnitus is not well understood, therefore  
45 leaving the disorder without a cure until today. The current study empirically explains how  
46 phantom perceptions are generated as a result of a maladaptive inference of the brain to  
47 uncertain            sensory            environments,            particularly            in            tinnitus.



## 48    **Introduction**

49        We live in a world with a variety of sensory information. To make sense of this rich  
50    sensory experience, the brain makes perceptual judgements and inferences that best explain  
51    the incoming sensory input based on its previous knowledge of the environment<sup>1</sup>. This  
52    process is called perceptual inference. One of the most influential models that forms the basis  
53    of perceptual decision making is the Bayesian predictive coding model where the brain  
54    maintains a generative representation of the environment with which it compares the sensory  
55    input<sup>2,3</sup>. When the incoming information changes, the brain assigns probabilistic weights to  
56    its input and predictions (prior) of the input based on the generative representation and  
57    calculates/updates its model (posterior/percept) of the world to what best makes sense of the  
58    uncertainty in its environment – thereby making a perceptual inference.

59        The aim of the current study is to empirically investigate the Bayesian Perceptual  
60    Inference (BPI) model by inducing phantom perceptions (i) in a group of healthy young  
61    adults who have no pre-existing conditions, to investigate the neural correlates of BPI and (ii)  
62    in a group of people with tinnitus (continuous ringing in the ear) to understand how the brain  
63    makes a perceptual inference in the presence of an pre-existing phantom percept.

64        Tinnitus, the perception of a continuous phantom sound in the absence of an external  
65    input<sup>4</sup>, may be hypothesised to be a maladaptive Bayesian Perceptual Inference (BPI) to  
66    changing auditory uncertainty<sup>5-7</sup>. The theory states that there may exist a tinnitus precursor  
67    whose precision increases in the presence of auditory anomalies<sup>8,9</sup>. The healthy brain  
68    accounts for this change by either reducing the precision of the input through top-down  
69    inhibitory connections or adjusting the prediction of the existing model to adapt to the  
70    changing auditory uncertainty to ultimately maintain the existing percept of “silence” in the  
71    absence of an external stimulus<sup>8,9</sup>. However, in tinnitus, the brain instead seems to be

72 changing its model of the world altogether by making a perceptual inference/decision to  
73 perceive a sound in the absence of an external stimulus as its own way of making sense of the  
74 uncertainty in the environment<sup>10</sup>.

75 To induce a phantom perception, we adapted a paradigm from a previously published  
76 study<sup>11</sup>. This paradigm consisted of training phase where participants learnt to associate a  
77 visual cue with an auditory target signal presented at different perceptual thresholds.  
78 According to the BPI model for multisensory perception, participants may make two types of  
79 perceptual judgements<sup>12,13</sup> – (i) that the two signals are coming from the same source, (ii) that  
80 the two signals are coming from independent sources. Therefore, when just the cue is  
81 presented and no target signal, participants making a same source judgement may be more  
82 likely to perceive an auditory phantom perception, since they tend to fuse the two signals into  
83 a single percept. However, participants making an independent source judgement may be less  
84 likely to perceive a phantom perception, since they tend to separate the sources of the two  
85 signals.

86 Past research indicates the neurophysiological and oscillatory signatures of the BPI model  
87 of multisensory perception through different studies. A recent study showed that the process  
88 of building evidence for making a BPI to a multisensory scene involves three stages<sup>14</sup> – (i)  
89 segregation of the auditory and visual information at the level of the sensory cortices (0 – 200  
90 ms post stimulus presentation), (ii) fusion of the auditory and visual signals into a single  
91 percept depending on the reliability of the signals encoded in the posterior parietal and  
92 temporal-parietal regions (200 – 400 ms post stimulus presentation) and (iii) causal inference  
93 of the source of the sensory uncertainties to produce a percept. From a neural oscillatory  
94 perspective, the precision of the predictions is encoded in alpha oscillations<sup>15,16</sup>. Several  
95 studies show changes in resting state alpha in tinnitus specifically showing increased

96 activity<sup>17</sup> and reduced variability<sup>18,19</sup>. However, there is no study, as far as we know that  
97 directly investigates the relevance of these neural oscillations from a BPI standpoint.

98 In healthy young adults, we hypothesise that those making single source judgements will  
99 have greater percentage of false alarms than those making independent source judgements.  
100 These participants will also show a stronger signal to integrating the visual and auditory  
101 information as one percept compared to those making independent source judgements. In  
102 tinnitus, we hypothesise that since there is an already existing chronic phantom percept in the  
103 auditory domain, there might be an interference in the formation of a new auditory phantom  
104 percept. For this reason, we additionally test the formation of a phantom percept in the visual  
105 domain by training patients to associate an auditory cue with an uncertain visual target, and  
106 testing for a visual illusion in the presence of just the auditory cue.

107 From the literature in the psychiatric domain, researchers postulate that the reason the  
108 brain perceives phantom percepts is because it makes very precise predictions of the  
109 environment based on its model and therefore instead of adjusting its predictions to adapt to  
110 environmental uncertainties, it ends up changing its perception of the environment  
111 altogether<sup>11,20</sup>. Therefore, if tinnitus were indeed a Bayesian Inference problem where  
112 patients make stronger predictions of a sensory environment, we would observe that tinnitus  
113 patients will have more false alarms to stimulus-absent trials compared to those with no  
114 tinnitus. Even in participants who make an independent source judgement about visual and  
115 auditory cues, we hypothesise to see changes in neural signatures of segregation, integration  
116 and causal inference in patients compared to controls indicating this strong-prior hypothesis  
117 in tinnitus. Furthermore, we expect this to be reflected in changes in the power and phase-  
118 locking of alpha oscillations while (i) learning the new sensory environment and (ii) while  
119 making a perceptual inference of the new sensory environment when the information in one  
120 of the domains become unavailable.

121

## 122 **Materials and Methods**

123 To test this hypothesis, the current study adapted a paradigm published by Powers and  
124 colleagues<sup>21</sup> to induce a conditioned illusion by simultaneously presenting an auditory and  
125 visual signal. Here, the original paradigm was modified to collect evoked response potentials  
126 (ERPs) using EEG and was implemented to induce illusions in the auditory and visual  
127 domains.

128

### 129 *Ethical statement*

130 This was a multi-site study. Part 1 of the study with healthy young adults took place at  
131 Trinity College Dublin. It was approved by the School of Psychology Research Ethics  
132 Committee and complied with the EU General Data Protection Regulation 2016 (GDPR).  
133 Participants were recruited from Trinity College Dublin's psychology students using the  
134 SONA system, in which participants are granted credits for participation. Other participants  
135 volunteered independently of the SONA system.

136 Part 2 of the study with tinnitus participants took place at The Brain Research Centre for  
137 Advanced Innovative & Interdisciplinary Neuromodulation (Brai3n) clinic in Ghent,  
138 Belgium. The patients were recruited from those who attended the clinic for treatment.  
139 Control participants were volunteers from the clinic and the community.

140

### 141 *Data and code availability statement*

142 The data and code are available with the corresponding author. They will be shared on  
143 email request. The anonymised data after removing the identifying personal information will  
144 be provided.



## Participants

### 1. Part 1 with healthy young adults:

There were 44 participants recruited in this part of the study. Data from 39 participants was included in the analysis. Participants were screened for chronic ear disorders such as Meniere's disease, ear infections and otosclerosis, in addition to neurological disorders such as tumours, mental disorders, and chronic headache. All participants underwent a pure tone hearing test with tones being produced bilaterally at thresholds of 500, 1000, 2000, 3000, 4000, 6000 and 8000Hz. Participants with hearing thresholds below 30 dB at any given frequency were excluded from participation.

Participants also completed a series of questionnaires for mood (Beck's Depression Index, Beck's Anxiety Index), and predisposition to auditory hallucinations (Launay-Hallucination Scale; PHVAS). As per these criteria, two participants were unable to participate due to mild to moderate hearing loss ( $n=1$ ), or mild depression as reflected by a BDI score ( $n=1$ ). From the remaining 42 participants, three participants failed to correctly perform the experiments (sleeping, repeat the same response throughout the task). This left us with data from 39 participants to analyse.

These 39 participants were split into those who were more likely (same-source perceivers) ( $M = 21.2$  years,  $SD = 3.3$  years; 8 males, 12 females) and less likely (independent source perceivers) ( $M = 21.3$  years,  $SD = 3.5$ ; 5 males, 14 females) to perceive an illusion based on a median split of behavioural responses to false alarms to stimulus-absent trials as explained below. The two groups were matched for age ( $t(37) = 0.107$ ,  $p = 0.915$ ), gender ( $\chi^2 = .821$ ,  $p = .365$ ), and audiogram ( $F(5, 185) = 2.01$ ,  $p = 0.079$ ) (Figure 1). These were determined using an independent samples  $t$ -test, a chi-square test and a repeated measures ANOVA with groups (same source and independent

source perceivers) as between-subjects variable, frequencies and side (left and right) as repeated measures.

## 2. Part 2 with patients with tinnitus and matched controls:

This part of the study consisted of 11 participants with tinnitus ( $M = 43.00$  years,  $SD = 14.40$  years; 4 males, 7 females) and 10 participants without tinnitus ( $M = 39.00$  years,  $SD = 17.49$  years; 6 males and 4 females). All participants underwent audiological measurements which included a pure tone audiogram testing the threshold of hearing at frequencies 125, 250, 500, 1000, 2000, 3000, 4000, 6000, and 8000Hz in both left and right ears according to the procedures prescribed by the British Society of Audiology.

The tinnitus characteristics such as the loudness and distress were measured using self-report questionnaires. In addition, the tinnitus type (3 patients with pure tone, 5 patients with noise-like, 1 patient with a combination and 2 patients with bells and crackling sounds) and laterality (2 patients with left-sided tinnitus, 2 patients with right-sided tinnitus, 4 patients with tinnitus on both ears equally, 3 patients with tinnitus on both ears but with dominant right-sided tinnitus) were also recorded to understand the heterogeneity of the group. Tinnitus loudness and distress were measured using a visual analogue scale (VAS) for loudness ( $M = 4.55$ ,  $SD = 1.91$ ) and distress ( $M = 3.48$ ,  $SD = 2.54$ ). This is a 10-cm scale with end points at a 0 = “no tinnitus”/“no distress” and 10 = “as loud as imaginable”/ “suicidal levels of distress”. They also completed a self-report questionnaire for Tinnitus Handicap Inventory (THI) ( $M = 49.09$ ,  $SD = 14.46$ ) which is designed to assess the tinnitus-related distress and impact on their lives. Most participants filled out the Dutch-translated versions of the questionnaires except a few who opted for the English versions.

The two groups were matched for age ( $t(19) = .57$ ,  $p = .573$ ,  $d = .25$ ), gender ( $\chi^2 = 1.17$ ,  $p = .279$ ) and overall audiogram ( $F(4.18, 309.84) = 1.002$ ,  $p = .416$ , partial  $\eta^2 = .063$ ) (Figure

1). These were determined using an independent samples *t*-test, a chi-square test and a repeated measures ANOVA with groups (tinnitus and control) as between-subjects variable, frequencies and side (left and right) as repeated measures. Similar to Part 1, exclusion criteria included Meniere's disease, chronic ear infections, otosclerosis, tumors, mental disorders and chronic eye disorders. All participants either had normal or corrected-to-normal vision. Patients presented with tinnitus anywhere between 3 months and 15 years.

### *Main Experiment – behavioural*

All participants, at both sites, underwent an experiment to induce an auditory illusion which had two parts – a behavioural and an electrophysiological part. In each part, the target stimulus (sound) embedded in noise was presented simultaneously with the cue (picture) in onset and duration. Participants were asked to press the right (or left) button on the mouse to indicate when they heard the target stimulus and the left (or right) button to indicate when they did not hear the target stimulus at the time the cue was presented as quickly and accurately as possible (during the behavioural session) and when prompted to give a response (during the electrophysiological recording session). The right or left mouse click corresponding to heard or did not hear was randomised in the study with the young adults and pseudorandomised between the tinnitus and control groups to ensure equal numbers. The tinnitus participants underwent an additional experiment similarly designed to induce a visual illusion.

### *Stimuli and trial structure*

#### *1. Auditory illusion*

The stimulus consisted of a 900 ms background white noise of intensity 40 dB (45 dB at the Belgium site) and a 10 ms rise-fall time and a 300 ms 1000 Hz pure tone target stimulus

with a rise-fall time of 10 ms embedded in the middle. The intensity of the pure tone target stimulus was determined using the QUEST thresholding paradigm explained below. The trial structure consisted of the stimulus and a 2400 ms response window that included the stimulus presentation time. A grey and black checkerboard served as the reliable visual cue and was synchronised in onset and duration to that of the target stimulus. The grey squares were at 25% brightness to maximise visual stimulation and minimise after-effects. The inter-trial interval was jittered between 1500 – 2000 ms. The trial structure is shown in Figure 2.

## 2. Visual illusion

The target stimulus consisted of a 200 ms sinusoidal Gabor with a visual angle of 3 cycles per degree embedded within 2 x 2 pixels of binary noise whose presentation was synchronised in onset and duration with that of a 500 Hz pure tone with a 10 ms rise-fall time and intensity of 60 dB that served as the reliable auditory cue. The contrast of the Gabor was determined by the QUEST thresholding paradigm explained below. This was followed by a response window of 2400 ms which included the stimulus duration, and the trials were jittered with an inter-trial duration of 1500 – 2000 ms. The trial structure is shown in Figure 2.

The auditory stimuli were presented binaurally through Sennheiser PRO headphones at both sites. At the Trinity site, the visual stimuli were presented on a 27” Isus Swift PG278QR monitor, placed approximately 85cm in front of the participant. At the Belgium site, the visual stimuli were presented on a 21” SAMSUNG computer screen placed at 171 cm in front of the participant.

## *QUEST*



The behavioural part was designed to determine the 75% likelihood threshold of the target stimulus in each domain. This was accomplished via the QUEST maximum likelihood-based procedure for threshold estimation coded through MATLAB Psychtoolbox 3.0. The QUEST algorithm was implemented in two 40-trial long initially ascending interleaved staircases of step size determined by the QUEST program based on the participant responses. The program terminated giving the 75% likelihood threshold of the target stimulus (amplitude of pure tone or contrast of the Gabor) embedded in noise. Additionally individual psychometric curves were fitted to obtain 50% and 25% likelihood points of the amplitude of the sound and contrast of the Gabor. The average thresholds at 75%, 50% and 25% likelihoods between the two runs were considered for the electrophysiological part of the experiment.

#### *Main experiment – electrophysiological*

During this part, EEG was recorded as the participants engaged in a structured presentation of stimuli as shown in Figure 2 which consisted of a disproportionately larger number of threshold-level stimuli in the initial runs followed by a disproportionately larger number of sub-threshold and absent stimuli in the later runs. The overall experiment consisted of 12 blocks, with each block consisting of 60 trials. 2 blocks made a functional run where participants were given a 30 second break between each functional run.

At the Trinity site, the trial structure consisted of a continuous background noise. The target stimulus was 300 ms long and the checkerboard was cued to the onset of the target stimulus. The stimulus presentation was followed by a 1000ms window to allow the ERP to develop. Following this, participants were prompted to indicate whether they heard the audio signal embedded in the background noise, with the right or left mouse button depending on the pseudorandomised condition and to rate their confidence on a 5 point scale from “Not

Sure”, to “Very Certain”. The response window was 1500 ms long and the confidence rating window was 2000 ms long. This was followed by 300-500 ms inter-trial jitter.

At the Belgium site, each trial was 3500 ms long with an inter-trial jitter of 100-300 ms, where the trigger was placed at the start of the trial. The stimuli were presented after a 300 ms delay. The auditory stimulus lasted 900 ms, where the embedded target stimulus was 300 ms long. The checkerboard cue was synchronised to the target stimulus. In the visual domain, the target Gabor stimulus embedded in noise was presented for 200 ms which was synchronised with the presentation of the 500 Hz pure tone cue. The stimulus presentation was followed by 800 ms and 1500 ms window in the auditory and visual experiments respectively to allow the evoked response to evolve before the participants were prompted to respond whether they heard a tone (in the auditory experiment) or saw a pattern (in the visual experiment) embedded in the noise structure or not by the right or left click of a mouse depending on the pseudorandomised condition. This response window lasted for 1500 ms in both experiments. Specifically, in the visual domain, to vary the noise structure of the target stimulus, the images were pseudo-randomly chosen from a pool of 112 noise structures embedded with Gabors of contrasts 75%, 50%, 25% likelihood thresholds and contrast of 0. The delayed response in the electrophysiological experiment allows for the motor potential from the mouse click to not contaminate the sensory-evoked potential of the audio-visual signals.

All trial structures are presented in Figure 2.

#### *EEG data collection and pre-processing*

At the Dublin site, the stimuli were presented through Psychopy which sent triggers to the BioSemi ActiView software. The EEG was sampled at 4096 Hz from a BioSemi ActiveTwo system. The data was collected using a 64 channel Biosemi EEG cap, in accordance with the

International 10-20 placement system. The data was pre-processed using MATLAB, EEGLAB v2021.1 and ERPLAB v8.20. The data was downsampled to 500 Hz, re-referenced to an average reference, and band-pass filtered between 0.55 – 44 Hz. The data was epoched from -300ms to +1300ms post onset on the stimulus, to capture the audio-evoked potential while avoiding the motor-evoked potential. An independent component analysis (ICA) was then performed to remove artifacts related to blinks, saccades, and muscle movements. Artifacts in all epochs were then detected and removed using a voltage threshold of  $\pm 90\mu\text{V}$  and manual inspection. Any channels that were removed during pre-processing were subsequently interpolated before the signal was processed.

At the Belgium site, the stimuli were presented through PsyTask controlled by WinEEG. The EEG was sampled using Mitsar 201 amplifiers at 250 Hz. The data was collected using a 19 channel Mitsar EEG cap designed using the International 10-20 placement system. The data was band-pass filtered online from 0.1 – 70 Hz and was collected with a reference close to Cz. Offline, the data was re-referenced to an average reference, filtered between 0.55 – 45 Hz, epoched between -400 and +3200 relative to the onset of the *stimulus*, cleaned for artifacts such as eyeblinks, saccades, muscle movements etc. using a temporal independent component analysis (ICA) using infomax algorithm. The data was further manually inspected for epochs with large deviations and were cleaned before comparing the two groups. A multivariate ANOVA to test the difference between the number of ICA components remaining in the two groups and two paradigms after cleaning reveal no significant differences (Wilk's  $\Lambda = .98$ ,  $F(2,18) = .14$ ,  $p = .87$ , partial  $\eta^2 = .015$ ).

### *Post-processing and analysis*

#### 1. Behavioural data:

The 75% likelihood threshold for each of the domains was compared between the two groups using an independent samples *t*-test. The percentage of hits and misses for the 75% threshold and the percentage of false alarms and correct responses for the stimulus-absent trials after accounting for the number of no-response trials, were compared between the two groups (same source vs independent source perceivers; controls vs tinnitus) using a chi-square analysis. Furthermore, the participants from the Belgium site, were further split into participants with and without false alarms (same source and independent source perceivers). The hits and misses for the 75% likelihood threshold trials and the number of false alarms and correct responses for same source and independent source perceivers were also separately evaluated using a chi-square analysis. The different chi-square analyses were corrected for multiple corrections using a Benjamini-Hochberg false discovery rate of  $\alpha = .25$ .

## 2. Electrophysiological data:

At the Dublin site, the ERPs same source and independent source perceivers were compared. At the Belgium site, the ERPs of the same source and independent source perceivers were compared between the two groups (controls and tinnitus) for the experiments in the two sensory domains. The hypothesis is that participants less and more likely to perceive an illusion amongst the young adults at the Dublin site and participants with and without false alarms amongst the relatively older adults at the Belgium make different perceptual inferences about the sensory environment when the auditory and visual stimuli are presented simultaneously – participants more likely to perceive false alarms possibly make an inference that the auditory and visual signals arise from the same source, those less likely to perceive false alarms possibly infer that they come from independent sources.

From a conceptual standpoint, the hits of the 75% threshold stimuli may be representative of participants' learning of the new sensory environment and the false alarms/correct



responses to the target stimulus-absent trials may be representative of the perceptual inference made by the brain in the current context.

#### *Event-related potential*

##### 1. Part 1 with healthy young adults

The single-trial EEG to the hits of 75% likelihood stimuli for same source (1761 trials across all participants) and independent source (2048 trials across all participants) perceivers were compared between the two groups using independent *t*-tests for the length of the epoch. The topographical plots for the hits were plotted for the most significant channel-time point clusters with the largest mean difference and the ERPs from the significant cluster of channels was represented alongside.

However, due to the nature of the two groups, there was a highly uneven number of trials between same source (991 trials across all participants) and independent source (292 trials across all participants) perceivers for the false alarms. To account for this, we opted to randomly select 292 trials from the same source perceivers group and perform a *t*-test between this sample of trials with all of the 292 trials for independent source perceivers. We repeated this procedure 100 times and determined which channel-time point clusters were significant in most of these iterations. The topographical plots for the false alarms were plotted for the channel-time point cluster that was significant in most of the iterations and the ERPs from the significant cluster of channels was represented alongside. The average amplitude for the false alarms across the significant channel-time point cluster was correlated to the percentage of false alarms using Spearmann correlation.

Cluster correction was performed to account for the family wise error rate using the Field Trip toolbox (Ostenveld et al., 2011) in Matlab. The neighbours of each channel were calculated using a standard template of neighbours provided in the Field trip documentation

for Biosemi 64 channel caps. The minimum number of neighbouring channels to form a cluster was thresholded at two channels. In this manner, a non-parametric cluster correction was applied by computing a permutation test of 5000 iterations at a cluster level alpha of 0.05 and an overall alpha of 0.025 for a two-tailed hypothesis. Following the  $t$ -tests, we applied a Bonferroni correction to the four  $t$ -tests (pre and post stimulus onset for two conditions), providing us with a new alpha level of .0125.

## 2. Part 2 with tinnitus patients and matched controls

The single trial EEG to the hits of the 75% threshold stimuli and false alarms/correct responses for the same source/independent source participants were compared between the two groups (controls and tinnitus) using independent  $t$ -tests. Correction for multiple comparison was performed using cluster correction using the FieldTrip toolbox in Matlab. The neighbours of each channel were calculated using a standard template of neighbours provided by FieldTrip for 19-channel EEG data. A cluster was determined in such a way that each channel would have at least two neighbours. This way a non-parametric cluster correction was applied by computing a permutation test of 5000 iterations at a cluster-level alpha of 0.05 and an overall alpha of 0.025 to account for a two tailed hypothesis. The tests were further corrected for multiple comparisons for the number of comparisons ran (4 conditions (hits and false alarms for same source perceiver; hits and correct responses for independent source perceivers) x 2 sensory domains x 2 time ranges (pre and post stimulus responses)) using Bonferroni correction (i.e.  $p < .003125$ ). The topographical plots were plotted for the most significant channel-time point clusters with the largest mean difference and the ERPs from the significant cluster of channels was represented alongside.

## *Time-frequency decomposition*

To further delve into neural correlates of the BPI model, a time-frequency decomposition was carried out for the hits of the 75% likelihood threshold stimuli (representing the establishment of predictions of the new sensory environment) and the false alarms/correct responses of the stimulus-absent trials (representing the perceptual inference). This was done by convolving a family of Morlet wavelets with a linearly increasing number of cycles between 2 cycles at 1 Hz and 15 cycles at 44 Hz, sampled at 500 Hz for Part 1 of the study and sampled at 250 Hz for Part 2 of the study. A baseline normalisation (-200 to -100 for Part 1 of the study and -400 to -200 ms for Part 2 of the study prior to stimulus presentation) was applied to the calculation. The differences in baseline normalisation parameters was due to the slight change in trial structure owing to the different data collection systems. The alpha band was defined between 8-12 Hz. The time-frequency decomposition was calculated for single trials (total power) for each person for the significant channel-time clusters obtained from the above ERP analysis.

#### 1. Part 1 with healthy young adults

The total power averaged across the significant time points for each of the channels identified as significant for the hits and false alarms were compared between the two groups with groups x conditions as fixed factor and channels and trials as random factors for each significant channel-time point cluster during stimulus presentation. If the interaction was significant, a further mixed model was conducted for each condition with groups as fixed factor and channels and time as random factors. Furthermore the same was carried with groups as fixed factor and channels and trials as random factors for the pre-stimulus time frame.

#### 2. Part 2 with patients with tinnitus and matched controls:

The total power averaged across the significant time points for each of the channels identified as significant for the hits, false alarms/correct responses for same source/independent source perceives were compared between the two groups (controls and tinnitus) with groups x conditions as fixed factor and channels and trials as random factors for each significant channel-time point cluster (during and post stimulus presentation) for each sensory domain (auditory, visual). These comparisons were corrected for multiple comparisons using the Benjamini-Hochberg False Discovery Rate with an alpha level = .25. If the interaction was significant, a further mixed model was conducted for each condition with groups as fixed factor and channels and time as random factors. A similar analysis was carried out for the visual domain with groups as fixed factor and channels and trials as random factors.

#### *Inter-trial phase clustering (ITPC)*

ITPC is the measure of phase locking across trials. The magnitude and phase angle of alpha phase locking for those conditions showing a significant difference in total power was calculated from the single trials using the formula below:

$$itpc_{mag} = abs(mean(e^{i*\theta}))$$

$$itpc_{phase} = angle(mean(e^{i*\theta}))$$

Where  $\theta$  is the vector of phase angles obtained from the convolution of the complex Morlet wavelets with the single trial data during time-frequency decomposition at each time point in the significant channel-timepoint cluster.

#### 1. Part 1 with healthy young adults

The average magnitude of inter-trial phase clustering was calculated from that of the significant time points for each significant channel and compared across the two groups and

the two conditions (Hits, False Alarms) using a mixed model with groups x conditions as fixed factor and channels as random factor during stimulus. A similar analysis was conducted pre-stimulus for the hits with groups as fixed factor and channels as random factors.

## 2. Part 2 with patients with tinnitus and matched controls

The average magnitude of inter-trial phase clustering was calculated from that of the significant time points for each significant channel and compared across the two groups using a mixed model with groups (tinnitus, controls) as fixed factor and channels as random factors for those comparisons that were identified as having a significant difference between the two groups from the previous analysis.

## Results

### *Behavioural results*

#### 1. Part 1 with healthy young adults

We observe no significant difference between the two groups in the 75% likelihood thresholds of the auditory ( $t(19) = .86, p = .398$ , Cohen's  $d = .38$ ) target stimuli.

For the same source perceivers, we observe no significant difference in the percentage of hits and misses between the two groups for the 75% threshold stimuli ( $X^2 = .92, p = .428$ ). However, we observe a significant difference between the two groups for the percentage of false alarms and correct responses for the stimulus-absent trials for the same source perceivers ( $X^2 = 7.27, p = .009$ ).

#### 2. Part 2 with patients with tinnitus and matched controls



We observe no significant difference between the two groups in the 75% likelihood thresholds of the auditory ( $t(19) = .86, p = .398$ , Cohen's  $d = .38$ ) and visual target stimuli ( $t(19) = .41, p = .690$ , Cohen's  $d = .17$ ).

For the same source perceivers in the auditory experiment, we observe no significant difference in the percentage of hits and misses between the two groups for the 75% threshold stimuli ( $X^2 = .05, p = .757$ ), for the false alarms and correct responses for the stimulus absent trials ( $X^2 = 0, p = .999$ ) or for the hits and misses for the 75% threshold stimuli for the independent source perceivers ( $X^2 = .38, p = .692$ ).

For the same source perceivers in the visual experiment, we observe no significant difference in the percentage of hits and misses between the two groups for the 75% threshold stimuli ( $X^2 = 1.93, p = .157$ ) or for hits and misses for the 75% threshold stimuli for the independent source perceivers ( $X^2 = 1.03, p = .32$ ). However, we observe a significant difference between the two groups for the percentage of false alarms and correct responses for the stimulus-absent trials for the same source perceivers ( $X^2 = 6.03, p = .014$ ).

All behavioural results are depicted in Figure 3.

### *ERP results*

#### *1. Part with healthy young adults*

We observe differences in the ERPs between the same source and independent source perceivers for the hits of the 75% likelihood stimulus trials (hits) and the false alarms of the stimulus absent trials in different time frames.

#### *Group comparison between same and independent source perceivers for false alarm trials*

We observe no significant difference in the ERP between the same source and independent source perceivers during pre- and post-stimulus epochs for false alarm trials. However, during stimulus presentation, there was a significantly more negative ERP amplitude for the same source perceivers group compared to the independent source perceivers group across occipital channels Oz, O1, O2, POz, PO3, PO4 during the timeframe from 280-316 ms post-stimulus onset. The average amplitude across the significant channel-time points are negatively correlated with the percentage of false alarms ( $r = -.43, p = .006$ ). This is shown in Figure 4.

#### *Group comparison between same and independent source perceivers for hit trials*

There was a significantly higher ERP amplitude response for the independent source compared to the same source perceivers during the pre-stimulus time frame from 254 – 134 ms pre-stimulus onset. This significant difference in amplitude was lateralised across right frontal channels. During stimulus presentation, the audio-visual signal evoked a significantly higher ERP amplitude in the same source perceiver group relative to the independent source perceiver group, distributed across channels PO8, P2, P4, CP4, CP6 and FP2 in the time frame from 194-260 ms post-stimulus onset. In the post-stimulus time window, there was a significantly higher ERP amplitude for the same source perceivers compared to the independent source perceivers distributed across frontal channels in the time window from 320-374 ms post-stimulus onset. This is shown in Figure 4.

## 2. Part 2 with patients with tinnitus and matched controls

We observe changes in the ERPs of the tinnitus compared to the control group for the hits of the 75% likelihood stimulus trials (hits), false alarms and correct responses of the stimulus absent trials in both the auditory and visual experiments. The participants divide into two

groups – one group with false alarms and one group without false alarms possibly because they apply different perceptual strategies to make sense of the environment.

*Group comparison between control and tinnitus for same source perceivers during the auditory task*

This subset of participants consisted of six control (4 males, 2 females; Mean Age = 28.33 years,  $SD = 9.43$ ) and tinnitus participants (4 males, 2 females, Mean Age = 36.16 years,  $SD = 12.89$ ) who are matched for age ( $t(10) = 1.20, p = .257$ , Cohen's  $d = .69$ ) and hearing loss ( $F(2.79, 195.988) = .60, p = .611$ , partial  $\eta^2 = .079$ ).

There was no significant difference in the ERP between the two groups during the pre-stimulus time frame for the hits or false alarms. During stimulus presentation, we observe increased ERP in the tinnitus compared to the control group for the hits and false alarms localised to the parietal electrodes. This change in responses are lateralised to the right for the hits. These results are depicted in figure 5.

Immediately following stimulus presentation, we observe a decrease in ERP responses for the hits and false alarms in the tinnitus group compared to the controls in a similar cluster of electrodes at the parietal and temporal-parietal regions. These results are depicted in Figure 6.

*Group comparison between control and tinnitus for same source perceivers during the visual task*

This subset of participants consisted of seven control (6 males, 1 females; Mean Age = 40.57 years,  $SD = 19.73$ ) and eight tinnitus participants (4 males, 4 females, Mean Age = 40.25 years,  $SD = 15.02$ ) who are matched for age ( $t(13) = .04, p = .972$ , Cohen's  $d = .02$ ) and hearing loss ( $F(3.99, 84.62) = .92, p = .461$ , partial  $\eta^2 = .077$ ).

There was significant reduction in amplitude of the ERP for the tinnitus group in the pre-stimulus time frame between -232 ms and 0 ms for the hits. However, there was no significant difference in the ERP amplitude between the two groups for the false alarms. These results are depicted in Figure 10. During and immediately following stimulus presentation, we observe an increased ERP response to the hits and false alarms in the tinnitus group compared to the controls. These changes are reflected in the parietal-occipital electrodes for the hits, but in the frontal and central electrodes for the false alarms. These results are depicted in Figures 5 and 6 respectively.

*Group comparison between controls and tinnitus for independent source perceivers during the auditory task*

This subset of participants consisted of three control (1 males, 2 females; Mean Age = 52.00 years,  $SD = 15.71$ ) and two tinnitus participants (0 males, 2 females, Mean Age = 59.5 years,  $SD = 4.94$ ) who are matched for age ( $t(3) = .63, p = .576$ , Cohen's  $d = .64$ ) and hearing loss ( $F(1.45, 233.74) = 1.73, p = .181$ , partial  $\eta^2 = .46$ ).

There was no significant difference in the amplitude of the ERP in the pre-stimulus time frame between the two groups for the hits or correct responses. During and immediately post stimulus presentation, we observe an increase in amplitude of the ERP in the tinnitus group compared to the controls for the hits and correct responses. These changes are localised to the parietal-occipital electrodes for both conditions. No significant difference is observed in the ERP between the two groups in the post stimulus condition for the correct responses. These results are depicted in Figure 7 and 8 respectively.

*Group comparison between controls and tinnitus for independent source perceivers during the visual task*

This subset of participants consisted of three control (0 males, 3 females; Mean Age = 35.33 years,  $SD = 13.42$ ) and tinnitus participants (0 males, 3 females, Mean Age = 50.33 years,  $SD = 11.67$ ) who are matched for age ( $t(4) = 1.46$ ,  $p = 2.18$ , Cohen's  $d = 1.19$ ) and hearing loss ( $F(1.68, 84.26) = .72$ ,  $p = .525$ , partial  $\eta^2 = .26$ ).

During and after stimulus presentation, we observe that the ERP of the tinnitus group is significantly lower in amplitude than that of the control group for the hits and correct responses. The changes in responses for the hits are localised to the parietal-occipital electrodes in both time ranges, whereas the changes in responses for the correct responses are localised to the frontal-central electrodes during stimulus presentation and to the parietal-occipital electrodes in the post stimulus response. These results are depicted in Figures 7 and 8 respectively.

#### *Time frequency analysis – total power*

##### *1. Auditory domain*

For the group of healthy young adults, we observe a significant group x condition interaction for the total alpha power during stimulus presentation ( $F(3, 30291.28) = 116.48$ ,  $p < .001$ , partial  $\eta^2 = .01$ ). For the hits, there was no significant difference in the alpha power between the same source and independent source perceivers ( $F(1, 22833.97) = 1.18$ ,  $p = .277$ , partial  $\eta^2 = .00005$ ), however there was a significant difference in alpha power between the two groups for the false alarms ( $F(1, 7658.94) = 65.54$ ,  $p < .001$ , partial  $\eta^2 = .008$ ).

For the same source perceivers, we observe a significant groups x conditions interaction for the total power in the auditory experiment for hits and false alarms during ( $F(3, 7974.15) = 3.28$ ,  $p = .020$ , partial  $\eta^2 = .001$ ) and post-stimulus presentation ( $F(3, 8939.06) = 7.15$ ,  $p < .001$ , partial  $\eta^2 = .002$ ). We observe a significant difference in the total alpha power for the hits ( $F(1, 4974.61) = 4.67$ ,  $p = .031$ , partial  $\eta^2 = .0009$ ) and false alarms ( $F(1, 2687.02) =$



4.12,  $p = .043$ , partial  $\eta^2 = .001$ ) for the tinnitus group compared to the control group during stimulus presentation. Post stimulus presentation, we observe no significant difference in total alpha power for the hits ( $F(1, 5983.41) = .79$ ,  $p = .374$ , partial  $\eta^2 = .0001$ ) but a significant difference for the false alarms ( $F(1, 2770) = 14.10$ ,  $p < .001$ , partial  $\eta^2 = .005$ ) for the tinnitus group compared to the control group.

For independent source perceivers, we observe no significant group x conditions interaction ( $F(3, 8255.61) = 1.44$ ,  $p = .229$ , partial  $\eta^2 = .0005$ ) between the hits and correct responses for the control and tinnitus groups.

These results are depicted in Figure 9.

## 2. Visual domain

For the same source perceivers, we observe a marginally significant groups x conditions interaction for the total alpha power in the visual domain for hits and false alarms during ( $F(3, 11967.59) = 2.37$ ,  $p = .069$ , partial  $\eta^2 = .0006$ ) and no significant difference post stimulus ( $F(3, 82.44) = 1.79$ ,  $p = .16$ , partial  $\eta^2 = .06$ ) presentation. During stimulus presentation, we observe no significant group difference in the total alpha power for the hits ( $F(1, 14151.16) = 3.15$ ,  $p = .076$ , partial  $\eta^2 = .0002$ ) but a significant increase in alpha power desynchronisation for the false alarms ( $F(1, 2289.39) = 4.86$ ,  $p = .028$ , partial  $\eta^2 = .002$ ).

For the independent source perceivers, we observe no significant group x condition interaction for the total alpha power for the hits and correct responses during stimulus presentation ( $F(3, 8255.61) = 1.44$ ,  $p = .229$ , partial  $\eta^2 = .0005$ ) but a significant effect for the post stimulus presentation ( $F(3, 13738.44) = 5.03$ ,  $p = .002$ , partial  $\eta^2 = .001$ ). Post stimulus presentation, there was no significant difference for the total alpha power for the hits ( $F(1, 5071.21) = .39$ ,  $p = .529$ , partial  $\eta^2 = .00008$ ) but there was for the correct responses ( $F(1, 10791.42) = 9.29$ ,  $p = .002$ , partial  $\eta^2 = .0009$ ).

These results are depicted in Figure 9.

#### *Time-frequency analysis – inter-trial phase clustering (ITPC)*

For the healthy young adults, ITPC magnitude for alpha showed a significant group x condition interaction ( $F(3,464) = 121.36, p < .001$ , partial  $\eta^2 = .44$ ) for the same source and independent source perceivers for the hits and false alarms during stimulus presentation. For the hits, there was no group difference between the two groups ( $F(1,232) = 1.90, p = .169$ , partial  $\eta^2 = .008$ ). However for the false alarms, a significant group difference was observed between the two groups ( $F(1,232) = 77.75, p < .001$ , partial  $\eta^2 = .25$ ) for the alpha ITPC. Furthermore, there was no significant group difference observed between the two groups before the onset of the hits ( $F(1,115) = .16, p = .689$ , partial  $\eta^2 = .001$ ). These results are shown in Figure 9.

For the same source perceivers during the auditory experiment, there was a significant group x condition interaction for the ITPC for the hits and false alarms during stimulus presentation ( $F(3,140) = 6.68, p < .001$ , partial  $\eta^2 = .12$ ). There was no significant group difference for the ITPC for the tinnitus and the control group for the hits ( $F(1,58) = 1.63, p = .207$ , partial  $\eta^2 = .027$ ), or false alarms ( $F(1,82) = 2.90, p = .096$ , partial  $\eta^2 = .034$ ). Post-stimulus presentation, there was a significant group x condition interaction for the ITPC for the hits and false alarms ( $F(3,152) = 26.48, p < .001$ , partial  $\eta^2 = .34$ ). For the hits, there was no significant group difference ( $F(1,69.43) = .71, p = .403$ , partial  $\eta^2 = .01$ ), but there was for the false alarms ( $F(1,82) = 8.95, p = .004$ , partial  $\eta^2 = .10$ ). Pre-stimulus presentation, there was a significant group difference between the controls and tinnitus group for the ITPC ( $F(1,83) = 19.02, p < .001$ , partial  $\eta^2 = .18$ ). These results are shown in Figure 9.

For the same source perceivers for the visual experiment, we observe a significant group x condition interaction for the alpha ITPC for the hits and false alarms ( $F(3,57.54) = 39.97, p <$

.001, partial  $\eta^2 = .67$ ) during stimulus presentation. There was no significant difference in the ITPC for the hits between the controls and tinnitus group ( $F(1,118.40) = .36, p = .551$ , partial  $\eta^2 = .003$ ) whereas there was a significant difference between the two groups for the false alarms ( $F(1,83) = 4.21, p = .043$ , partial  $\eta^2 = .05$ ). For the independent source perceivers, we observe a significant group x condition interaction for the alpha ITPC for the hits and correct responses ( $F(3,98.13) = 5.92, p < .001$ , partial  $\eta^2 = .15$ ) post stimulus presentation. There was no significant group difference between the controls and tinnitus group for the hits ( $F(1,58) = 2.91, p = .094$ , partial  $\eta^2 = .05$ ) or the correct responses ( $F(1,34) = .20, p = .656$ , partial  $\eta^2 = .006$ ). These figures are shown in Figure 9.

## Discussion

The current study investigated the mechanism of the BPI model by experimentally inducing a phantom perception in (i) a group of healthy young adults and (ii) a group with chronic phantom perception. In both situations, we studied the difference in neural processes between participants who were more and less likely to perceive a phantom perception thereby revealing how they make perceptual inferences about a newly learned sensory environment. All participants were exposed to the simultaneous presentation of a cue with an uncertain target stimulus, one of which was visual and the other was auditory. As the experiment proceeded, the threshold of the target stimulus was varied and the stimulus was absent in most trials towards the end of the experiment. The hypothesis was that people who were more likely to perceive an illusion would make stronger associations between the cue and target stimulus. Furthermore, the theory is that tinnitus patients make more precise predictions of the sensory environment based on their perceptual model of the world and therefore, when exposed to a new sensory environment such as the above, they may be more likely to perceive an illusion in the domain of the target stimulus when only the cue was presented.

One of the first observations of the data is that participants employ different strategies to process their sensory environment. They divide into two categories – those who are more likely to perceive an illusion and those who are less likely. This bifurcation of the groups may be attributed to the way participants make a causal inference about the source of the signals which is explained by the Bayesian Causal Inference model<sup>22-24</sup>. According to this model people process multisensory information in 3 stages – (1) segregation of the individual input streams in their respective sensory cortices, (2) integration into a fused percept, (3) causally inferring the source of the signals. In step (3) participants could either infer that the visual and auditory information come from (i) the same source or (ii) independent sources. Those who adopt a same-source strategy tend to fuse the two streams of sensory input into one percept, whereas the others do not. Therefore, when presented with just the cue, participants adopting strategy (i) will likely perceive an illusion of the missing sensory input.

#### *Experimental induction of phantom perception in healthy young adults*

In this group, we observed two phases – (i) the learning phase i.e. during the simultaneous presentation of the target and cue stimulus and (ii) the inferential phase during the stimulus absent trials. We observed an increase in ERP amplitude for same source perceivers during the during and following the presentation of the simultaneous target and cue stimuli compared to that of the independent source perceivers. Topographically this was lateralised to the right temporo-parietal regions. A review of literature surrounding this region reveals its function in both contextual updating of the internal model based on the current sensory environment reflecting a change in expectation of upcoming events<sup>25</sup>. The increased amplitude in the group that makes a same source judgement, possibly make stronger predictions about the upcoming stimuli therefore reflecting the learning of the environment and updating of the current perceptual model to one that fits this sensory environment.

This is reflected in the difference in amplitude of the ERP and the alpha power for the false alarms for the two groups – i.e. in the inferential phase. We observe a more negative amplitude for the same source perceivers compared to the independent source perceivers. This amplitude is also correlated to the percentage of false alarms – i.e. people who are more likely to perceive an illusion have a more negative amplitude during the perception of the illusion. The topographical plots show an orientation of the dipole to the frontal and fronto-temporal regions as shown by previous studies. However, the significant difference in 80% of the tests is observed at the negative end of the dipole. Furthermore, the negative end of the dipole is oriented towards the posterior occipital regions of the brain also showing the stronger encoding of stimulus segregation in the independent source perceivers.

The change in the ERP is also accompanied by a change in the alpha power and phase clustering. We observe decreased alpha power – or a desynchronization of the total alpha power accompanied by a significant reduction in its phase clustering. Alpha desynchronisation during auditory perception has been shown in the past<sup>26</sup>.

#### *Examining a clinical model of phantom perception - patients with tinnitus and matched controls*

From a behavioural standpoint we observe that tinnitus patients are more likely than a control group to perceive an illusion in the visual domain where the reliability of the visual input is varied and that of the auditory input is a constant. Whereas, in the auditory domain, they are as likely as the control group to perceive an illusion when the auditory information is unreliable, and the visual information is a constant. From these results, it may be likely that tinnitus patients make stronger predictions of the sensory environment when the auditory signal is reliable.



From the ERP responses we observe three distinct components of the BPI model – segregation, integration and perceptual inference. The absence of the distinction between the segregation and integration components in the young adult group, may be a factor of ageing. We know from previous literature that multisensory processing is different with age.

Particularly delving into the electrophysiology of the mechanism of the visual illusions, we observe an increase in ERP amplitude in tinnitus compared to controls while learning the sensory environment (i.e. during hits of the 75% likelihood threshold stimuli) during both the segregation (within 200 ms of stimulus onset) and integration (200-400 ms of stimulus onset) time frames of the inferential and while making a same-source inference when only the auditory cue was presented (i.e. during and after stimulus presentation while perceiving the false alarms). However, in participants without illusions, i.e. those who adopt an independent source strategy of perceptual inference, we observe that the amplitude of the ERP is lower in the tinnitus compared to the controls during both the learning phase i.e. hits and the perceptual inference phase i.e. during the reporting of correct responses.

It is interesting to observe that during the learning phase in both strategies, the difference in ERP amplitudes are localised to the posterior parietal electrodes possibly corresponding to the regions of multisensory integration<sup>14,23,24</sup> and differences in perceptual inferences are localised to fronto-central electrodes, which are hypothesised to be involved in drawing an inference<sup>14,23,24</sup>. The increase in amplitude in the same source strategy in the tinnitus group during the integration time frame possibly represents an increased sensitivity to fusing audio-visual signals into a single percept compared to controls, and the decrease in amplitude during the independent source strategy shows a decreased sensitivity to fusing audio-visual signals into one percept. Furthermore, this pattern is replayed when a perceptual inference is made (i.e. during the false alarms in the same source strategy cohort, and during the correct responses in the independent source strategy cohort). Furthermore, these neural signatures of

perceptual inference are also accompanied by a change in alpha activity where we observe increased synchronisation of alpha during the perception of false alarms and increased desynchronization during the correct responses.

The precision of the predictions of the model are encoded in alpha oscillations and here it represents the predictability from the same source. In the same source cohort, it's more precisely coming from the same source and in the independent source cohort it is significantly less precisely coming from the same source or more precisely coming from different sources. In other words, no matter what the model of the sensory environment made the tinnitus group seem to make stronger predictions of these models, which is observed when they make a perceptual inference of the learnt model.

During the auditory experiment, although behaviourally we observe no differences between the two groups, electrophysiologically we observe changes in the amplitude of the ERP. Here, we observe that the ERP amplitude is increased during the segregation time frame during learning (hits) and perceptual inference (false alarms) but decreased during the integration time frame for all the above conditions in the same source cohort. In the independent source cohort, we observe that there is an increase in ERP amplitude during the segregation time frame during learning (hits) and perceptual inference (correct responses) which is maintained for learning (hits) into the integration time frame, but not for perceptual inference (correct responses). It is interesting to note that unlike in the visual domain, where the perceptual inference was drawn from the frontal regions, here the perceptual inference is drawn from the posterior parietal regions. The predictive coding literature in tinnitus postulates that perceiving a phantom percept becomes the new default state of the brain<sup>8,10</sup> and this state is integrated into the internal representation and be by the default mode network, particularly the posterior cingulate cortex<sup>27</sup>. Furthermore, changes in alpha activity show increased desynchronisation during learning and decreased desynchronisation during

perceptual inference, showing that learning of the new sensory environment may be precise, but the inference drawn from it may be also reflecting the interruption made by the ongoing strong auditory phantom percept.

### *Building a perceptual inference*

From both sets of experiments, we observe (i) participants who are more likely to perceive an illusion, whether they have an existing chronic condition, or they are healthy young adults, make strong associations with the cue and the target stimulus. This means when there is an omission of the target, these people are more likely to “fill in” the missing information based on their strong prediction of the environment.

We also observe (ii) that the regions which are involved in building this perceptual inference are those from the temporal-parietal-occipital regions, where activity in these regions depend on whether they are participants who make a same source or independent source judgement.

Particularly from the results of the clinical model of phantom perception we observe that (iii) the tinnitus brain possibly makes stronger predictions about the sensory environment when the auditory signal is reliable. This may be a neural correlate of a precursor to chronic domain-specific phantom perception since the most common denominator to tinnitus generation is an auditory anomaly. Therefore, it is possible that people who make stronger predictions of the sensory scene when their domain-specific cues are reliable and may be susceptible to developing a chronic perception in the future, following a deafferentation.

Finally, we observe that patients with a chronic auditory phantom percept who do adopt an independent source strategy to inferring the causes of multisensory cues are possibly more reliant on visual information (a domain with sensory integrity). We observe from the ERPs of this cohort, that when the visual signal is reliable, there is increased activation in the posterior

783 parietal regions, and when the visual signal is unreliable, a decreased activation in the  
784 posterior parietal regions. Therefore, future studies may also want to investigate the role of  
785 cross-modal plasticity in patients with a chronic auditory phantom percept which maybe a  
786 compensation to the increased auditory uncertainty.

### 788 *Implications*

789 The current study confirms that simple auditory phantom perceptions is generated as a  
790 result of building strong prior beliefs about the environment. From an academic standpoint,  
791 the current study adds to the literature an empirical estimation and application of the BPI  
792 model of perception using a normative and clinical population. We learn that phantom  
793 perception is a natural way of the brain to “fill in” for the missing information. However, it  
794 also poses a question, whether the people who are more likely to perceive a phantom  
795 perception in the normative group – i.e. the people who perceive the auditory and visual  
796 information from the same source, are predisposed to developing a chronic phantom  
797 perception in the future. This can be addressed through longitudinal studies that can follow  
798 up with these participants to determine if they go on to develop chronic phantom perceptions,  
799 not only in the auditory but in other domains as well.

800 From a clinical perspective, the current study is the first to show this as a possible  
801 mechanism of action for chronic clinical conditions like tinnitus, where psychiatric  
802 complaints are less prevalent. Furthermore, it also indicates that patients with tinnitus are  
803 more reliant on the visual domain information and more sensitive to uncertainty in the visual  
804 domain. This is a particularly interesting finding especially because tinnitus is most often  
805 accompanied by changes in the auditory pathways. This makes the identification of an  
806 objective marker for tinnitus an extremely challenging process. However, indications from  
807 the current study that patients with tinnitus are sensitive to changes in a sensory domain that

is peripherally in tact can expand the search of an objective marker for tinnitus into other reliable sensory domains. This is immensely beneficial for the clinic in both diagnosis of tinnitus and treatment evaluation.

## **Conclusion**

The current study shows that participants who are likely to perceive a phantom perception are likely to merge the sources of a multisensory scene. They build a strong perceptual model of their environment and “fill in” for the missing information, if any. This is also observed in patients with a chronic phantom perception, both in the domain of the phantom percept and in a domain irrelevant to the phantom percept. In the domain of the phantom percept, we observe that there is a rivalry between the existing percept and the induced percept therefore the inference being drawn from regions related to internal processing. However, in the domain irrelevant to the chronic percept, we observe the inference drawn from more frontal regions thereby converging with the evidence found in healthy young adults.

## 823    **References**

- 824    1    Aggelopoulos, N. C. Perceptual inference. *Neuroscience & Biobehavioral Reviews*  
825        **55**, 375-392 (2015). <https://doi.org/10.1016/j.neubiorev.2015.05.001>
- 826    2    Friston, K. & Kiebel, S. Predictive coding under the free-energy principle.  
827        *Philosophical transactions of the Royal Society of London. Series B, Biological*  
828        *sciences* **364**, 1211-1221 (2009). <https://doi.org/10.1098/rstb.2008.0300>
- 829    3    Knill, D. C. & Pouget, A. The Bayesian brain: the role of uncertainty in neural coding  
830        and computation. *Trends Neurosci* **27**, 712-719 (2004).  
831        <https://doi.org/10.1016/j.tins.2004.10.007>
- 832    4    Baguley, D., McFerran, D. & Hall, D. Tinnitus. *The Lancet* **382**, 1600-1607 (2013).
- 833    5    De Ridder, D., Vanneste, S. & Freeman, W. The Bayesian brain: Phantom percepts  
834        resolve sensory uncertainty. *Neuroscience & Biobehavioral Reviews* **44**, 4-15 (2014).  
835        <https://doi.org/10.1016/j.neubiorev.2012.04.001>
- 836    6    De Ridder, D., Joos, K. & Vanneste, S. The Enigma of the Tinnitus-Free Dream State  
837        in a Bayesian World. *Neural Plasticity* **2014**, 612147 (2014).  
838        <https://doi.org/10.1155/2014/612147>
- 839    7    Mohan, A. & Vanneste, S. Adaptive and maladaptive neural compensatory  
840        consequences of sensory deprivation-From a phantom percept perspective. *Progress*  
841        *in neurobiology* **153**, 1-17 (2017). <https://doi.org/10.1016/j.pneurobio.2017.03.010>
- 842    8    Sedley, W., Friston, K. J., Gander, P. E., Kumar, S. & Griffiths, T. D. An Integrative  
843        Tinnitus Model Based on Sensory Precision. *Trends in neurosciences* **39**, 799-812  
844        (2016). <https://doi.org/10.1016/j.tins.2016.10.004>
- 845    9    Hullfish, J., Sedley, W. & Vanneste, S. Prediction and perception: Insights for (and  
846        from) tinnitus. *Neuroscience and biobehavioral reviews* **102**, 1-12 (2019).  
847        <https://doi.org/10.1016/j.neubiorev.2019.04.008>
- 848    10    Sedley, W., Alter, K., Gander, P. E., Berger, J. & Griffiths, T. D. Exposing  
849        Pathological Sensory Predictions in Tinnitus Using Auditory Intensity Deviant  
850        Evoked Responses. *The Journal of Neuroscience* **39**, 10096 (2019).  
851        <https://doi.org/10.1523/JNEUROSCI.1308-19.2019>
- 852    11    Powers, A. R., Mathys, C. & Corlett, P. R. Pavlovian conditioning-induced  
853        hallucinations result from overweighting of perceptual priors. *Science (New York,*  
854        *N.Y.)* **357**, 596-600 (2017). <https://doi.org/10.1126/science.aan3458>
- 855    12    Körding, K. P. *et al.* Causal Inference in Multisensory Perception. *PLOS ONE* **2**, e943  
856        (2007). <https://doi.org/10.1371/journal.pone.0000943>
- 857    13    Rohe, T., Ehrlis, A.-C. & Noppeney, U. The neural dynamics of hierarchical Bayesian  
858        causal inference in multisensory perception. *Nature Communications* **10**, 1907 (2019).  
859        <https://doi.org/10.1038/s41467-019-09664-2>
- 860    14    Cao, Y., Summerfield, C., Park, H., Giordano, B. L. & Kayser, C. Causal Inference in  
861        the Multisensory Brain. *Neuron* **102**, 1076-1087.e1078 (2019).  
862        <https://doi.org/10.1016/j.neuron.2019.03.043>
- 863    15    Arnal, L. H. & Giraud, A. L. Cortical oscillations and sensory predictions. *Trends*  
864        *Cogn Sci* **16**, 390-398 (2012). <https://doi.org/10.1016/j.tics.2012.05.003>
- 865    16    Sedley, W. *et al.* Neural signatures of perceptual inference. *eLife* **5**, e11476 (2016).  
866        <https://doi.org/10.7554/eLife.11476>
- 867    17    Lan, L. *et al.* Alterations of brain activity and functional connectivity in transition  
868        from acute to chronic tinnitus. *Human Brain Mapping* **42**, 485-494 (2021).  
869        <https://doi.org/10.1002/hbm.25238>
- 870    18    Schlee, W. *et al.* Reduced Variability of Auditory Alpha Activity in Chronic Tinnitus.  
871        *Neural Plasticity* **2014**, 436146 (2014). <https://doi.org/10.1155/2014/436146>

- 872 19 Weisz, N., Moratti, S., Meinzer, M., Dohrmann, K. & Elbert, T. Tinnitus perception  
873 and distress is related to abnormal spontaneous brain activity as measured by  
874 magnetoencephalography. *PLoS medicine* **2**, e153 (2005).
- 875 20 Corlett, P. R. *et al.* Hallucinations and Strong Priors. *Trends in Cognitive Sciences* **23**,  
876 114-127 (2019). [https://doi.org:https://doi.org/10.1016/j.tics.2018.12.001](https://doi.org/https://doi.org/10.1016/j.tics.2018.12.001)
- 877 21 Powers, A. R., Mathys, C. & Corlett, P. R. Pavlovian conditioning&#x2013induced  
878 hallucinations result from overweighting of perceptual priors. *Science* **357**, 596-600  
879 (2017). <https://doi.org:doi:10.1126/science.aan3458>
- 880 22 Shams, L. & Beierholm, U. Bayesian causal inference: A unifying neuroscience  
881 theory. *Neuroscience & Biobehavioral Reviews* **137**, 104619 (2022).  
882 <https://doi.org:https://doi.org/10.1016/j.neubiorev.2022.104619>
- 883 23 Rohe, T. & Noppeney, U. Cortical Hierarchies Perform Bayesian Causal Inference in  
884 Multisensory Perception. *PLOS Biology* **13**, e1002073 (2015).  
885 <https://doi.org:10.1371/journal.pbio.1002073>
- 886 24 Kayser, C. & Shams, L. Multisensory Causal Inference in the Brain. *PLOS Biology*  
887 **13**, e1002075 (2015). <https://doi.org:10.1371/journal.pbio.1002075>
- 888 25 Geng, J. J. & Vossel, S. Re-evaluating the role of TPJ in attentional control:  
889 Contextual updating? *Neuroscience & Biobehavioral Reviews* **37**, 2608-2620 (2013).  
890 <https://doi.org:https://doi.org/10.1016/j.neubiorev.2013.08.010>
- 891 26 Weisz, N., Hartmann, T., Müller, N., Lorenz, I. & Obleser, J. Alpha rhythms in  
892 audition: cognitive and clinical perspectives. *Frontiers in psychology* **2**, 73 (2011).
- 893 27 Song, J.-J. *et al.* The balance between Bayesian inference and default mode  
894 determines the generation of tinnitus from decreased auditory input: A volume  
895 entropy-based study. *Human Brain Mapping* **42**, 4059-4073 (2021).  
896 <https://doi.org:https://doi.org/10.1002/hbm.25539>

897

898



## 899 **Figure Legends**

900 **Figure 1:** Demographics of the participants from the two sets of studies. The figure shows  
901 overall summary statistics of the age, gender and hearing profiles of the two groups – same  
902 source, independent source perceivers in Part 1 with healthy young adults (displayed on the  
903 left) and tinnitus and control groups in Part 2 of the study (displayed on the right). The purple  
904 bars and lines represent the independent source perceivers group and the green bars and lines  
905 represent the same source perceivers group. The red bars and lines represent the tinnitus  
906 group and the blue bars and lines represent the control group.

907 **Figure 2:** Summary of methods. The figure displays the trial structure along with the duration  
908 of the stimulus, length of the response window and inter-trial intervals for the auditory and  
909 visual experiments during the behavioural and electrophysiological sections. The figure also  
910 displays the number of trials per block and the number of threshold-level, sub-threshold level  
911 and absent-trials across each block in the top right corner. This structure was retained for the  
912 two experiments.

913 **Figure 3:** Summary of results of the behavioural session. The figure displays the difference  
914 between the two groups – same source, independent source perceivers for Part 1 for auditory;  
915 tinnitus, control groups for Part 2 for auditory and visual thresholds in the first row. For Part  
916 1, percentage of hits and misses for the 75% likelihood stimuli, false alarms and correct  
917 responses for the stimulus-absent trials are displayed in the second row. The purple bars  
918 represent the independent source and the green bars represent the same source perceivers.  
919 The third and fourth row display the percentage of hits and misses for the 75% likelihood  
920 stimuli, false alarms and correct responses for the stimulus-absent trials for the tinnitus and  
921 control groups who are same source and independent source perceivers. The red bars are  
922 representative of the tinnitus groups and blue bars are that of the control group.

**Figure 4:** Summary of ERP results for the healthy young adults. The figure depicts the scalp maps and evoked response potentials for the hits and false alarms during stimulus presentation (top panels) and post stimulus presentation (bottom panels). The topographical plots are average amplitudes over the significant time points; the channels in bold show the significant cluster and bright green line on the ERP shows the significant time points. The ERP in dark green is indicative of the ERP of the significant cluster from the same source perceiver group and the ERP in purple is indicative of the independent source perceiver group.

**Figure 5:** Summary of ERP results for participants with false alarms during stimulus presentation in the auditory and visual experiments. The figure depicts the scalp maps and evoked response potentials for the hits and false alarms in the auditory (top panels) and visual (bottom panels) experiments. The topographical plots are average amplitudes over the significant time points; the channels in bold show the significant cluster and green line on the ERP shows the significant time points. The ERP in red is indicative of the ERP of the significant cluster from the tinnitus group and the ERP in blue is indicative of the same in the control group.

**Figure 6:** Summary of ERP results for participants with false alarms immediately after stimulus presentation in the auditory and visual experiments. The figure depicts the scalp maps and evoked response potentials for the hits and false alarms in the auditory (top panels) and visual (bottom panels) experiments. The topographical plots are average amplitudes over the significant time points; the channels in bold show the significant cluster and green line on the ERP shows the significant time points. The ERP in red is indicative of the ERP of the significant cluster from the tinnitus group and the ERP in blue is indicative of the same in the control group.

**Figure 7:** Summary of ERP results for participants without false alarms during stimulus presentation in the auditory and visual experiments. The figure depicts the scalp maps and evoked response potentials for the hits and correct responses in the auditory (top panels) and visual (bottom panels) experiments. The topographical plots are average amplitudes over the significant time points; the channels in bold show the significant cluster and green line on the ERP shows the significant time points. The ERP in red is indicative of the ERP of the significant cluster from the tinnitus group and the ERP in blue is indicative of the same in the control group.

**Figure 8:** Summary of ERP results for participants without false alarms immediately after stimulus presentation in the auditory and visual experiments. The figure depicts the scalp maps and evoked response potentials for the hits and correct responses in the auditory (top panels) and visual (bottom panels) experiments. The topographical plots are average amplitudes over the significant time points; the channels in bold show the significant cluster and green line on the ERP shows the significant time points. The ERP in red is indicative of the ERP of the significant cluster from the tinnitus group and the ERP in blue is indicative of the same in the control group.

**Figure 9:** Summary of time frequency analysis for the total alpha power and inter-trial phase clustering during and post stimulus. The top panel depicts the significant interactions during stimulus presentation for the auditory experiment with the healthy young adults. The purple bars are representative of the total alpha power in the independent source perceiver group and the green bar is representative of that of the same source perceiver group. The purple lines are representative of the ITPC in the independent source perceiver group and the green bar is representative of that of the same source perceiver group. The middle and lower panel shows the significant interactions during and post stimulus presentation for the auditory and visual experiments respectively for patients with tinnitus and their matched controls. The red bars

are representative of the total alpha power in the tinnitus group and the blue bar is representative of that of the control group. The red lines are representative of the ITPC for the tinnitus group and the blue lines are representative of that of the control group.

**Figure 10:** Summary of time frequency analysis for the total alpha power and inter-trial phase clustering pre stimulus. The top panel depicts the significant interactions pre-stimulus presentation for the auditory experiment with the healthy young adults. The purple bars are representative of the total alpha power in the independent source perceiver group and the green bar is representative of that of the same source perceiver group. The purple lines are representative of the ITPC in the independent source perceiver group and the green bar is representative of that of the same source perceiver group. The lower panel shows the significant interactions pre-stimulus presentation for the visual experiment for patients with tinnitus and their matched controls. The red bars are representative of the total alpha power in the tinnitus group and the blue bar is representative of that of the control group. The red lines are representative of the ITPC for the tinnitus group and the blue lines are representative of that of the control group.

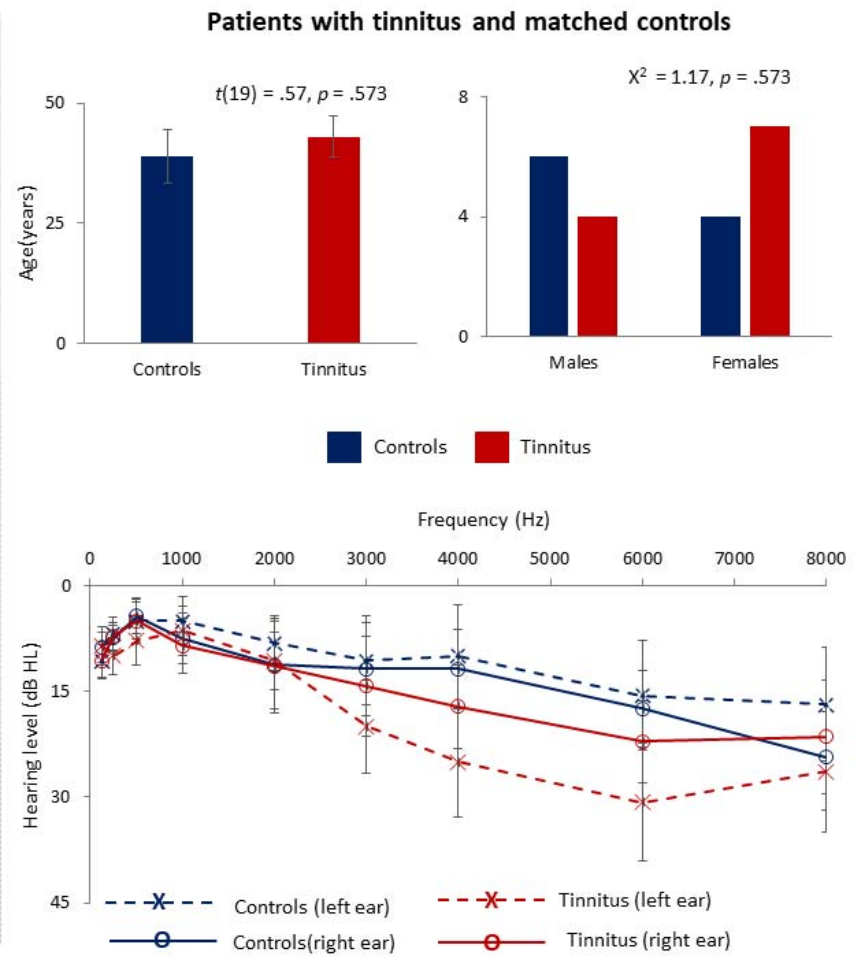
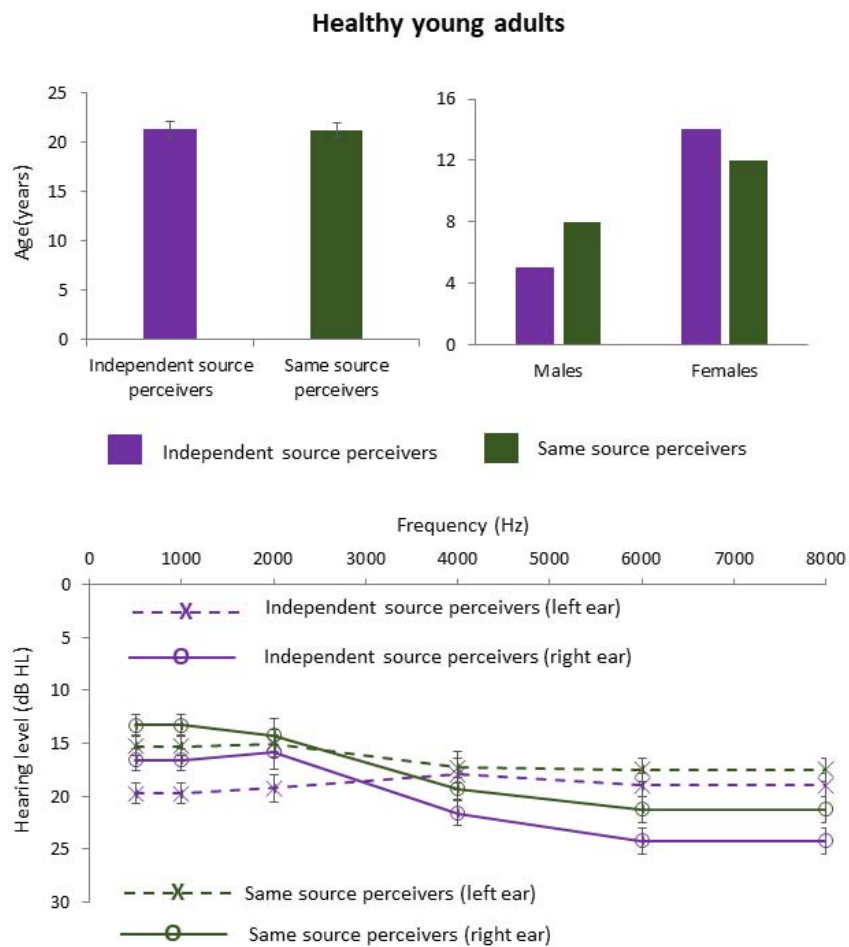
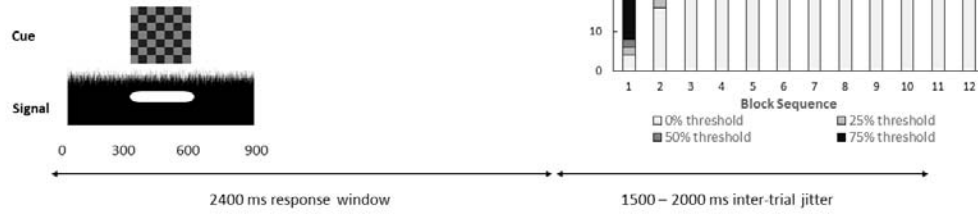


Figure 1

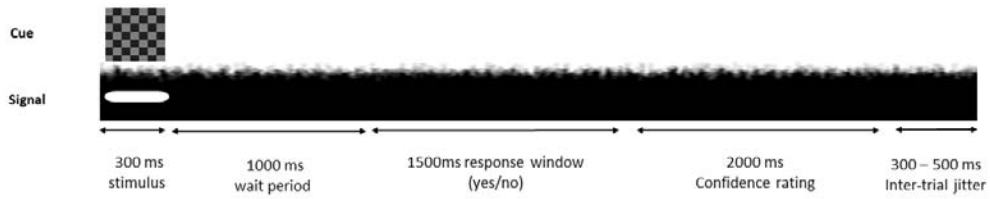
## Trial presentation across blocks in both auditory and visual experiments

### Auditory experiment

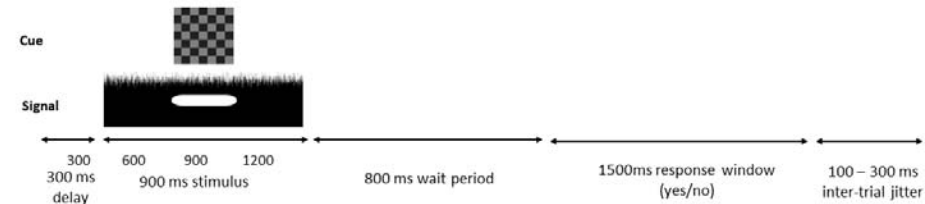
#### *Behavioral trial structure to determine threshold level*



#### *ERP trial structure (Healthy young adults)*



#### *ERP trial structure (Tinnitus vs Controls)*

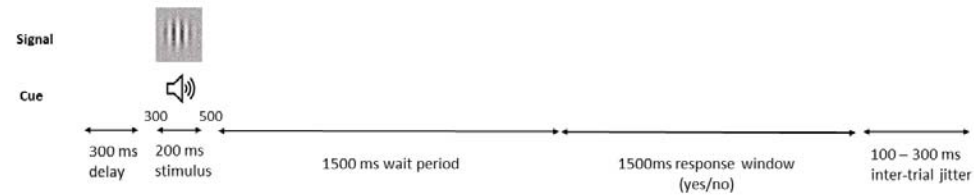


### Visual experiment

#### *Behavioral trial structure to determine threshold level*



#### *ERP trial structure*



990

991

Figure 2

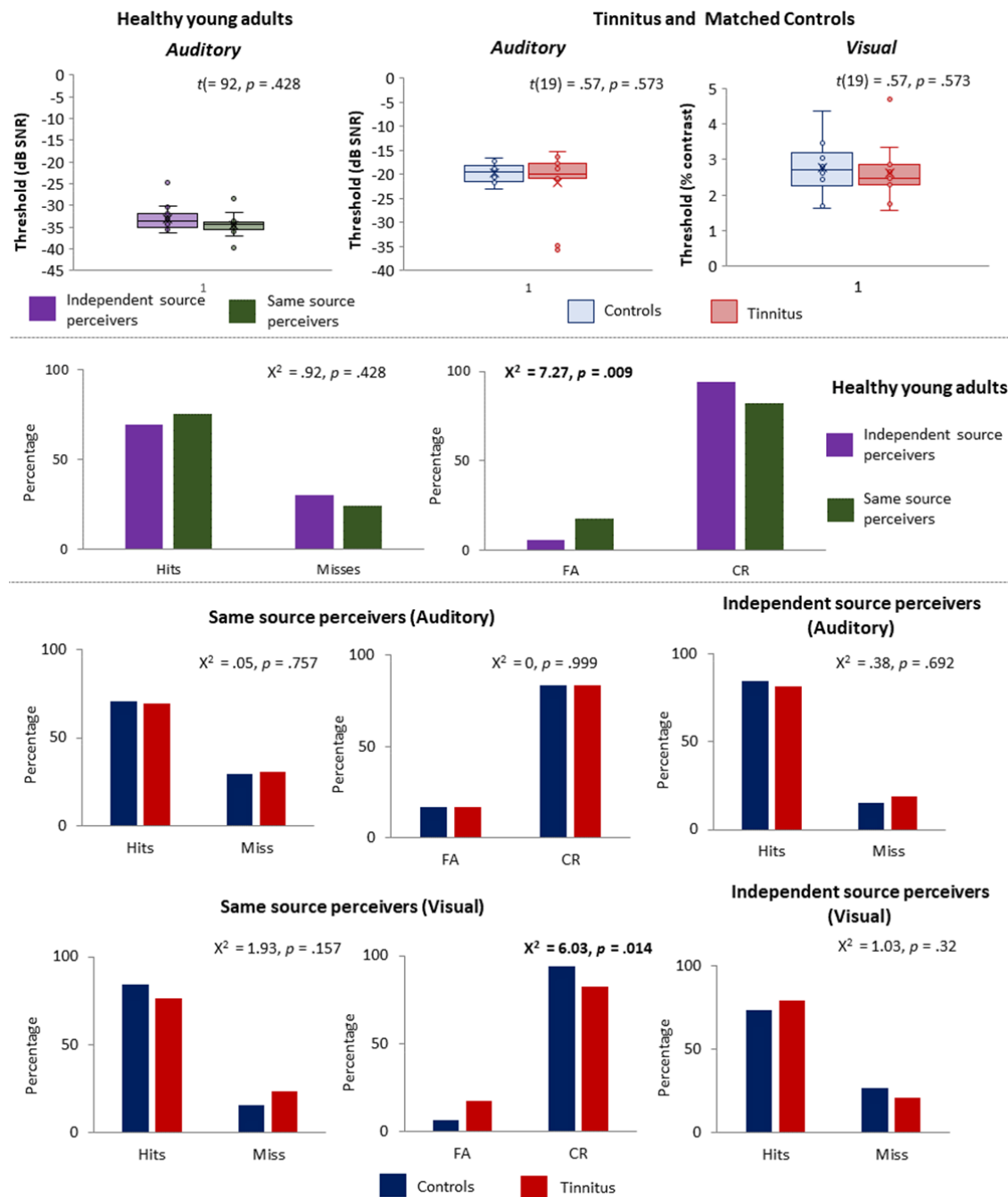


Figure 3



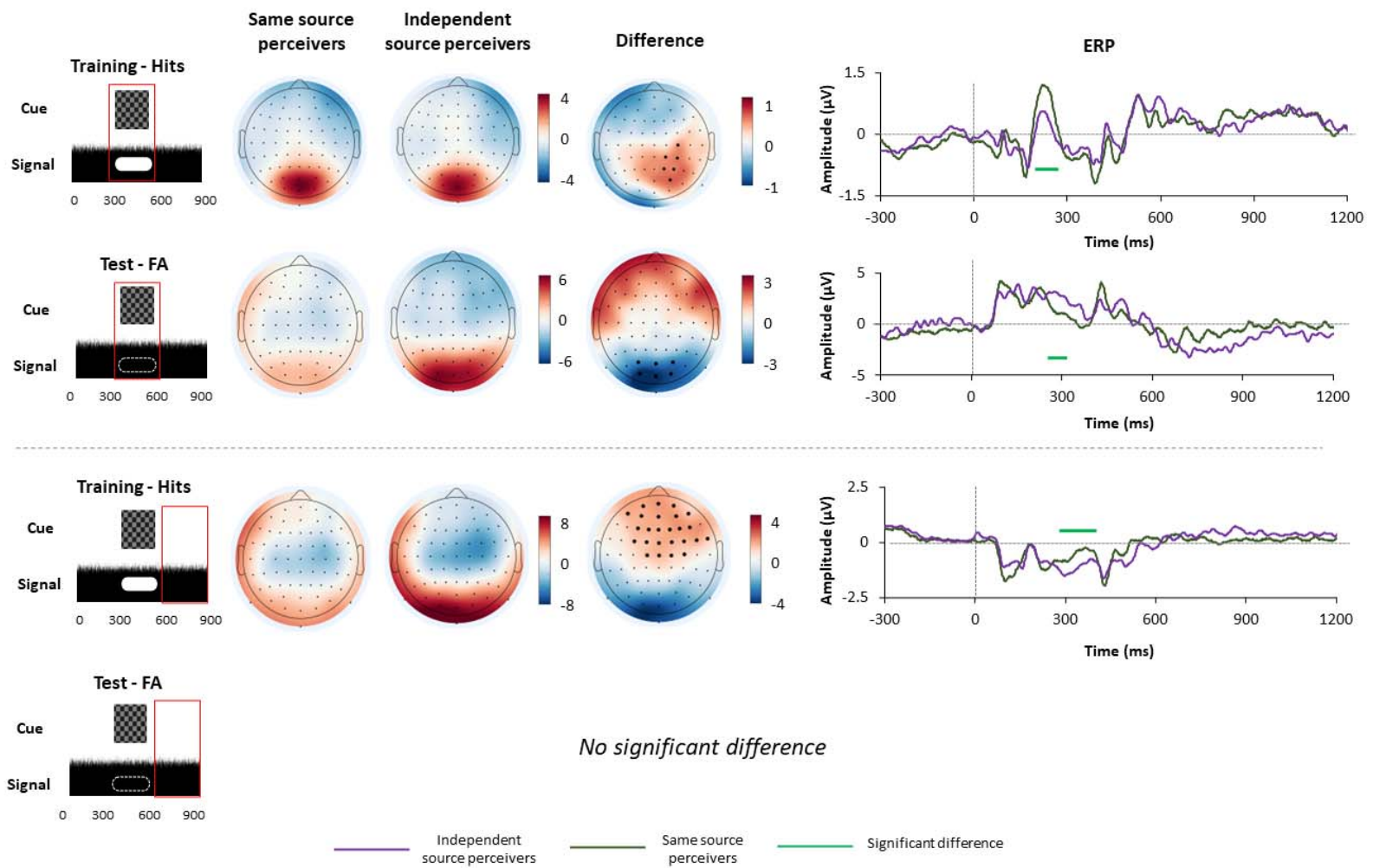


Figure 4

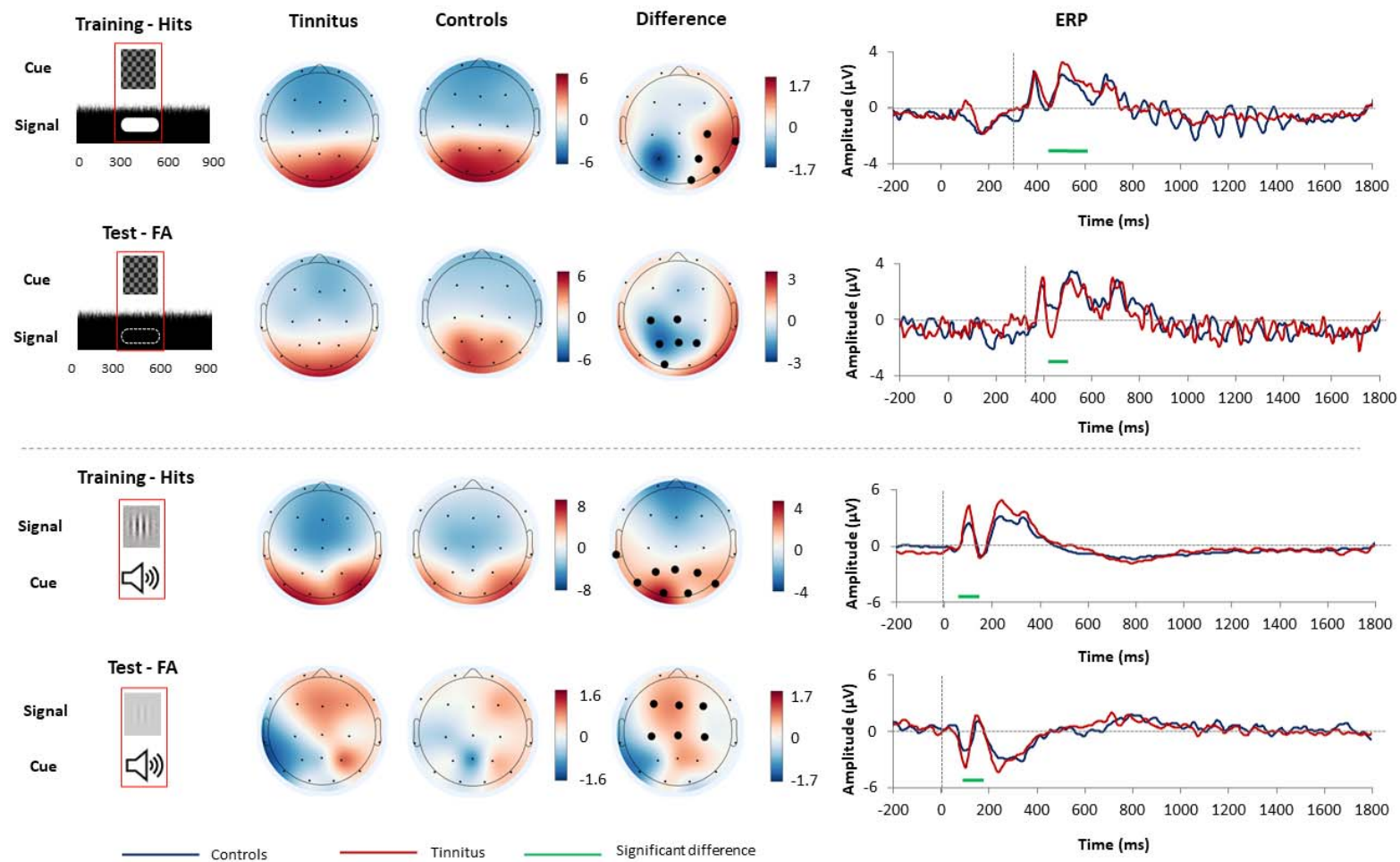


Figure 5

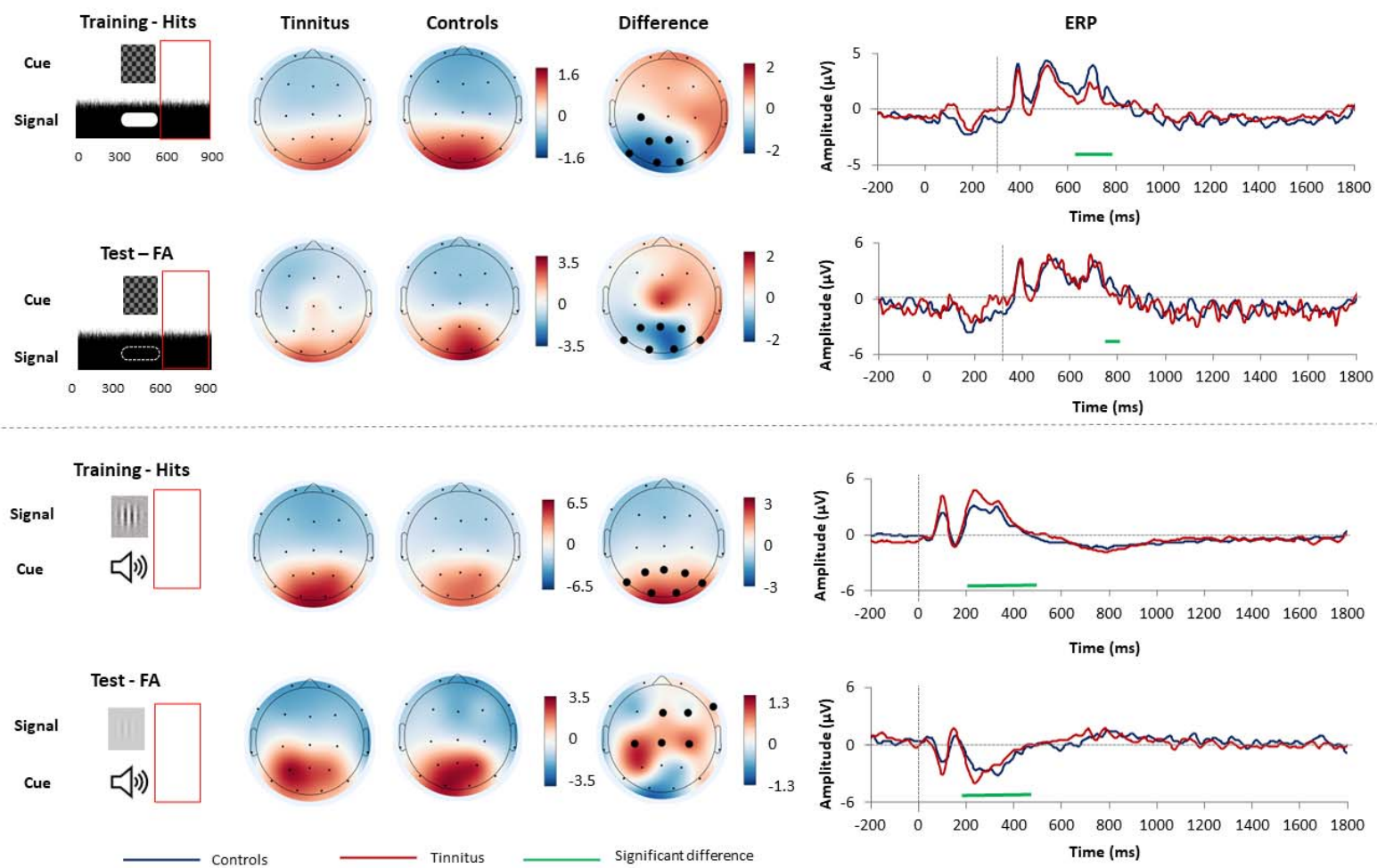


Figure 6

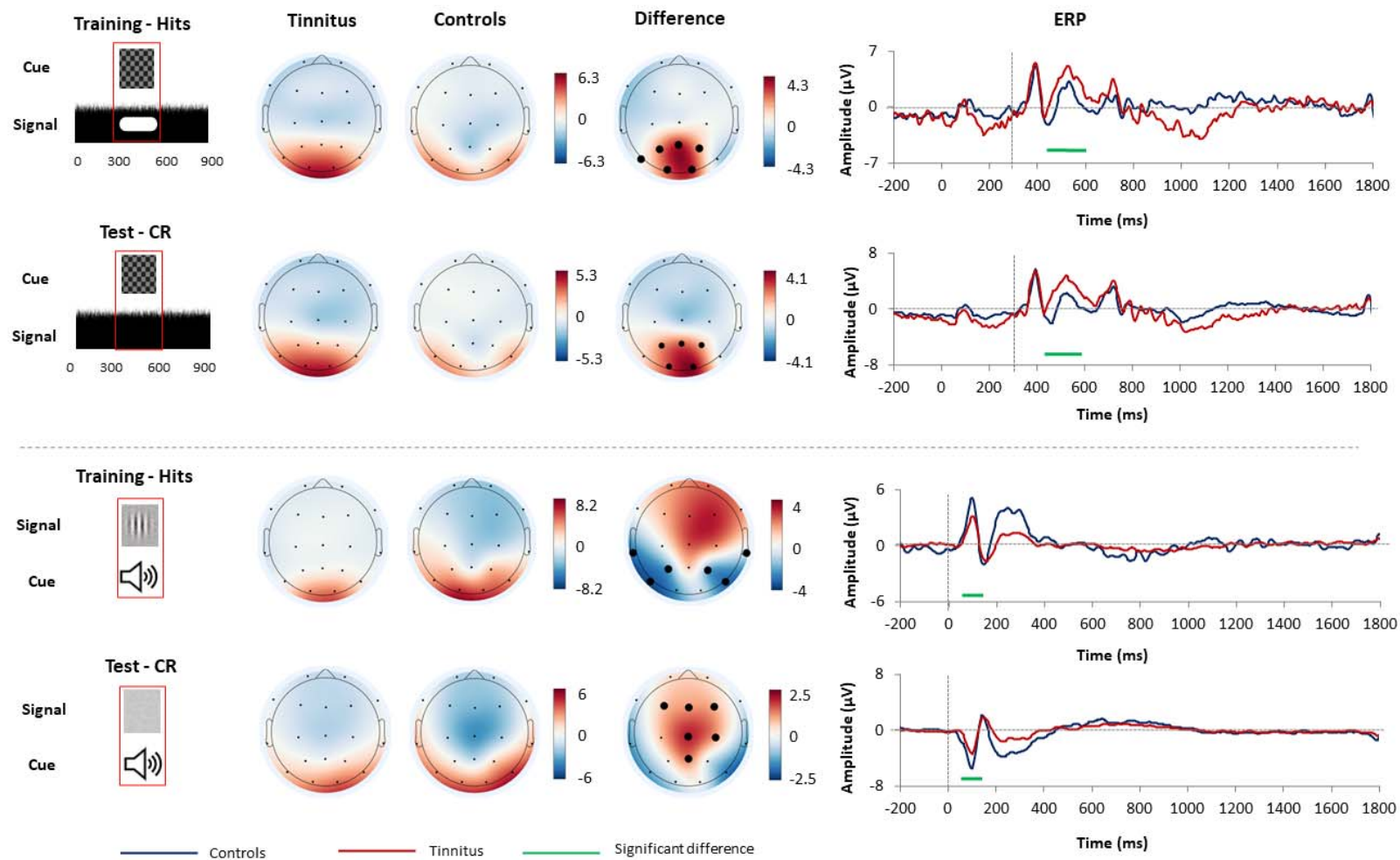
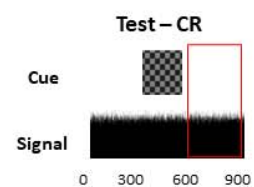
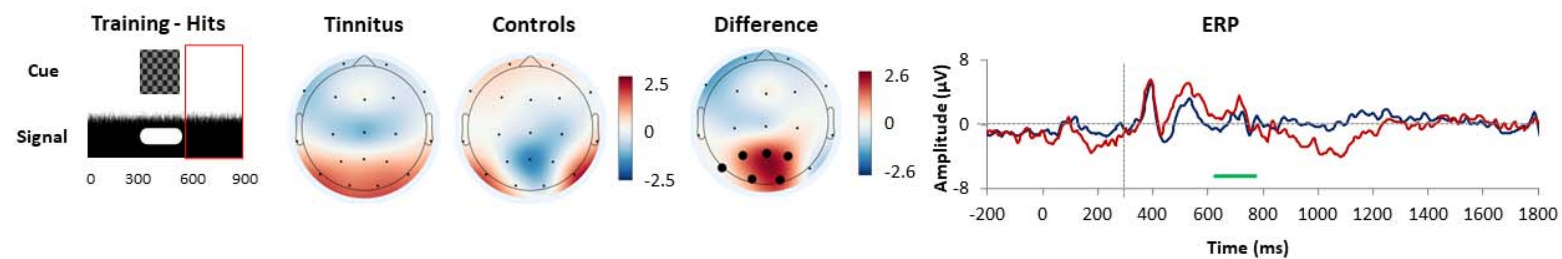
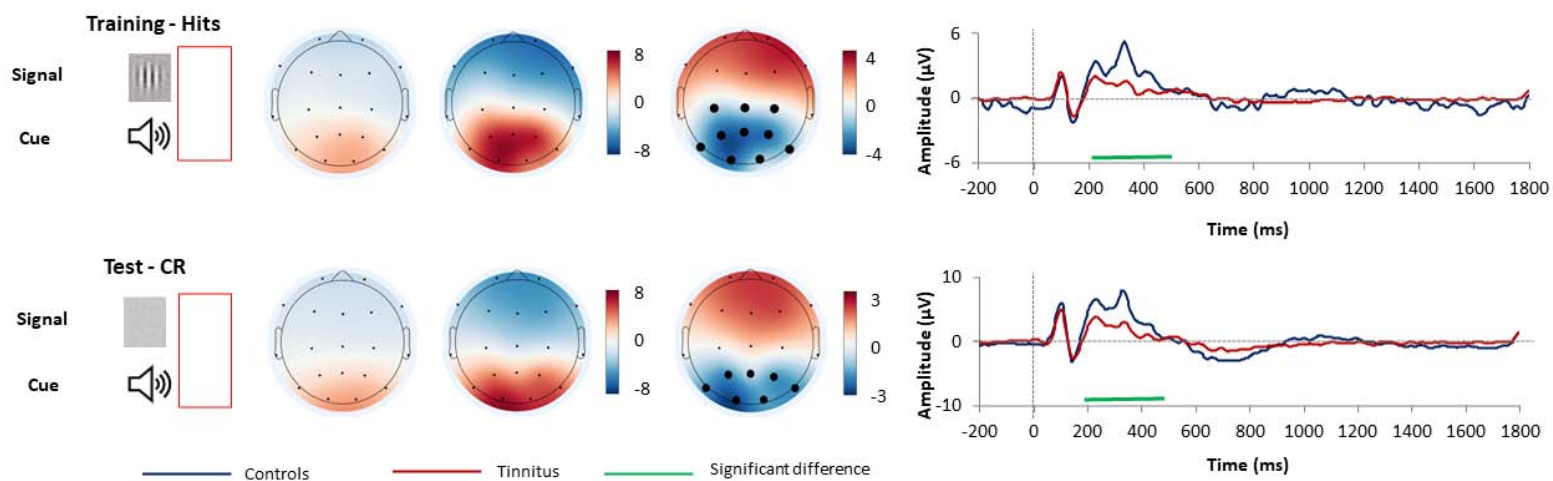


Figure 7





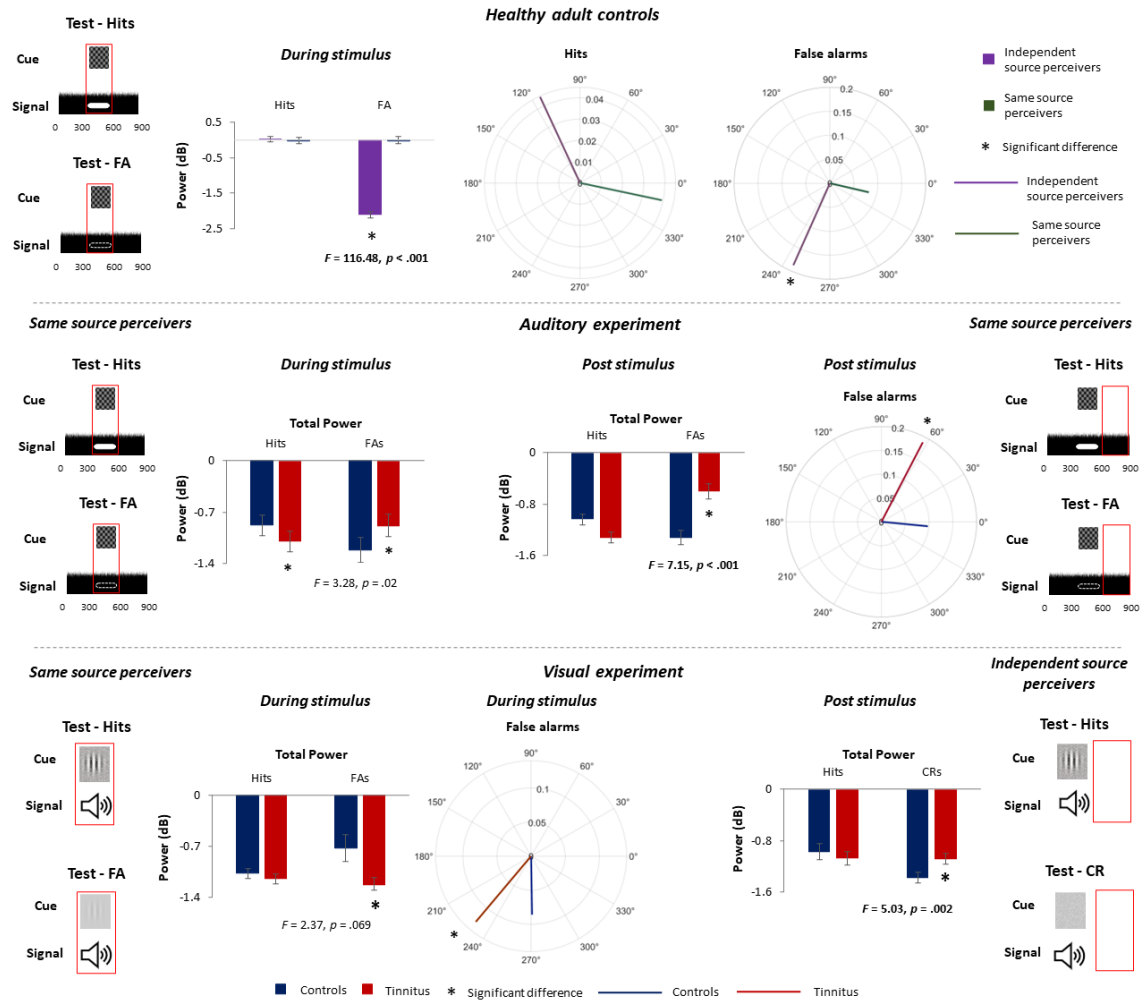
*No significant difference*



1003

1004

Figure 8



1005

1006

Figure 9

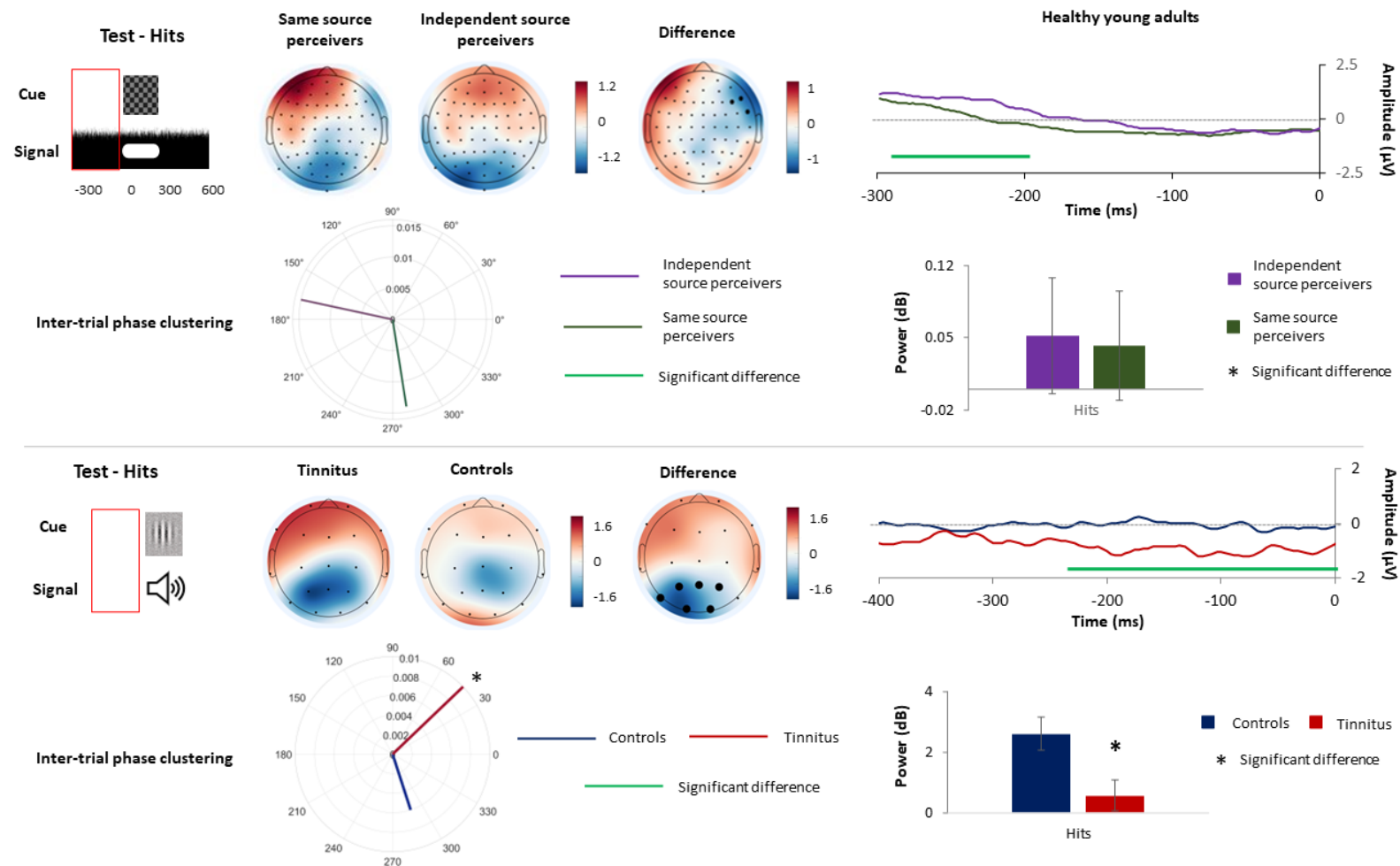


Figure 10





## Chronic auditory phantom perception – a sensory or a systemic disorder?

Journal:	<i>Psychophysiology</i>
Manuscript ID	PsyP-2023-0272
Wiley - Manuscript type:	Original Article
Date Submitted by the Author:	20-Sep-2023
Complete List of Authors:	Yasoda-Mohan, Anusha; Trinity College Faubert, Jocelyn Ost, Jan Kropotov, Juri; Institute of the Human Brain of Russian Academy of Sciences, laboratory of neurobiology of action programming Vanneste, Sven
Keywords:	Auditory Processes < Content/Topics, Visual Processes < Content/Topics, ERPs < Methods, Hearing/Vision Impaired < Groups Studied
Abstract:	The perception of a continuous phantom in a sensory domain in the absence of an external stimulus is explained as a maladaptive compensation of aberrant predictive coding, a proposed unified theory of brain functioning. If this were true, these changes would occur not only in the domain of the phantom percept but in other sensory domains as well. We confirm this hypothesis by using tinnitus (continuous phantom sound) as a model and probe the predictive coding mechanism using the established local-global oddball paradigm in both the auditory and visual domains. We observe that tinnitus patients are sensitive to changes in predictive coding not only in the auditory but also in the visual domain. We report changes in well-established components of event-related EEG such as the mismatch negativity, late positive potential and during the anticipatory pre-stimulus signal. Furthermore, deviations in stimulus characteristics were correlated with hearing loss and deviations in context with the tinnitus percept itself. These results provide an empirical confirmation that aberrant perceptions are a symptom of a systemic disorder transcending the domain of the percept.

SCHOLARONE™  
Manuscripts

1  
2  
3  
4  
5  
6  
7  
8  
9  
10  
11  
12  
13  
14  
15  
16  
17  
18  
19  
20  
21  
22  
23  
24  
25  
26  
27  
28  
29  
30  
31  
32  
33  
34  
35  
36  
37  
38  
39  
40  
41  
42  
43  
44  
45  
46  
47  
48  
49  
50  
51  
52  
53  
54  
55  
56  
57  
58  
59  
60

**Impact statement**

        This study is the first to show that phantom perceptions affect neural processes in sensory domains other than the one it occurs in, confirming that they are systemic solutions generated by the brain. This enables us to search for biomarkers of phantom percepts in more intact sensory systems rather than deafferented ones.

## Chronic auditory phantom perception – a sensory or a systemic disorder?

Anusha Yasoda-Mohan<sup>1,2</sup>, Jocelyn Faubert<sup>3</sup>, Jan Ost<sup>4</sup>, Juri D. Kropotov<sup>5</sup> & Sven

Vanneste<sup>1,2,4\*</sup>

1. Lab for Clinical and Integrative Neuroscience, Trinity College Institute for Neuroscience, School of Psychology, Trinity College Dublin, Ireland

2. Global Brain Health Institute, Trinity College Dublin, Ireland.

3. Faubert Lab, School of Optometry, University of Montreal, Montreal, Canada

4. Brain Research Center for Advanced International Innovative and Interdisciplinary Neuromodulation, Ghent, Belgium.

5. N.P. Bechtereva Institute of the Human Brain of Russian Academy of Sciences, St. Petersburg, Russia.

**Keywords:** tinnitus, predictive coding, sensory prediction error, contextual prediction error, strong-priors

**Correspondence to:** Sven Vanneste, Lab for Clinical and Integrative Neuroscience, Institute for Neuroscience, School of Psychology, Trinity College Dublin, College Green, Dublin 2, Ireland. Email: [sven.vanneste@tcd.ie](mailto:sven.vanneste@tcd.ie). Website: [www.lab-clint.org](http://www.lab-clint.org).

**Abstract**

The perception of a continuous phantom in a sensory domain in the absence of an external stimulus is explained as a maladaptive compensation of aberrant predictive coding, a proposed unified theory of brain functioning. If this were true, these changes would occur not only in the domain of the phantom percept but in other sensory domains as well. We confirm this hypothesis by using tinnitus (continuous phantom sound) as a model and probe the predictive coding mechanism using the established local-global oddball paradigm in both the auditory and visual domains. We observe that tinnitus patients are sensitive to changes in predictive coding not only in the auditory but also in the visual domain. We report changes in well-established components of event-related EEG such as the mismatch negativity, late positive potential and during the anticipatory pre-stimulus signal. Furthermore, deviations in stimulus characteristics were correlated with hearing loss and deviations in context with the tinnitus percept itself. These results provide an empirical confirmation that aberrant perceptions are a symptom of a systemic disorder transcending the domain of the percept.

## Introduction

The predictive coding model is now widely gaining recognition and consensus to explain the integrated functioning of the brain. The theory is that the brain maintains an internal prediction model with which it compares the incoming sensory information to produce its perception of the environment around it<sup>1-3</sup>. The difference between the prediction and the input is called a prediction error<sup>2</sup>. If the error is large and strong, it modifies the internal model by changing the prediction and thereby the percept<sup>2</sup>.

Perceptual disorders in different sensory domains such as tinnitus (a phantom ringing in the ears)<sup>4</sup>, chronic pain<sup>5</sup>, phantom smell<sup>6</sup> and taste<sup>7</sup>, Charles Bonnet syndrome<sup>8</sup> where patients perceive phantom images that are illogically related to the surrounding and other hallucinatory experiences are discussed as a maladaptive compensation of an aberration in the brain's predictive coding system<sup>3</sup>. This aberration is most commonly brought on by loss of sensory information in the domain of the phantom percept – hearing loss<sup>9</sup>, damage to peripheral nerve endings in the extremities<sup>10</sup>, sensorineural loss in the olfactory or gustatory system<sup>11</sup>, macular degeneration<sup>12</sup> etc. respectively. Although the deafferentation is limited to the sensory domain of the phantom percept, predictive coding is a much broader, higher-order systemic process that controls all the senses. So, the question now arises if the maladaptive predictive processing of the brain in any of these disorders is just limited to the domain of deafferentation or if it is a symptom of a disorder in higher-order processing that extends to other sensory domains as well.

In the current study, we use tinnitus as a model and probe the predictive coding system in the sensory domain of the percept and deafferentation (auditory) and a domain that is independent of it (visual). Tinnitus is a simple auditory phantom percept which is rarely accompanied by symptoms of psychosis<sup>13</sup>. The predictive coding model of tinnitus is comprehensively discussed by several researchers in the field and attempts to provide a universal and integrated explanation to the generation of a very heterogeneous disorder<sup>2,3,14,15</sup>.

The hypothesis is that the input to the model is a tinnitus precursor signal which becomes more precise and influential in the presence of hearing loss or other changes in the bottom-up pathways<sup>15</sup>. If this maladaptive activity is not minimised by the top-down inhibitory system, the prediction error produced by the strong tinnitus precursor signal can override the current prediction of perceiving silence in the absence of an external sound source and updating it to perceiving tinnitus<sup>15</sup>. With time, the brain learns that perceiving tinnitus may be the new normal leading to a chronic tinnitus percept that is difficult to modify<sup>15</sup>. The empirical evidence for tinnitus being a disorder of predictive coding is becoming more concrete<sup>16,17</sup>. In a recent study, the authors showed that tinnitus patients were more sensitive to auditory prediction errors<sup>18</sup> encoded by the previously well-established local-global oddball paradigm<sup>19-21</sup>. We are particularly interested if this maladaptive predictive processing in tinnitus surpasses the auditory domain to reflect changes in other sensory domains as well.

The current study uses the auditory (similar to the recent study<sup>18</sup>) and an equivalent visual adaptation of the local-global oddball paradigm to probe the predictive coding system of the brain and investigate maladaptive changes in tinnitus compared to non-tinnitus participants. Here we investigate two types of prediction errors – sensory and contextual – based on whether we change the *input* to the model or the *prediction* of the model. These prediction errors are empirically quantified using evoked response potential (ERPs) corresponding to the different stimulus sequences which are recorded using EEG. Subtracting the ERP of the frequent (standard, expected omission) from that of the rare (deviant, unexpected omission) sequences will generate a prediction error signal which has two signature components – (1) mismatch negativity (MMN), (2) late positive potential popularly known as the P300<sup>22,23</sup>. The MMN was first discovered in the auditory domain as a negative going potential between 100-250 ms post-stimulus onset in the frontal electrodes that encodes an automatic deviance in stimulus characteristics<sup>22</sup>. This has been explained under both the predictive coding framework<sup>24-26</sup> and

also under the neural adaptation framework where the change reflects a deviation from the adaptation of the neural groups to repetitive stimuli<sup>27,28</sup>. The MMN was later also identified in the visual domain<sup>29</sup>. In the context of the difference between the two omission sequences, the MMN becomes an early omission response capturing the pre-attentive, hierarchical predictive process<sup>21</sup>. The P300 is an attention-driven component which is a positive going potential 250 ms post-stimulus onset<sup>21,23</sup> that requires the participant to engage in the task actively or passively. In a three-stimulus oddball paradigm, where there are two rare stimuli with different probabilities, the more deviant stimulus shows a positive going potential in the fronto-central electrodes marking a shift in attention and the deviant with the less deviant stimulus shows a positive going potential in the parietal electrodes<sup>18,22,30</sup>.

Based on these previous findings, we hypothesise that if tinnitus were purely an auditory predictive processing disorder, we would expect to observe a significant difference between the tinnitus and control group in the prediction errors produced by sensory and contextual changes in the incoming stimuli during the MMN and P300 time frames only in the auditory but not in the visual domain. However, if tinnitus were more a systemic problem, these differences would transcend its domain of deafferentation (auditory) and be reflected in another sensory domain that is independent of it (visual) as well. Given the mechanistic similarity between tinnitus and other phantom percepts, showing that phantom percepts present changes in predictive coding reflected in sensory systems other than the domain of the percept would be a pivotal finding in understanding the neural mechanism underlying different perceptual disorders. One of the implications of this would be to propose the idea that phantom percepts may be a symptom of a higher-order systemic problem and the domain it manifests in may be triggered by the domain in which the deafferentation occurs i.e., hearing loss producing tinnitus or damage to nerve endings in extremities producing chronic pain etc.



**Materials and Methods**

The current study used the well-established local-global oddball paradigm and was implemented in both the auditory and visual domains. The participants consisted of participants with and without tinnitus. The study consisted of 4 blocks of auditory and visual stimulation with the experiment lasting up to an hour with breaks in between each block.

*Ethical statement*

The study was approved by the ethical committee at Trinity College Dublin and was in accordance with the Declaration of Helsinki. All participants gave explicit consent to participate. Tinnitus participants were patients who visited the Brain Research center for Advanced Innovative & Interdisciplinary Neuromodulation (Brai3n) clinic in Ghent, Belgium. Control participants were volunteers from the clinic and the community.

*Data and code availability statement*

The data and code are present with the corresponding author. They will be available on email request. Interested members may email the corresponding author. The anonymised data will be provided after removing the identifying personal information. The code will also be distributed on request with the corresponding author. The code may also be downloaded from [https://github.com/anushaYmohan/Tinnitus\\_aud\\_vis\\_ERP.git](https://github.com/anushaYmohan/Tinnitus_aud_vis_ERP.git)

*Participants*

The study consists of 16 participants with tinnitus ( $M = 47.87$  years,  $SD = 15.04$  years; 10 males, 6 females) and 13 participants without tinnitus ( $M = 42.85$  years,  $SD = 16.14$  years; 5 males and 8 females). The study was powered based on a recently published study<sup>31</sup>. The two groups were matched for age ( $t(27) = .87, p = .394, d = .32$ ), gender( $\chi^2 = 1.66, p = .197$ ) and

overall audiogram ( $F(3.34,60.68) = .822, p = .497$ , partial  $\eta^2 = .043$ ). These were determined using an independent samples  $t$ -test, a chi-square test and a repeated measures ANOVA with groups (tinnitus and control) as between-subjects variable, frequencies (explained below in the audiogram section) and side (left and right) as repeated measures. Exclusion criteria included Meniere's disease, chronic ear infections, otosclerosis, tumors, mental disorders and chronic eye disorders. All participants either had normal or corrected-to-normal vision. Patients presented with tinnitus anywhere between 3 months and 20 years.

### *Audiological and behavioural measures*

All participants underwent audiological measurements which included a pure tone audiogram testing the threshold of hearing at frequencies 125, 250, 500, 1000, 2000, 3000, 4000, 6000, and 8000Hz in both left and right ears according to the procedures prescribed by the British Society of Audiology. The overall audiogram of the participants from the two groups were matched as indicated above with the two groups showing a significant difference in the mean hearing loss calculated as the mean of the audiological thresholds at all frequencies in both ears ( $t(26) = 2.15, p = .041, d = .83$ ). However, there was no difference between the two groups for the measure of hearing disability measured at speech frequencies which is the mean of the hearing thresholds at 500, 1000, 2000 and 4000 Hz ( $t(26) = 1.79, p = .08, d = .69$ ) as used by the World Health Organisation<sup>32</sup>. This is particularly important given that the auditory stimulus is centered at 500 Hz. The pure tone audiogram, mean hearing loss and hearing disability thresholds for the two groups are displayed in Figure 1.

The tinnitus characteristics such as the loudness and distress were measured using self-report questionnaires. In addition, the tinnitus type (10 patients with pure tone, 2 patients with noise-like and 3 patients with a combination, 1 missing value) and laterality (3 patients with left-sided tinnitus, 2 patients with right-sided tinnitus, 5 patients with tinnitus on both ears

equally, 4 patients with tinnitus on both ears but with dominant left-sided tinnitus and no one with tinnitus on both ear with a dominant right-sided tinnitus, 2 missing values) were also recorded to understand the heterogeneity of the group. Tinnitus loudness and distress were measured using a visual analogue scale (VAS) for loudness ( $M = 5.24$ ,  $SD = 2.39$ ) and distress ( $M = 4.39$ ,  $SD = 2.51$ ). This is a 10-cm scale with end points at a 0 = “no tinnitus”/”no distress” and 10 = “as loud as imaginable”/ “suicidal levels of distress”. They also completed a self-report questionnaire for Tinnitus Handicap Inventory (THI) ( $M = 49.12$ ,  $SD = 20.24$ ) which is designed to assess the tinnitus-related distress and impact on their lives. Most participants filled out the Dutch-translated versions of the questionnaires except a few who opted for the English versions.

*Event-related potential (ERP) study using an oddball paradigm*

The main study encapsulates the use of EEG to record brain activity in response to auditory and visual stimuli that are played in a specific paradigm developed by Wacongne and colleagues<sup>21</sup>. The auditory segment consisted of three different stimulus sequences as shown in Figure 2 presented in different probabilities. The standard sequence consisted of four 500 Hz tones followed by one white noise burst; the deviant sequence consisted of five 500 Hz tones and the omission sequence consisted of four 500 Hz tones and a silence in the place of the 5<sup>th</sup> stimulus. Each stimulus was 50 ms in duration with a 7 ms rise-fall time separated by 250 ms. The sequences were matched to have the same RMS power. This particular paradigm was chosen based on the results of a recent paper<sup>31</sup>. The sounds were played binaurally through stereo headphones.

All stimuli were played at the most comfortable loudness level following the procedure of the recently published study<sup>31</sup>. This was determined by presenting the sequence with five tones at varying loudness levels going from full volume on the headphones (84 dB SPL) in 5

1  
2  
3 dB attenuation steps until it was 40 dB softer than the original sound and then increased in 5  
4  
5 dB attenuation steps back to full volume. For every sequence the participant was asked to rate  
6  
7 the loudness on a scale of 1 – 7, where 7 = “uncomfortably loud” and 1 = “very soft”. 4 was  
8  
9 considered most comfortable loudness. For those patients who were uncomfortable going  
10  
11 through the procedure since some of the sounds could be uncomfortably loud, we played some  
12  
13 of the softer sounds and let them choose what level they wanted to hear. The standard sequence  
14  
15 of the 4 tones followed by noise burst was chosen at the same attenuation level as the level  
16  
17 picked by the participant.  
18  
19  
20

21  
22 The visual equivalent of this paradigm consisted of 2 cycles per degree (cpd) sinusoidal  
23  
24 gratings and a visual noise. 2 cpd was used because this falls under the low-mid frequency range  
25  
26 just like the auditory stimuli. The standard visual sequence consisted of four sinusoidal gratings  
27  
28 followed by one visual noise stimulus (2x2 pixel binary noise); the deviant sequence was five  
29  
30 sinusoidal gratings; the omission sequence was 4 sinusoidal gratings followed by a blank screen  
31  
32 where the stimulus should’ve been. All stimuli were 100% contrast played on a grey mean  
33  
34 luminance background (49.58 cd/m<sup>2</sup>). The luminance output was gamma corrected and we used  
35  
36 the ‘Noisy Bits’ method for producing a continuous luminance resolution<sup>33</sup>. The image  
37  
38 dimensions were 1440 x 900 pixels with a bit depth of 24. The sinusoidal gratings of 900 pixels  
39  
40 in diameter was placed at the center of the image. The participants sat at 171 cm from the screen.  
41  
42 The stimuli were played on a 21” LED Dell Monitor.  
43  
44  
45

46  
47 The auditory and visual paradigms were played in four blocks – three blocks of oddball  
48  
49 presentation and one block consisting solely of omission sequences. Each block consisted of  
50  
51 125 trials. In the oddball blocks, 25 trials of the standard were first presented followed by 100  
52  
53 trials of standard, deviant and omission sequences pseudorandomly presented at 75%, 15% and  
54  
55 10% probability respectively so that no two similar type of deviants were presented  
56  
57 continuously and there were at least 2 standard between similar deviants. The omission block  
58  
59  
60

consisted of 125 trials of omission sequences. The inter-trial interval was jittered between 1400 – 1600 ms. This resulted in 300 standard, 45 deviant, 30 unexpected omission and 125 expected omission trials. The order of presentation was randomised between the visual and auditory paradigms and between the oddball and omission blocks in each paradigm. A short break was given between each block and between each paradigm.

*EEG data collection and pre-processing*

The stimuli were presented using PsyTask which was controlled by the WinEEG software. The EEG was sampled using Mitsar 201 amplifiers at 250 Hz. The data was collected using a 19 channel Mitsar EEG cap designed using the International 10-20 placement system. The data was band-pass filtered online from 0.1 – 70 Hz and was collected with a reference close to Cz. Offline, the data was re-referenced to an average reference, filtered between 0.55 – 45 Hz, cleaned for artifacts such as eyeblinks, saccades, muscle movements etc. using a temporal independent component analysis (ICA) using infomax algorithm and epoched between -400 and +2352 relative to the onset of the first stimulus of the sequence. The data was further manually inspected for epochs with large deviations and were cleaned before comparing the two groups. A multivariate ANOVA to test the difference between the number of ICA components remaining in the two groups and two paradigms after cleaning reveal no significant differences ( $F(2,26) = 1.14, p = .334, \text{partial } \eta^2 = .08$ ).

*ERP post processing and analysis*

The prediction error is defined as the difference between the incoming sensory input and the existing prediction<sup>2</sup>. When auditory and visual stimuli are presented in an oddball paradigm, the frequent sequence creates a sensory memory trace which acts as a prediction or expectation of the incoming input. The rare sequence creates a deviance from the expectation and the

1  
2  
3 difference between the two can be regarded as the prediction error. The prediction error signal  
4  
5 was calculated from the averaged ERPs from the single trial responses to each stimulus  
6  
7 sequence resulting in three different conditions in both the auditory and visual paradigms for  
8  
9 all participants: (1) deviant – standard; (2) unexpected omission – standard; (3) unexpected  
10  
11 omission – expected omission. The first two prediction errors represent a deviance in the  
12  
13 expectation of the sensory information of the 5<sup>th</sup> stimulus and represent a prediction error that  
14  
15 is driven by changes in stimulus characteristics. In (3), the stimulus characteristics of the  
16  
17 expected and unexpected stimuli are the same, but the difference between these stimuli is purely  
18  
19 a difference in expectation and can be conceived as a prediction error driven by changes in  
20  
21 contextual information  
22  
23  
24  
25

26         Given that there is a difference between the number of trials in the standard, deviant,  
27  
28 expected and unexpected omission sequences, the frequent stimuli were randomly chosen from  
29  
30 the available number to match the number of rare stimuli for each person, in each condition  
31  
32 mentioned above. The average ERP was calculated across the responses of the both the stimulus  
33  
34 sequences for all conditions and then subtracted as indicated above. This was repeated 45 times  
35  
36 for condition (1) and 30 times for conditions (2) and (3) for each participant in both groups and  
37  
38 both sensory paradigms. These numbers were based on the math that there will be 45 trials for  
39  
40 the deviant responses and 30 trials for the unexpected omission response given their 15% and  
41  
42 10% distribution over three blocks respectively. The average across the iterations were  
43  
44 compared between the two groups using an independent *t*-test for the length of the post-stimulus  
45  
46 epoch starting from the onset of the 5<sup>th</sup> stimulus for all channels using FieldTrip accounting for  
47  
48 the single trials. The result was cluster corrected at  $\alpha = 0.05$  and the number of comparisons  
49  
50 were corrected using Bonferroni correction at  $p = 0.008$  (for 6 conditions).  
51  
52  
53  
54  
55

56         The topographical plots were plotted for the mean of the time points that showed a  
57  
58 significant difference in the time frame of the MMN (100 – 250 ms) and P300 (> 250 ms) for  
59  
60

both the auditory and visual paradigms. The cluster of electrodes were determined from the result of the ERP analysis based on which electrodes showed a significant difference in similar time points in the time frames mentioned above. This resulted in three clusters for each condition mentioned above – MMN, early P300 and late P300 for all three prediction error conditions and an extra pre-stimulus timeframe for prediction error condition (3). The ERP for one of the electrodes in the cluster was plotted with the time points showing the significant difference between the two groups in the each of the time frames analysed above.

*Post-hoc correlation with behavioural data for the tinnitus group*

The mean amplitude in the pre-stimulus, MMN, early and late P300 components from the significant channel-time point clusters from the auditory domains for the prediction error conditions (1) and (2) were correlated with the mean hearing loss. The mean amplitude in the pre-stimulus, MMN, early and late P300 timeframes from the significant channel-time point clusters from both domains for the prediction error condition (3) was correlated with the VAS for loudness. The resulting correlations (for the timeframes and sensory domains) were corrected for multiple comparisons using Benjamini-Hoschburg method using a false discovery rate of 0.30.

**Results**

Overall, there is a significant difference between ERPs of the controls and tinnitus groups in each of the prediction error conditions. The pattern of significant difference between the two groups for the prediction error conditions (1) and (2) in the visual domain and for prediction error condition (2) in the auditory domain show a similar trend. However, the pattern of significant difference between the two groups for prediction error (1) in auditory domain is

quite the opposite. Interestingly, the pattern of significant difference between the two groups for prediction error condition (3) show a similar trend in both the auditory and visual domains.

*Prediction error condition 1: Difference between standard and deviant stimulus sequences*

In the auditory domain, we observe a significant difference between tinnitus and control groups in the pre-stimulus, MMN (100 – 250 ms), early P300 (300-500 ms) and late P300 (500-700 ms) time frames. Particularly, we observe an increase in negative polarity for the pre-stimulus in the parietal electrodes, MMN time frame in the frontal electrodes, a decrease in positivity in the early and increase in positivity in the late P300 time frame in the parietal and frontal electrodes respectively. The cluster of electrodes showing significant difference are shown in BOLD on the first rows of the Figures 3, 4, 5 and 6 with the corresponding ERP showing one of the electrodes with the significant time points. The channel-time point clusters that were significant in the post-stimulus epoch had a  $t$ -value ranging between 296.94 and 2234.7 and in the pre-stimulus between 281.12 and 1230.7 with  $p < .001$ . The clusters plotted are the ones with the highest  $t$ -value.

In the visual domain, we also observe a significant difference between the tinnitus and control groups in the pre-stimulus, MMN (100 – 250 ms), early (300 – 400 ms) and late (500 – 1000 ms) time frames. From a topographical view, we observe an increase in lateralised positivity in the prestimulus condition, a less negative amplitude shown as an increase in positivity in the posterior-occipital electrodes corresponding to the decreased negativity of the ERP in the MMN timeframe for the tinnitus group. On the other hand, we observe an increase in positivity of the mean early P300 amplitude and a decrease in positivity of the late mean P300 amplitude in the parietal-occipital electrodes which is reflected in the corresponding ERP. The channel-time point clusters there were significant in the post-stimulus epoch had a  $t$ -value ranging between 498.41 and 4075.9 and in the pre-stimulus between 229.15 and 1381 with  $p <$



.001. The cluster of electrodes showing these changes are signified in BOLD. These changes are reflected in row 3 in Figures 3, 4, 5 and 6. The clusters plotted are the ones with the highest  $t$ -value.

*Prediction error condition 2: Difference between standard and unexpected omission stimulus sequence*

In the auditory domain, we observe a significant difference between the two groups in the pre-stimulus, MMN (100 – 250 ms), early P300 (250 – 600 ms) and late P300 (700-900 ms). Particularly, we observe an increased positivity and decreased negativity in the tinnitus group shown as an increased positivity in the parietal-occipital and central-parietal electrodes in the pre-stimulus and MMN time frame respectively. On the contrary, we observe an increase in positivity of the early P300 amplitude in the fronto-central electrodes and a decrease in positivity of the late P300 amplitude in central-posterior electrodes in the tinnitus group. These changes are reflected in the corresponding ERPs. The channel-time points showing a significant difference between the two groups in the post-stimulus epoch has a  $t$ -value ranging between 294.36 and 1313.88 and in the pre-stimulus between 235.27 and 2094.6 with  $p < .001$ . The cluster of electrodes showing these changes are shown in BOLD. These changes are reflected in row 2 in Figures 3, 4, 5 and 6.

In the visual domain, we see a pattern similar to the auditory domain with significant difference between the two groups in the pre-stimulus, MMN (100 – 200 ms), early P300 (300 – 400 ms) and late P300 (650 – 950 ms) timeframes. We observe an increase of positivity in the pre-stimulus condition lateralised to the left. In the rest of the conditions, the similarity in pattern of changes with the auditory domain, although changes in electrode location, maintains the same trend. We observe a decrease in negativity of the MMN in the tinnitus group represented by the red cluster of electrodes in the parietal-occipital electrodes; increase in

positivity of the early P300 and decrease in positivity of the late P300 amplitude in the parietal-occipital cluster of electrodes. These changes are evident in the respective ERPs. The channel-time point cluster showing a significant difference between the two groups in the post-stimulus epoch has a  $t$ -value ranging between 562.76 and 2084.4 and in the pre-stimulus between 240.83 and 1860 with  $p < .001$ . The cluster of electrodes showing these changes are shown in BOLD. These changes are reflected in row 4 in Figures 3, 4, 5 and 6.

*Prediction error condition 3: Difference between expected and unexpected omission sequences*

In the auditory domain, we observe a significant difference between the controls and tinnitus groups in the pre-stimulus, MMN (100 – 250 ms), early P300 (250 – 400 ms) and late P300 (500 – 700 ms) timeframes. Particularly, we observe increased positivity in the pre-stimulus, MMN, early P300 and late P300 amplitude in the parietal-occipital, fronto-central electrodes and central-parietal electrodes in the tinnitus group. These changes are reflected in the ERP shown correspondingly. The channel-time point cluster showing a significant difference between the two groups in post-stimulus epoch has a  $t$ -value ranging between 294.93 and 2068 and in the pre-stimulus between 228.63 and 1903.9 with  $p < .001$ . The cluster of electrodes showing these changes are shown in BOLD.

In the visual domain, we observe a very similar effect as the auditory domain with a significant difference between the tinnitus and controls groups in the MMN (100 – 200 ms), early P300 (300 – 400 ms) and late P300 (500 – 1000 ms) timeframes. Particularly, we observe an increase in positivity in the MMN amplitude in the electrodes in the occipital region; an increased positivity in early P300 amplitude in the frontal and late P300 amplitude in the central electrodes in the tinnitus group. These changes are reflected in the ERP shown correspondingly. The channel-time points showing a significant difference between the two groups in the post-

stimulus epoch has a  $t$ -value ranging between 322.85 and 3120.8 and in the pre-stimulus between 293.35 and 3015.7 with  $p < .001$ . The cluster of electrodes showing these changes are shown in BOLD.

The changes in the auditory and visual domain are represented in Figure 7 and the results of the changes in the sensory and contextual prediction errors in the tinnitus group in the three timeframes are summarised in Table 1.

*Post-hoc correlations with behavioural data*

For prediction error condition 1, mean hearing loss was not significantly correlated with the mean amplitude in the pre-stimulus ( $r = -.005, p = .987$ ), in the MMN timeframe ( $r = .30, p = .271$ ), early P300 ( $r = -.06, p = .815$ ) and late P300 ( $r = -.27, p = .334$ ) time frames. For prediction error condition 2, mean hearing loss was not significantly correlated with the mean amplitude of the ERP in the pre-stimulus ( $r = .10, p = .713$ ), MMN ( $r = -.11, p = .699$ ), mean early P300 ( $r = .24, p = .393$ ) and late P300 ( $r = -.20, p = .469$ ) time frames.

For prediction error condition 3, in the auditory domain, VAS for loudness was not significantly correlated with the mean amplitude of the ERP in the pre-stimulus ( $r = .03, p = .904$ ), MMN ( $r = .04, p = .871$ ), early P300 ( $r = -.05, p = .841$ ) and late P300 ( $r = .08, p = .766$ ) time frames in the auditory domain. However, in the visual domain, VAS for loudness was significantly correlated with the mean amplitude of the ERP in the early P300 ( $r = .60, p = .014$ ), but not in the pre-stimulus ( $r = .08, p = .774$ ), MMN ( $r = -.39, p = .131$ ) and late P300 ( $r = .23, p = .393$ ) time frames. These correlations are show in Figure 7.

**Discussion**

In the current study we use tinnitus as a model to investigate if phantom perception is a result of aberrant predictive processing only in their respective deafferented sensory domains or

whether it reflects an anomaly in higher-order predictive processing which extends to other sensory domains as well. We probe the predictive coding system using auditory and visual stimuli designed using the well-established local-global oddball paradigm<sup>21</sup> with three stimulus sequences (standard, deviant, omission). Subtracting the responses of frequent (standard, expected omission) from the rare (deviant, unexpected omission) sequences, we get two kinds of prediction errors – sensory and contextual. Sensory prediction errors characterise a deviance based on changing the stimulus characteristics of the incoming information, whereas contextual prediction errors characterise a deviance based on changing the expectation of the same incoming information. We demonstrate that tinnitus affects processing of sensory and contextual prediction errors in the deafferented sensory domain (auditory) and a domain independent of it (visual).

### *Effect of phantom perception on sensory prediction errors*

Previous research in tinnitus about changes in prediction errors was solely conducted in the auditory domain. Most work surrounded the examination of the MMN and these results were inconsistent across studies showing increased<sup>34</sup>, decreased<sup>35,36</sup> or no changes<sup>37</sup> in MMN amplitude in the tinnitus group when tones were presented at frequencies distant from that of their hearing loss (similar to the current study). In schizophrenia, however, research showed a consistent and robust decrease in MMN amplitude<sup>38,39</sup>. Furthermore, studies in patients with hallucinations reveal decreased MMN amplitude compared to non-hallucinating patients and healthy controls<sup>39</sup>.

In the auditory domain, the pattern of sensitivity of the tinnitus group to sensory prediction errors across the different timeframes depends on the stimulus characteristics of the incoming stimulus. In the pre-stimulus, MMN and late P300 timeframe, patients are more sensitive to a deviance but less sensitive to an absence of the 5<sup>th</sup> stimulus than controls. However, in the early

P300 timeframe, patients are less sensitive to a deviance and more sensitive to the absence of the 5<sup>th</sup> stimulus than controls. The MMN and P300 to the deviant with the lower probability (omission) was observed in the frontal electrodes and the P300 to the deviant with the higher probability (deviant) was observed in the parietal electrodes. This former is called a P3a whereas the latter is called a P3b and the location of these components depending on the probability of the deviants and sensory domain has been established in the classic oddball literature<sup>23,40,41</sup>.

On the contrary, the pattern of sensitivity of the tinnitus group to sensory prediction errors across the different timeframes is consistent for both conditions in the visual domain. Patients are less sensitive in the pre-stimulus, MMN and late P300 timeframes but more sensitive in the early P300 timeframe to both sensory prediction errors (i.e., (1) deviant – standard and (2) unexpected omission – standard) than controls. This variability in processing sensory prediction errors between the visual and auditory domain, may be attributed to the fact that tinnitus patients have hearing loss, which is not compensated during the task, whereas any deficits in processing the visual field is corrected using spectacles. Although not reflected in the correlation, in the presence of deafferentation, we observe an increase in the automatic response to a deviant stimulus, but a decrease in higher order processing of the stimulus-driven prediction error. It is important to note that the pattern of changes in sensitivity of tinnitus patients to the omission of the 5<sup>th</sup> auditory stimulus is similar to that of both prediction errors in the visual domain (which, for the purposes of this task, is free of deafferentation). Previous research argues that changes in the brain response to the omission of a stimulus can only be explained by predictive coding and not by neural adaptation theories<sup>21</sup>. Therefore, the changes in both sensory prediction errors in the visual domain and prediction error (2) in the auditory domain may be directly attributed to aberrations in a higher-order predictive coding system orchestrated by the presence of tinnitus.

### *Effect of phantom perception on contextual prediction errors*

Unlike with sensory prediction errors, the tinnitus group is more sensitive to prediction errors driven by changes in the context of the incoming stimulus compared to controls, in all timeframes in both the auditory and visual domains. This is consistent with the recently published study<sup>18</sup>. In the auditory domain, the early omission response of the contextual prediction errors is observed in the frontal electrodes, whereas its visual equivalent is observed in the occipital electrodes. Apart from that, the changes in the early and late P300 components in the tinnitus group in the auditory and visual domains seem to originate from similar sources seen from the similarity in the location of the dipole. The consistency of the results between the auditory and visual domain and the correlation of the amplitude of the early omission response in the auditory domain with the loudness of the tinnitus controlling for hearing loss and age, provide compelling evidence that this may be a correlate of the phantom perception itself rather than the hearing loss. Furthermore, from the results of the recently published study and our current study, we observe that irrespective of the amount of hearing loss, tinnitus patients are more sensitive to contextual prediction errors which further bolsters these prediction errors as a possible neural correlate of phantom perception.

Sensitivity to changes in the context of the incoming stimulus in tinnitus is also seen in the pre-stimulus timeframe. The pre-stimulus timeframe reflects the anticipation to the upcoming information<sup>16</sup>. In the auditory domain, we observed decreased sensitivity to this anticipation in tinnitus in the central electrodes which was different from the results of the recently published study<sup>18</sup>. This difference may be attributed to the auditory deafferentation. In the presence of hearing loss, the incoming auditory signals become less precise than there was no hearing loss, and possibly reflect in the anticipatory signal in the pre-stimulus condition. This may also be seen from the visual domain (where deafferentation is compensated by spectacles) that the

anticipatory signal is more positive in the central electrodes as observed in the recent study. Changes in the anticipatory signal support the strong-prior hypothesis of generation of hallucinations<sup>42-44</sup>. The authors argue that patients who are more likely to perceive hallucinations tend to allocate abnormally more weight to the prediction rather than the incoming stimulus. Therefore, the resulting percept is biased towards the prediction<sup>45</sup>. In the example of tinnitus, irrespective of whether the evidence the brain receives is enough to support tinnitus perception, if the person tends to place abnormally high weight to predicting the occurrence of tinnitus, their percept would be shifted closer towards perceiving tinnitus. This is referred to by some researchers as an “inferential leap”<sup>46</sup> and would explain why tinnitus develops irrespective of the hearing loss. With experience dependent plasticity, this acute tinnitus perception could become chronic thereby changing the default prediction of the brain<sup>15</sup>.

The changes in pre-stimulus anticipatory signal localised to the central-parietal electrodes is in support of this hypothesis. Such an orientation of the dipole possibly reflects changes in activity originating in the posterior cingulate cortex (PCC). The PCC is a key hub in the default mode network whose vital function is to generate a mental model of the self<sup>47</sup>. The PCC plays a central role in self-perception, supporting internally-directed cognition, regulating the focus of attention, and autopilot behaviour<sup>48,49</sup>. Furthermore, the PCC is associated with the detection of environmental changes, subsequent alterations in prior predictions<sup>50</sup> and is also a part of the auditory predictive coding network<sup>18</sup>. A possible increase in activity in the PCC during the anticipatory phase in the tinnitus group may be reflective of a different state of the brain than the control group.

*A predictive coding approach to treatment strategies*

Considering the sensory and contextual prediction errors from the framework of the tinnitus predictive coding model, we see that tinnitus patients are less sensitive to changes in input

characteristics and more sensitive to changes in prediction. This is an important finding providing an explanation as to why most treatments fail to change the tinnitus percept. According to the predictive coding model, chronic tinnitus is the new prediction, or the new state of the brain<sup>15</sup>. Treatments like sound stimulation<sup>51-53</sup>, hearing aids<sup>54</sup> and cochlear implants<sup>55</sup> etc. can be viewed from this perspective as changing the input to the brain. However, from the current study, we observe that providing a different auditory input (prediction error (1)) may be impacting the hearing loss rather than the tinnitus itself. From the visual domain, where there is no practical deafferentation, and from prediction error (2) in the auditory domain, we observe that the tinnitus itself may be neurophysiologically less sensitive to changes to just the characteristics of the incoming input. This could explain why sometimes the tinnitus comes back when the treatment is stopped – because they do not attempt to change the state of the brain, but just the input that it receives. Therefore, a more effective way may be to leverage the increased sensitivity of tinnitus to changes in predictions as a driving force to work with modulating the state of the brain, in addition to existing methods to modulate the input to the brain, for long-term suppression of the tinnitus percept itself.

### *Limitations*

The current study provides empirical evidence to phantom percepts being a systemic disorder rather than an auditory processing disorder. However, like any other study, it comes with some limitations. It is important to keep in mind that sensory ERP signals are accompanied by noise. Although the current study looks at group differences, it will be important to keep in mind the low number of trials in the unexpected omission condition while interpreting the results. This has been addressed by equating the number of trials in the expected and unexpected omission conditions. Secondly, it is important to keep in mind that increase and decrease in sensitivity to auditory and visual ERP components explains the positioning of the dipoles. Even



though at a scalp level there may be a negative polarity at some electrodes, the source level information might be different. Therefore, it would be beneficial to perform this experiment inside an MRI scanner to better grasp the source-level changes of these scalp-level potentials.

**Conclusion**

From the current study, we therefore see that phantom percepts not only reflect changes in predictive coding in their own sensory domains but transcend to other sensory domains. Particularly patients with phantom perception are differently sensitive to prediction errors driven by changes in stimulus characteristics and changes in context. We provide neural correlates that are specific to the deafferentation and to the percept itself showing that the changes in the predictive coding model are not dependent on the domain of deafferentation. Furthermore, the consistency between the results of the auditory and visual domain for contextual prediction errors and the positive correlation between the mean amplitude of the early pre-attentive auditory processing and the loudness measure provides compelling evidence that phantom percepts are not simply an auditory predictive processing disorder but possibly a symptom of a more systemic change in the higher-order predictive coding mechanism transcending the auditory domain. Furthermore, in a disease state, the perception of sensory phantoms may be reflective of a change of the state of the brain in terms of a change in the prediction to perceive the phantom as the new default.

### **Funding**

One of the authors was funded by the Government of Ireland Postdoctoral Fellowship 2020-2022 (GOIPD/2020/663) and the Royal Irish Academy Charlemont Grant 2021 and another one of the authors was funded by the State Assignment of the Ministry of Education and Science of the Russian Federation.

### **Competing interest**

The authors have no competing interests.

### **Data availability statement**

The data will be made available on request by email to the corresponding author.

**Table 1: Summary of results showing changes in the mean amplitude of the sensory and contextual prediction errors in the tinnitus group compared to the control group for the different timeframes**

Condition	Sensory domain	Pre-stimulus	MMN	Early P300	Late P300
<i>Sensory prediction errors</i>					
Deviant (-) Standard	Auditory	↓ (-628ms to -496ms) in parietal electrodes	↑ (175-260ms) in frontal electrodes	↓ (348-452ms) in parietal electrodes	↑ (644-836ms) in frontal electrodes
	Visual	↑ (-144ms to -48ms) in parietal electrodes	↓ (156-348ms) in occipital electrodes	↓ (448-612ms) in parietal - occipital electrodes	↓ (820-916ms) in occipital electrodes
Omission (-) Standard	Auditory	↑ (-440ms to -240ms) in parietal electrodes	↑ (124-256ms) in parietal electrodes	↑ (500-600ms) in frontal-central electrodes	↓ (900-1088ms) in parietal electrodes
	Visual	↑ (-196ms to 0ms) in central electrodes	↓ (136-228ms) in occipital electrodes	↑ (320-408ms) in occipital electrodes	↓ (788-952ms) in occipital electrodes
<i>Contextual prediction errors</i>					
Unexpected omission (-)	Auditory	↑ (-700ms to -528ms) in parietal electrodes	↑ (0-188ms) in frontal electrodes	↑ (252-412ms) in frontal electrodes	↑ (500-700ms) in parietal electrodes
Expected omission	Visual	↑ (-472ms to -112ms) in central electrodes	↑ (92-192ms) in occipital electrodes	↑ (316-76ms) in frontal electrodes	↑ (780-956ms) in parietal electrodes

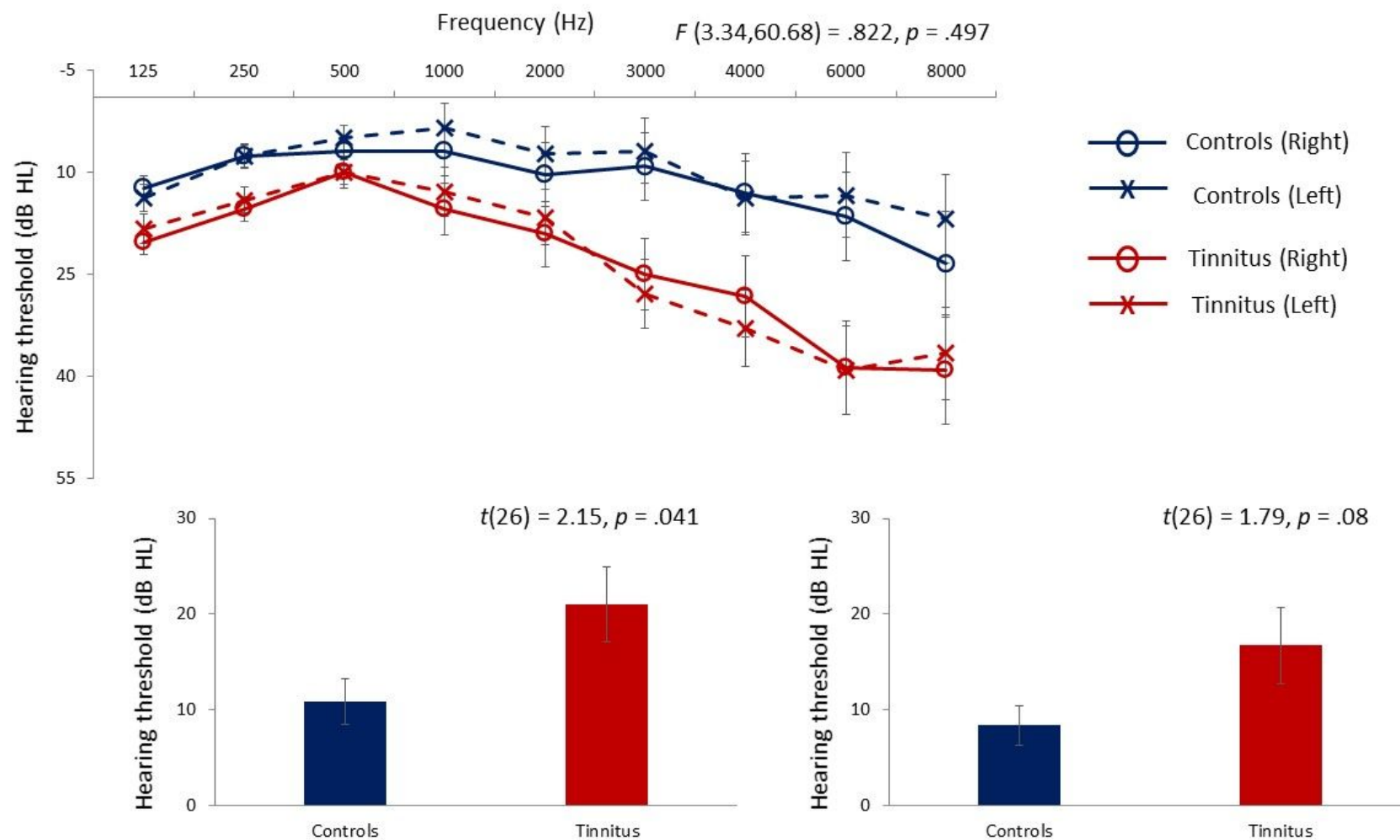


Figure 1

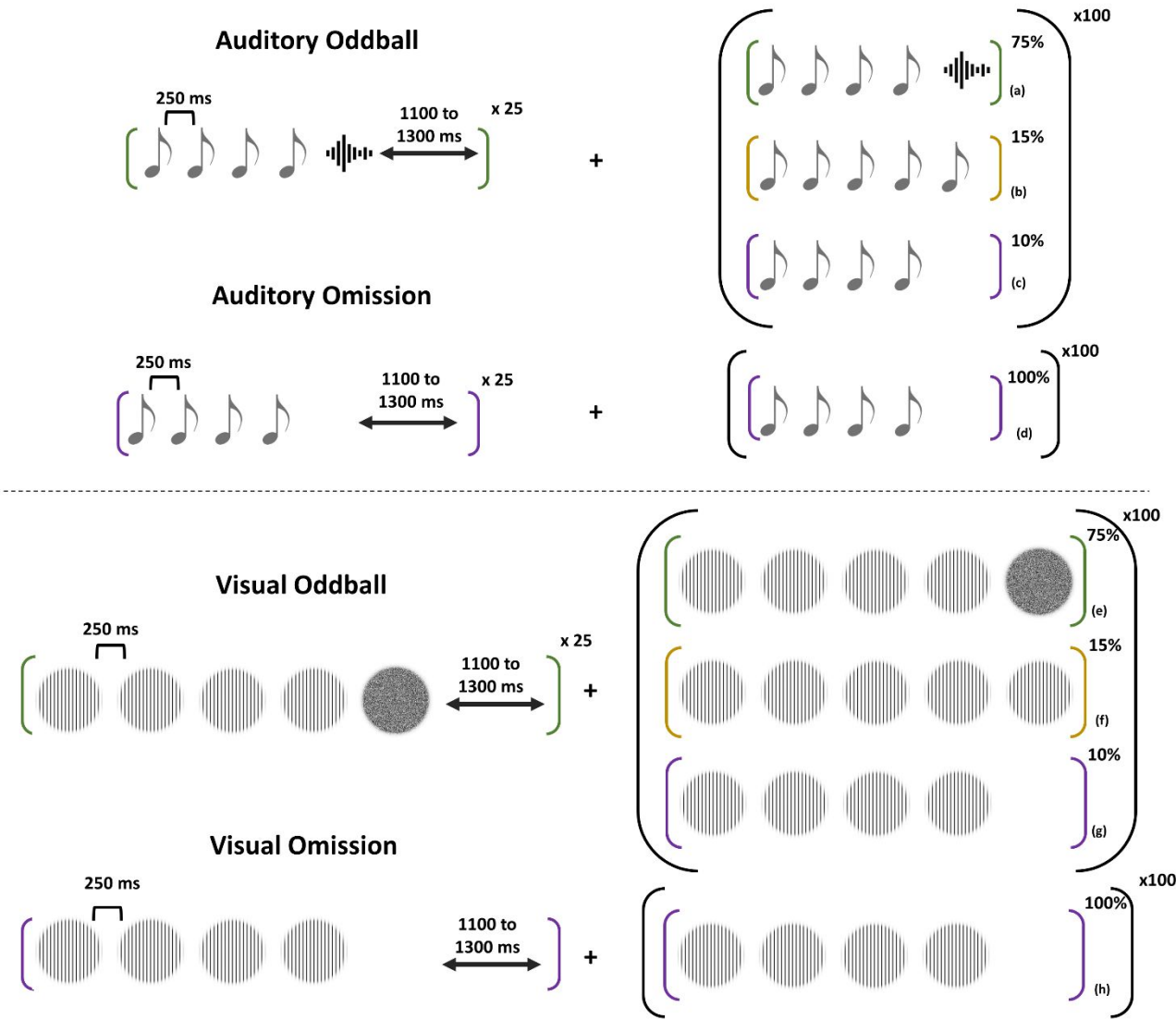


Figure 2

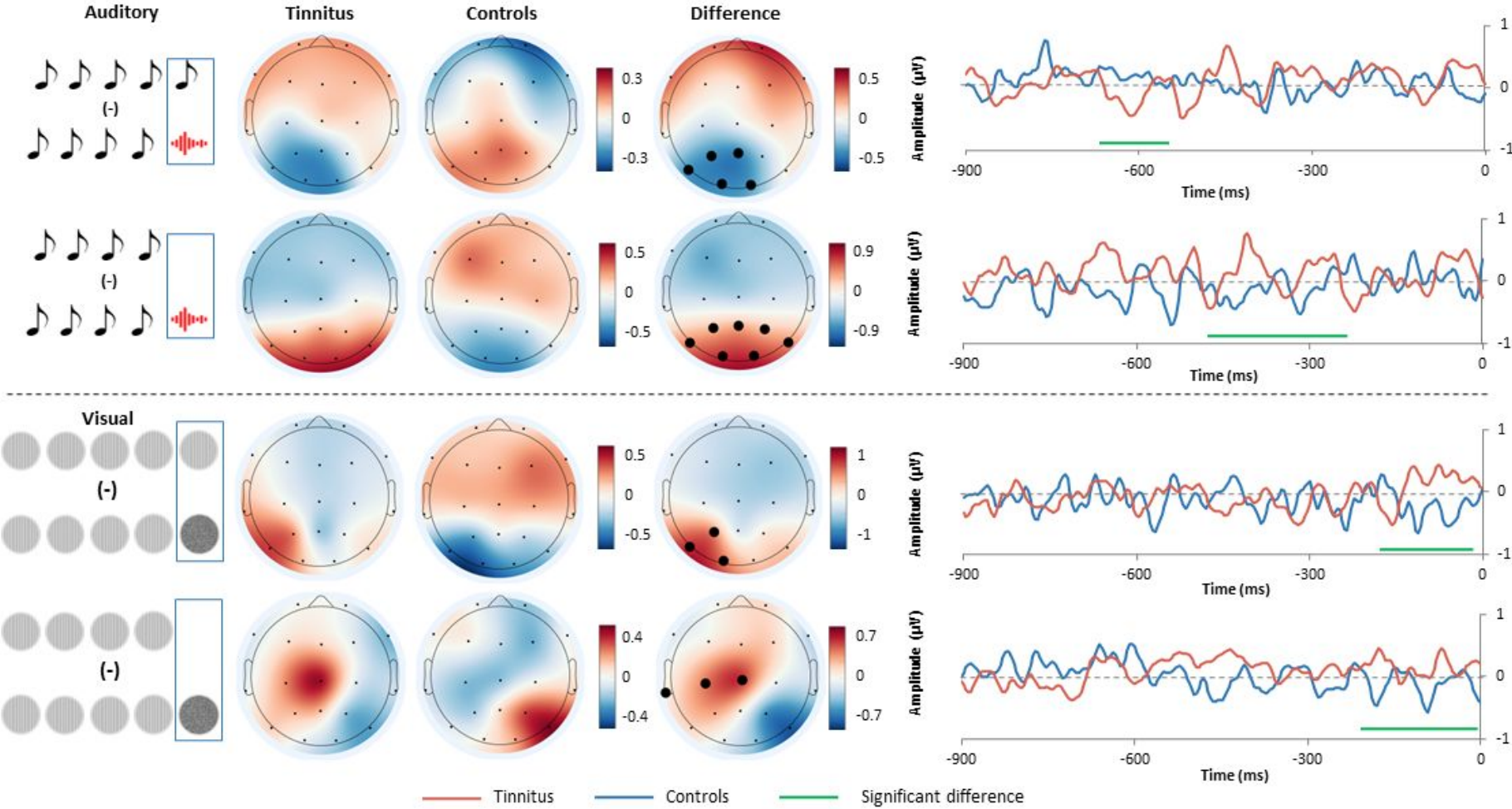


Figure 3



1  
2  
3  
4  
5  
6  
7  
8  
9  
10  
11  
12  
13  
14  
15  
16  
17  
18  
19  
20  
21  
22  
23  
24  
25  
26  
27  
28  
29  
30  
31  
32  
33  
34  
35  
36  
37  
38  
39  
40  
41  
42  
43  
44  
45  
46

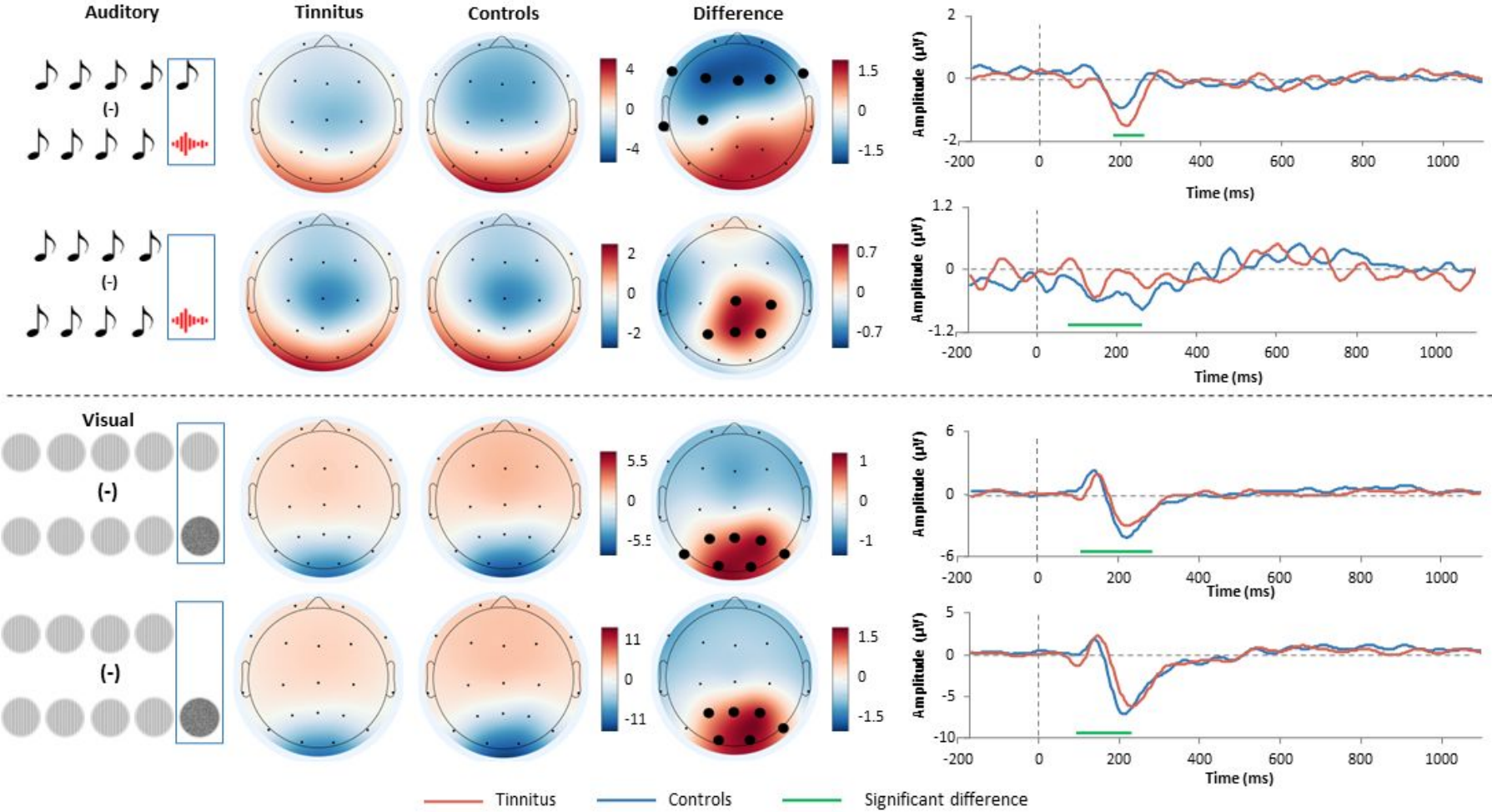


Figure 4

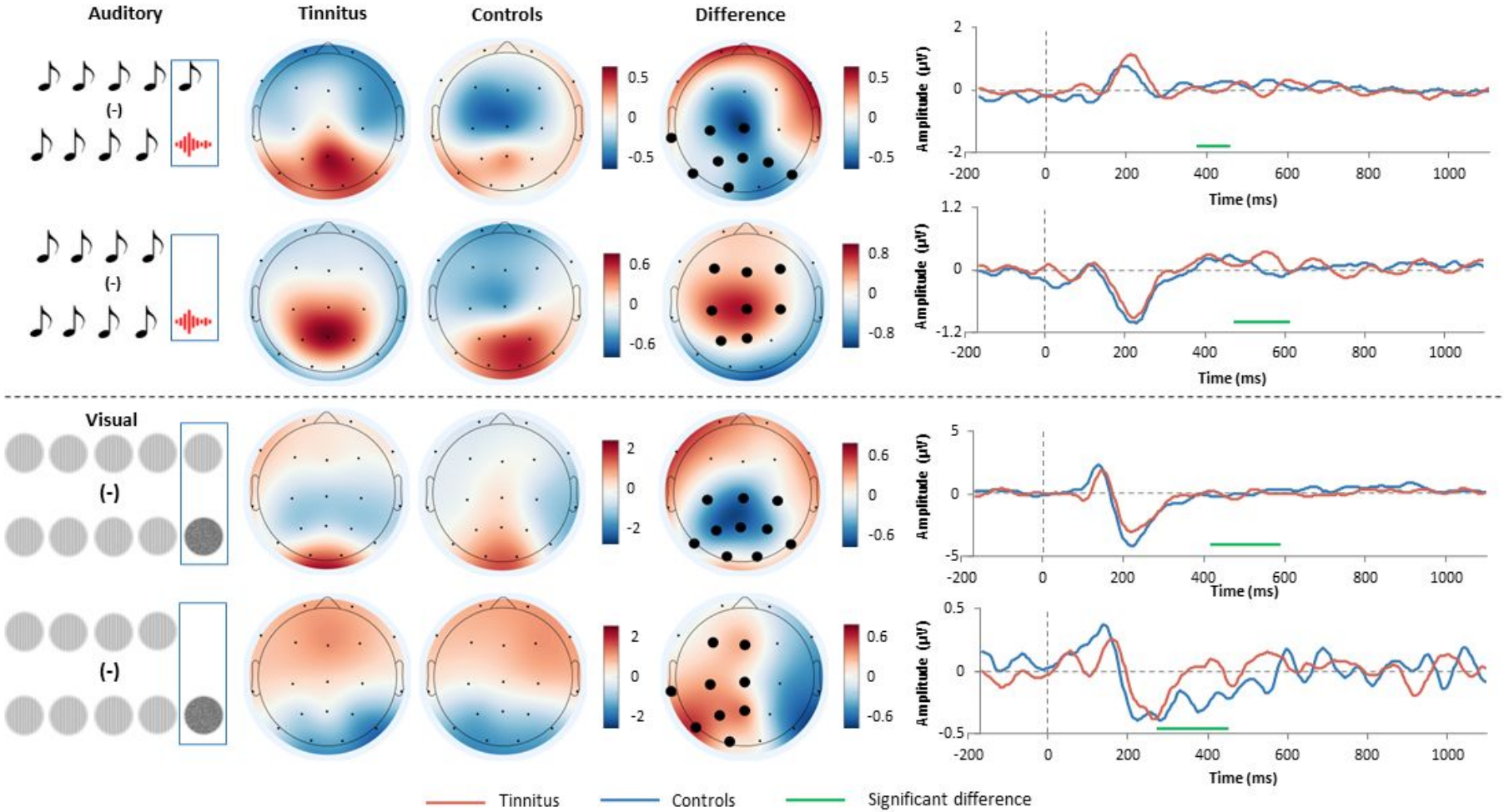


Figure 5



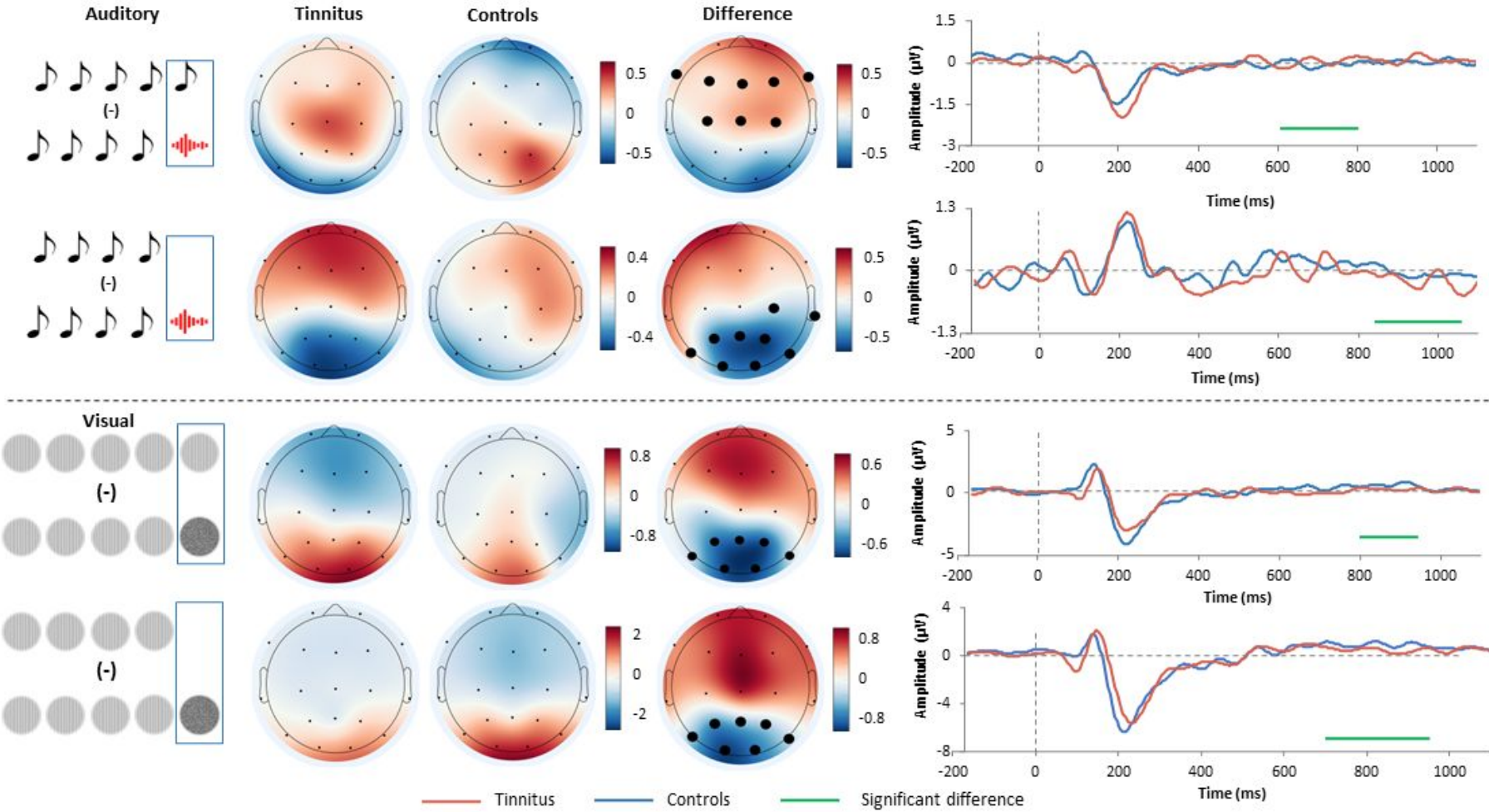


Figure 6

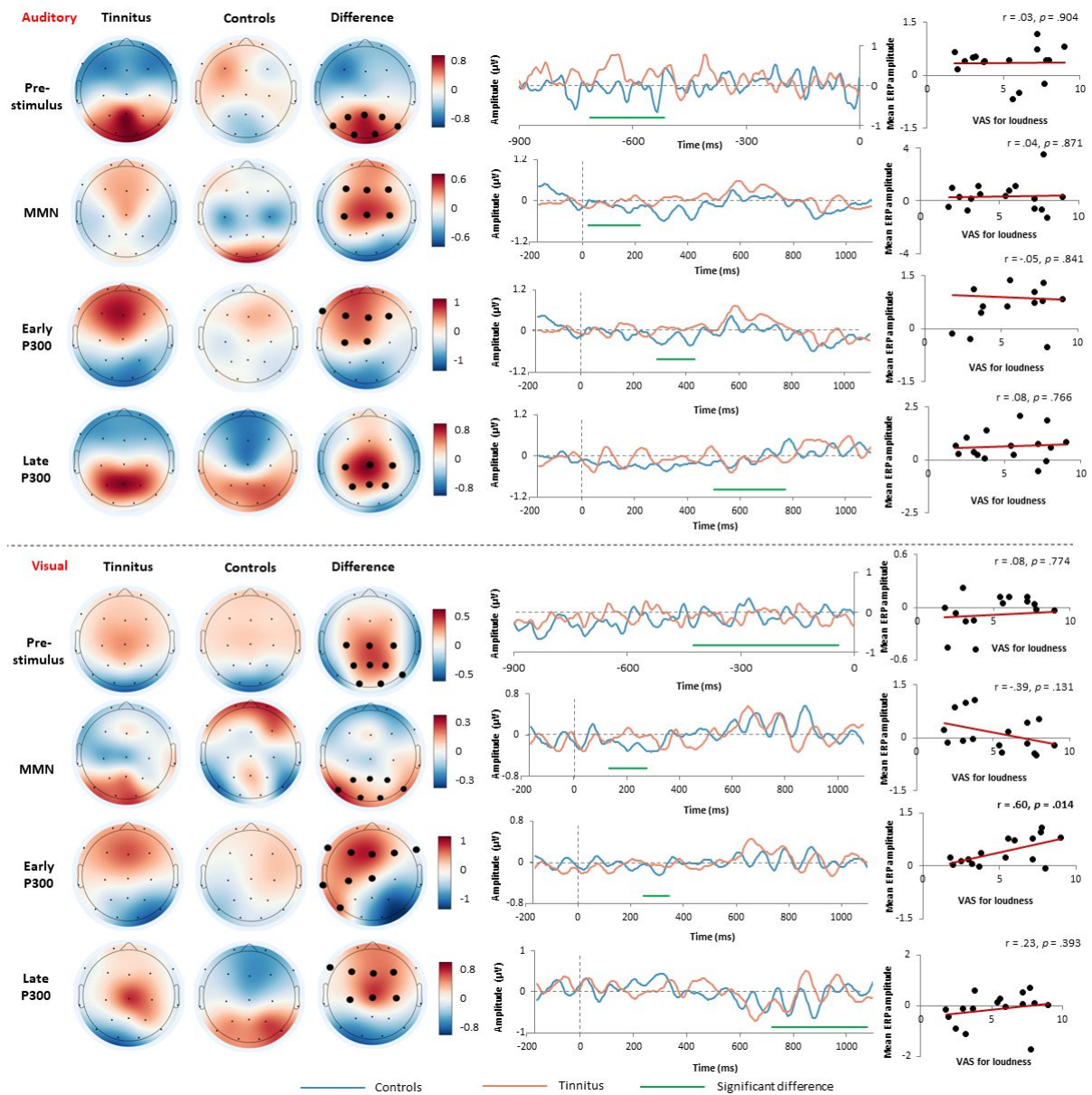


Figure 7

References

1. Rao RP, Ballard DH. Predictive coding in the visual cortex: a functional interpretation of some extra-classical receptive-field effects. *Nature neuroscience*. 1999;2(1):79-87.

2. Hullfish J, Sedley W, Vanneste S. Prediction and perception: Insights for (and from) tinnitus. *Neuroscience & Biobehavioral Reviews*. 2019/07/01/ 2019;102:1-12. doi:<https://doi.org/10.1016/j.neubiorev.2019.04.008>

3. Mohan A, Vanneste S. Adaptive and maladaptive neural compensatory consequences of sensory deprivation—From a phantom percept perspective. *Progress in neurobiology*. 2017;153:1-17.

4. Baguley D, McFerran D, Hall D. Tinnitus. *The Lancet*. 2013;382(9904):1600-1607.

5. Cohen SP, Vase L, Hooten WM. Chronic pain: an update on burden, best practices, and new advances. *The Lancet*. 2021;397(10289):2082-2097.

6. Grouios G. Phantom smelling. *Perceptual and motor skills*. 2002;94(3):841-850.

7. Maheswaran T, Abikshyeet P, Sitra G, Gokulanathan S, Vaithiyanadane V, Jeelani S. Gustatory dysfunction. *Journal of pharmacy & bioallied sciences*. 2014;6(Suppl 1):S30.

8. Schadlu AP, Schadlu R, Shepherd JB. Charles Bonnet syndrome: a review. *Current opinion in ophthalmology*. 2009;20(3):219-222.

9. Jansen E, Helleman H, Dreschler W, De Laat J. Noise induced hearing loss and other hearing complaints among musicians of symphony orchestras. *International archives of occupational and environmental health*. 2009;82(2):153-164.

10. Baron R. Mechanisms of disease: neuropathic pain—a clinical perspective. *Nature clinical practice Neurology*. 2006;2(2):95-106.

11. Wrobel BB, Leopold DA. Clinical assessment of patients with smell and taste disorders. *Otolaryngologic Clinics of North America*. 2004;37(6):1127-1142.

12. Kester EM. Charles Bonnet syndrome: case presentation and literature review. *Optometry-Journal of the American Optometric Association*. 2009;80(7):360-366.

13. Eggermont J. Tinnitus: some thoughts about its origin. *The Journal of Laryngology & Otology*. 1984;98(S9):31-37.

14. De Ridder D, Vanneste S, Freeman W. The Bayesian brain: Phantom percepts resolve sensory uncertainty. *Neuroscience & Biobehavioral Reviews*. 2014/07/01/ 2014;44:4-15. doi:<https://doi.org/10.1016/j.neubiorev.2012.04.001>
15. Sedley W, Friston KJ, Gander PE, Kumar S, Griffiths TD. An Integrative Tinnitus Model Based on Sensory Precision. *Trends Neurosci*. 2016;39(12):799-812. doi:10.1016/j.tins.2016.10.004
16. Partyka M, Demarchi G, Roesch S, *et al*. Phantom auditory perception (tinnitus) is characterised by stronger anticipatory auditory predictions. *bioRxiv*. 2019:869842. doi:10.1101/869842
17. Sedley W, Alter K, Gander PE, Berger J, Griffiths TD. Exposing Pathological Sensory Predictions in Tinnitus Using Auditory Intensity Deviant Evoked Responses. *The Journal of Neuroscience*. 2019;39(50):10096. doi:10.1523/JNEUROSCI.1308-19.2019
18. Mohan A, Luckey A, Weisz N, Vanneste S. Predisposition to domain-wide maladaptive changes in predictive coding in auditory phantom perception. *NeuroImage*. 2021:118813.
19. Bekinschtein TA, Dehaene S, Rohaut B, Tadel F, Cohen L, Naccache L. Neural signature of the conscious processing of auditory regularities. *Proceedings of the National Academy of Sciences*. 2009;106(5):1672-1677.
20. Chao ZC, Takaura K, Wang L, Fujii N, Dehaene S. Large-scale cortical networks for hierarchical prediction and prediction error in the primate brain. *Neuron*. 2018;100(5):1252-1266. e3.
21. Wacongne C, Labyt E, van Wassenhove V, Bekinschtein T, Naccache L, Dehaene S. Evidence for a hierarchy of predictions and prediction errors in human cortex. *Proceedings of the National Academy of Sciences*. 2011;108(51):20754-20759.
22. Näätänen R, Paavilainen P, Titinen H, Jiang D, Alho K. Attention and mismatch negativity. *Psychophysiology*. 1993;30(5):436-450.
23. Polich J. Updating P300: an integrative theory of P3a and P3b. *Clinical neurophysiology*. 2007;118(10):2128-2148.
24. Garrido MI, Kilner JM, Kiebel SJ, Friston KJ. Dynamic causal modeling of the response to frequency deviants. *Journal of Neurophysiology*. 2009;101(5):2620-2631.
25. Garrido MI, Kilner JM, Kiebel SJ, Friston KJ. Evoked brain responses are generated by feedback loops. *Proceedings of the National Academy of Sciences*. 2007;104(52):20961-20966.

26. Wacongne C, Changeux J-P, Dehaene S. A neuronal model of predictive coding accounting for the mismatch negativity. *Journal of Neuroscience*. 2012;32(11):3665-3678.
27. May PJ, Tiitinen H. Mismatch negativity (MMN), the deviance-elicited auditory deflection, explained. *Psychophysiology*. 2010;47(1):66-122.
28. Garrido MI, Kilner JM, Stephan KE, Friston KJ. The mismatch negativity: a review of underlying mechanisms. *Clinical neurophysiology*. 2009;120(3):453-463.
29. Stefanics G, Kremláček J, Czigler I. Visual mismatch negativity: a predictive coding view. Review. *Front Hum Neurosci*. 2014-September-16 2014;8(666)doi:10.3389/fnhum.2014.00666
30. Nakao M, Barsky AJ, Nishikitani M, Yano E, Murata K. Somatosensory amplification and its relationship to somatosensory, auditory, and visual evoked and event-related potentials (P300). *Neuroscience letters*. 2007;415(2):185-189.
31. Mohan A, Luckey A, Weisz N, Vanneste S. Predisposition to domain-wide maladaptive changes in predictive coding in auditory phantom perception. *NeuroImage*. 2021;Accepted
32. Mathers C, Smith A, Concha M. Global burden of hearing loss in the year 2000. *Global burden of Disease*. 2000;18(4):1-30.
33. Allard R, Faubert J. The noisy-bit method for digital displays: Converting a 256 luminance resolution into a continuous resolution. *Behavior Research Methods*. 2008/08/01 2008;40(3):735-743. doi:10.3758/BRM.40.3.735
34. El-Minawi MS, Dabbous AO, Hamdy MM, Sheta SM. Does changes in mismatch negativity after tinnitus retraining therapy using tinnitus pitch as deviant stimulus, reflect subjective improvement in tinnitus handicap? *Hearing, Balance and Communication*. 2018;16(3):182-196.
35. Asadpour A, Jahed M, Mahmoudian S. Aberrant Frequency Related Change-Detection Activity in Chronic Tinnitus. *Frontiers in Neuroscience*. 2020;14
36. Sendesen E, Erbil N, Türkyılmaz MD. The mismatch negativity responses of individuals with tinnitus with normal extended high-frequency hearing—is it possible to use mismatch negativity in the evaluation of tinnitus? *European Archives of Oto-Rhino-Laryngology*. 2021:1-10.

37. Weisz N, Voss S, Berg P, Elbert T. Abnormal auditory mismatch response in tinnitus sufferers with high-frequency hearing loss is associated with subjective distress level. *BMC Neurosci.* 2004;5(1):1-9.
38. Umbricht D, Krljes S. Mismatch negativity in schizophrenia: a meta-analysis. *Schizophrenia research.* 2005;76(1):1-23.
39. Fisher DJ, Labelle A, Knott VJ. The right profile: mismatch negativity in schizophrenia with and without auditory hallucinations as measured by a multi-feature paradigm. *Clinical Neurophysiology.* 2008;119(4):909-921.
40. O'Connell RG, Balsters JH, Kilcullen SM, *et al.* A simultaneous ERP/fMRI investigation of the P300 aging effect. *Neurobiology of aging.* 2012;33(10):2448-2461.
41. Wronka E, Kaiser J, Coenen AM. The auditory P3 from passive and active three-stimulus oddball paradigm. 2008;
42. Corlett PR, Horga G, Fletcher PC, Alderson-Day B, Schmack K, Powers III AR. Hallucinations and strong priors. *Trends Cogn Sci.* 2019;23(2):114-127.
43. Powers AR, Mathys C, Corlett PR. Pavlovian conditioning–induced hallucinations result from overweighting of perceptual priors. *Science.* 2017;357(6351):596-600.
44. Cassidy CM, Balsam PD, Weinstein JJ, *et al.* A perceptual inference mechanism for hallucinations linked to striatal dopamine. *Current Biology.* 2018;28(4):503-514. e4.
45. Pezzulo G, Maisto D, Barca L, Van den Bergh O. Symptom perception from a predictive processing perspective. *Clinical Psychology in Europe.* 2019;1(4):1-14.
46. Van den Bergh O, Witthöft M, Petersen S, Brown RJ. Symptoms and the body: taking the inferential leap. *Neuroscience & Biobehavioral Reviews.* 2017;74:185-203.
47. Koban L, Gianaros PJ, Kober H, Wager TD. The self in context: brain systems linking mental and physical health. *Nature Reviews Neuroscience.* 2021;22(5):309-322.
48. Leech R, Sharp DJ. The role of the posterior cingulate cortex in cognition and disease. *Brain.* 2014;137(1):12-32.
49. Vatansever D, Menon DK, Stamatakis EA. Default mode contributions to automated information processing. *Proceedings of the National Academy of Sciences.* 2017;114(48):12821-12826.



1  
2  
3  
4  
5  
6  
7  
8  
9  
10  
11  
12  
13  
14  
15  
16  
17  
18  
19  
20  
21  
22  
23  
24  
25  
26  
27  
28  
29  
30  
31  
32  
33  
34  
35  
36  
37  
38  
39  
40  
41  
42  
43  
44  
45  
46  
47  
48  
49  
50  
51  
52  
53  
54  
55  
56  
57  
58  
59  
60

50. Pearson JM, Heilbronner SR, Barack DL, Hayden BY, Platt ML. Posterior cingulate cortex: adapting behavior to a changing world. *Trends Cogn Sci.* 2011;15(4):143-151.

51. Marks KL, Martel DT, Wu C, *et al.* Auditory-somatosensory bimodal stimulation desynchronizes brain circuitry to reduce tinnitus in guinea pigs and humans. *Science translational medicine.* 2018;10(422)

52. Conlon B, Hamilton C, Hughes S, *et al.* Noninvasive Bimodal Neuromodulation for the Treatment of Tinnitus: Protocol for a Second Large-Scale Double-Blind Randomized Clinical Trial to Optimize Stimulation Parameters. *JMIR Res Protoc.* 2019;8(9):e13176-e13176. doi:10.2196/13176

53. Tyler R, Cacace A, Stocking C, *et al.* Vagus nerve stimulation paired with tones for the treatment of tinnitus: a prospective randomized double-blind controlled pilot study in humans. *Scientific reports.* 2017;7(1):1-11.

54. Kikidis D, Vassou E, Markatos N, Schlee W, Iliadou E. Hearing Aid Fitting in Tinnitus: A Scoping Review of Methodological Aspects and Effect on Tinnitus Distress and Perception. *Journal of Clinical Medicine.* 2021;10(13):2896.

55. Arts RA, George EL, Stokroos RJ, Vermeire K. Cochlear implants as a treatment of tinnitus in single-sided deafness. *Current opinion in otolaryngology & head and neck surgery.* 2012;20(5):398-403.

### Figure legends

**Figure 1:** Hearing assessment in the tinnitus and control groups. The pure tone audiogram thresholds at the different frequencies are shown for the controls (blue) and the tinnitus (groups). The mean hearing loss calculated over all the frequencies, and the mean hearing disability calculated for 500, 1000, 2000, 4000 Hz are displayed for the controls (blue) and tinnitus (red) groups. The error bars represent standard error.

**Figure 2:** A visual representation of the local-global oddball paradigm adapted to the auditory and visual domain. The top section represents the auditory paradigm where each tone represents a 500 Hz pure tone and the signal represents a white noise burst. The bottom section represents the visual paradigm where each sinusoidal grating is designed at 3 cpd and the noise stimulus is a white noise. In both paradigms the standard is played 25 times to establish the global rule and standard-deviant-omission sequences are played at 75%-15%-10% probability. The omission sequence is also played separately at 100%.

**Figure 3:** Scalp maps and event-related potentials for the prediction error generated by the subtraction of the responses of the two deviants and the standard in the pre-stimulus timeframe. Scalp maps show the mean amplitude in the pre-stimulus time frame for the tinnitus group, control group and the difference between the two groups in the auditory (upper section) and visual (lower sections) domains. The event-related potentials show the prediction error response of the controls (blue) and tinnitus (red) group and the significant difference between them (green line). The electrodes in BOLD show the electrodes that show a significant difference at all time points indicated by the green line.

**Figure 4:** Scalp maps and event-related potentials for the prediction error generated by the subtraction of the responses of the two deviants and the standard in the MMN timeframe. Scalp maps show the mean amplitude in the mis-match negativity time frame for the tinnitus group, control group and the difference between the two groups in the auditory (upper



section) and visual (lower sections) domains. The event-related potentials show the prediction error response of the controls (blue) and tinnitus (red) group and the significant difference between them (green line). The “0” time point corresponds to the onset of the 5<sup>th</sup> stimulus in the sequence. The electrodes in BOLD show the electrodes that show a significant difference at all time points indicated by the green line.

**Figure 5:** Scalp maps and event-related potentials for the prediction error generated by subtraction of the responses of the two deviants and the standard in the early P300 timeframe. Scalp maps show the mean amplitude in the early P300 time frame for the tinnitus group, control group and the difference between the two groups in the auditory (upper section) and visual (lower sections) domains. The event-related potentials show the prediction error response of the controls (blue) and tinnitus (red) group and the significant difference between them (green line). The “0” time point corresponds to the onset of the 5<sup>th</sup> stimulus in the sequence. The electrodes in BOLD show the electrodes that show a significant difference at all time points indicated by the green line.

**Figure 6:** Scalp maps and event-related potentials for the prediction error generated by the subtraction of the responses of the two deviants and the standard in the late P300 timeframe. Scalp maps show the mean amplitude in the late P300 time frame for the tinnitus group, control group and the difference between the two groups in the auditory (upper section) and visual (lower sections) domains. The event-related potentials show the prediction error response of the controls (blue) and tinnitus (red) group and the significant difference between them (green line). The “0” time point corresponds to the onset of the 5<sup>th</sup> stimulus in the sequence. The electrodes in BOLD show the electrodes that show a significant difference at all time points indicated by the green line.

**Figure 7:** Scalp maps, event-related responses and correlations for the prediction error generated by the subtraction of the unexpected omission from the expected omission. Scalp

maps show the mean amplitude in the pre-stimulus, mis-match negativity, early and late P300 time frames for the tinnitus group, control group and the difference between the two groups in the auditory (upper section) and visual (lower sections) domains. The event-related potentials show the response of the controls (blue) and tinnitus (red) group and the significant difference between them (green line). The electrodes in BOLD show the electrodes that show a significant difference at all time points indicated by the green line. The numbers in the correlations represent the unstandardised residuals VAS for loudness and mean amplitude of the corresponding ERP component after controlling for mean hearing loss.



# The use of non-invasive brain stimulation in auditory perceptual learning: A review

Yvette Grootjans<sup>a</sup>, Gabriel Byczynski<sup>a</sup>, Sven Vanneste<sup>a,b,\*</sup>

<sup>a</sup> Lab for Clinical and Integrative Neuroscience, Trinity Institute for Neuroscience, School of Psychology, Trinity College Dublin, Ireland

<sup>b</sup> Global Brain Health Institute, Institute of Neuroscience, Trinity College Dublin, Ireland

## ARTICLE INFO

### Keywords:

Auditory perceptual learning  
Auditory cortex  
Neural mechanisms  
Plasticity  
Non-invasive brain stimulation  
Frequency discrimination

## ABSTRACT

Auditory perceptual learning is an experience-dependent form of auditory learning that can improve substantially throughout adulthood with practice. A key mechanism associated with perceptual learning is synaptic plasticity. In the last decades, an increasingly better understanding has formed about the neural mechanisms related to auditory perceptual learning. Research in animal models found an association between the functional organization of the primary auditory cortex and frequency discrimination ability. Several studies observed an increase in the area of representation to be associated with improved frequency discrimination. Non-invasive brain stimulation techniques have been related to the promotion of plasticity. Despite its popularity in other fields, non-invasive brain stimulation has not been used much in auditory perceptual learning. The present review has discussed the application of non-invasive brain stimulation methods in auditory perceptual learning by discussing the mechanisms, current evidence and challenges, and future directions.

## 1. Introduction

Traditionally, the auditory system has been viewed as a genetically determined system largely dependent on critical developmental periods (Hensch, 2005). However, in recent years multiple studies have shown that the auditory system continuously reorganizes itself in response to either lesioning, or to behavioural training via auditory input (Irvine et al., 2001; Irvine, 2018a). In the former, lesion-induced pattern changes of input cause sensory cortices to modify in response. In one study, it was shown in cats that cochlear lesioning resulted in an expanded representation of adjacent cochlear regions (a mechanism further discussed later in this paper) (Rajan et al., 1993). In humans with tinnitus, a similar pattern was found, as magnetoencephalographic (MEG) recordings showed a shift in cortical representation of tinnitus, suggesting pathologically-induced plasticity (Muhlnickel et al., 1998). Alternatively, auditory plasticity has also been shown to result from behavioural training, including learning. This form of learning is called auditory perceptual learning. Perceptual learning has been used as an umbrella term for experience-dependent learning which includes a wide variety of sensory modalities, such as visual, auditory, tactile, taste, and olfaction (Gold et al., 2010). Early studies observed a dramatic

improvement in the ability of humans to distinguish between two tactile stimuli on the skin through training (Gibson, 1953, 1969). These changes occurred within days, and therefore too rapid to be caused by an increase in peripheral receptors, instead it was hypothesised that it involved changes in the central nervous system (Gold et al., 2010). For many years, research into perceptual learning has been dominated by visual studies, and only more recently has auditory perceptual learning become a topic of interest (Irvine, 2018b). auditory perceptual learning can be studied using a variety of tasks, including frequency discrimination, interval discrimination, spatial hearing, intensity discrimination, and tone pattern learning (Wright et al., 2009).

Through animal research, various ideas have emerged on the neural and cortical processes that underlie auditory perceptual learning. These studies have particularly focused on auditory frequency discrimination (Polley et al., 2006; Recanzone et al., 1993). A reason being that frequency discrimination is easily applicable to animal models. Animal models have revealed a possible role of map plasticity in the primary auditory cortex (A1) in auditory perceptual learning by showing an increased cortical area of representation in the A1 for behaviourally trained frequencies (Polley et al., 2006; Recanzone et al., 1993). The finding that the auditory system is plastic is promising, especially for

\* Corresponding author at: Lab for Clinical & Integrative Neuroscience, School of Psychology, Global Brain Health Institute, Institute of Neuroscience, Trinity College Dublin, College Green 2, Dublin, Ireland.

E-mail address: [sven.vanneste@tcd.ie](mailto:sven.vanneste@tcd.ie) (S. Vanneste).

<https://doi.org/10.1016/j.heares.2023.108881>

Received 2 June 2023; Received in revised form 8 August 2023; Accepted 25 August 2023

Available online 29 August 2023

0378-5955/© 2023 Elsevier B.V. All rights reserved.

methods like non-invasive brain stimulation which have been related to the promotion of plasticity in the brain (Huang et al., 2017). Non-invasive brain stimulation is a relatively novel technique used to identify the functional role of specific brain structures, and it can provide valuable information about the relationship between brain and behavior (Cirillo et al., 2017). As perceptual learning can be substantially improved during adulthood through practice, there is scientific interest in the ability to modulate auditory perceptual learning via non-invasive brain stimulation. A handful of studies have used non-invasive brain stimulation for auditory perceptual learning, but with mixed results, possibly due to methodological differences between these studies (Simonsmeier et al., 2018). Overall, there seems to be a lack of consensus in the field on how non-invasive brain stimulation could be applied for auditory perceptual learning. In the current review, we will discuss how non-invasive brain stimulation methods could be used for auditory perceptual learning. A narrative review was chosen in this context because of the sparse literature available on this topic, with this review we would like to provide an overview on what is currently being done and what might be valuable for future studies to focus on. This review begins by providing a concise overview of what is known about the mechanisms of action associated with auditory perceptual learning. Then we will summarize and discuss studies that have used non-invasive brain stimulation to modulate auditory perceptual learning. Lastly, we will discuss the current challenges of applying non-invasive brain stimulation in auditory perceptual learning research, and our recommendations for future research.

## 2. Mechanisms of auditory perceptual learning

To discuss how non-invasive brain stimulation could be applied in auditory perceptual learning, it is important to first understand the mechanisms of action associated with auditory perceptual learning. Before perceptual learning can take place, the incoming stimulus first needs to be processed. Auditory input travels first through the outer ear, ear canal, and then eardrum (Saenz et al., 2014). Soundwaves vibrate the eardrum, and these vibrations are then amplified by the auditory ossicles. The amplified waves enter the inner ear, and then the cochlear, see Fig. 1. Filled with fluid, vibrations in the cochlea are picked up by hair cells, converting the waves to electrical signals. The cochlea is also tonotopically organized, with the base tuned to higher frequencies, and decreasing toward the apex, tuned to low frequencies (Hackett, 2015; Musiek et al., 2018; von Bekesy, 1970). After transduction, the signal is

transmitted by the cochlear nerve, sending tonotopic projections from the auditory nerve (Peterson et al., 2022). Next, the site of binaural convergence, information is transmitted to the superior olivary complex. The signal then travels to the nuclei of the lateral lemniscus, which itself has two regions: the ventral nucleus, and the dorsal nucleus. The ventral nucleus receives information from the central cochlear nucleus and is not tonotopically organized, however the inferior colliculus, at the roof of the mesencephalon, is organized (in the central nucleus) tonotopically, receiving inputs from the cochlear nuclei, and the superior olivary complex (Musiek et al., 2018). Lastly between the inferior colliculus and the auditory cortex is the thalamic relay, the medial geniculate nucleus. Similar to the inferior colliculus, the ventral division of the medial geniculate nucleus displays tonotopy, and projects to the core areas of the auditory cortex (primary and associated). The auditory cortex is also organized tonotopically, similar to the distribution of the cochlea, with a gradient of neurons preferentially responding to high or low frequencies (Peterson et al., 2022).

Studies that investigate the functional organization of the A1 use electrophysiological measures to map the A1 by identifying the frequency within a neuron's receptive field to which it is maximally sensitive, called the characteristic frequency (CF) (Saenz et al., 2014). Related to this is the so-called 'best frequency', which represents the frequency that evokes the strongest response (Saenz et al., 2014).

Early studies have argued for a role of map plasticity underlying auditory perceptual learning (Polley et al., 2006; Recanzone et al., 1993). For example, Recanzone and colleagues (Recanzone et al., 1993) were one of the first to find an increased cortical area of representation for behaviourally trained frequencies. In the study, monkeys were trained on a frequency discrimination task while tonotopic organization was measured through the recording of the number of neurons in A1 with CFs in the frequency range used during the task. A correlation was found between improvement on the trained frequency in a frequency discrimination task and an increase in the cortical area of representation pertaining to that frequency. Additionally, Polley and colleagues (Polley et al., 2006) also found an expansion of cortical representations for trained frequencies in rats both in A1 and in the suprarhinal auditory field, a secondary higher auditory field. The inclusion of a secondary higher auditory field made it possible to investigate whether tonotopic map plasticity is guided by bottom-up or top-down factors. The expectation was that plasticity in the suprarhinal auditory field would be influenced by top-down factors, whereas reorganization in A1 would indicate bottom-up factors. Additionally, the task was designed in a way

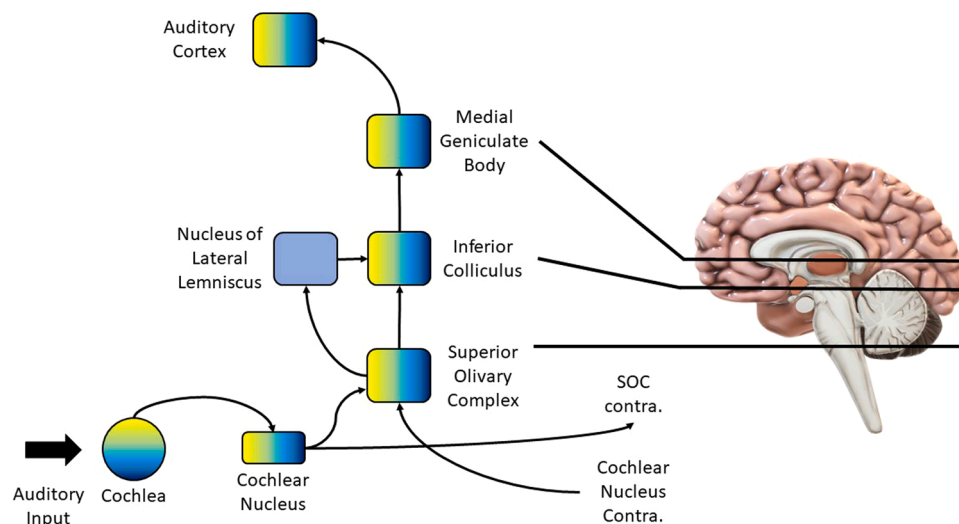


**Fig. 1.** Central auditory pathway. Auditory input first travels through the auditory canal where it reaches the inner ear. Through the auditory nerve, the sound reaches the brain, where it travels along the central auditory pathway. The auditory information is transmitted through a series of nuclei before it reaches the auditory cortex.

to observe whether the type of stimulus that was attended to, could influence the magnitude of the respective cortical area. These studies found an increased cortical area of representation in A1 for behaviourally trained frequencies. However, there are also several studies that have failed to find map plasticity associated with improved auditory perceptual learning (Brown et al., 2004; Thomas et al., 2020; Witte et al., 2005). A number of models for auditory plasticity have emerged over the years. The Weinberger model by Weinberger and colleagues (Weinberger, 2007) highlighted the importance of sensory structures in memory and associative learning. Although, associative learning is different from perceptual learning, the two concepts are closely related. Through classical conditioning studies, Weinberger and colleagues (Weinberger, 2004) initially proposed a model with multiple key brain structures in associative receptive field plasticity, including the nucleus basalis, the amygdala, the brainstem, and the magnocellular medial geniculate nucleus. With their model they showed auditory plasticity in many of these structures, making the field switch from only focusing on plasticity in A1 to looking at subcortical structures. The nucleus basalis and its cholinergic projections is especially important in long-term plasticity according to the Weinberger model (Weinberger, 2007). Suga and colleagues (Suga et al., 2003) agreed on the importance of the nucleus basalis in plasticity but also proposed in their alternative model which included the descending auditory system, suggesting that plasticity that develops in the association cortex is relayed via the amygdala to the inferior colliculus, which then promotes plasticity in A1. (Suga et al., 2003; Weinberger, 2007) Bajo and colleagues (Bajo et al., 2010) further stressed the role of the descending auditory pathways, by showing that lesions in these pathways did not affect sound-localization in ferrets but did severely affect localization learning. Their results indicated that descending projections from A1 is responsible for learning and that concurrent plasticity might occur subcortically. Therefore, a shift in the literature occurred of only focusing on plasticity in A1 to also observing plasticity in subcortical structures. This was further investigated by Edeline and colleagues (Edeline et al., 2011), they stimulated the locus coeruleus – a small brainstem structure with noradrenergic projections – paired with a tone frequency while recording cells both in the auditory cortex and the auditory thalamus. They observed plasticity in both the cortex and the thalamus because of locus coeruleus-tone pairing, indicating plasticity at the thalamic and cortical level and the importance of the locus coeruleus-noradrenergic pathway in promoting auditory plasticity. In the work of Shore and colleagues (Shore et al., 2006), another structure in the brainstem, the cochlear nucleus, has been highlighted as having an important role in auditory plasticity (Koehler et al., 2013; Shore et al., 2006). The cochlear nucleus' principal output are fusiform cells, and a hyperactivity in these cells has been suggested to be related to tinnitus, a phantom auditory perception (Dehmel et al., 2012; Koehler et al., 2013; Stefanescu et al., 2015).

Another leading hypothesis that should be mentioned in relation to perceptual learning and plasticity is the expansion-renormalization model for plasticity and learning (Reed et al., 2011). Reed and colleagues (Reed et al., 2011) applied nucleus basalis stimulation through a surgical implant while presenting rats with a frequency discrimination task. This was based on findings that nucleus basalis stimulation paired with tone presentations leads to stimulus-specific tonotopic map expansions in A1 and the secondary auditory cortex possibly by mimicking nucleus basalis activity during periods of arousal (Froemke et al., 2007; Kilgard et al., 1998; Puckett et al., 2007). The results showed cortical map plasticity to be associated with learning, but not as much with performance. Reed and colleagues (Reed et al., 2011) made this distinction by using nucleus basalis stimulation-tone pairing to cause auditory map expansions before discrimination learning to assess learning. Performance was assessed by pairing nucleus basalis stimulation with tones in rats that had already learned the task. They found that the nucleus basalis stimulation-tone pairing enhanced tone frequency discrimination learning. No difference in discrimination ability was found between the paired group and the control group after they had

already learned the task, indicating that performance on a well-learned task could not be further improved through nucleus basalis stimulation-tone pairing, specifically for the low tone group. Based on this finding, the expansion-renormalization model for plasticity and learning was formulated (Reed et al., 2011). Unlike the earlier hypothesis that suggested that improved frequency discrimination is due to large scale cortical map reorganization, this model has suggested that improved frequency discrimination may be due to a temporary increase of a cortical representation only for the duration of the task. After learning is complete, the map is hypothesised to return to its “normal” organization. Although this model is more generally applicable to learning and plasticity, in this instance it will be discussed in relation to auditory perceptual learning. According to the expansion-renormalization model, the process of auditory perceptual learning consists of two stages. In the expansion stage, neuromodulators are repeatedly released during the discrimination of a target frequency. Due to the release of these neuromodulators, the cortical map expands by increasing the number of neural circuits related to that frequency. After map expansion, the neural circuits associated with the stimulus will be more easily available. According to this model, after learning is complete, the map will return to its “normal” organization. Froemke and colleagues (Froemke et al., 2013) have shown results in favor of the expansion-renormalization model. They studied neural activity in rats in vivo by applying nucleus basalis stimulation paired with tone presentations. Indeed, the findings indicate that nucleus basalis stimulation-tone pairing induced increased excitation of the paired input, while decreasing excitation for the stimuli that originally evoked the largest response. This finding argues for an optimization of the underlying neural circuits as a response to the trained frequency. Interestingly, they also recorded long-term changes and observed that inhibition at the paired input recovered and returned to its default organization.

The findings discussed up to here are a brief representation of what has been done in the field so far, for a full review on the mechanisms underlying auditory perceptual learning see Irvine and colleagues (Irvine, 2018b). Overall, there seems to be a lack of agreement between studies on the mechanisms related to auditory perceptual learning, but the majority agrees that neural plasticity is involved.

### 3. Non-invasive brain stimulation and auditory perceptual learning

The finding that the auditory system is plastic is promising, especially for methods like non-invasive brain stimulation which have been related to the promotion of plasticity in the brain (Huang et al., 2017). Non-invasive brain stimulation is a relatively novel technique used to identify the functional role of specific brain structures (Cirillo et al., 2017).

Most studies investigating non-invasive brain stimulation in relation to auditory perceptual learning have used transcranial electrical stimulation. Transcranial electrical stimulation is a non-invasive, cost-effective, highly tolerable, and convenient method (Hoy et al., 2010). There are three types of transcranial electrical stimulation that are most commonly used: transcranial direct current stimulation (tDCS), transcranial alternating current stimulation (tACS), and transcranial random noise stimulation (tRNS). tDCS applies a weak direct electrical current to the scalp through two or more electrodes, either in an anodal or cathodal fashion (Woods et al., 2016). The effects of tDCS are believed to occur due to the manipulation of ion channels or a shift in the electrical gradients across the neural membrane (He et al., 2020). Motor studies have shown that when an anodal electrode was applied over the primary motor cortex, it enhanced corticospinal excitability, whereas the cathodal electrode diminished it (He et al., 2020; Nitsche et al., 2005). From these observations in the motor cortex, it was concluded that anodal stimulation enhances cortical excitability, whereas cathodal stimulation suppressed it. In contrast, tACS applies a sinusoidal current to the scalp

and is believed to induce frequency dependent effects through modulation of endogenous oscillations in the brain (He et al., 2020). Similar to tACS, tRNS also uses alternating currents, but with tRNS the stimulation frequency continuously changes within a spectrum of oscillations.

There are a few studies that have used non-invasive brain stimulation to investigate its effects on auditory perceptual learning. The stimulated brain area is mostly the A1 because of its intuitive relation to auditory learning.

Mathys and colleagues (Mathys et al., 2010) investigated the effects of cathodal and anodal tDCS applied to the Heschl's gyrus on a pitch direction discrimination task. In this task, participants were asked to indicate whether a second tone was higher or lower than the first. Before the stimulation was applied, the participants engaged in a practice session without tDCS. A day later, three tDCS sessions took place each with a day in between. In the stimulation groups, participants received stimulation over the right or left Heschl's gyrus, and results showed that cathodal tDCS on the Heschl's gyrus interferes with pitch direction discrimination ability. More specifically, they found a greater contribution to this interference by the right Heschl's gyrus compared to the left. Although an inhibiting effect was found during cathodal stimulation, no significant effects were found in the anodal stimulation group. Mathys and colleagues (Mathys et al., 2010) used *offline* stimulation in their study, meaning the stimulation was not delivered during the task, but before or after. In this case, stimulation was delivered before the task. Similarly, Loui and colleagues (Loui et al., 2010) applied offline cathodal tDCS to the superior temporal gyrus and the inferior frontal gyrus before a pitch matching task, chosen because this skill is impaired in tone-deaf people (Loui et al., 2008). Participants were presented with a pure tone and were asked to reproduce the tone by humming. Stimulation was delivered on four separate days for 20 min over four target regions: the left posterior superior temporal gyrus, left posterior inferior frontal gyrus, right posterior superior temporal gyrus, and right posterior inferior frontal gyrus. The fifth day, sham stimulation was applied. After each stimulation session, the participant engaged in the pitch matching task. They found a disruption in pitch matching after cathodal tDCS was delivered to the left posterior inferior frontal gyrus. Additionally, they report that stimulation over the right posterior superior temporal gyrus produced marginal disruptions in pitch matching. There were no effects of stimulation found on the right posterior inferior frontal gyrus and left posterior superior temporal gyrus. In contrast, Tang and Hammond (Tang et al., 2013) used *online* stimulation, meaning the stimulation was delivered during the task. Participants were trained on a frequency discrimination task for two days. Anodal or sham tDCS was applied over the right auditory cortex only on the first day of testing but not on the second day. They found that anodal tDCS applied over the right auditory cortex impaired frequency discrimination. The authors argued that this was due to tDCS affecting temporal coding, shown through the result of a decreased frequency selectivity – a measure related to place coding – at 2000 Hz but not at 1000 Hz. Temporal processes seem to play a dominant role at lower frequencies, whereas place processes are more dominant at higher frequencies (Johnson, 1980). Similarly, Matsushita and colleagues (Matsushita et al., 2015) found a disruption in pitch discrimination learning when anodal tDCS was applied over the right temporal cortex. Participants were trained on a micromelody pitch discrimination task for three consecutive days. The task consisted of a pair of micromelodies, and the participant was asked to indicate whether the two items were the same or different. On the first day, the baseline performance was measured without applying tDCS. The next day, participants received tDCS while performing the same task as on the first day. On the third day, the participant performed the task again without receiving any tDCS. The sample was divided in three groups: the anodal group, the cathodal group, and the sham group. Cathodal tDCS did not have a significant effect on pitch discrimination learning. When replicating their initial study, Matsushita and colleagues (Matsushita et al., 2021) found the same result that applying anodal tDCS over the right auditory cortex disrupts pitch learning.

Furthermore, they recorded electrophysiological data through MEG. MEG was recorded before, during, and after tDCS. MEG data showed that tDCS to the left or right auditory cortex induced an ipsilateral decrease in N1m amplitude during stimulation. In conclusion, this study showed a significant association between pitch threshold changes and the degree of decrease of N1m induced by tDCS in the right auditory cortex.

Lega and colleagues (Lega et al., 2016) used another type of non-invasive brain stimulation, transcranial magnetic stimulation (TMS), to look at the role of the cerebellum in pitch and timbre discrimination. TMS uses magnetic stimulation to deliver single pulse, double pulse, online repetitive pulse, or offline repetitive pulse to the brain (Parkin et al., 2015). The effect of the stimulation on cortical activity is dependent on the type of pulse. For example, single pulse displays excitatory effects, whereas repetitive pulse has an inhibitory effect (Parkin et al., 2015). Lega and colleagues (Lega et al., 2016) applied offline repetitive TMS at 1 Hz to the right cerebellum expecting an inhibiting effect on performance. Participants performed two tasks – a pitch discrimination and a timbre discrimination task – before and after they received TMS. They found that offline repetitive TMS at 1 Hz impaired pitch discrimination ability but not timbre discrimination. These results show a possible association between the subcortical cerebellum and pitch discrimination ability.

So far, studies investigating the effects of non-invasive brain stimulation on auditory perceptual learning produced mixed results. On one hand, cathodal tDCS on the right auditory cortex – specifically, Heschl's gyrus – has shown to disrupt pitch discrimination performance (Mathys et al., 2010). On the other hand, anodal tDCS that is thought to have an excitatory effect on the brain, displayed the same disruptive effect (Matsushita et al., 2015, 2021; Tang et al., 2013). Other brain regions that have been linked to auditory perceptual learning are the left posterior inferior frontal gyrus and the cerebellum (Lega et al., 2016; Loui et al., 2010). Interestingly, none of the studies using non-invasive brain stimulation led to an improvement in performance on an auditory perceptual learning task. An overview of the stimulated areas and non-invasive brain stimulation techniques used in auditory perceptual learning studies can be found in Fig. 2.

#### 4. Challenges and future directions

The conflicting results found in studies applying non-invasive brain stimulation to auditory perceptual learning could be explained by methodological differences. The first difference lies in the use of offline stimulation versus online stimulation. So far, no studies have examined the effects of online versus offline stimulation in auditory perceptual learning directly. However, a study investigating the effect of online versus offline transcranial electrical stimulation in visual perceptual learning found that offline stimulation applied to the primary visual cortex increased visual perceptual learning whereas online tDCS did not improve performance (Pirulli et al., 2013). Although visual perceptual learning and auditory perceptual learning have different underlying mechanisms both are based on experience-dependent learning. Therefore, future research may benefit from further exploring online and offline stimulation in auditory perceptual learning.

Another crucial difference is whether a study used stimulation of learning or stimulation of test performance. In a stimulation of learning paradigm, the subject participates in a learning phase first while receiving stimulation before or during this phase, concurrently the participant is tested on a learning outcome measure (Simonsmeier et al., 2018). In contrast, in stimulation of test performance, participants receive brain stimulation before or during their performance on a test without any learning phase beforehand. Simonsmeier and colleagues (Simonsmeier et al., 2018) argues for an underestimation of the beneficial effects of transcranial electrical stimulation due to a lack of differentiation in studies between stimulation of learning and stimulation of test performance. With their meta-analysis, they showed that



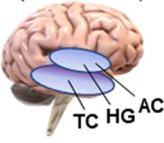
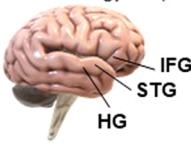
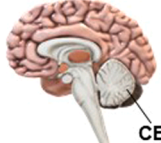
Type of stimulation	Anodal transcranial direct current stimulation (tDCS)	Cathodal transcranial direct current stimulation (tDCS)	Repetitive transcranial magnetic stimulation (rTMS)
Target areas	Right auditory cortex (AC) Heschl's gyrus (HG) Right temporal cortex (TC) 	Heschl's gyrus (HG) Superior temporal gyrus (STG) Inferior frontal gyrus (IFG) 	Cerebellum (CB) 
Current	20-25 minutes at 1.0 - 2.0 mA	20-25 minutes at 1.0 - 2.0 mA	Repeated sessions at 1 Hz
References	Mathys et al. (2010), Tang & Hammond (2013), Matsushita et al. (2015), Matsushita et al. (2021)	Mathys et al. (2010), Loui et al. (2010)	Lega et al. (2016)

Fig. 2. Schematic overview of studies. Overview of non-invasive brain stimulation applied in auditory perceptual learning studies.

transcranial electrical stimulation in the learning phase is more effective than transcranial electrical stimulation in the test phase on a variety of cognitive tasks. When looking at the studies mentioned here, half of the studies used stimulation of learning (Matsushita et al., 2015, 2021; Tang et al., 2013) and the other half stimulation of test performance (Lega et al., 2016; Loui et al., 2010; Mathys et al., 2010). What could also be considered is the type of stimulation that is used. The studies discussed above that used transcranial electrical stimulation, all used tDCS. Considering the methodological differences between the three types of transcranial electrical stimulation, it is important to evaluate which one suits the current modality best. Although no studies have directly investigated the effects of tACS on auditory perceptual learning, there are some studies that looked at the effects of tACS on auditory cortex excitability (Hyvärinen et al., 2018; Wang et al., 2021, 2023). Wang and colleagues (Wang et al., 2021) investigated the effects of tACS on the auditory cortex by using the auditory steady-state response (ASSR) – a measure used to assess activity in the auditory pathway – and found that tACS had an inhibitory effect on 40 Hz ASSR, implying that tACS might modulate cortical activity in the auditory cortex. In contrast, Van Doren et al. (2014) found that temporal tRNS increased the power of the 40 Hz ASSR. These studies indicate that not only tDCS can modulate cortical activity in the auditory cortex, but tACS and tRNS also seem to do so. Therefore, future studies may benefit from using tACS and tRNS in relation to auditory perceptual learning. Furthermore, another suggestion has been offered for the conflicting results in transcranial electrical stimulation studies. Namely, it has been proposed that the effects of transcranial electrical stimulation might be more likely to be due to stimulation of peripheral nerves in the skin and not only by direct stimulation of the cortex (Asamoah et al., 2019). The hypothesis of peripheral nerve stimulation has been supported by a study by Vöröslakos and colleagues (Vöröslakos et al., 2018) who showed that only 25 to 50 percent of the applied current reaches the brain due to the high electrical resistance of the skull. Indeed, our research group has found an enhancing effect on learning and memory when delivering stimulation to the greater occipital nerve (Luckey et al., 2022, 2020; Vanneste et al., 2020). By using occipital nerve stimulation, the locus coeruleus-noradrenaline pathway might be activated via the peripheral nervous system (Bear et al., 1986; Martins et al., 2015; Vanneste et al., 2020). The locus coeruleus-noradrenaline pathway has shown to promote arousal through the influence of the nucleus of the solitary tract (McIntyre et al., 2012). Concurrently, arousal has shown to improve

frequency discrimination by reducing noise correlations (Downer et al., 2015; Lin et al., 2019). Animal studies have shown that pairing perceptual learning with stimulation of the locus coeruleus in rats enhanced auditory perceptual learning through the release of noradrenaline in the auditory cortex (Glennon et al., 2019; Martins et al., 2015). They found that activation of the locus coeruleus paired with pure tones led to long-term responses in formerly silent cells indicating plasticity. Behaviourally, an accelerated learning rate for a new tone in the rats that received locus coeruleus stimulation compared to the control group was observed. These studies suggest that the locus coeruleus plays an important role in auditory perceptual learning, and by using occipital nerve stimulation, the locus coeruleus might be activated in humans (Vanneste et al., 2020). These findings also tie in with the earlier discussed study by Edeline and colleagues (Edeline et al., 2011) in which they found plasticity in the auditory thalamus as a result of locus coeruleus stimulation (Bajo et al., 2010; Edeline et al., 2011). A similar pathway exists for other peripheral nerves including the vagus nerve, in which stimulation increases the noradrenergic release from the locus coeruleus, and in some studies has been associated with increased retention performance and consolidation (Ghacibeh et al., 2006; Jacobs et al., 2020). Vagus nerve stimulation has also been shown to act on the basal forebrain from projections of the nucleus of the solitary tract, which further suggests that the basal forebrain-aCh system can be activation via vagus nerve stimulation, as it has been shown that vagus nerve stimulation evoked activity of the cholinergic axons in the auditory cortex (Mridha et al., 2021). Other pathways that have been stimulated transcutaneously are the trigeminal and dorsal column pathways to the dorsal cochlear nucleus by Wu and colleagues (Wu et al., 2015). They used transcutaneous electrical stimulation of the face and neck in rats to activate these pathways combined with an auditory stimulus. They observed long-lasting changes in the firing rates of the fusiform cells as a result of the stimulation, indicating stimulus time dependent plasticity in these cells.

To conclude, both anodal and cathodal tDCS applied to the auditory cortex disrupt auditory perceptual learning (Mathys et al., 2010; Matsushita et al., 2015, 2021). Additionally, rTMS to the cerebellum also showed a disruption in auditory perceptual learning (Lega et al., 2016). The mechanisms underlying the disruption are unclear. There are major differences in the application of stimulation in these studies. While some studies used online stimulation, others used offline stimulation with wide variety in the amount of stimulation sessions. It may improve

future research in auditory perceptual learning to establish a protocol to be used in non-invasive brain stimulation studies by using knowledge from other fields. In addition, most studies thus far have applied stimulation to the auditory cortex. However, there are many studies that show plasticity in the auditory system starts subcortically (Bajo et al., 2010; Carcagno et al., 2011; Edeline et al., 2011; Lega et al., 2016; Wu et al., 2015). Therefore, we suggest future research to not only target the A1 but also focus on the subcortical structures in the auditory pathway, including the cochlear nucleus, the locus coeruleus, or the nucleus basalis as a way to stimulate plasticity and possibly enhance auditory perceptual learning. In humans, these subcortical structures could be activated non-invasively through the use of peripheral nerve stimulation. This might enhance our understanding of the auditory pathways and the subcortical structures involved with auditory perceptual learning. A further understanding could be useful in auditory disorders, for example in speech disorders, tinnitus, or for cochlear implant users.

## 5. Conclusion

The different techniques used in research related to auditory perceptual learning have all contributed substantially to a better understanding of the neural mechanisms underlying perceptual learning. From these studies, it has become clear that synaptic plasticity is key in understanding auditory perceptual learning. Research in animal models have shown an association between tonotopic map plasticity in the A1 and improved frequency discrimination. By using non-invasive brain stimulation, cortical activity can be modulated and promoted which has provided the field with further understanding of the brain areas involved with auditory perceptual learning. Although non-invasive brain stimulation seems to have these enhancing effects in other domains, in the auditory domain the effect seems to be mostly disruptive. However, many methodological differences have been found between these studies and there is not only a pressing need for more studies in this area, but also more agreement in the application of non-invasive brain stimulation in auditory perceptual learning studies – with regards to the timing of stimulation, the type of stimulation, and the stimulated brain area. We suggest exploring peripheral nerve stimulation for subcortical structures to understand more about the auditory pathways. From these studies, a better understanding of the mechanisms of auditory perceptual learning in humans can be established which will be relevant for understanding how perceptual learning occurs.

## CRedit authorship contribution statement

**Yvette Grootjans:** Writing – original draft, Writing – review & editing. **Gabriel Byczynski:** Writing – review & editing. **Sven Vanneste:** Writing – review & editing.

## Declaration of Competing Interest

None.

## Data availability

No data was used for the research described in the article.

## Funding

This research did not receive any specific grant from funding agencies in the public, commercial, or not-for-profit sectors.

## References

Asamoah, B., Khatoun, A., Mc Laughlin, M., 2019. tACS motor system effects can be caused by transcutaneous stimulation of peripheral nerves. *Nat. Commun.* 10, 266.

- Bajo, V.M., Nodal, F.R., Moore, D.R., King, A.J., 2010. The descending corticocollicular pathway mediates learning-induced auditory plasticity. *Nat. Neurosci.* 13, 253–260.
- Bear, M.F., Singer, W., 1986. Modulation of visual cortical plasticity by acetylcholine and noradrenaline. *Nature* 320, 172–176.
- Brown, M., Irvine, D.R., Park, V.N., 2004. Perceptual learning on an auditory frequency discrimination task by cats: association with changes in primary auditory cortex. *Cereb. Cortex* 14, 952–965.
- Carcagno, S., Plack, C.J., 2011. Subcortical plasticity following perceptual learning in a pitch discrimination task. *J. Assoc. Res. Otolaryngol.* 12, 89–100.
- Cirillo, G., Di Pino, G., Capone, F., Ranieri, F., Florio, L., Todesco, V., Tedeschi, G., Funke, K., Di Lazzaro, V., 2017. Neurobiological after-effects of non-invasive brain stimulation. *Brain Stimul.* 10, 1–18.
- Dehmel, S., Pradhan, S., Koehler, S., Bledsoe, S., Shore, S., 2012. Noise overexposure alters long-term somatosensory-auditory processing in the dorsal cochlear nucleus—possible basis for tinnitus-related hyperactivity? *J. Neurosci.* 32, 1660–1671.
- Downer, J.D., Niwa, M., Sutter, M.L., 2015. Task engagement selectively modulates neural correlations in primary auditory cortex. *J. Neurosci.* 35, 7565–7574.
- Edeline, J.-M., Manunta, Y., Hennevin, E., 2011. Induction of selective plasticity in the frequency tuning of auditory cortex and auditory thalamus neurons by locus coeruleus stimulation. *Hear. Res.* 274, 75–84.
- Froemke, R.C., Merzenich, M.M., Schreiner, C.E., 2007. A synaptic memory trace for cortical receptive field plasticity. *Nature* 450, 425–429.
- Froemke, R.C., Carcea, I., Barker, A.J., Yuan, K., Seybold, B.A., Martins, A.R., Zaika, N., Bernstein, H., Wachs, M., Levis, P.A., Polley, D.B., Merzenich, M.M., Schreiner, C.E., 2013. Long-term modification of cortical synapses improves sensory perception. *Nat. Neurosci.* 16, 79–88.
- Ghacibeh, G.A., Shenker, J.I., Shenal, B., Uthman, B.M., Heilman, K.M., 2006. The influence of vagus nerve stimulation on memory. *Cogn. Behav. Neurol.* 19, 119–122.
- Gibson, E.J., 1953. Improvement in perceptual judgments as a function of controlled practice or training. *Psychol. Bull.* 50, 401–431.
- Gibson, E.J., 1969. *Principles of Perceptual Learning and Development*. Appleton-Century-Crofts. East Norwalk, CT, US.
- Glennon, E., Carcea, I., Martins, A.R.O., Multani, J., Shehu, I., Svirsky, M.A., Froemke, R.C., 2019. Locus coeruleus activation accelerates perceptual learning. *Brain Res.* 1709, 39–49.
- Gold, J.I., Watanabe, T., 2010. Perceptual learning. *Curr. Biol.* 20, R46–R48.
- Hackett, T.A., 2015. Chapter 2 - Anatomic organization of the auditory cortex. In: Aminoff, M.J., Boller, F., Swaab, D.F., (Eds.), *Handbook of Clinical Neurology*, Vol. 129. Elsevier, pp. 27–53.
- He, W., Fong, P.Y., Leung, T.W.H., Huang, Y.Z., 2020. Protocols of non-invasive brain stimulation for neuroplasticity induction. *Neurosci. Lett.* 719, 133437.
- Hensch, T.K., 2005. Critical period plasticity in local cortical circuits. *Nat. Rev. Neurosci.* 6, 877–888.
- Hoy, K.E., Fitzgerald, P.B., 2010. Brain stimulation in psychiatry and its effects on cognition. *Nat. Rev. Neurol.* 6, 267–275.
- Huang, Y.Z., Lu, M.K., Antal, A., Classen, J., Nitsche, M., Ziemann, U., Ridding, M., Hamada, M., Ugawa, Y., Jaberzadeh, S., Suppa, A., Paulus, W., Rothwell, J., 2017. Plasticity induced by non-invasive transcranial brain stimulation: a position paper. *Clin. Neurophysiol.* 128, 2318–2329.
- Hyvärinen, P., Choi, D., Demarchi, G., Aarnisalo, A.A., Weisz, N., 2018. tACS-mediated modulation of the auditory steady-state response as seen with MEG. *Hear. Res.* 364, 90–95.
- Irvine, D.R., Rajan, R., Brown, M., 2001. Injury- and use-related plasticity in adult auditory cortex. *Audiol. Neurotol.* 6, 192–195.
- Irvine, D.R.F., 2018a. Plasticity in the auditory system. *Hear. Res.* 362, 61–73.
- Irvine, D.R.F., 2018b. Auditory perceptual learning and changes in the conceptualization of auditory cortex. *Hear. Res.* 366, 3–16.
- Jacobs, H.I., Priovoulos, N., Riphagen, J.M., Poser, B.A., Napadow, V., Uludag, K., Sclocco, R., Ivanov, D., Verhey, F.R., 2020. Transcutaneous vagus nerve stimulation increases locus coeruleus function and memory performance in older individuals: featured research and focused topic sessions: interventions targeting the noradrenergic system in Alzheimer's and neurodegenerative disease. *Alzheimer's Dementia* 16, e044766.
- Johnson, D.H., 1980. The relationship between spike rate and synchrony in responses of auditory-nerve fibers to single tones. *J. Acoust. Soc. Am.* 68, 1115–1122.
- Kilgard, M.P., Merzenich, M.M., 1998. Cortical map reorganization enabled by nucleus basalis activity. *Science* 279, 1714–1718.
- Koehler, S.D., Shore, S.E., 2013. Stimulus-timing dependent multisensory plasticity in the guinea pig dorsal cochlear nucleus. *PLoS ONE* 8, e59828.
- Lega, C., Vecchi, T., D'Angelo, E., Cattaneo, Z., 2016. A TMS investigation on the role of the cerebellum in pitch and timbre discrimination. *Cerebellum Ataxias* 3, 6.
- Lin, P.A., Asinof, S.K., Edwards, N.J., Isaacson, J.S., 2019. Arousal regulates frequency tuning in primary auditory cortex. *Proc. Natl. Acad. Sci. U. S. A.* 116, 25304–25310.
- Loui, P., Hohmann, A., Schlaug, G., 2010. Inducing disorders in pitch perception and production: a reverse-engineering approach. *Proc. Meet. Acoust.* 9, 50002.
- Loui, P., Guenther, F.H., Mathys, C., Schlaug, G., 2008. Action-perception mismatch in tone-deafness. *Curr. Biol.* 18, R331–R332.
- Luckey, A.M., McLeod, S.L., Mohan, A., Vanneste, S., 2022. Potential role for peripheral nerve stimulation on learning and long-term memory: a comparison of alternating and direct current stimulations. *Brain Stimul.* 15, 536–545.
- Luckey, A.M., McLeod, S.L., Robertson, L.H., To, W.T., Vanneste, S., 2020. Greater occipital nerve stimulation boosts associative memory in older individuals: a randomized trial. *Neurorehabil. Neural Repair.* 34, 1020–1029.
- Martins, A.R.O., Froemke, R.C., 2015. Coordinated forms of noradrenergic plasticity in the locus coeruleus and primary auditory cortex. *Nat. Neurosci.* 18, 1483–1492.



- Mathys, C., Loui, P., Zheng, X., Schlaug, G., 2010. Non-invasive brain stimulation applied to Heschl's gyrus modulates pitch discrimination. *Front. Psychol.* 1, 193.
- Matsushita, R., Andoh, J., Zatorre, R.J., 2015. Polarity-specific transcranial direct current stimulation disrupts auditory pitch learning. *Front. Neurosci.* 9, 174.
- Matsushita, R., Puschmann, S., Baillet, S., Zatorre, R.J., 2021. Inhibitory effect of tDCS on auditory evoked response: simultaneous MEG-tDCS reveals causal role of right auditory cortex in pitch learning. *Neuroimage* 233, 117915.
- McIntyre, C.K., McGaugh, J.L., Williams, C.L., 2012. Interacting brain systems modulate memory consolidation. *Neurosci. Biobehav. Rev.* 36, 1750–1762.
- Mridha, Z., de Gee, J.W., Shi, Y., Alkashgari, R., Williams, J., Suminski, A., Ward, M.P., Zhang, W., McGinley, M.J., 2021. Graded recruitment of pupil-linked neuromodulation by parametric stimulation of the vagus nerve. *Nat. Commun.* 12, 1539.
- Muhlnickel, W., Elbert, T., Taub, E., Flor, H., 1998. Reorganization of auditory cortex in tinnitus. *Proc. Natl. Acad. Sci. U.S.A.* 95, 10340–10343.
- Musiek, F.E., Baran, J.A., 2018. The Auditory System: Anatomy, physiology, and Clinical Correlates. Plural Publishing.
- Nitsche, M.A., Seeber, A., Frommann, K., Klein, C.C., Rochford, C., Nitsche, M.S., Fricke, K., Liebetanz, D., Lang, N., Antal, A., Paulus, W., Tergau, F., 2005. Modulating parameters of excitability during and after transcranial direct current stimulation of the human motor cortex. *J. Physiol.* 568, 291–303.
- Parkin, B.L., Ekhtiari, H., Walsh, V.F., 2015. Non-invasive human brain stimulation in cognitive neuroscience: a primer. *Neuron* 87, 932–945.
- Peterson, D.C., Reddy, V., Hamel, R.N., 2022. Neuroanatomy, Auditory Pathway. StatPearls, Treasure Island (FL). StatPearls Publishing, Copyright © 2022, StatPearls Publishing LLC.
- Pirulli, C., Fertonani, A., Miniussi, C., 2013. The role of timing in the induction of neuromodulation in perceptual learning by transcranial electric stimulation. *Brain Stimul.* 6, 683–689.
- Polley, D.B., Steinberg, E.E., Merzenich, M.M., 2006. Perceptual learning directs auditory cortical map reorganization through top-down influences. *J. Neurosci.* 26, 4970–4982.
- Puckett, A.C., Pandya, P.K., Moucha, R., Dai, W., Kilgard, M.P., 2007. Plasticity in the rat posterior auditory field following nucleus basalis stimulation. *J. Neurophysiol.* 98, 253–265.
- Rajan, R., Irvine, D.R., Wise, L.Z., Heil, P., 1993. Effect of unilateral partial cochlear lesions in adult cats on the representation of lesioned and unlesioned cochleas in primary auditory cortex. *J. Comp. Neurol.* 338, 17–49.
- Recanzone, G.H., Schreiner, C.E., Merzenich, M.M., 1993. Plasticity in the frequency representation of primary auditory cortex following discrimination training in adult owl monkeys. *J. Neurosci.* 13, 87–103.
- Reed, A., Riley, J., Carraway, R., Carrasco, A., Perez, C., Jakkamsetti, V., Kilgard, M.P., 2011. Cortical map plasticity improves learning but is not necessary for improved performance. *Neuron* 70, 121–131.
- Saenz, M., Langers, D.R.M., 2014. Tonotopic mapping of human auditory cortex. *Hear. Res.* 307, 42–52.
- Shore, S.E., Zhou, J., 2006. Somatosensory influence on the cochlear nucleus and beyond. *Hear. Res.* 216–217, 90–99.
- Simonsmeier, B.A., Grabner, R.H., Hein, J., Krenz, U., Schneider, M., 2018. Electrical brain stimulation (tES) improves learning more than performance: a meta-analysis. *Neurosci. Biobehav. Rev.* 84, 171–181.
- Stefanescu, R.A., Koehler, S.D., Shore, S.E., 2015. Stimulus-timing-dependent modifications of rate-level functions in animals with and without tinnitus. *J. Neurophysiol.* 113, 956–970.
- Suga, N., Ma, X., 2003. Multiparametric corticofugal modulation and plasticity in the auditory system. *Nat. Rev. Neurosci.* 4, 783–794.
- Tang, M.F., Hammond, G.R., 2013. Anodal transcranial direct current stimulation over auditory cortex degrades frequency discrimination by affecting temporal, but not place, coding. *Eur. J. Neurosci.* 38, 2802–2811.
- Thomas, M.E., Lane, C.P., Chaudron, Y.M.J., Cisneros-Franco, J.M., de Villers-Sidani, É., 2020. Modifying the adult rat tonotopic map with sound exposure produces frequency discrimination deficits that are recovered with training. *J. Neurosci.* 40, 2259–2268.
- Van Doren, J., Langguth, B., Schecklmann, M., 2014. Electroencephalographic effects of transcranial random noise stimulation in the auditory cortex. *Brain Stimul.* 7, 807–812.
- Vanneste, S., Mohan, A., Yoo, H.B., Huang, Y., Luckey, A.M., McLeod, S.L., Tabet, M.N., Souza, R.R., McIntyre, C.K., Chapman, S., Robertson, I.H., To, W.T., 2020. The peripheral effect of direct current stimulation on brain circuits involving memory. *Sci. Adv.* 6.
- von Békésy, G., 1970. Travelling waves as frequency analysers in the cochlea. *Nature* 225, 1207–1209.
- Voroslakos, M., Takeuchi, Y., Brinyiczki, K., Zombori, T., Oliva, A., Fernandez-Ruiz, A., Kozak, G., Kincses, Z.T., Ivanyi, B., Buzsáki, G., Berenyi, A., 2018. Direct effects of transcranial electric stimulation on brain circuits in rats and humans. *Nat. Commun.* 9, 483.
- Wang, Y., Dong, G., Shi, L., Yang, T., Chen, R., Wang, H., Han, G., 2021. Depression of auditory cortex excitability by transcranial alternating current stimulation. *Neurosci. Lett.* 742, 135559.
- Wang, Y., Zhang, Y., Hou, P., Dong, G., Shi, L., Li, W., Wei, R., Li, X., 2023. Excitability changes induced in the human auditory cortex by transcranial alternating current stimulation. *Neurosci. Lett.* 792, 136960.
- Weinberger, N.M., 2004. Specific long-term memory traces in primary auditory cortex. *Nat. Rev. Neurosci.* 5, 279–290.
- Weinberger, N.M., 2007. Associative representational plasticity in the auditory cortex: a synthesis of two disciplines. *Learn. Mem.* 14, 1–16.
- Witte, R.S., Kipke, D.R., 2005. Enhanced contrast sensitivity in auditory cortex as cats learn to discriminate sound frequencies. *Cognit. Brain Res.* 23, 171–184.
- Woods, A.J., Antal, A., Bikson, M., Boggio, P.S., Brunoni, A.R., Celnik, P., Cohen, L.G., Fregni, F., Herrmann, C.S., Kappenman, E.S., Knotkova, H., Liebetanz, D., Miniussi, C., Miranda, P.C., Paulus, W., Priori, A., Reato, D., Stagg, C., Wenderoth, N., Nitsche, M.A., 2016. A technical guide to tDCS, and related non-invasive brain stimulation tools. *Clin. Neurophysiol.* 127, 1031–1048.
- Wright, B.A., Zhang, Y., 2009. Insights into human auditory processing gained from perceptual learning. *The Cognitive Neurosciences*, 4th ed. Massachusetts Institute of Technology, Cambridge, MA, US, pp. 353–365.
- Wu, C., Martel, D., Shore, S., 2015. Transcutaneous induction of stimulus timing dependent plasticity in dorsal cochlear nucleus. *Front. Syst. Neurosci.* 9.



# Peripheral nerve stimulation: A neuromodulation-based approach

Alison M. Luckey<sup>a,b</sup>, Katherine Adcock<sup>a,b</sup>, Sven Vanneste<sup>a,b,c,\*</sup>,<sup>1</sup>

<sup>a</sup> Lab for Clinical & Integrative Neuroscience, School of Psychology, Trinity College Dublin, Dublin, Ireland

<sup>b</sup> Trinity College Institute for Neuroscience, Trinity College Dublin, Dublin, Ireland

<sup>c</sup> Global Brain Health Institute, Trinity College Dublin, Dublin, Ireland

## ARTICLE INFO

### Keywords:

Direct current stimulation  
Locus coeruleus  
Reticular formation  
Occipital nerve stimulation  
Vagus nerve stimulation  
Trigeminal nerve stimulation

## ABSTRACT

Recent technological improvements have positioned us at the threshold of innovative discoveries that will assist in new perspectives and avenues of research. Increased attention has been directed towards peripheral nerve stimulation, particularly of the vagus, trigeminal, or greater occipital nerve, due to their unique pathway that engages neural circuits within networks involved in higher cognitive processes. Here, we question whether the effects of transcutaneous electrical stimulation are mediated by synergistic interactions of multiple neuromodulatory networks, considering this pathway is shared by more than one neuromodulatory system. By spotlighting this attractive transcutaneous pathway, this opinion piece aims to acknowledge the contributions of four vital neuromodulators and prompt researchers to consider them in future investigations or explanations.

## 1. A shift from transcranial to transcutaneous

Over the past decade, investigations researching ways to boost synaptic plasticity have attracted attention from a broad array of professional fields, including neuroscience, engineering, and even the U.S. Department of Defense – which in 2017 began funding research to exploit neuromodulation interventions to improve and accelerate training of military personnel via the activation of peripheral nerves to tune neural networks responsible for vital cognitive skills. However, the field's understanding of the underlying neurophysiological mechanism(s) of peripheral nerve stimulation remains limited and opposes the prevailing mechanistic explanation of non-invasive neuromodulation methods, namely transcranial electrical stimulation (tES), including direct and alternate current stimulation (see Box 1).

Lately, the debate concerning the transcranial versus transcutaneous mechanism has gained new prominence in light of recent investigations unveiling striking evidence that suggests a transcutaneous mechanism may be more suitable and plausible (Fig. 1) (Liu et al., 2018). Calculations on a realistic head model and validation studies in both animal and human experiments have indicated that only 25 (up to 50) percent of the applied current reaches the brain due to the high electrical resistance of the skull, while the remaining current is shunted through extracranial soft tissues (Liu et al., 2018; Voroslakos et al., 2018). Additionally, tES

delivered at peak 1 mA induced an electrical field of approximately 0.2 V/m when measured at the cortex, a level that contains an inadequate threshold to initiate an action potential in cortical neurons (Liu et al., 2018; Voroslakos et al., 2018). It is important to note that the maximal electric field for 1 mA peak intensity amounts to <0.5 V/m in other independent studies with the use of intracranial electrodes (Huang et al., 2017; Opitz et al., 2016). Furthermore, human cadaver and in vivo rat experiments indicated that for brain networks to be adequately modified directly, an electric current of approximately 6 mA would need to be administered to the scalp (Voroslakos et al., 2018). Regrettably, this requisite of 6 mA would considerably exceed the latest safety guidelines of <4 mA for tES application (Bikson et al., 2016; Thair et al., 2017). Alternatively, tES delivered at 1 mA results in an electrical field that surpasses 20 V/m in the scalp and engages peripheral nerves inside the scalp (Asamoah et al., 2019), initiating the action potentials needed to indirectly modify brain activity (So et al., 2004).

Recently, a perspective piece has endorsed the alternative, peripheral route, referencing the prior assumption of how the effects of tES transpire solely due to the weak, subthreshold electric field it generates in the cortex as being an oversimplification (van Boekholdt et al., 2021). The authors suggest that observed tES effects are instead triggered through peripheral stimulation of the ascending reticular activating system, which promotes the release of noradrenaline from the locus

\* Correspondence to: Lab for Clinical & Integrative Neuroscience, School of Psychology, Global Brain Health Institute, Institute of Neuroscience, Trinity College Dublin, College Green 2, Dublin, Ireland.

E-mail address: [sven.vanneste@tcd.ie](mailto:sven.vanneste@tcd.ie) (S. Vanneste).

<sup>1</sup> website: <http://www.lab-clint.org>.

<https://doi.org/10.1016/j.neubiorev.2023.105180>

Received 28 October 2022; Received in revised form 23 March 2023; Accepted 11 April 2023

Available online 12 April 2023

0149-7634/© 2023 The Author(s). Published by Elsevier Ltd. This is an open access article under the CC BY license (<http://creativecommons.org/licenses/by/4.0/>).

coeruleus (LC) throughout the brain (van Boekholdt et al., 2021). Building upon this alternative explanation, we provide evidence from several studies to extend this understanding and go beyond the noradrenergic system. We question whether the effects of tES and other forms of neuromodulation are mediated by additional neuromodulatory networks. In the following sections, we discuss an attractive transcutaneous pathway, followed by evidence highlighting the contributions of other vital neuromodulators that researchers might want to consider in future investigations or explanations.

## 2. Proposed transcutaneous pathway

Directly stimulating the trigeminal and the occipital nerve is an acknowledged and longstanding technique for neuropathic pain suppression and managing headache syndromes (Helm et al., 2021; Slavin, 2011; Zhou et al., 2021). Moreover, attention has been directed towards peripheral stimulation of these nerves due to their unique pathway that engages neural circuits within networks that are highly involved in higher cognitive processes (see Fig. 2). The trigeminal nerve begins in

the brain and travels throughout the head to where the nerve endings span across the face and forehead (Rea, 2015). On the other hand, the greater occipital nerve arises from the C2 spinal nerve with several branches innervating the posterior occiput up to the scalp vertex (Weiner and Alo, 2018). These two nerves are interlinked (Busch et al., 2006) and presumably encompass many traditional anterior and posterior electrode montages of non-invasive stimulation utilized by current experimental studies (van Boekholdt et al., 2021) (see Box 3). Of particular importance, targeting either the trigeminal or greater occipital nerve via cutaneous electrodes establishes communication gateways from the periphery to the brain via the specific afferent fibers that project to the brainstem and synapse onto the nucleus tractus solitarius (NTS); various rodent studies have used anterograde neuronal tracers to demonstrate these connections (Adair et al., 2020; Caous et al., 2001; de Sousa Buck et al., 2001; Menetrey and Basbaum, 1987). From the NTS, the information is then integrated and relayed across the brainstem amongst networks within the complex reticular formation (Kawai, 2018), whereby sensory information is processed via the thalamocortical networks (Halassa and Sherman, 2019), and environmental or

### Box 1

Traditional account of transcranial direct and alternate current stimulation.

One of the most significant current discussions regarding non-invasive stimulation techniques is whether much of the electrical current modulating the excitability of neurons is provided transcranially, directly and in a regionally constrained manner, or transcutaneously, where the current flow primarily affects neural circuits indirectly via peripheral nerves. The predominant understanding of transcranial direct current stimulation (tDCS) proposes that it employs a unidirectional, direct current at a low or weak intensity (1–2 mA) via two or more strategically placed electrodes (at least one anode and one cathode) in order to transmit the current from the device to the scalp in an effort to polarize the region (Nitsche and Paulus, 2000; Nitsche et al., 2005). In doing so, tDCS aims to modulate cortical excitability and spontaneous activity through subthreshold alterations on neuronal resting membrane potentials, thus increasing or decreasing the neuron's likelihood to fire an action potential (Nitsche and Paulus, 2000; Reed and Cohen Kadosh, 2018; Woods et al., 2016). Prior to the usage of tDCS, it is necessary to consider all components of the methodological design, such as the size and placement of the electrodes and selection of a tolerable stimulus protocol (i.e., current intensity) (Woods et al., 2016), given that they are key indicators of current density and the distribution of the electrical field (Jackson et al., 2016). Further attention is advised to the current intensity and stimulation duration, owing to their potential to substantially impact short- and long-term effects produced by tDCS (Nitsche and Paulus, 2000).

Effects generated by tDCS have been deemed similar to long-term potentiation and long-term depression (Kronberg et al., 2017). The ability to produce such outcomes has accelerated tDCS' usage as a treatment option for various neurocognitive disorders associated with plasticity deficits (Jahshan et al., 2017) and tDCS' capability to modify plasticity for memory stabilization (Zhao and Woodman, 2021). Moreover, a relatively recent model, known as activity-selective, suggests that it is preferential to target neuronal populations that are simultaneously active when applying tDCS while also taking into account the state of the brain when stimulation is administered, thereby generating stimulus-specific brain state effects via tDCS (Boroda et al., 2020). It is of note that this has been emphasized in prior research, whereby it was suggested that tDCS be employed with the behavior it strives to modulate (Fritsch et al., 2010), therefore, gaining momentum as an explanation of cognitive enhancement when tasks are aided by t/DCS (Kronberg et al., 2020; Podda et al., 2016).

Distinguishing itself from tDCS, transcranial alternate current stimulation (tACS) omits the unidirectional voltage component and influences the polarization of neurons via sinusoidal fluctuations of the membrane potential (Tavakoli and Yun, 2017). tACS exerts a sine wave current between the anode and cathode electrodes in a half-cycle fashion to modify the spike-timing activity of individual neurons. Five mechanisms have been proposed for how tACS modifies brain activity, likely depending on the estimated field intensity being generated: stochastic resonance, rhythm resonance, temporal bias of spikes, network entrainment, and imposed pattern (Liu et al., 2018). Most conventionally, tACS is characterized to enhance brain oscillations via neural entrainment or synchronized firing of neurons through external stimuli (Reinhart and Nguyen, 2019; Tavakoli and Yun, 2017). To entrain endogenous oscillations, tACS delivers an exogenous oscillation at an equal or increased frequency to enhance the existing oscillation's power (i.e., amplitude), whereas transmitting a signal below the intrinsic frequency will reduce the intrinsic oscillation (Antal and Herrmann, 2016). Frequency, intensity, and phase are three parameters of tACS oscillations that each play a significant role in defining the direction and cyclical pattern of the delivered stimulation (Antal and Herrmann, 2016).

Cortical oscillations are fundamental processes underlying cognition and behavior (Buzsaki and Draguhn, 2004). Moreover, alterations in neuronal synchrony have been identified during the early stages of neurodegenerative disorders (Ahnaou et al., 2017), increasing studies utilizing tACS to intervene with and modulate synchrony to restore oscillatory activity. tACS may be applied across a wide array of frequency ranges, typically within conventional electroencephalography frequencies (0.01–80 Hz), and is generally considered to be brain-state dependent, such that the effect of tACS is influenced by the state the brain is in at the time of application. Accordingly, tACS requires a more concrete stimulation paradigm when preparing experimental study designs or intervention protocols, such that researchers need to predetermine the sought-after cognitive-behavioral processes to identify the underlying native oscillatory properties and frequencies of these processes to entrain the associated oscillations (Woods et al., 2016). Entraining oscillations at a fixed frequency in specific brain areas enables the researchers to extract causal inferences between brain modulation and obtained effects, such as improved communication leading to improved cognition and/or behavior (Herrmann et al., 2013). Although neural entrainment transpiring is yet to be unanimously supported (Beliaeva et al., 2021), the rationale that tACS' frequency may be applied at the exact frequency rhythm fundamental for optimal brain functioning results in favoring frequency-specific synchrony effect via tACS (Reinhart and Nguyen, 2019).

arousal information, as well as other states of vigilance and novelty, will additionally activate LC noradrenergic projections from the brainstem throughout major cortical and subcortical regions (Berridge and Waterhouse, 2003). Therefore, this proposed transcutaneous pathway that emphasizes enhanced LC noradrenergic activation, thereby generating excitatory or inhibitory effects on neural activity (Salgado et al., 2016), has been described as the missing mechanistic link that may underpin the effects of non-invasive brain stimulation (van Boekholdt et al., 2021), and points to an attractive mediator of neuromodulation.

### 3. Activation of locus coeruleus noradrenaline pathway

Due to its vast connectedness and activation responses, we propose that the LC be considered a principal target for peripheral nerve stimulation. The LC noradrenaline system was previously thought to solely regulate arousal and autonomic functions (Berridge and Waterhouse, 2003); however, a greater understanding of organizational afferent projections to the LC has led to a widespread agreement that the LC noradrenaline system is one of the four principle neuromodulatory networks heavily engaged in physiological processes including being a significant contributor to signal transduction and synaptic plasticity required for the LC's dual involvement in behaviors and cognition (Avery and Krichmar, 2017; Poe et al., 2020; Samuels and Szabadi, 2008).

Recent research by our laboratory has endorsed peripheral nerve stimulation via non-invasive stimulation of the greater occipital nerve (NITESGON) to (1) upregulate the LC noradrenaline system, (2) confirm that the occipital nerve was sufficient to induce these changes, and (3) suggest an augmentation of memory performance (see Box 2) (Vanneste et al., 2020). The vagus nerve has also been proposed to activate the same transcutaneous pathway leading to the NTS and LC when stimulated (Yap et al., 2020). This pathway has led to vagus nerve stimulation (VNS) being investigated as an approach to modifying neuroplasticity (Farmer et al., 2020; Yap et al., 2020). Moreover, stimulation of the left cervical vagus nerve has received FDA approval for treating intractable

epilepsy and depression (Farmer et al., 2020) and has been incorporated into rehabilitation programs for various neurological disorders, including ischemic stroke (Engineer et al., 2019; Hays, 2016). Like trigeminal and occipital nerve stimulation, the underlying mechanics of VNS are not yet fully comprehended; however, a proliferation of investigations into VNS have provided a greater understanding than trigeminal and occipital nerve stimulation. For example, Hulsey and colleagues (2017) assessed an extensive range of VNS parameters in rats to show that short bursts and low thresholds (starting at 0.1 mA) prompted phasic LC activity; greater intensities and pulse width increased the phasic activity while varying frequencies impacted timing but not the maximum activity of the LC (Hulsey et al., 2017). These findings demonstrate that VNS can activate the LC and modulate neural activity, suggesting that the LC could mediate the effect observed in VNS research (Hulsey et al., 2017). In a follow-up study, Hulsey and colleagues (2019) demonstrated that left-VNS paired with training resulted in over double the amount of motor cortex area dedicated to proximal forelimb movements detected when compared to the sham and the immunotoxin injected groups; this depletion of noradrenaline innervation to the motor cortex demonstrated the requirement of noradrenergic activity to be a mediator of VNS-directed plasticity (Hulsey et al., 2019).

Taken together, these studies have identified the LC noradrenergic system to be engaged by non-invasive stimulation of the greater occipital nerve and invasive stimulation of the vagus nerve, thus providing merit to its usage to enhance cortical plasticity and improve memory performance.

### 4. Activation of other neuromodulatory pathways

Considering how the vagus, trigeminal, and greater occipital nerve share a pathway leading to nuclei in the brainstem, particularly the NTS, we extracted parallels from preclinical studies employing VNS to highlight other ascending neuromodulatory systems, including the serotonergic, cholinergic, and dopaminergic systems (Brougher et al., 2021a; Hulsey et al., 2016; Hulsey et al., 2019), that have been suggestive of

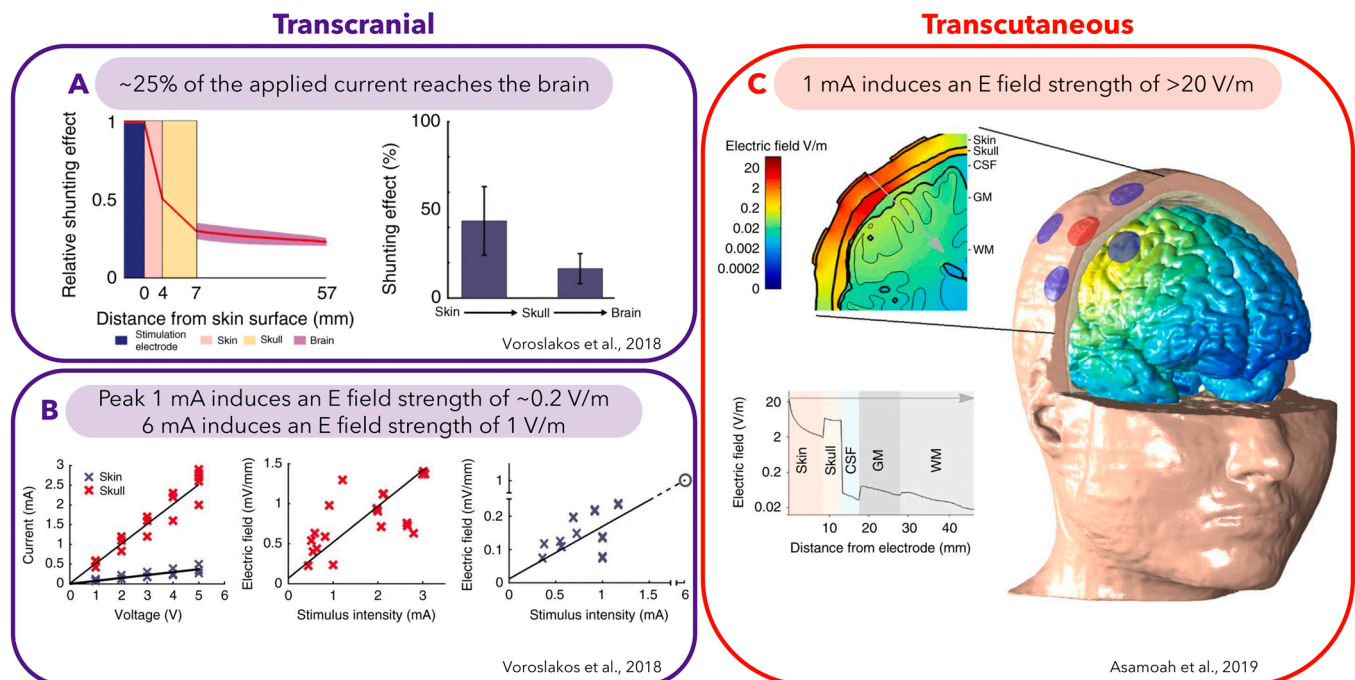


**Fig. 1.** Comparison of electric fields of a transcranial mechanism (Voroslakos et al., 2018) versus a transcutaneous mechanism (Asamoah et al., 2019) (A) Voroslakos and colleagues (2018) demonstrated that due to the shunting effect, approximately 25% (up to 50%) of the applied current reaches the brain. (B) Additionally, Voroslakos and colleagues (2018) presented the relationship between the stimulation intensity and the electric field strength for both transcutaneous (scalp) and subcutaneous (skull with scalp removed) stimulation. (C) Asamoah et al. (2019) illustrated the electric field strength distribution amongst different tissues; using a more focused montage, 1 mA of tACS induces an E field strength of >20 V/m.



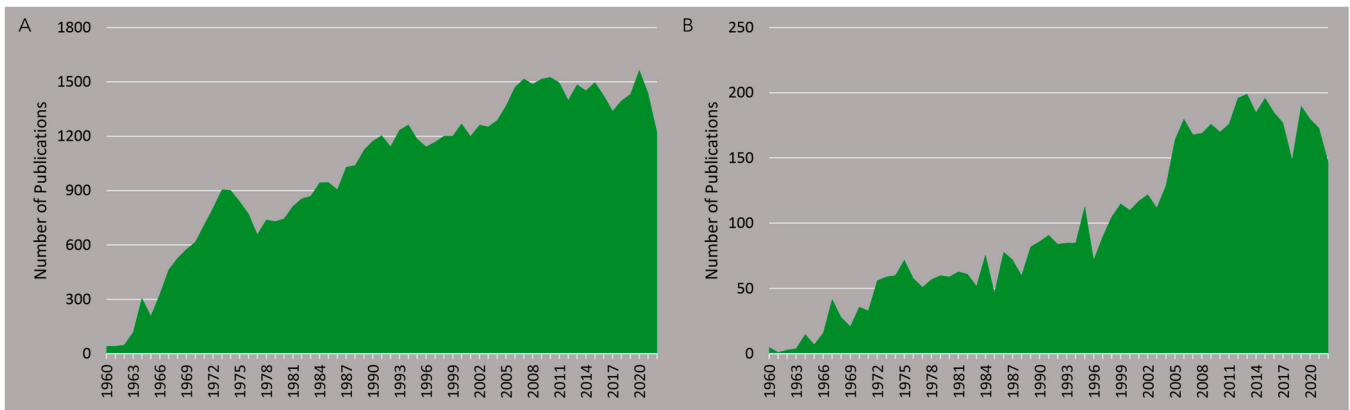


**Fig. 2.** An overview papers published using PubMed from 1960 to 2022 (a) Using peripheral nerve stimulation as keyword (b) Using trigeminal and occipital nerve stimulation as keywords.

### Box 3

The vagus, trigeminal and occipital nerve.

The trigeminal nerve (cranial nerve V) is a cranial nerve responsible for sensation in the face and motor functions such as biting and chewing; it is the most complex of the cranial nerves. Its name derives from each of the two nerves (one on each side of the pons) having three major branches: the ophthalmic nerve, the maxillary nerve, and the mandibular nerve. The ophthalmic and maxillary nerves are purely sensory, whereas the mandibular nerve supplies motor as well as functions. Adding to the complexity of this nerve is that autonomic nerve fibers as well as special sensory fibers (taste) are contained within it. The motor division of the trigeminal nerve derives from the basal plate of the embryonic pons, and the sensory division originates in the cranial neural crest. Sensory information from the face and body is processed by parallel pathways in the central nervous system.

The greater occipital nerve is a nerve of the head. It is a spinal nerve, specifically the medial branch of the dorsal primary ramus of cervical spinal nerve 2. It arises from between the first and second cervical vertebrae, ascends, and then passes through the semispinalis muscle. It ascends further to supply the skin along the posterior part of the scalp to the vertex. It supplies sensation to the scalp at the top of the head, over the ear and over the parotid glands.

### Box 2

Non-invasive stimulation of the greater occipital nerve.

The effects of NITESGON on the LC noradrenaline activity were measured via three common proxy measures: pupillometry, salivary  $\alpha$ -amylase, and neurophysiology [event-related potentials (ERPs)]. This enabled us to track changes (significant increases) from baseline measurements; however, caution should be applied considering these proxy measures possess limitations such as being substantially variable and the potential of other brain regions and monoamine neurotransmitters associated with changes (Jones et al., 2020; Joshi, 2021; Joshi and Gold, 2020). Nevertheless, significant intercorrelations were found amongst the three proxy measures, suggesting that NITESGON can induce changes in LC activity, thus promoting noradrenaline release.

The second set of experiments, including a direct and indirect route of occipital nerve stimulation, were designed to substantiate the transcutaneous mechanism that drives the memory-effect of NITESGON (Vanneste et al., 2020). A more invasive technique directly stimulated the greater occipital nerve in rats to improve memory performance during inhibitory avoidance and object recognition tasks. Additionally, a group of participants received a topical skin anesthetic (lidocaine/prilocaine) cream during initial learning with stimulation to block the activation of peripheral nerves (Kumar et al., 2015). Seven days later, participants with no anesthesia cream demonstrated enhanced memory recollection, indicating effects are driven by peripheral nerve stimulation. Together, these studies suggest that invasive and non-invasive occipital nerve stimulation directly affects memory (Vanneste et al., 2020). These memory improvements have since been replicated in younger and older adult populations and by utilizing transcranial alternating current stimulation (tACS) with salivary  $\alpha$ -amylase concentration levels used to substantiate noradrenergic activation (Luckey et al., 2022; Luckey et al., 2020). These replications divert from proposed limitations associated with age and endorse that other neuromodulation devices are capable of activating transcutaneous pathways.

acting synergistically along with the noradrenergic system to contribute to plasticity to influence behaviors and cognition.

The researchers of the aforementioned preclinical studies carried out additional experiments to examine the significance of other neurotransmitters, such as acetylcholine, originating from the nucleus basalis, and serotonin, originating from the dorsal raphe nucleus, to the

plasticity processes to identify whether neuromodulatory systems can substitute for other networks so that plasticity is not forfeited (Hulsey et al., 2016; Hulsey et al., 2019). Results obtained from intracortical microstimulation motor mapping again demonstrated that left-VNS during training resulted in more than double the percentage of proximal forelimb movements detected compared to the sham and

immunotoxin groups, demonstrating the requirement of serotonergic and cholinergic activity each to be facilitators of VNS-directed plasticity (Hulsey et al., 2016; Hulsey et al., 2019). Multiple neuromodulatory systems being necessary aligns with previous research that exhibited various neuromodulators could cooperatively govern plasticity and how the absence of any of these specific neuromodulators could not be replaced by other neuromodulatory networks also being activated by VNS.

In light of the evidence exhibiting cortical plasticity's dependency on multiple neuromodulators, a second group of researchers sought to determine if cortical dopamine, a neuromodulator originating from the ventral tegmental area (VTA) or substantia nigra pars compacta (SNc), was required for VNS-induced plasticity in the motor cortex. Unexpectedly, the depletion of cortical dopamine did not affect cortical plasticity (Brougher et al., 2021b). However, recent findings of the right nodose ganglion projecting to the NTS and activating dopamine via the VTA and the left nodose ganglion having no such effect (Han et al., 2018) prompted the researchers to compare how stimulation to the right cervical vagus nerve and the traditional left cervical vagus nerve affected behavior and dopaminergic activity from the midbrain when employing matching VNS parameters (Brougher et al., 2021a). Results indicated that right-VNS enhanced activation of the midbrain dopaminergic system and resulted in a more significant number of forelimb movements compared to the left-VNS group (Brougher et al., 2021a). These findings suggest that the preclinical and clinical protocol of traditional left-VNS is unsuitable for driving dopaminergic activity or enhancing behavior. However, right-VNS may be exploited to preferentially promote plasticity via the midbrain dopaminergic systems (Brougher et al., 2021a).

Taken together, the evidence from these studies suggests that lesions in three neuromodulatory networks prevented VNS-movement pairing from generating cortical plasticity, specifically the dorsal raphe nucleus serotonergic and nucleus basalis cholinergic networks. Moreover, the additional findings evoke the potential of right-VNS being an effective intervention to promote dopamine-dependent plasticity. Collectively, the observed results insinuate that cortical serotonin, acetylcholine, and dopamine are each essential to plasticity and can be driven by peripheral nerve stimulation.

## 5. Critical implications for transcutaneous stimulation

Empirical findings within this opinion piece provide an initial understanding of various neuromodulators that can be activated via peripheral nerve stimulation. Taken together, these findings suggest a role for peripheral nerve stimulation in improving or restoring neuroplasticity. For instance, a recent investigation sought to determine if lesions in the nucleus basalis blocking VNS-induced plasticity would consequently affect the efficacy of VNS when paired with motor rehabilitation (Meyers et al., 2019), given that VNS has previously been used to improve recovery after injury (Ganzer et al., 2018; Meyers et al., 2018). Results indicated that VNS during rehabilitation showed repaired motor map representations and improved volitional forelimb function compared to groups that rehabilitated without VNS or received delayed VNS. To address a more causal role, a second set of experiments blocked acetylcholine to further investigate VNS's effect on plasticity and recovery. Results demonstrated that VNS during rehabilitation reversed maladaptive plasticity and helped improve recovery, whereas blocking acetylcholine prevented recovery even when receiving VNS during rehabilitation, thus highlighting cortical acetylcholine's critical function in restoring brain circuits (Meyers et al., 2019).

As demonstrated by the preclinical studies, peripheral nerve stimulation activates these four main neuromodulators (Brougher et al., 2021a; Hulsey et al., 2016; Hulsey et al., 2019), and evidence suggests these neuromodulators are essential for neuroplasticity and, therefore, underlie the effectiveness of peripheral nerve stimulation (Meyers et al., 2019). Through interactions with other brain regions and within the

neuromodulatory systems, neuromodulators are responsible for signaling risk and reward, uncertainty and novelty, and thus directly influence higher-order cognitive functions, including attention, decision-making, goal-directed behavior, and emotion (Avery and Krichmar, 2017). Accordingly, utilizing peripheral nerve stimulation as a therapeutic intervention to upregulate these neuromodulators or as an adjunctive treatment to enhance neuroplasticity may be a suitable approach, considering that a range of neurocognitive and psychiatric disorders are associated with downregulated neuromodulatory systems or plasticity deficits (Avery and Krichmar, 2017; Briand et al., 2007). For example, mood disorders and depression have been linked to impairments in the connections between the serotonergic pathway and the prefrontal cortex (Liu et al., 2019). Moreover, associations regarding malfunction in the cholinergic pathway and disorders of memory, attention deficit hyperactivity disorder, and schizophrenia have been acknowledged (Scarr et al., 2013), whereas abnormal noradrenergic and dopaminergic activity, respectively, have been associated with neurological and psychiatric disorders, most notably Alzheimer's and Parkinson's disease (Beardmore et al., 2021; Latif et al., 2021). Given that previous evidence has spotlighted these neuromodulators' significant role, utilizing peripheral nerve stimulation represents a potential therapeutic strategy.

## 6. Concluding remarks and future perspectives

Research to date has not yet determined the mechanism(s) of non-invasive neuromodulation methods. The significance of this issue has grown in light of recent evidence suggesting that standard electrode montages applied directly to the scalp result in peripheral nerves sustaining electric fields significantly greater in strength than those measured in the cortex (Asamoah et al., 2019). These findings have begun to shift researchers' position away from the prevailing transcranial mechanism toward favoring a transcutaneous approach. The advantage of these novel non-invasive methods of stimulation is that they are easy to apply at a relatively low cost that are easy to be used in a home setting.

This opinion piece aimed to provide greater insight into a bottom-up transcutaneous pathway shared by four neuromodulatory systems (Fig. 3). This proposed concept lays the groundwork for future investigations into peripheral nerve stimulation being an optimal strategy to modulate neuroplasticity in key brain regions that contribute to relevant cognitive processes or brain regions impacted by neurological disease and psychiatric disorders.

A recent perspective piece proposed that the effects of non-invasive brain stimulation may be attributable to the activation of a peripheral pathway that promotes LC noradrenergic activity, especially considering that a myriad of tDCS studies utilize anterior and posterior electrode montages, many of which engage with the trigeminal and the occipital nerve (van Boekholdt et al., 2021). Per this peripheral route, information is transmitted from the trigeminal and occipital nerve to a common hub, the brainstem. Within the brainstem, information is integrated, relayed, and projected from the NTS throughout widespread regions of the central nervous system. However, despite identifying this promising transcutaneous pathway, many factors of peripheral nerve stimulation remain unclear and require further investigation (see Outstanding Questions). Although limited research regarding stimulation of the trigeminal and greater occipital nerve exists, this pathway sharing a central hub with the vagus nerve suggests that stimulation of these nerves can have similar effects to VNS. Therefore, assimilating evidence from VNS literature has helped to detail other neuromodulatory systems, including the serotonergic, cholinergic, and dopaminergic systems, that may be activated when the trigeminal and greater occipital nerves are stimulated.

Although both trigeminal and greater occipital nerve stimulation share a common neural pathway, it does not exclude that both types of nerve stimulation also activate additional pathways that do not overlap.

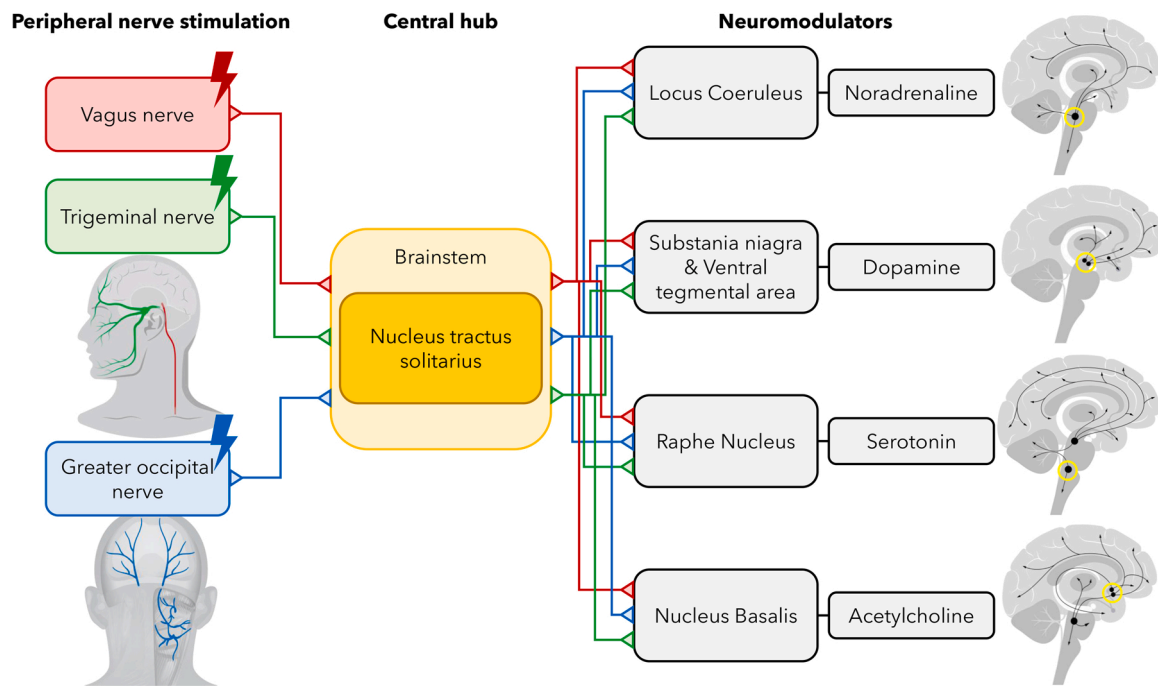


**Fig. 3.** A transcutaneous pathway shared by four neuromodulatory systems. In this proposed transcutaneous mechanism, tES electrodes may be placed amongst cites that stimulate either the trigeminal or greater occipital nerve – likewise, stimulating the cervical vagus nerve via a handheld device applied to the neck or stimulating the auricular vagus nerve via electrodes within ear regions (for VNS recommendations see (Farmer et al., 2020)). Activation of these nerves will send ascending projections to the brainstem, particularly the NTS. From here, there is potential to activate four core neuromodulatory systems, including the far-reaching LC noradrenergic, nucleus basalis cholinergic, raphe nucleus serotonergic, and the SNc and VTA dopaminergic neurotransmitter networks.

It is also difficult to compare trigeminal and greater occipital nerve stimulation as well as the outcome of different labs. At this point there is no consistency in the application of different parameters for trigeminal and greater occipital nerve stimulation including for example amplitude (mA), current (direct versus alternating), specific site of stimulation.

Per this evidence, it is suggested that cortical noradrenaline, serotonin, acetylcholine, and dopamine are each imperative to plasticity (Brougher et al., 2021a; Hulsey et al., 2016; Hulsey et al., 2019). Furthermore, it can be speculated that these neuromodulators underlie the effectiveness of peripheral nerve stimulation (Meyers et al., 2019); however, whether, and if so, how, these multiple neurotransmitter systems work synergistically to modulate certain behaviors and cognition when activated by transcutaneous stimulation of either of these peripheral nerves needs further investigation.

#### Outstanding Questions.

- Seeing that variables such as charge density have shown to alter the effects of non-invasive brain stimulation, it is necessary to discern what the optimal stimulation parameters and variables of stimulating the vagus, trigeminal, and greater occipital nerve are for optimal efficacy, including length of stimulation, number of sessions, and more. Additionally, how do optimal stimulation parameters change based on the peripheral nerve and the neuromodulatory system being targeted?
- Previous research has highlighted that the timing of stimulation may need to vary based upon the desired stimulation effect. Taking this into consideration, it is critical to determine when peripheral nerve stimulation should occur (i.e., online or offline) to produce its desired outcome. Also, does peripheral nerve stimulation need to be paired with a task to activate a specific pathway to see the desired effect?
- Is there an interaction between multiple neuromodulators to optimize peripheral nerve stimulation? If so, how much interaction is required, and how would the multiple neuromodulators interactions

be affected by various pharmacological blockades? Would this then affect the stimulation's efficacy?

- Although modelling calculations support that minimal amounts of direct current reach the cortex, and when they do, the electrical field is inadequate to cause significant effects, it is still unknown how much, if any, direct current contributes to the effect of non-invasive stimulation. Do the minimal amounts of direct current stimulation that reach the cortex contribute to the effects of peripheral nerve stimulation?
- Prior research has identified beneficial effects of alternative neuromodulatory techniques such as TMS and tACS. Considering these effects are similar to those seen from tDCS, could these effects be attributed to these techniques stimulating peripheral nerves?
- What are the effects on behaviour and cognition? How specific are these effects?

#### Data Availability

No data was used for the research described in the article.

#### References

- Adair, D., Truong, D., Esmailpour, Z., Gebodh, N., Borges, H., Ho, L., Bremner, J.D., Badran, B.W., Napadow, V., Clark, V.P., Bikson, M., 2020. Electrical stimulation of cranial nerves in cognition and disease. *Brain Stimul.* 13, 717–750.
- Ahnaou, A., Moechars, D., Raeymaekers, L., Biermans, R., Manyakov, N.V., Bottelbergs, A., Wintmolders, C., Van Kolen, K., Van De Casteele, T., Kemp, J.A., Drinkenburg, W.H., 2017. Emergence of early alterations in network oscillations and functional connectivity in a tau seeding mouse model of Alzheimer's disease pathology. *Sci. Rep.* 7, 14189.
- Antal, A., Herrmann, C.S., 2016. Transcranial alternating current and random noise stimulation: possible mechanisms. *Neural Plast.* 2016, 3616807.
- Asamoah, B., Khatoun, A., Mc Laughlin, M., 2019. tACS motor system effects can be caused by transcutaneous stimulation of peripheral nerves. *Nat. Commun.* 10, 266.
- Avery, M.C., Krichmar, J.L., 2017. Neuromodulatory systems and their interactions: a review of models, theories, and experiments. *Front Neural Circuits* 11, 108.
- Beardmore, R., Hou, R., Darekar, A., Holmes, C., Boche, D., 2021. The Locus Coeruleus in aging and alzheimer's disease: a postmortem and brain imaging review. *J. Alzheimers Dis.* 83, 5–22.

- Beliaeva, V., Savvateev, I., Zerbi, V., Polania, R., 2021. Toward integrative approaches to study the causal role of neural oscillations via transcranial electrical stimulation. *Nat. Commun.* 12, 2243.
- Berridge, C.W., Waterhouse, B.D., 2003. The locus coeruleus-noradrenergic system: modulation of behavioral state and state-dependent cognitive processes. *Brain Res. Brain Res. Rev.* 42, 33–84.
- Bikson, M., Grossman, P., Thomas, C., Zannou, A.L., Jiang, J., Adnan, T., Mourdoukoutas, A.P., Kronberg, G., Truong, D., Boggio, P., Brunoni, A.R., Charvet, L., Fregni, F., Fritsch, B., Gillick, B., Hamilton, R.H., Hampstead, B.M., Jankord, R., Kirton, A., Knotkova, H., Liebetanz, D., Liu, A., Loo, C., Nitsche, M.A., Reis, J., Richardson, J.D., Rotenberg, A., Turkeltaub, P.E., Woods, A.J., 2016. Safety of transcranial direct current stimulation: evidence based update 2016. *Brain Stimul.* 9, 641–661.
- van Boekholdt, L., Kerstens, S., Khatoun, A., Asamoah, B., Mc Laughlin, M., 2021. tDCS peripheral nerve stimulation: a neglected mode of action? *Mol. Psychiatry* 26, 456–461.
- Boroda, E., Sponheim, S.R., Fiecas, M., Lim, K.O., 2020. Transcranial direct current stimulation (tDCS) elicits stimulus-specific enhancement of cortical plasticity. *Neuroimage* 211, 116598.
- Briand, L.A., Gritton, H., Howe, W.M., Young, D.A., Sarter, M., 2007. Modulators in concert for cognition: modulator interactions in the prefrontal cortex. *Prog. Neurobiol.* 83, 69–91.
- Brougher, J., Aziz, U., Adari, N., Chaturvedi, M., Jules, A., Shah, I., Syed, S., Thorn, C.A., 2021a. Self-administration of right vagus nerve stimulation activates midbrain dopaminergic nuclei. *Front. Neurosci.* 15, 782786.
- Brougher, J., Sanchez, C.A., Aziz, U.S., Gove, K.F., Thorn, C.A., 2021b. Vagus nerve stimulation induced motor map plasticity does not require cortical dopamine. *Front. Neurosci.* 15, 693140.
- Busch, V., Jakob, W., Juergens, T., Schulte-Mattler, W., Kaube, H., May, A., 2006. Functional connectivity between trigeminal and occipital nerves revealed by occipital nerve blockade and nociceptive blink reflexes. *Cephalalgia* 26, 50–55.
- Buzsaki, G., Draguhn, A., 2004. Neuronal oscillations in cortical networks. *Science* 304, 1926–1929.
- Caous, C.A., de Sousa Buck, H., Lindsey, C.J., 2001. Neuronal connections of the paratrigeminal nucleus: a topographic analysis of neurons projecting to bulbar, pontine and thalamic nuclei related to cardiovascular, respiratory and sensory functions. *Auton. Neurosci.* 94, 14–24.
- Engineer, N.D., Kimberley, T.J., Prudente, C.N., Dawson, J., Tarver, W.B., Hays, S.A., 2019. Targeted Vagus Nerve Stimulation for Rehabilitation After Stroke. *Front. Neurosci.* 13, 280.
- Farmer, A.D., Strzelczyk, A., Finisguerra, A., Gourine, A.V., Gharabaghi, A., Hasan, A., Burger, A.M., Jaramillo, A.M., Mertens, A., Majid, A., Verkuil, B., Badran, B.W., Ventura-Bort, C., Gaul, C., Beste, C., Warren, C.M., Quintana, D.S., Hammerer, D., Frerri, E., Frangos, E., Tobaldini, E., Kaniusas, E., Rosenow, F., Capone, F., Panetsos, F., Ackland, G.L., Kaithwas, G., O'Leary, G.H., Genheimer, H., Jacobs, H.I. L., Van Diest, I., Schoenen, J., Redgrave, J., Fang, J., Deuchars, J., Szeles, J.C., Thayer, J.F., More, K., Vonck, K., Steenbergen, L., Vianna, L.C., McTeague, L.M., Ludwigg, M., Veldhuizen, M.G., De Cock, M., Casazza, M., Keute, M., Bikson, M., Andreatta, M., D'Agostini, M., Weymar, M., Betts, M., Prigge, M., Kaess, M., Roden, M., Thai, M., Schuster, N.M., Montano, N., Hansen, N., Kroemer, N.B., Rong, P., Fischer, R., Howland, R.H., Sclocco, R., Sellaro, R., Garcia, R.G., Bauer, S., Gancheva, S., Stavrakis, S., Kampusch, S., Deuchars, S.A., Wehner, S., Laborde, S., Usichenko, T., Polak, T., Zaehle, T., Borges, U., Teckentrup, V., Jandackova, V.K., Napadow, V., Koenig, J., 2020. International consensus based review and recommendations for minimum reporting standards in research on transcutaneous vagus nerve stimulation (Version 2020). In: *Front. Hum. Neurosci.* 14, 568051.
- Fritsch, B., Reis, J., Martinowich, K., Schambra, H.M., Ji, Y., Cohen, L.G., Lu, B., 2010. Direct current stimulation promotes BDNF-dependent synaptic plasticity: potential implications for motor learning. *Neuron* 66, 198–204.
- Ganzer, P.D., Darrow, M.J., Meyers, E.C., Solorzano, B.R., Ruiz, A.D., Robertson, N.M., Adcock, K.S., James, J.T., Jeong, H.S., Becker, A.M., Goldberg, M.P., Pruitt, D.T., Hays, S.A., Kilgard, M.P., Rennaker 2nd, R.L., 2018. Closed-loop neuromodulation restores network connectivity and motor control after spinal cord injury. *Elife* 7.
- Halassa, M.M., Sherman, S.M., 2019. Thalamocortical circuit motifs: a general framework. *Neuron* 103, 762–770.
- Han, W., Tellez, L.A., Perkins, M.H., Perez, I.O., Qu, T., Ferreira, J., Ferreira, T.L., Quinn, D., Liu, Z.W., Gao, X.B., Kaelberer, M.M., Bohorquez, D.V., Shammah-Lagnado, S.J., de Lartigue, G., de Araujo, I.E., 2018. A neural circuit for gut-induced reward. *Cell* 175, 665–678 e623.
- Hays, S.A., 2016. Enhancing rehabilitative therapies with vagus nerve stimulation. *Neurotherapeutics* 13, 382–394.
- Helm, S., Shirsat, N., Calodney, A., Abd-Elseyed, A., Kloth, D., Soin, A., Shah, S., Trescot, A., 2021. Peripheral nerve stimulation for chronic pain: a systematic review of effectiveness and safety. *Pain. Ther.* 10, 985–1002.
- Herrmann, C.S., Rach, S., Neuling, T., Struber, D., 2013. Transcranial alternating current stimulation: a review of the underlying mechanisms and modulation of cognitive processes. *Front. Hum. Neurosci.* 7, 279.
- Huang, Y., Liu, A.A., Lafon, B., Friedman, D., Dayan, M., Wang, X., Bikson, M., Doyle, W. K., Devinsky, O., Parra, L.C., 2017. Measurements and models of electric fields in the in vivo human brain during transcranial electric stimulation. *Elife* 6.
- Hulse, D.R., Hays, S.A., Khodaparast, N., Ruiz, A., Das, P., Rennaker 2nd, R.L., Kilgard, M.P., 2016. Reorganization of motor cortex by vagus nerve stimulation requires cholinergic innervation. *Brain Stimul.* 9, 174–181.
- Hulse, D.R., Riley, J.R., Loerwald, K.W., Rennaker 2nd, R.L., Kilgard, M.P., Hays, S.A., 2017. Parametric characterization of neural activity in the locus coeruleus in response to vagus nerve stimulation. *Exp. Neurol.* 289, 21–30.
- Hulse, D.R., Shedd, C.M., Sarker, S.F., Kilgard, M.P., Hays, S.A., 2019. Norepinephrine and serotonin are required for vagus nerve stimulation directed cortical plasticity. *Exp. Neurol.* 320, 112975.
- Jackson, M.P., Rahman, A., Lafon, B., Kronberg, G., Ling, D., Parra, L.C., Bikson, M., 2016. Animal models of transcranial direct current stimulation: Methods and mechanisms. *Clin. Neurophysiol.* 127, 3425–3454.
- Jahshan, C., Wynn, J.K., Mathalon, D.H., Green, M.F., 2017. Cognitive correlates of visual neural plasticity in schizophrenia. *Schizophr. Res.* 190, 39–45.
- Jones, E.J., Rohleder, N., Schreier, H.M.C., 2020. Neuroendocrine coordination and youth behavior problems: a review of studies assessing sympathetic nervous system and hypothalamic-pituitary-adrenal axis activity using salivary alpha amylase and salivary cortisol. *Horm. Behav.* 122, 104750.
- Joshi, S., 2021. Pupillometry: arousal state or state of mind? *Curr. Biol.* 31, R32–R34.
- Joshi, S., Gold, J.I., 2020. Pupil size as a window on neural substrates of cognition. *Trends Cogn. Sci.* 24, 466–480.
- Kawai, Y., 2018. Differential ascending projections from the male rat caudal nucleus of the tractus solitarius: an interface between local microcircuits and global macrocircuits. *Front. Neuroanat.* 12, 63.
- Kronberg, G., Bridi, M., Abel, T., Bikson, M., Parra, L.C., 2017. Direct current stimulation modulates LTP and LTD: activity dependence and dendritic effects. *Brain Stimul.* 10, 51–58.
- Kronberg, G., Rahman, A., Sharma, M., Bikson, M., Parra, L.C., 2020. Direct current stimulation boosts hebbian plasticity in vitro. *Brain Stimul.* 13, 287–301.
- Kumar, M., Chawla, R., Goyal, M., 2015. Topical anesthesia. *J. Anaesthesiol. Clin. Pharm.* 31, 450–456.
- Latif, S., Jahangeer, M., Maknoon Razia, D., Ashiq, M., Ghaffar, A., Akram, M., El Allam, A., Bouyahya, A., Garipova, L., Ali Shariati, M., Thiruvengadam, M., Azam Ansari, M., 2021. Dopamine in Parkinson's disease. *Clin. Chim. Acta* 522, 114–126.
- Liu, A., Voroslakos, M., Kronberg, G., Henin, S., Krause, M.R., Huang, Y., Opitz, A., Mehta, A., Pack, C.C., Krekelberg, B., Berenyi, A., Parra, L.C., Melloni, L., Devinsky, O., Buzsaki, G., 2018. Immediate neurophysiological effects of transcranial electrical stimulation. *Nat. Commun.* 9, 5092.
- Liu, Y., Zhao, J., Fan, X., Guo, W., 2019. Dysfunction in serotonergic and noradrenergic systems and somatic symptoms in psychiatric disorders. *Front. Psychiatry* 10, 286.
- Luckey, A.M., McLeod, S.L., Robertson, I.H., To, W.T., Vanneste, S., 2020. Greater occipital nerve stimulation boosts associative memory in older individuals: a randomized trial. *Neurorehabil. Neural Repair*, 1545968320943573.
- Luckey, A.M., McLeod, S.L., Mohan, A., Vanneste, S., 2022. Potential role for peripheral nerve stimulation on learning and long-term memory: a comparison of alternating and direct current stimulations. *Brain Stimul.* 15, 536–545.
- Menetrey, D., Basbaum, A.I., 1987. Spinal and trigeminal projections to the nucleus of the solitary tract: a possible substrate for somatovisceral and viscerovisceral reflex activation. *J. Comp. Neurol.* 255, 439–450.
- Meyers, E.C., Solorzano, B.R., James, J., Ganzer, P.D., Lai, E.S., Rennaker 2nd, R.L., Kilgard, M.P., Hays, S.A., 2018. Vagus nerve stimulation enhances stable plasticity and generalization of stroke recovery. *Stroke* 49, 710–717.
- Meyers, E.C., Kasliwal, N., Solorzano, B.R., Lai, E., Bendale, G., Berry, A., Ganzer, P.D., Romero-Ortega, M., Rennaker 2nd, R.L., Kilgard, M.P., Hays, S.A., 2019. Enhancing plasticity in central networks improves motor and sensory recovery after nerve damage. *Nat. Commun.* 10, 5782.
- Nitsche, M.A., Paulus, W., 2000. Excitability changes induced in the human motor cortex by weak transcranial direct current stimulation. *J. Physiol.* 527 (3), 633–639 (Pt).
- Nitsche, M.A., Seeber, A., Frommann, K., Klein, C.C., Rochford, C., Nitsche, M.S., Fricke, K., Liebetanz, D., Lang, N., Antal, A., Paulus, W., Tergau, F., 2005. Modulating parameters of excitability during and after transcranial direct current stimulation of the human motor cortex. *J. Physiol.* 568, 291–303.
- Opitz, A., Falchier, A., Yan, C.G., Yeagle, E.M., Linn, G.S., Megevdand, P., Thielscher, A., Deborah, A.R., Milham, M.P., Mehta, A.D., Schroeder, C.E., 2016. Spatiotemporal structure of intracranial electric fields induced by transcranial electric stimulation in humans and nonhuman primates. *Sci. Rep.* 6, 31236.
- Podda, M.V., Cocco, S., Mastrodonato, A., Fusco, S., Leone, L., Barbati, S.A., Colussi, C., Ripoli, C., Grassi, C., 2016. Anodal transcranial direct current stimulation boosts synaptic plasticity and memory in mice via epigenetic regulation of Bdnf expression. *Sci. Rep.* 6, 22180.
- Poe, G.R., Foote, S., Eschenko, O., Johansen, J.P., Bouret, S., Aston-Jones, G., Harley, C. W., Manahan-Vaughan, D., Weinschenker, D., Valentino, R., Berridge, C., Chandler, D.J., Waterhouse, B., Sara, S.J., 2020. Locus coeruleus: a new look at the blue spot. *Nat. Rev. Neurosci.* 21, 644–659.
- Rea, P., 2015. Trigeminal Nerve, Regional Nerve Blocks in Anesthesia and Pain Therapy. Springer, pp. 133–160.
- Reed, T., Cohen Kadosh, R., 2018. Transcranial electrical stimulation (tES) mechanisms and its effects on cortical excitability and connectivity. *J. Inherit. Metab. Dis.*
- Reinhart, R.M.G., Nguyen, J.A., 2019. Working memory revived in older adults by synchronizing rhythmic brain circuits. *Nat. Neurosci.* 22, 820–827.
- Salgado, H., Trevino, M., Atzori, M., 2016. Layer- and area-specific actions of norepinephrine on cortical synaptic transmission. *Brain Res.* 1641, 163–176.
- Samuels, E.R., Szabadi, E., 2008. Functional neuroanatomy of the noradrenergic locus coeruleus: its roles in the regulation of arousal and autonomic function part I: principles of functional organisation. *Curr. Neuropharmacol.* 6, 235–253.
- Scarr, E., Gibbons, A.S., Neo, J., Udawela, M., Dean, B., 2013. Cholinergic connectivity: its implications for psychiatric disorders. *Front. Cell Neurosci.* 7, 55.
- Slavin, K.V., 2011. History of peripheral nerve stimulation. *Prog. Neurol. Surg.* 24, 1–15.
- So, P.P., Stuchly, M.A., Nyenhuis, J.A., 2004. Peripheral nerve stimulation by gradient switching fields in magnetic resonance imaging. *IEEE Trans. Biomed. Eng.* 51, 1907–1914.



- de Sousa Buck, H., Caous, C.A., Lindsey, C.J., 2001. Projections of the paratrigeminal nucleus to the ambiguus, rostroventrolateral and lateral reticular nuclei, and the solitary tract. *Auton. Neurosci.* 87, 187–200.
- Tavakoli, A.V., Yun, K., 2017. Transcranial alternating current stimulation (tACS) mechanisms and protocols. *Front Cell Neurosci.* 11, 214.
- Thair, H., Holloway, A.L., Newport, R., Smith, A.D., 2017. Transcranial direct current stimulation (tDCS): a beginner's guide for design and implementation. *Front Neurosci.* 11, 641.
- Vanneste, S., Mohan, A., Yoo, H.B., Huang, Y., Luckey, A.M., McLeod, S.L., Tabet, M.N., Souza, R.R., McIntyre, C.K., Chapman, S., Robertson, I.H., To, W.T., 2020. The peripheral effect of direct current stimulation on brain circuits involving memory. *Sci. Adv.* 6.
- Voroslakos, M., Takeuchi, Y., Brinyiczki, K., Zombori, T., Oliva, A., Fernandez-Ruiz, A., Kozak, G., Kincses, Z.T., Ivanyi, B., Buzsaki, G., Berenyi, A., 2018. Direct effects of transcranial electric stimulation on brain circuits in rats and humans. *Nat. Commun.* 9, 483.
- Weiner, R.L., Alo, K.M., 2018. Occipital nerve stimulation for treatment of intractable headache syndromes. *Neuromodulation. Elsevier*, pp. 773–782.
- Woods, A.J., Antal, A., Bikson, M., Boggio, P.S., Brunoni, A.R., Celnik, P., Cohen, L.G., Fregni, F., Herrmann, C.S., Kappenman, E.S., Knotkova, H., Liebetanz, D., Miniussi, C., Miranda, P.C., Paulus, W., Priori, A., Reato, D., Stagg, C., Wenderoth, N., Nitsche, M.A., 2016. A technical guide to tDCS, and related non-invasive brain stimulation tools. *Clin. Neurophysiol.* 127, 1031–1048.
- Yap, J.Y.Y., Keatch, C., Lambert, E., Woods, W., Stoddart, P.R., Kameneva, T., 2020. Critical review of transcutaneous vagus nerve stimulation: challenges for translation to clinical practice. *Front Neurosci.* 14, 284.
- Zhao, C., Woodman, G.F., 2021. Converging evidence that neural plasticity underlies transcranial direct-current stimulation. *J. Cogn. Neurosci.* 33, 146–157.
- Zhou, S., Hussain, N., Abd-Elseyed, A., Boulos, R., Hakim, M., Gupta, M., Weaver, T., 2021. Peripheral nerve stimulation for treatment of headaches: an evidence-based review. *Biomedicines* 9.



# Peripheral nerve stimulation: A neuromodulation-based approach

Alison M. Luckey<sup>a,b</sup>, Katherine Adcock<sup>a,b</sup>, Sven Vanneste<sup>a,b,c,\*</sup>,<sup>1</sup>

<sup>a</sup> Lab for Clinical & Integrative Neuroscience, School of Psychology, Trinity College Dublin, Dublin, Ireland

<sup>b</sup> Trinity College Institute for Neuroscience, Trinity College Dublin, Dublin, Ireland

<sup>c</sup> Global Brain Health Institute, Trinity College Dublin, Dublin, Ireland

## ARTICLE INFO

### Keywords:

Direct current stimulation  
Locus coeruleus  
Reticular formation  
Occipital nerve stimulation  
Vagus nerve stimulation  
Trigeminal nerve stimulation

## ABSTRACT

Recent technological improvements have positioned us at the threshold of innovative discoveries that will assist in new perspectives and avenues of research. Increased attention has been directed towards peripheral nerve stimulation, particularly of the vagus, trigeminal, or greater occipital nerve, due to their unique pathway that engages neural circuits within networks involved in higher cognitive processes. Here, we question whether the effects of transcutaneous electrical stimulation are mediated by synergistic interactions of multiple neuromodulatory networks, considering this pathway is shared by more than one neuromodulatory system. By spotlighting this attractive transcutaneous pathway, this opinion piece aims to acknowledge the contributions of four vital neuromodulators and prompt researchers to consider them in future investigations or explanations.

## 1. A shift from transcranial to transcutaneous

Over the past decade, investigations researching ways to boost synaptic plasticity have attracted attention from a broad array of professional fields, including neuroscience, engineering, and even the U.S. Department of Defense – which in 2017 began funding research to exploit neuromodulation interventions to improve and accelerate training of military personnel via the activation of peripheral nerves to tune neural networks responsible for vital cognitive skills. However, the field's understanding of the underlying neurophysiological mechanism(s) of peripheral nerve stimulation remains limited and opposes the prevailing mechanistic explanation of non-invasive neuromodulation methods, namely transcranial electrical stimulation (tES), including direct and alternate current stimulation (see [Box 1](#)).

Lately, the debate concerning the transcranial versus transcutaneous mechanism has gained new prominence in light of recent investigations unveiling striking evidence that suggests a transcutaneous mechanism may be more suitable and plausible ([Fig. 1](#)) ([Liu et al., 2018](#)). Calculations on a realistic head model and validation studies in both animal and human experiments have indicated that only 25 (up to 50) percent of the applied current reaches the brain due to the high electrical resistance of the skull, while the remaining current is shunted through extracranial soft tissues ([Liu et al., 2018](#); [Voroslakos et al., 2018](#)). Additionally, tES

delivered at peak 1 mA induced an electrical field of approximately 0.2 V/m when measured at the cortex, a level that contains an inadequate threshold to initiate an action potential in cortical neurons ([Liu et al., 2018](#); [Voroslakos et al., 2018](#)). It is important to note that the maximal electric field for 1 mA peak intensity amounts to <0.5 V/m in other independent studies with the use of intracranial electrodes ([Huang et al., 2017](#); [Opitz et al., 2016](#)). Furthermore, human cadaver and in vivo rat experiments indicated that for brain networks to be adequately modified directly, an electric current of approximately 6 mA would need to be administered to the scalp ([Voroslakos et al., 2018](#)). Regrettably, this requisite of 6 mA would considerably exceed the latest safety guidelines of <4 mA for tES application ([Bikson et al., 2016](#); [Thair et al., 2017](#)). Alternatively, tES delivered at 1 mA results in an electrical field that surpasses 20 V/m in the scalp and engages peripheral nerves inside the scalp ([Asamoah et al., 2019](#)), initiating the action potentials needed to indirectly modify brain activity ([So et al., 2004](#)).

Recently, a perspective piece has endorsed the alternative, peripheral route, referencing the prior assumption of how the effects of tES transpire solely due to the weak, subthreshold electric field it generates in the cortex as being an oversimplification ([van Boekholdt et al., 2021](#)). The authors suggest that observed tES effects are instead triggered through peripheral stimulation of the ascending reticular activating system, which promotes the release of noradrenaline from the locus

\* Correspondence to: Lab for Clinical & Integrative Neuroscience, School of Psychology, Global Brain Health Institute, Institute of Neuroscience, Trinity College Dublin, College Green 2, Dublin, Ireland.

E-mail address: [sven.vanneste@tcd.ie](mailto:sven.vanneste@tcd.ie) (S. Vanneste).

<sup>1</sup> website: <http://www.lab-clint.org>.

<https://doi.org/10.1016/j.neubiorev.2023.105180>

Received 28 October 2022; Received in revised form 23 March 2023; Accepted 11 April 2023

Available online 12 April 2023

0149-7634/© 2023 The Author(s). Published by Elsevier Ltd. This is an open access article under the CC BY license (<http://creativecommons.org/licenses/by/4.0/>).

coeruleus (LC) throughout the brain (van Boekholdt et al., 2021). Building upon this alternative explanation, we provide evidence from several studies to extend this understanding and go beyond the noradrenergic system. We question whether the effects of tES and other forms of neuromodulation are mediated by additional neuromodulatory networks. In the following sections, we discuss an attractive transcutaneous pathway, followed by evidence highlighting the contributions of other vital neuromodulators that researchers might want to consider in future investigations or explanations.

## 2. Proposed transcutaneous pathway

Directly stimulating the trigeminal and the occipital nerve is an acknowledged and longstanding technique for neuropathic pain suppression and managing headache syndromes (Helm et al., 2021; Slavin, 2011; Zhou et al., 2021). Moreover, attention has been directed towards peripheral stimulation of these nerves due to their unique pathway that engages neural circuits within networks that are highly involved in higher cognitive processes (see Fig. 2). The trigeminal nerve begins in

the brain and travels throughout the head to where the nerve endings span across the face and forehead (Rea, 2015). On the other hand, the greater occipital nerve arises from the C2 spinal nerve with several branches innervating the posterior occiput up to the scalp vertex (Weiner and Alo, 2018). These two nerves are interlinked (Busch et al., 2006) and presumably encompass many traditional anterior and posterior electrode montages of non-invasive stimulation utilized by current experimental studies (van Boekholdt et al., 2021) (see Box 3). Of particular importance, targeting either the trigeminal or greater occipital nerve via cutaneous electrodes establishes communication gateways from the periphery to the brain via the specific afferent fibers that project to the brainstem and synapse onto the nucleus tractus solitarius (NTS); various rodent studies have used anterograde neuronal tracers to demonstrate these connections (Adair et al., 2020; Caous et al., 2001; de Sousa Buck et al., 2001; Menetrey and Basbaum, 1987). From the NTS, the information is then integrated and relayed across the brainstem amongst networks within the complex reticular formation (Kawai, 2018), whereby sensory information is processed via the thalamocortical networks (Halassa and Sherman, 2019), and environmental or

### Box 1

Traditional account of transcranial direct and alternate current stimulation.

One of the most significant current discussions regarding non-invasive stimulation techniques is whether much of the electrical current modulating the excitability of neurons is provided transcranially, directly and in a regionally constrained manner, or transcutaneously, where the current flow primarily affects neural circuits indirectly via peripheral nerves. The predominant understanding of transcranial direct current stimulation (tDCS) proposes that it employs a unidirectional, direct current at a low or weak intensity (1–2 mA) via two or more strategically placed electrodes (at least one anode and one cathode) in order to transmit the current from the device to the scalp in an effort to polarize the region (Nitsche and Paulus, 2000; Nitsche et al., 2005). In doing so, tDCS aims to modulate cortical excitability and spontaneous activity through subthreshold alterations on neuronal resting membrane potentials, thus increasing or decreasing the neuron's likelihood to fire an action potential (Nitsche and Paulus, 2000; Reed and Cohen Kadosh, 2018; Woods et al., 2016). Prior to the usage of tDCS, it is necessary to consider all components of the methodological design, such as the size and placement of the electrodes and selection of a tolerable stimulus protocol (i.e., current intensity) (Woods et al., 2016), given that they are key indicators of current density and the distribution of the electrical field (Jackson et al., 2016). Further attention is advised to the current intensity and stimulation duration, owing to their potential to substantially impact short- and long-term effects produced by tDCS (Nitsche and Paulus, 2000).

Effects generated by tDCS have been deemed similar to long-term potentiation and long-term depression (Kronberg et al., 2017). The ability to produce such outcomes has accelerated tDCS' usage as a treatment option for various neurocognitive disorders associated with plasticity deficits (Jahshan et al., 2017) and tDCS' capability to modify plasticity for memory stabilization (Zhao and Woodman, 2021). Moreover, a relatively recent model, known as activity-selective, suggests that it is preferential to target neuronal populations that are simultaneously active when applying tDCS while also taking into account the state of the brain when stimulation is administered, thereby generating stimulus-specific brain state effects via tDCS (Boroda et al., 2020). It is of note that this has been emphasized in prior research, whereby it was suggested that tDCS be employed with the behavior it strives to modulate (Fritsch et al., 2010), therefore, gaining momentum as an explanation of cognitive enhancement when tasks are aided by t/DCS (Kronberg et al., 2020; Podda et al., 2016).

Distinguishing itself from tDCS, transcranial alternate current stimulation (tACS) omits the unidirectional voltage component and influences the polarization of neurons via sinusoidal fluctuations of the membrane potential (Tavakoli and Yun, 2017). tACS exerts a sine wave current between the anode and cathode electrodes in a half-cycle fashion to modify the spike-timing activity of individual neurons. Five mechanisms have been proposed for how tACS modifies brain activity, likely depending on the estimated field intensity being generated: stochastic resonance, rhythm resonance, temporal bias of spikes, network entrainment, and imposed pattern (Liu et al., 2018). Most conventionally, tACS is characterized to enhance brain oscillations via neural entrainment or synchronized firing of neurons through external stimuli (Reinhart and Nguyen, 2019; Tavakoli and Yun, 2017). To entrain endogenous oscillations, tACS delivers an exogenous oscillation at an equal or increased frequency to enhance the existing oscillation's power (i.e., amplitude), whereas transmitting a signal below the intrinsic frequency will reduce the intrinsic oscillation (Antal and Herrmann, 2016). Frequency, intensity, and phase are three parameters of tACS oscillations that each play a significant role in defining the direction and cyclical pattern of the delivered stimulation (Antal and Herrmann, 2016).

Cortical oscillations are fundamental processes underlying cognition and behavior (Buzsaki and Draguhn, 2004). Moreover, alterations in neuronal synchrony have been identified during the early stages of neurodegenerative disorders (Ahnaou et al., 2017), increasing studies utilizing tACS to intervene with and modulate synchrony to restore oscillatory activity. tACS may be applied across a wide array of frequency ranges, typically within conventional electroencephalography frequencies (0.01–80 Hz), and is generally considered to be brain-state dependent, such that the effect of tACS is influenced by the state the brain is in at the time of application. Accordingly, tACS requires a more concrete stimulation paradigm when preparing experimental study designs or intervention protocols, such that researchers need to predetermine the sought-after cognitive-behavioral processes to identify the underlying native oscillatory properties and frequencies of these processes to entrain the associated oscillations (Woods et al., 2016). Entraining oscillations at a fixed frequency in specific brain areas enables the researchers to extract causal inferences between brain modulation and obtained effects, such as improved communication leading to improved cognition and/or behavior (Herrmann et al., 2013). Although neural entrainment transpiring is yet to be unanimously supported (Beliaeva et al., 2021), the rationale that tACS' frequency may be applied at the exact frequency rhythm fundamental for optimal brain functioning results in favoring frequency-specific synchrony effect via tACS (Reinhart and Nguyen, 2019).

arousal information, as well as other states of vigilance and novelty, will additionally activate LC noradrenergic projections from the brainstem throughout major cortical and subcortical regions (Berridge and Waterhouse, 2003). Therefore, this proposed transcutaneous pathway that emphasizes enhanced LC noradrenergic activation, thereby generating excitatory or inhibitory effects on neural activity (Salgado et al., 2016), has been described as the missing mechanistic link that may underpin the effects of non-invasive brain stimulation (van Boekholdt et al., 2021), and points to an attractive mediator of neuromodulation.

### 3. Activation of locus coeruleus noradrenaline pathway

Due to its vast connectedness and activation responses, we propose that the LC be considered a principal target for peripheral nerve stimulation. The LC noradrenaline system was previously thought to solely regulate arousal and autonomic functions (Berridge and Waterhouse, 2003); however, a greater understanding of organizational afferent projections to the LC has led to a widespread agreement that the LC noradrenaline system is one of the four principle neuromodulatory networks heavily engaged in physiological processes including being a significant contributor to signal transduction and synaptic plasticity required for the LC's dual involvement in behaviors and cognition (Avery and Krichmar, 2017; Poe et al., 2020; Samuels and Szabadi, 2008).

Recent research by our laboratory has endorsed peripheral nerve stimulation via non-invasive stimulation of the greater occipital nerve (NITESGON) to (1) upregulate the LC noradrenaline system, (2) confirm that the occipital nerve was sufficient to induce these changes, and (3) suggest an augmentation of memory performance (see Box 2) (Vanneste et al., 2020). The vagus nerve has also been proposed to activate the same transcutaneous pathway leading to the NTS and LC when stimulated (Yap et al., 2020). This pathway has led to vagus nerve stimulation (VNS) being investigated as an approach to modifying neuroplasticity (Farmer et al., 2020; Yap et al., 2020). Moreover, stimulation of the left cervical vagus nerve has received FDA approval for treating intractable

epilepsy and depression (Farmer et al., 2020) and has been incorporated into rehabilitation programs for various neurological disorders, including ischemic stroke (Engineer et al., 2019; Hays, 2016). Like trigeminal and occipital nerve stimulation, the underlying mechanics of VNS are not yet fully comprehended; however, a proliferation of investigations into VNS have provided a greater understanding than trigeminal and occipital nerve stimulation. For example, Hulsey and colleagues (2017) assessed an extensive range of VNS parameters in rats to show that short bursts and low thresholds (starting at 0.1 mA) prompted phasic LC activity; greater intensities and pulse width increased the phasic activity while varying frequencies impacted timing but not the maximum activity of the LC (Hulsey et al., 2017). These findings demonstrate that VNS can activate the LC and modulate neural activity, suggesting that the LC could mediate the effect observed in VNS research (Hulsey et al., 2017). In a follow-up study, Hulsey and colleagues (2019) demonstrated that left-VNS paired with training resulted in over double the amount of motor cortex area dedicated to proximal forelimb movements detected when compared to the sham and the immunotoxin injected groups; this depletion of noradrenaline innervation to the motor cortex demonstrated the requirement of noradrenergic activity to be a mediator of VNS-directed plasticity (Hulsey et al., 2019).

Taken together, these studies have identified the LC noradrenergic system to be engaged by non-invasive stimulation of the greater occipital nerve and invasive stimulation of the vagus nerve, thus providing merit to its usage to enhance cortical plasticity and improve memory performance.

### 4. Activation of other neuromodulatory pathways

Considering how the vagus, trigeminal, and greater occipital nerve share a pathway leading to nuclei in the brainstem, particularly the NTS, we extracted parallels from preclinical studies employing VNS to highlight other ascending neuromodulatory systems, including the serotonergic, cholinergic, and dopaminergic systems (Brougher et al., 2021a; Hulsey et al., 2016; Hulsey et al., 2019), that have been suggestive of

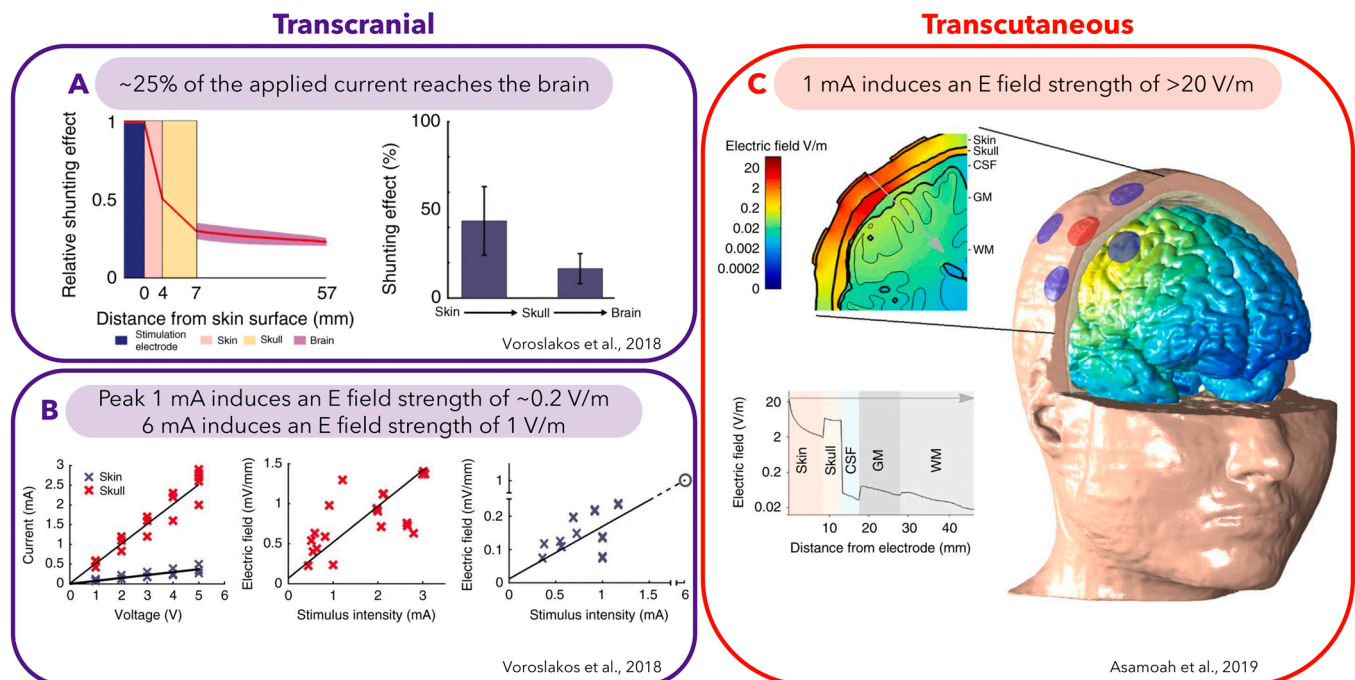


**Fig. 1.** Comparison of electric fields of a transcranial mechanism (Voroslakos et al., 2018) versus a transcutaneous mechanism (Asamoah et al., 2019) (A) Voroslakos and colleagues (2018) demonstrated that due to the shunting effect, approximately 25% (up to 50%) of the applied current reaches the brain. (B) Additionally, Voroslakos and colleagues (2018) presented the relationship between the stimulation intensity and the electric field strength for both transcutaneous (scalp) and subcutaneous (skull with scalp removed) stimulation. (C) Asamoah et al. (2019) illustrated the electric field strength distribution amongst different tissues; using a more focused montage, 1 mA of tACS induces an E field strength of >20 V/m.

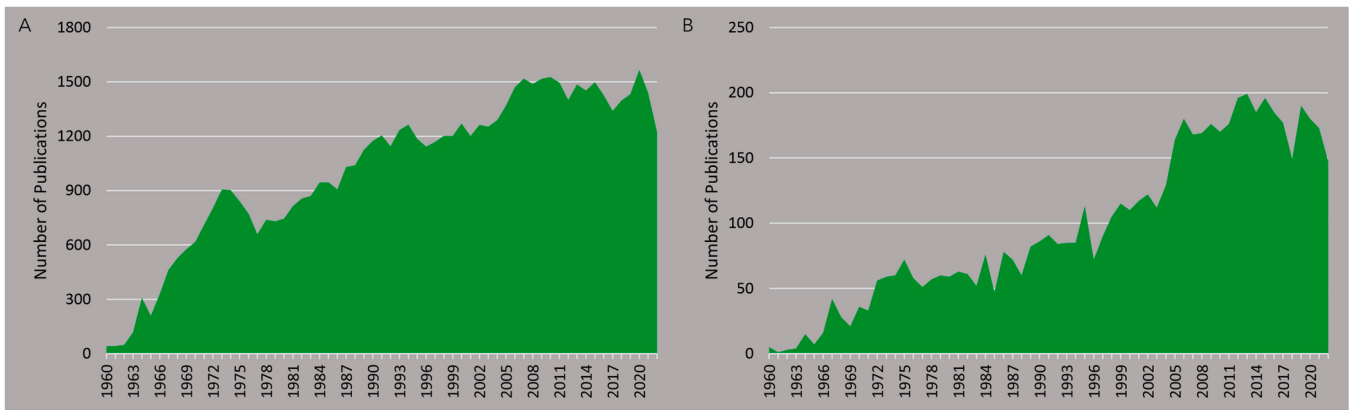


**Fig. 2.** An overview papers published using PubMed from 1960 to 2022 (a) Using peripheral nerve stimulation as keyword (b) Using trigeminal and occipital nerve stimulation as keywords.

### Box 3

The vagus, trigeminal and occipital nerve.

The trigeminal nerve (cranial nerve V) is a cranial nerve responsible for sensation in the face and motor functions such as biting and chewing; it is the most complex of the cranial nerves. Its name derives from each of the two nerves (one on each side of the pons) having three major branches: the ophthalmic nerve, the maxillary nerve, and the mandibular nerve. The ophthalmic and maxillary nerves are purely sensory, whereas the mandibular nerve supplies motor as well as functions. Adding to the complexity of this nerve is that autonomic nerve fibers as well as special sensory fibers (taste) are contained within it. The motor division of the trigeminal nerve derives from the basal plate of the embryonic pons, and the sensory division originates in the cranial neural crest. Sensory information from the face and body is processed by parallel pathways in the central nervous system.

The greater occipital nerve is a nerve of the head. It is a spinal nerve, specifically the medial branch of the dorsal primary ramus of cervical spinal nerve 2. It arises from between the first and second cervical vertebrae, ascends, and then passes through the semispinalis muscle. It ascends further to supply the skin along the posterior part of the scalp to the vertex. It supplies sensation to the scalp at the top of the head, over the ear and over the parotid glands.

### Box 2

Non-invasive stimulation of the greater occipital nerve.

The effects of NITESGON on the LC noradrenaline activity were measured via three common proxy measures: pupillometry, salivary  $\alpha$ -amylase, and neurophysiology [event-related potentials (ERPs)]. This enabled us to track changes (significant increases) from baseline measurements; however, caution should be applied considering these proxy measures possess limitations such as being substantially variable and the potential of other brain regions and monoamine neurotransmitters associated with changes (Jones et al., 2020; Joshi, 2021; Joshi and Gold, 2020). Nevertheless, significant intercorrelations were found amongst the three proxy measures, suggesting that NITESGON can induce changes in LC activity, thus promoting noradrenaline release.

The second set of experiments, including a direct and indirect route of occipital nerve stimulation, were designed to substantiate the transcutaneous mechanism that drives the memory-effect of NITESGON (Vanneste et al., 2020). A more invasive technique directly stimulated the greater occipital nerve in rats to improve memory performance during inhibitory avoidance and object recognition tasks. Additionally, a group of participants received a topical skin anesthetic (lidocaine/prilocaine) cream during initial learning with stimulation to block the activation of peripheral nerves (Kumar et al., 2015). Seven days later, participants with no anesthesia cream demonstrated enhanced memory recollection, indicating effects are driven by peripheral nerve stimulation. Together, these studies suggest that invasive and non-invasive occipital nerve stimulation directly affects memory (Vanneste et al., 2020). These memory improvements have since been replicated in younger and older adult populations and by utilizing transcranial alternating current stimulation (tACS) with salivary  $\alpha$ -amylase concentration levels used to substantiate noradrenergic activation (Luckey et al., 2022; Luckey et al., 2020). These replications divert from proposed limitations associated with age and endorse that other neuromodulation devices are capable of activating transcutaneous pathways.

acting synergistically along with the noradrenergic system to contribute to plasticity to influence behaviors and cognition.

The researchers of the aforementioned preclinical studies carried out additional experiments to examine the significance of other neurotransmitters, such as acetylcholine, originating from the nucleus basalis, and serotonin, originating from the dorsal raphe nucleus, to the

plasticity processes to identify whether neuromodulatory systems can substitute for other networks so that plasticity is not forfeited (Hulsey et al., 2016; Hulsey et al., 2019). Results obtained from intracortical microstimulation motor mapping again demonstrated that left-VNS during training resulted in more than double the percentage of proximal forelimb movements detected compared to the sham and



immunotoxin groups, demonstrating the requirement of serotonergic and cholinergic activity each to be facilitators of VNS-directed plasticity (Hulsey et al., 2016; Hulsey et al., 2019). Multiple neuromodulatory systems being necessary aligns with previous research that exhibited various neuromodulators could cooperatively govern plasticity and how the absence of any of these specific neuromodulators could not be replaced by other neuromodulatory networks also being activated by VNS.

In light of the evidence exhibiting cortical plasticity's dependency on multiple neuromodulators, a second group of researchers sought to determine if cortical dopamine, a neuromodulator originating from the ventral tegmental area (VTA) or substantia nigra pars compacta (SNc), was required for VNS-induced plasticity in the motor cortex. Unexpectedly, the depletion of cortical dopamine did not affect cortical plasticity (Brougher et al., 2021b). However, recent findings of the right nodose ganglion projecting to the NTS and activating dopamine via the VTA and the left nodose ganglion having no such effect (Han et al., 2018) prompted the researchers to compare how stimulation to the right cervical vagus nerve and the traditional left cervical vagus nerve affected behavior and dopaminergic activity from the midbrain when employing matching VNS parameters (Brougher et al., 2021a). Results indicated that right-VNS enhanced activation of the midbrain dopaminergic system and resulted in a more significant number of forelimb movements compared to the left-VNS group (Brougher et al., 2021a). These findings suggest that the preclinical and clinical protocol of traditional left-VNS is unsuitable for driving dopaminergic activity or enhancing behavior. However, right-VNS may be exploited to preferentially promote plasticity via the midbrain dopaminergic systems (Brougher et al., 2021a).

Taken together, the evidence from these studies suggests that lesions in three neuromodulatory networks prevented VNS-movement pairing from generating cortical plasticity, specifically the dorsal raphe nucleus serotonergic and nucleus basalis cholinergic networks. Moreover, the additional findings evoke the potential of right-VNS being an effective intervention to promote dopamine-dependent plasticity. Collectively, the observed results insinuate that cortical serotonin, acetylcholine, and dopamine are each essential to plasticity and can be driven by peripheral nerve stimulation.

## 5. Critical implications for transcutaneous stimulation

Empirical findings within this opinion piece provide an initial understanding of various neuromodulators that can be activated via peripheral nerve stimulation. Taken together, these findings suggest a role for peripheral nerve stimulation in improving or restoring neuroplasticity. For instance, a recent investigation sought to determine if lesions in the nucleus basalis blocking VNS-induced plasticity would consequently affect the efficacy of VNS when paired with motor rehabilitation (Meyers et al., 2019), given that VNS has previously been used to improve recovery after injury (Ganzer et al., 2018; Meyers et al., 2018). Results indicated that VNS during rehabilitation showed repaired motor map representations and improved volitional forelimb function compared to groups that rehabilitated without VNS or received delayed VNS. To address a more causal role, a second set of experiments blocked acetylcholine to further investigate VNS's effect on plasticity and recovery. Results demonstrated that VNS during rehabilitation reversed maladaptive plasticity and helped improve recovery, whereas blocking acetylcholine prevented recovery even when receiving VNS during rehabilitation, thus highlighting cortical acetylcholine's critical function in restoring brain circuits (Meyers et al., 2019).

As demonstrated by the preclinical studies, peripheral nerve stimulation activates these four main neuromodulators (Brougher et al., 2021a; Hulsey et al., 2016; Hulsey et al., 2019), and evidence suggests these neuromodulators are essential for neuroplasticity and, therefore, underlie the effectiveness of peripheral nerve stimulation (Meyers et al., 2019). Through interactions with other brain regions and within the

neuromodulatory systems, neuromodulators are responsible for signaling risk and reward, uncertainty and novelty, and thus directly influence higher-order cognitive functions, including attention, decision-making, goal-directed behavior, and emotion (Avery and Krichmar, 2017). Accordingly, utilizing peripheral nerve stimulation as a therapeutic intervention to upregulate these neuromodulators or as an adjunctive treatment to enhance neuroplasticity may be a suitable approach, considering that a range of neurocognitive and psychiatric disorders are associated with downregulated neuromodulatory systems or plasticity deficits (Avery and Krichmar, 2017; Briand et al., 2007). For example, mood disorders and depression have been linked to impairments in the connections between the serotonergic pathway and the prefrontal cortex (Liu et al., 2019). Moreover, associations regarding malfunction in the cholinergic pathway and disorders of memory, attention deficit hyperactivity disorder, and schizophrenia have been acknowledged (Scarr et al., 2013), whereas abnormal noradrenergic and dopaminergic activity, respectively, have been associated with neurological and psychiatric disorders, most notably Alzheimer's and Parkinson's disease (Beardmore et al., 2021; Latif et al., 2021). Given that previous evidence has spotlighted these neuromodulators' significant role, utilizing peripheral nerve stimulation represents a potential therapeutic strategy.

## 6. Concluding remarks and future perspectives

Research to date has not yet determined the mechanism(s) of non-invasive neuromodulation methods. The significance of this issue has grown in light of recent evidence suggesting that standard electrode montages applied directly to the scalp result in peripheral nerves sustaining electric fields significantly greater in strength than those measured in the cortex (Asamoah et al., 2019). These findings have begun to shift researchers' position away from the prevailing transcranial mechanism toward favoring a transcutaneous approach. The advantage of these novel non-invasive methods of stimulation is that they are easy to apply at a relatively low cost that are easy to be used in a home setting.

This opinion piece aimed to provide greater insight into a bottom-up transcutaneous pathway shared by four neuromodulatory systems (Fig. 3). This proposed concept lays the groundwork for future investigations into peripheral nerve stimulation being an optimal strategy to modulate neuroplasticity in key brain regions that contribute to relevant cognitive processes or brain regions impacted by neurological disease and psychiatric disorders.

A recent perspective piece proposed that the effects of non-invasive brain stimulation may be attributable to the activation of a peripheral pathway that promotes LC noradrenergic activity, especially considering that a myriad of tDCS studies utilize anterior and posterior electrode montages, many of which engage with the trigeminal and the occipital nerve (van Boekholdt et al., 2021). Per this peripheral route, information is transmitted from the trigeminal and occipital nerve to a common hub, the brainstem. Within the brainstem, information is integrated, relayed, and projected from the NTS throughout widespread regions of the central nervous system. However, despite identifying this promising transcutaneous pathway, many factors of peripheral nerve stimulation remain unclear and require further investigation (see Outstanding Questions). Although limited research regarding stimulation of the trigeminal and greater occipital nerve exists, this pathway sharing a central hub with the vagus nerve suggests that stimulation of these nerves can have similar effects to VNS. Therefore, assimilating evidence from VNS literature has helped to detail other neuromodulatory systems, including the serotonergic, cholinergic, and dopaminergic systems, that may be activated when the trigeminal and greater occipital nerves are stimulated.

Although both trigeminal and greater occipital nerve stimulation share a common neural pathway, it does not exclude that both types of nerve stimulation also activate additional pathways that do not overlap.

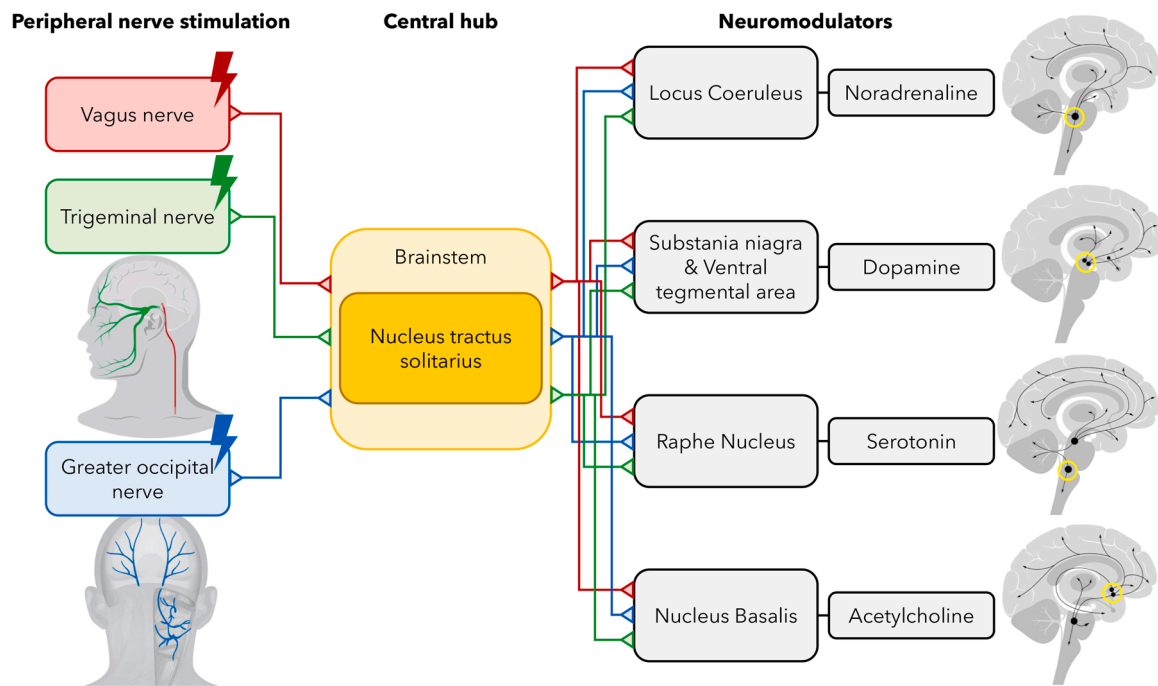


**Fig. 3.** A transcutaneous pathway shared by four neuromodulatory systems. In this proposed transcutaneous mechanism, tES electrodes may be placed amongst cites that stimulate either the trigeminal or greater occipital nerve – likewise, stimulating the cervical vagus nerve via a handheld device applied to the neck or stimulating the auricular vagus nerve via electrodes within ear regions (for VNS recommendations see (Farmer et al., 2020)). Activation of these nerves will send ascending projections to the brainstem, particularly the NTS. From here, there is potential to activate four core neuromodulatory systems, including the far-reaching LC noradrenergic, nucleus basalis cholinergic, raphe nucleus serotonergic, and the SNc and VTA dopaminergic neurotransmitter networks.

It is also difficult to compare trigeminal and greater occipital nerve stimulation as well as the outcome of different labs. At this point there is no consistency in the application of different parameters for trigeminal and greater occipital nerve stimulation including for example amplitude (mA), current (direct versus alternating), specific site of stimulation.

Per this evidence, it is suggested that cortical noradrenaline, serotonin, acetylcholine, and dopamine are each imperative to plasticity (Brougher et al., 2021a; Hulsey et al., 2016; Hulsey et al., 2019). Furthermore, it can be speculated that these neuromodulators underlie the effectiveness of peripheral nerve stimulation (Meyers et al., 2019); however, whether, and if so, how, these multiple neurotransmitter systems work synergistically to modulate certain behaviors and cognition when activated by transcutaneous stimulation of either of these peripheral nerves needs further investigation.

#### Outstanding Questions.

- Seeing that variables such as charge density have shown to alter the effects of non-invasive brain stimulation, it is necessary to discern what the optimal stimulation parameters and variables of stimulating the vagus, trigeminal, and greater occipital nerve are for optimal efficacy, including length of stimulation, number of sessions, and more. Additionally, how do optimal stimulation parameters change based on the peripheral nerve and the neuromodulatory system being targeted?
- Previous research has highlighted that the timing of stimulation may need to vary based upon the desired stimulation effect. Taking this into consideration, it is critical to determine when peripheral nerve stimulation should occur (i.e., online or offline) to produce its desired outcome. Also, does peripheral nerve stimulation need to be paired with a task to activate a specific pathway to see the desired effect?
- Is there an interaction between multiple neuromodulators to optimize peripheral nerve stimulation? If so, how much interaction is required, and how would the multiple neuromodulators interactions

be affected by various pharmacological blockades? Would this then affect the stimulation's efficacy?

- Although modelling calculations support that minimal amounts of direct current reach the cortex, and when they do, the electrical field is inadequate to cause significant effects, it is still unknown how much, if any, direct current contributes to the effect of non-invasive stimulation. Do the minimal amounts of direct current stimulation that reach the cortex contribute to the effects of peripheral nerve stimulation?
- Prior research has identified beneficial effects of alternative neuromodulatory techniques such as TMS and tACS. Considering these effects are similar to those seen from tDCS, could these effects be attributed to these techniques stimulating peripheral nerves?
- What are the effects on behaviour and cognition? How specific are these effects?

#### Data Availability

No data was used for the research described in the article.

#### References

- Adair, D., Truong, D., Esmailpour, Z., Gebodh, N., Borges, H., Ho, L., Bremner, J.D., Badran, B.W., Napadow, V., Clark, V.P., Bikson, M., 2020. Electrical stimulation of cranial nerves in cognition and disease. *Brain Stimul.* 13, 717–750.
- Ahnaou, A., Moechars, D., Raeymaekers, L., Biermans, R., Manyakov, N.V., Bottelbergs, A., Wintmolders, C., Van Kolen, K., Van De Casteele, T., Kemp, J.A., Drinkenburg, W.H., 2017. Emergence of early alterations in network oscillations and functional connectivity in a tau seeding mouse model of Alzheimer's disease pathology. *Sci. Rep.* 7, 14189.
- Antal, A., Herrmann, C.S., 2016. Transcranial alternating current and random noise stimulation: possible mechanisms. *Neural Plast.* 2016, 3616807.
- Asamoah, B., Khatoun, A., Mc Laughlin, M., 2019. tACS motor system effects can be caused by transcutaneous stimulation of peripheral nerves. *Nat. Commun.* 10, 266.
- Avery, M.C., Krichmar, J.L., 2017. Neuromodulatory systems and their interactions: a review of models, theories, and experiments. *Front Neural Circuits* 11, 108.
- Beardmore, R., Hou, R., Darekar, A., Holmes, C., Boche, D., 2021. The Locus Coeruleus in aging and alzheimer's disease: a postmortem and brain imaging review. *J. Alzheimers Dis.* 83, 5–22.

- Beliaeva, V., Savvateev, I., Zerbi, V., Polania, R., 2021. Toward integrative approaches to study the causal role of neural oscillations via transcranial electrical stimulation. *Nat. Commun.* 12, 2243.
- Berridge, C.W., Waterhouse, B.D., 2003. The locus coeruleus-noradrenergic system: modulation of behavioral state and state-dependent cognitive processes. *Brain Res. Brain Res. Rev.* 42, 33–84.
- Bikson, M., Grossman, P., Thomas, C., Zannou, A.L., Jiang, J., Adnan, T., Mourdoukoutas, A.P., Kronberg, G., Truong, D., Boggio, P., Brunoni, A.R., Charvet, L., Fregni, F., Fritsch, B., Gillick, B., Hamilton, R.H., Hampstead, B.M., Jankord, R., Kirton, A., Knotkova, H., Liebetanz, D., Liu, A., Loo, C., Nitsche, M.A., Reis, J., Richardson, J.D., Rotenberg, A., Turkeltaub, P.E., Woods, A.J., 2016. Safety of transcranial direct current stimulation: evidence based update 2016. *Brain Stimul.* 9, 641–661.
- van Boekholdt, L., Kerstens, S., Khatoun, A., Asamoah, B., Mc Laughlin, M., 2021. tDCS peripheral nerve stimulation: a neglected mode of action? *Mol. Psychiatry* 26, 456–461.
- Boroda, E., Sponheim, S.R., Fiecas, M., Lim, K.O., 2020. Transcranial direct current stimulation (tDCS) elicits stimulus-specific enhancement of cortical plasticity. *Neuroimage* 211, 116598.
- Briand, L.A., Gritton, H., Howe, W.M., Young, D.A., Sarter, M., 2007. Modulators in concert for cognition: modulator interactions in the prefrontal cortex. *Prog. Neurobiol.* 83, 69–91.
- Brougher, J., Aziz, U., Adari, N., Chaturvedi, M., Jules, A., Shah, I., Syed, S., Thorn, C.A., 2021a. Self-administration of right vagus nerve stimulation activates midbrain dopaminergic nuclei. *Front. Neurosci.* 15, 782786.
- Brougher, J., Sanchez, C.A., Aziz, U.S., Gove, K.F., Thorn, C.A., 2021b. Vagus nerve stimulation induced motor map plasticity does not require cortical dopamine. *Front. Neurosci.* 15, 693140.
- Busch, V., Jakob, W., Juergens, T., Schulte-Mattler, W., Kaube, H., May, A., 2006. Functional connectivity between trigeminal and occipital nerves revealed by occipital nerve blockade and nociceptive blink reflexes. *Cephalalgia* 26, 50–55.
- Buzsaki, G., Draguhn, A., 2004. Neuronal oscillations in cortical networks. *Science* 304, 1926–1929.
- Caous, C.A., de Sousa Buck, H., Lindsey, C.J., 2001. Neuronal connections of the paratrigeminal nucleus: a topographic analysis of neurons projecting to bulbar, pontine and thalamic nuclei related to cardiovascular, respiratory and sensory functions. *Auton. Neurosci.* 94, 14–24.
- Engineer, N.D., Kimberley, T.J., Prudente, C.N., Dawson, J., Tarver, W.B., Hays, S.A., 2019. Targeted Vagus Nerve Stimulation for Rehabilitation After Stroke. *Front. Neurosci.* 13, 280.
- Farmer, A.D., Strzelczyk, A., Finisguerra, A., Gourine, A.V., Gharabaghi, A., Hasan, A., Burger, A.M., Jaramillo, A.M., Mertens, A., Majid, A., Verkuil, B., Badran, B.W., Ventura-Bort, C., Gaul, C., Beste, C., Warren, C.M., Quintana, D.S., Hammerer, D., Frerri, E., Frangos, E., Tobaldini, E., Kaniusas, E., Rosenow, F., Capone, F., Panetsos, F., Ackland, G.L., Kaithwas, G., O'Leary, G.H., Genheimer, H., Jacobs, H.I. L., Van Diest, I., Schoenen, J., Redgrave, J., Fang, J., Deuchars, J., Szeles, J.C., Thayer, J.F., More, K., Vonck, K., Steenbergen, L., Vianna, L.C., McTeague, L.M., Ludwig, M., Veldhuizen, M.G., De Cock, M., Casazza, M., Keute, M., Bikson, M., Andreatta, M., D'Agostini, M., Weymar, M., Betts, M., Prigge, M., Kaess, M., Roden, M., Thai, M., Schuster, N.M., Montano, N., Hansen, N., Kroemer, N.B., Rong, P., Fischer, R., Howland, R.H., Sclocco, R., Sellaro, R., Garcia, R.G., Bauer, S., Gancheva, S., Stavrakis, S., Kampusch, S., Deuchars, S.A., Wehner, S., Laborde, S., Usichenko, T., Polak, T., Zaehle, T., Borges, U., Teckentrup, V., Jandackova, V.K., Napadow, V., Koenig, J., 2020. International consensus based review and recommendations for minimum reporting standards in research on transcutaneous vagus nerve stimulation (Version 2020). In: *Front. Hum. Neurosci.* 14, 568051.
- Fritsch, B., Reis, J., Martinowich, K., Schambra, H.M., Ji, Y., Cohen, L.G., Lu, B., 2010. Direct current stimulation promotes BDNF-dependent synaptic plasticity: potential implications for motor learning. *Neuron* 66, 198–204.
- Ganzer, P.D., Darrow, M.J., Meyers, E.C., Solorzano, B.R., Ruiz, A.D., Robertson, N.M., Adcock, K.S., James, J.T., Jeong, H.S., Becker, A.M., Goldberg, M.P., Pruitt, D.T., Hays, S.A., Kilgard, M.P., Rennaker 2nd, R.L., 2018. Closed-loop neuromodulation restores network connectivity and motor control after spinal cord injury. *Elife* 7.
- Halassa, M.M., Sherman, S.M., 2019. Thalamocortical circuit motifs: a general framework. *Neuron* 103, 762–770.
- Han, W., Tellez, L.A., Perkins, M.H., Perez, I.O., Qu, T., Ferreira, J., Ferreira, T.L., Quinn, D., Liu, Z.W., Gao, X.B., Kaelberer, M.M., Bohorquez, D.V., Shammah-Lagnado, S.J., de Lartigue, G., de Araujo, I.E., 2018. A neural circuit for gut-induced reward. *Cell* 175, 665–678 e623.
- Hays, S.A., 2016. Enhancing rehabilitative therapies with vagus nerve stimulation. *Neurotherapeutics* 13, 382–394.
- Helm, S., Shirsat, N., Calodney, A., Abd-Elseyed, A., Kloth, D., Soin, A., Shah, S., Trescot, A., 2021. Peripheral nerve stimulation for chronic pain: a systematic review of effectiveness and safety. *Pain. Ther.* 10, 985–1002.
- Herrmann, C.S., Rach, S., Neuling, T., Struber, D., 2013. Transcranial alternating current stimulation: a review of the underlying mechanisms and modulation of cognitive processes. *Front. Hum. Neurosci.* 7, 279.
- Huang, Y., Liu, A.A., Lafon, B., Friedman, D., Dayan, M., Wang, X., Bikson, M., Doyle, W. K., Devinsky, O., Parra, L.C., 2017. Measurements and models of electric fields in the in vivo human brain during transcranial electric stimulation. *Elife* 6.
- Hulse, D.R., Hays, S.A., Khodaparast, N., Ruiz, A., Das, P., Rennaker 2nd, R.L., Kilgard, M.P., 2016. Reorganization of motor cortex by vagus nerve stimulation requires cholinergic innervation. *Brain Stimul.* 9, 174–181.
- Hulse, D.R., Riley, J.R., Loerwald, K.W., Rennaker 2nd, R.L., Kilgard, M.P., Hays, S.A., 2017. Parametric characterization of neural activity in the locus coeruleus in response to vagus nerve stimulation. *Exp. Neurol.* 289, 21–30.
- Hulse, D.R., Shedd, C.M., Sarker, S.F., Kilgard, M.P., Hays, S.A., 2019. Norepinephrine and serotonin are required for vagus nerve stimulation directed cortical plasticity. *Exp. Neurol.* 320, 112975.
- Jackson, M.P., Rahman, A., Lafon, B., Kronberg, G., Ling, D., Parra, L.C., Bikson, M., 2016. Animal models of transcranial direct current stimulation: Methods and mechanisms. *Clin. Neurophysiol.* 127, 3425–3454.
- Jahshan, C., Wynn, J.K., Mathalon, D.H., Green, M.F., 2017. Cognitive correlates of visual neural plasticity in schizophrenia. *Schizophr. Res.* 190, 39–45.
- Jones, E.J., Rohleder, N., Schreier, H.M.C., 2020. Neuroendocrine coordination and youth behavior problems: a review of studies assessing sympathetic nervous system and hypothalamic-pituitary-adrenal axis activity using salivary alpha amylase and salivary cortisol. *Horm. Behav.* 122, 104750.
- Joshi, S., 2021. Pupillometry: arousal state or state of mind? *Curr. Biol.* 31, R32–R34.
- Joshi, S., Gold, J.I., 2020. Pupil size as a window on neural substrates of cognition. *Trends Cogn. Sci.* 24, 466–480.
- Kawai, Y., 2018. Differential ascending projections from the male rat caudal nucleus of the tractus solitarius: an interface between local microcircuits and global macrocircuits. *Front. Neuroanat.* 12, 63.
- Kronberg, G., Bridi, M., Abel, T., Bikson, M., Parra, L.C., 2017. Direct current stimulation modulates LTP and LTD: activity dependence and dendritic effects. *Brain Stimul.* 10, 51–58.
- Kronberg, G., Rahman, A., Sharma, M., Bikson, M., Parra, L.C., 2020. Direct current stimulation boosts hebbian plasticity in vitro. *Brain Stimul.* 13, 287–301.
- Kumar, M., Chawla, R., Goyal, M., 2015. Topical anesthesia. *J. Anaesthesiol. Clin. Pharm.* 31, 450–456.
- Latif, S., Jahangeer, M., Maknoon Razia, D., Ashiq, M., Ghaffar, A., Akram, M., El Allam, A., Bouyahya, A., Garipova, L., Ali Shariati, M., Thiruvengadam, M., Azam Ansari, M., 2021. Dopamine in Parkinson's disease. *Clin. Chim. Acta* 522, 114–126.
- Liu, A., Voroslakos, M., Kronberg, G., Henin, S., Krause, M.R., Huang, Y., Opitz, A., Mehta, A., Pack, C.C., Krekelberg, B., Berenyi, A., Parra, L.C., Melloni, L., Devinsky, O., Buzsaki, G., 2018. Immediate neurophysiological effects of transcranial electrical stimulation. *Nat. Commun.* 9, 5092.
- Liu, Y., Zhao, J., Fan, X., Guo, W., 2019. Dysfunction in serotonergic and noradrenergic systems and somatic symptoms in psychiatric disorders. *Front. Psychiatry* 10, 286.
- Luckey, A.M., McLeod, S.L., Robertson, I.H., To, W.T., Vanneste, S., 2020. Greater occipital nerve stimulation boosts associative memory in older individuals: a randomized trial. *Neurorehabil. Neural Repair*, 1545968320943573.
- Luckey, A.M., McLeod, S.L., Mohan, A., Vanneste, S., 2022. Potential role for peripheral nerve stimulation on learning and long-term memory: a comparison of alternating and direct current stimulations. *Brain Stimul.* 15, 536–545.
- Menetrey, D., Basbaum, A.I., 1987. Spinal and trigeminal projections to the nucleus of the solitary tract: a possible substrate for somatovisceral and viscerovisceral reflex activation. *J. Comp. Neurol.* 255, 439–450.
- Meyers, E.C., Solorzano, B.R., James, J., Ganzer, P.D., Lai, E.S., Rennaker 2nd, R.L., Kilgard, M.P., Hays, S.A., 2018. Vagus nerve stimulation enhances stable plasticity and generalization of stroke recovery. *Stroke* 49, 710–717.
- Meyers, E.C., Kasliwal, N., Solorzano, B.R., Lai, E., Bendale, G., Berry, A., Ganzer, P.D., Romero-Ortega, M., Rennaker 2nd, R.L., Kilgard, M.P., Hays, S.A., 2019. Enhancing plasticity in central networks improves motor and sensory recovery after nerve damage. *Nat. Commun.* 10, 5782.
- Nitsche, M.A., Paulus, W., 2000. Excitability changes induced in the human motor cortex by weak transcranial direct current stimulation. *J. Physiol.* 527 (3), 633–639 (Pt).
- Nitsche, M.A., Seeber, A., Frommann, K., Klein, C.C., Rochford, C., Nitsche, M.S., Fricke, K., Liebetanz, D., Lang, N., Antal, A., Paulus, W., Tergau, F., 2005. Modulating parameters of excitability during and after transcranial direct current stimulation of the human motor cortex. *J. Physiol.* 568, 291–303.
- Opitz, A., Falchier, A., Yan, C.G., Yeagle, E.M., Linn, G.S., Megevard, P., Thielscher, A., Deborah, A.R., Milham, M.P., Mehta, A.D., Schroeder, C.E., 2016. Spatiotemporal structure of intracranial electric fields induced by transcranial electric stimulation in humans and nonhuman primates. *Sci. Rep.* 6, 31236.
- Podda, M.V., Cocco, S., Mastrodonato, A., Fusco, S., Leone, L., Barbati, S.A., Colussi, C., Ripoli, C., Grassi, C., 2016. Anodal transcranial direct current stimulation boosts synaptic plasticity and memory in mice via epigenetic regulation of Bdnf expression. *Sci. Rep.* 6, 22180.
- Poe, G.R., Foote, S., Eschenko, O., Johansen, J.P., Bouret, S., Aston-Jones, G., Harley, C. W., Manahan-Vaughan, D., Weinschenker, D., Valentino, R., Berridge, C., Chandler, D.J., Waterhouse, B., Sara, S.J., 2020. Locus coeruleus: a new look at the blue spot. *Nat. Rev. Neurosci.* 21, 644–659.
- Rea, P., 2015. Trigeminal Nerve, Regional Nerve Blocks in Anesthesia and Pain Therapy. Springer, pp. 133–160.
- Reed, T., Cohen Kadosh, R., 2018. Transcranial electrical stimulation (tES) mechanisms and its effects on cortical excitability and connectivity. *J. Inherit. Metab. Dis.*
- Reinhart, R.M.G., Nguyen, J.A., 2019. Working memory revived in older adults by synchronizing rhythmic brain circuits. *Nat. Neurosci.* 22, 820–827.
- Salgado, H., Trevino, M., Atzori, M., 2016. Layer- and area-specific actions of norepinephrine on cortical synaptic transmission. *Brain Res.* 1641, 163–176.
- Samuels, E.R., Szabadi, E., 2008. Functional neuroanatomy of the noradrenergic locus coeruleus: its roles in the regulation of arousal and autonomic function part I: principles of functional organisation. *Curr. Neuropharmacol.* 6, 235–253.
- Scarr, E., Gibbons, A.S., Neo, J., Udawela, M., Dean, B., 2013. Cholinergic connectivity: its implications for psychiatric disorders. *Front. Cell Neurosci.* 7, 55.
- Slavin, K.V., 2011. History of peripheral nerve stimulation. *Prog. Neurol. Surg.* 24, 1–15.
- So, P.P., Stuchly, M.A., Nyenhuis, J.A., 2004. Peripheral nerve stimulation by gradient switching fields in magnetic resonance imaging. *IEEE Trans. Biomed. Eng.* 51, 1907–1914.



- de Sousa Buck, H., Caous, C.A., Lindsey, C.J., 2001. Projections of the paratrigeminal nucleus to the ambiguus, rostroventrolateral and lateral reticular nuclei, and the solitary tract. *Auton. Neurosci.* 87, 187–200.
- Tavakoli, A.V., Yun, K., 2017. Transcranial alternating current stimulation (tACS) mechanisms and protocols. *Front Cell Neurosci.* 11, 214.
- Thair, H., Holloway, A.L., Newport, R., Smith, A.D., 2017. Transcranial direct current stimulation (tDCS): a beginner's guide for design and implementation. *Front Neurosci.* 11, 641.
- Vanneste, S., Mohan, A., Yoo, H.B., Huang, Y., Luckey, A.M., McLeod, S.L., Tabet, M.N., Souza, R.R., McIntyre, C.K., Chapman, S., Robertson, I.H., To, W.T., 2020. The peripheral effect of direct current stimulation on brain circuits involving memory. *Sci. Adv.* 6.
- Voroslakos, M., Takeuchi, Y., Brinyiczki, K., Zombori, T., Oliva, A., Fernandez-Ruiz, A., Kozak, G., Kincses, Z.T., Ivanyi, B., Buzsaki, G., Berenyi, A., 2018. Direct effects of transcranial electric stimulation on brain circuits in rats and humans. *Nat. Commun.* 9, 483.
- Weiner, R.L., Alo, K.M., 2018. Occipital nerve stimulation for treatment of intractable headache syndromes. *Neuromodulation. Elsevier*, pp. 773–782.
- Woods, A.J., Antal, A., Bikson, M., Boggio, P.S., Brunoni, A.R., Celnik, P., Cohen, L.G., Fregni, F., Herrmann, C.S., Kappenman, E.S., Knotkova, H., Liebetanz, D., Miniussi, C., Miranda, P.C., Paulus, W., Priori, A., Reato, D., Stagg, C., Wenderoth, N., Nitsche, M.A., 2016. A technical guide to tDCS, and related non-invasive brain stimulation tools. *Clin. Neurophysiol.* 127, 1031–1048.
- Yap, J.Y.Y., Keatch, C., Lambert, E., Woods, W., Stoddart, P.R., Kameneva, T., 2020. Critical review of transcutaneous vagus nerve stimulation: challenges for translation to clinical practice. *Front Neurosci.* 14, 284.
- Zhao, C., Woodman, G.F., 2021. Converging evidence that neural plasticity underlies transcranial direct-current stimulation. *J. Cogn. Neurosci.* 33, 146–157.
- Zhou, S., Hussain, N., Abd-Elseyed, A., Boulos, R., Hakim, M., Gupta, M., Weaver, T., 2021. Peripheral nerve stimulation for treatment of headaches: an evidence-based review. *Biomedicines* 9.

# Making memories last using the peripheral effect of direct current stimulation

Alison M Luckey<sup>1</sup>, Lauren S McLeod<sup>2</sup>, Yuefeng Huang<sup>3</sup>, Anusha Mohan<sup>1</sup>, Sven Vanneste<sup>1\*</sup>

<sup>1</sup>Global Brain Health Institute and Institute of Neuroscience, Trinity College Dublin, Dublin, Ireland; <sup>2</sup>School of Medicine, Texas Tech School of Medicine, Lubbock, United States; <sup>3</sup>Department of Psychiatry, Icahn School of Medicine at Mount Sinai, New York, United States

**Abstract** Most memories that are formed are forgotten, while others are retained longer and are subject to memory stabilization. We show that non-invasive transcutaneous electrical stimulation of the greater occipital nerve (NITESGON) using direct current during learning elicited a long-term memory effect. However, it did not trigger an immediate effect on learning. A neurobiological model of long-term memory proposes a mechanism by which memories that are initially unstable can be strengthened through subsequent novel experiences. In a series of studies, we demonstrate NITESGON's capability to boost the retention of memories when applied shortly before, during, or shortly after the time of learning by enhancing memory consolidation via activation and communication in and between the locus coeruleus pathway and hippocampus by plausibly modulating dopaminergic input. These findings may have a significant impact for neurocognitive disorders that inhibit memory consolidation such as Alzheimer's disease.

\*For correspondence:  
sven.vanneste@tcd.ie

**Competing interest:** The authors declare that no competing interests exist.

**Funding:** See page 30

**Received:** 15 November 2021

**Preprinted:** 06 July 2022

**Accepted:** 18 May 2023

**Published:** 19 May 2023

**Reviewing Editor:** Lila Davachi, Columbia University, United States

© Copyright Luckey et al. This article is distributed under the terms of the [Creative Commons Attribution License](https://creativecommons.org/licenses/by/4.0/), which permits unrestricted use and redistribution provided that the original author and source are credited.

## Editor's evaluation

This is a landmark study showing that non-invasive transcutaneous electrical stimulation of the greater occipital nerve (NITESGON) can improve long-term memory. The authors provide compelling evidence that applying NITESGON during learning causally influences memory behavior. This method is novel and the work presented herein will be valuable to a broad range of scientists and clinicians interested in manipulations to improve memory and cognition more broadly.

## Introduction

Research on enhancing and preserving human memory has substantially increased in the last few decades due largely to the prevalence and inexorable condition of Alzheimer's disease (AD). Early behavioral indicators of AD include a decline in an individual's ability to retain learned information and remember events, situations, and objects, alluding to synaptic connections losing strength as AD emerges (*Reza-Zaldivar et al., 2020*). As a result, recent investigations have begun assessing the perspective clinical significance of therapeutic non-invasive brain stimulation techniques to modify neuroplasticity and upregulate neuronal excitability in different neurological conditions, including memory deficits (*Lefaucheur et al., 2017*).

There is an ongoing debate about whether non-invasive electrical stimulation of the scalp modulates the excitability of neurons directly (*Vöröslakos et al., 2018; Liu et al., 2018*). Interestingly, a series of experiments in rats and humans isolated the transcranial and transcutaneous mechanisms of

non-invasive electrical stimulation and showed that the reported effects are mainly caused by transcutaneous stimulation of peripheral nerves (Vöröslakos *et al.*, 2018; Asamoah *et al.*, 2019). Similarly, it was demonstrated that nerve stimulation paired with an auditory or motor task could induce targeted plasticity in animals (Engineer *et al.*, 2011; Porter *et al.*, 2012). In addition, our recent work suggests that non-invasive transcutaneous electrical stimulation of the greater occipital nerve (NITESGON) using direct current utilizes a pathway that arises from the C2 spinal nerve to establish communication gateways from the periphery to the brain via afferent fibers that project to the brainstem and synapse onto the nucleus tractus solitarius (NTS); various rodent studies have used antero-grade neuronal tracers to demonstrate these connections (Adair *et al.*, 2020; Caous *et al.*, 2001; de Sousa Buck *et al.*, 2001; Menétrey and Basbaum, 1987). From the NTS, the information is then integrated among networks within the complex reticular formation and relayed across the brainstem through major cortical and subcortical regions (Kawai, 2018). Furthermore, our work demonstrated that NITESGON during learning induces improvements in memory recall in younger (18–25 years) and older (>55 years) adults up to 28 days after learning (Luckey *et al.*, 2020; Vanneste *et al.*, 2020). Intriguingly, NITESGON yielded a long-term memory effect but did not trigger an immediate effect on learning, suggesting that the effect is generated during the consolidation of memories (Vanneste *et al.*, 2020; Luckey *et al.*, 2020) as opposed to during the learning or encoding of new memories.

Most episodic-like memories that are formed are forgotten, while others are retained for longer periods of time and are subject to memory stabilization (Squire, 1992; Squire *et al.*, 1992; Tonegawa *et al.*, 2018). This is referred to as synaptic consolidation, a process that stabilizes new information into memory over a timespan of minutes to hours (Squire *et al.*, 2015). To illustrate the neurobiological account of synaptic consolidation, Frey and Morris introduced a plasticity model known as the synaptic tag-and-capture hypothesis that has proposed a cellular mechanism explaining how new memories that are initially weak and unstable are tagged to be captured by late-phase long-term potentiation (LTP) to become stable (Morris and Frey, 1997; Frey and Morris, 1997). This synaptic tag-and-capture mechanism has since been translated into a learning and memory paradigm referred to as behavioral tagging (Moncada *et al.*, 2015; Viola *et al.*, 2014). Behavioral tagging proposes weak training that typically generates short-term memory can utilize the tag-and-capture process to consolidate into a stabilized long-term memory when a weak event is preceded or followed by a strong or novel event within a limited time window (Moncada *et al.*, 2015; Viola *et al.*, 2014; Dunsmoor *et al.*, 2022). The neural mechanism that controls this novelty response is the locus coeruleus–noradrenaline (LC–NA) pathway (Vankov *et al.*, 1995; Takeuchi *et al.*, 2016). Animal research further indicates that direct electrical stimulation of the LC modulates hippocampal synaptic consolidation (Lemon and Manahan-Vaughan, 2012; McGaugh, 2004; Cahill and McGaugh, 1998). We hypothesize that NITESGON modulates projections to the hippocampus via the LC–NA system and induces memory stabilization by modulating synaptic consolidation in the hippocampus via the mechanism of behavioral tagging.

The present study tests the above hypothesis questioning if NITESGON induces a long-term memory effect by strengthening memories via behavioral tagging across eight experiments. The first set of experiments aims to confirm the behavioral tagging hypothesis as the potential mechanism inducing memory consolidation via NITESGON, whereby the second set of experiments examines the underlying brain network involved in synaptic consolidation and investigates the underlying neural mechanism that is associated with behavioral tagging induced by NITESGON.

## Results

### Experiment 1. NITESGON during or immediately after training

The idea behind behavioral tagging suggests that weak memories that are regularly unstable and likely to be forgotten will solidify following a novel experience (Moncada *et al.*, 2015; Viola *et al.*, 2014; Dunsmoor *et al.*, 2022). That is, consolidation is facilitated by applying a strong stimulus alongside a weak stimulus within a critical time window. Recent research revealed a direct link between the LC and behavioral tagging, attributable to the pivotal role the LC plays during the presentation of a salient or arousing event (i.e., strong stimulus) (Sara, 2009; Poe *et al.*, 2020), as well as being at the helm of regulating the synthesis of new proteins required for memory consolidation in the hippocampus (Moncada, 2017). Furthermore, studies have shown modulation of memory consolidation

with increases in stress and arousal that are mediated via the LC pathway (McGaugh, 2004; Cahill and McGaugh, 1998). Moreover, animal research has indicated that direct electrical stimulation of the LC modulates hippocampal synaptic transmission fundamental for memory consolidation (Lemon and Manahan-Vaughan, 2012).

Seeing that NITESGON activates the LC pathway, which plays an important role in memory consolidation, we hypothesize that participants will be able to establish long-term memories upon modulating the LC both during learning, as shown before (Luckey et al., 2020; Vanneste et al., 2020), as well as immediately after learning. This will directly test if NITESGON plays a more central role during encoding or the consolidation phase of memory. To test this hypothesis, participants learned a word-association task and were tested 7 days later on how many word associations they were able to recall correctly. Active or sham NITESGON was applied via electrodes placed over the left and right C2 nerve dermatome at a constant current of 1.5 mA either during or immediately after learning the word-association task on visit 1.

To further explore the effect of NITESGON, resting-state EEG (rsEEG) and salivary  $\alpha$ -amylase (sAA) were collected immediately before and after NITESGON on visit 1. Previous research has revealed an increase in sAA, a putative marker of endogenous NA activity, immediately following NITESGON (Luckey et al., 2020; Vanneste et al., 2020). Furthermore, previous investigations have demonstrated that LC discharge enhances the synchronization of gamma activity in the hippocampus in rats (Hajós et al., 2003) and have identified gamma oscillations' critical role in long-term memory formation and the potential to predict subsequent recall (Osipova et al., 2006; Sederberg et al., 2003). Based on these findings, we hypothesized that NITESGON would induce an increase in sAA and gamma activity in the medial temporal lobe that will correlate with successful recall during the second visit 7 days after learning the task.

On visit 1, no difference was observed regarding the number of word associations learned between the three condition groups (i.e., sham NITESGON during learning and after learning, active NITESGON during learning and sham NITESGON after learning, or sham NITESGON during learning and active NITESGON after learning) ( $F = 0.24$ ,  $p = 0.79$ ; see **Figure 1a**), thus indicating that NITESGON had no effect on learning the word-association task. Results revealed a significant difference in memory recall 7 days after NITESGON was applied either during learning ( $46.09 \pm 15.06\%$ ,  $p = 0.012$ ) or after learning the task ( $47.65 \pm 13.27\%$ ,  $p = 0.005$ ) relative to the sham condition employed during both learning and immediately after learning the task ( $33.38 \pm 12.57\%$ ) ( $F = 5.24$ ,  $p = 0.009$ ; see **Figure 1b**). However, no difference was attained on recall 7 days later between the conditions of NITESGON applied during learning the task or immediately after learning the task ( $p = 0.75$ ). A significant increase in sAA ( $F = 7.69$ ,  $p = 0.010$ ; see **Figure 1c**) was revealed during learning (before:  $88.79 \pm 50.48$  vs. after:  $149.82.6 \pm 82.67$ ;  $p < 0.001$ ) and after learning in comparison to the sham group (before:  $100.28 \pm 41.95$  vs. after:  $114.30 \pm 41.02$ ;  $p = 0.14$ ). Memory recall 7 days later correlated with the difference in sAA levels on visit 1 (pre vs. post) ( $r = 0.59$ ,  $p < 0.001$ ; **Figure 1d**;  $r_s = 0.62$ ,  $p < 0.001$ ; **Figure 1—figure supplement 1**). Looking at the individual correlations for each group separately, we found a significant correlation for the active groups (i.e., NITESGON during learning  $r = 0.47$ ,  $p = 0.09$  and after learning [ $r = 0.78$ ,  $p < 0.001$ ]) between memory recall 7 days later and sAA levels on visit 1 (pre vs. post). No significant correlation was obtained for the sham group ( $r = 0.27$ ,  $p = 0.31$ ). Memory recollection 7 days after stimulation was associated with increased gamma power in the medial temporal cortex as well as the precuneus and dorsal lateral prefrontal cortex immediately after stimulation ( $r = 0.42$ ,  $p = 0.011$ ; see **Figure 1e**).

## Experiment 2. NITESGON during second task – retroactive strengthening of memories

Experiment 1 suggests that NITESGON generates an effect during the consolidation phase as opposed to the learning-encoding phase due to no effect of NITESGON being exhibited during learning between the different groups, but both stimulating during and after learning the task induced a long-term memory effect. Bearing in mind the definition of behavioral tagging that indicates that the pairing of a strong stimulus and a weak stimulus within a critical time window can induce memory stabilization of the weak stimulus, NITESGON can be seen as the mechanism that induces a similar action as a strong stimulus, and through the mechanism of behavioral tagging strengthen the weak stimulus (i.e., the word-association task).

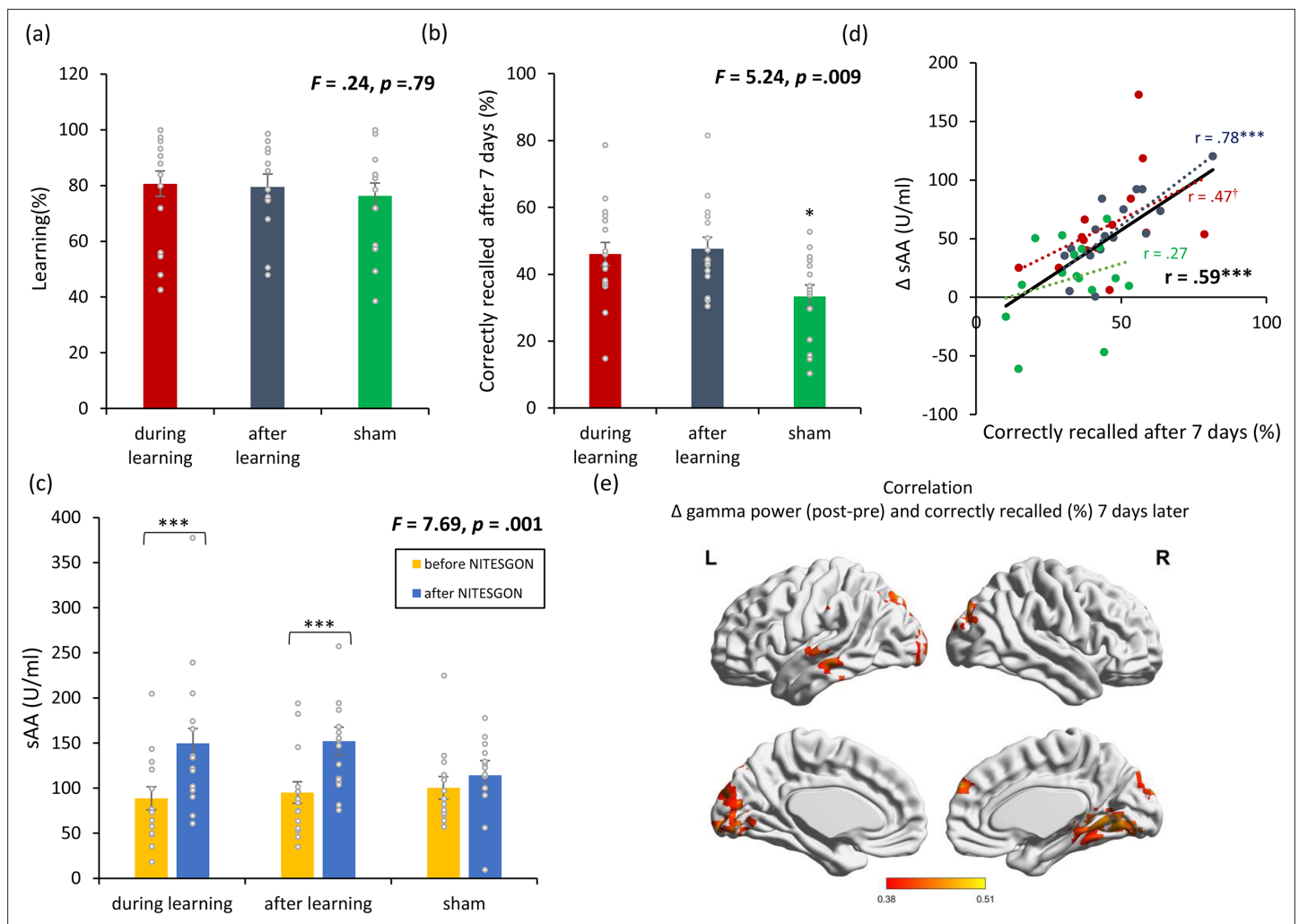


**Figure 1.** Non-invasive transcutaneous electrical stimulation of the greater occipital nerve (NITESGON) immediately after training can enhance memory with **Figure 1—figure supplement 1**. **(a)** No difference was observed in the cumulative learning rate between active and sham NITESGON during or immediately after the study phase of the word-association memory task. **(b)** NITESGON during or immediately after the word-association memory task can improve memory recall 7 days after the study phase for the active relative to the sham group. **(c)** After NITESGON salivary  $\alpha$ -amylase (sAA) levels increase for both active groups, but not for sham NITESGON. **(d)** Memory recall 7 days later correlates with the difference in sAA levels during the first visit (pre vs. post study phase). **(e)** Improved memory recall 7 days after stimulation is associated with increased activity in the medial temporal lobe as well as anterior and posterior cingulate cortex immediately after NITESGON for the gamma frequency band. Error bars, standard error of the mean (s.e.m.). Asterisks represent significant differences (\* $p < 0.05$ ; \*\* $p < 0.01$ ; \*\*\* $p < 0.001$ ),  $\Delta$ sAA levels are the subtraction of sAA levels before NITESGON from sAA levels immediately after NITESGON.

The online version of this article includes the following figure supplement(s) for figure 1:

**Figure supplement 1.** To avoid the potential outliers would drive the Pearson correlation between a memory recall 7 days after learning the task and the difference in salivary  $\alpha$ -amylase (sAA) levels (difference between before and after stimulation on day 1), a Spearman rank correlation was calculated to cross validate our findings.

Prior research on behavioral tagging has shown that items paired with an electric shock (i.e., Pavlovian fear conditioning task) had a retroactive memory effect on items learned before the fear conditioning task (Dunsmoor et al., 2015). This provided evidence for a generalized retroactive memory enhancement, whereby information can be retroactively credited as relevant, and therefore remembered (Dunsmoor et al., 2015). Interestingly, LC activation occurs in close relation to the intensity of the Pavlovian behavior (Bouret and Richmond, 2009). Hence, to explore the effect of the LC on behavioral tagging, we verified if NITESGON applied during a second task would result in a significant retroactive memory effect on the first task as predicted by behavioral tagging.

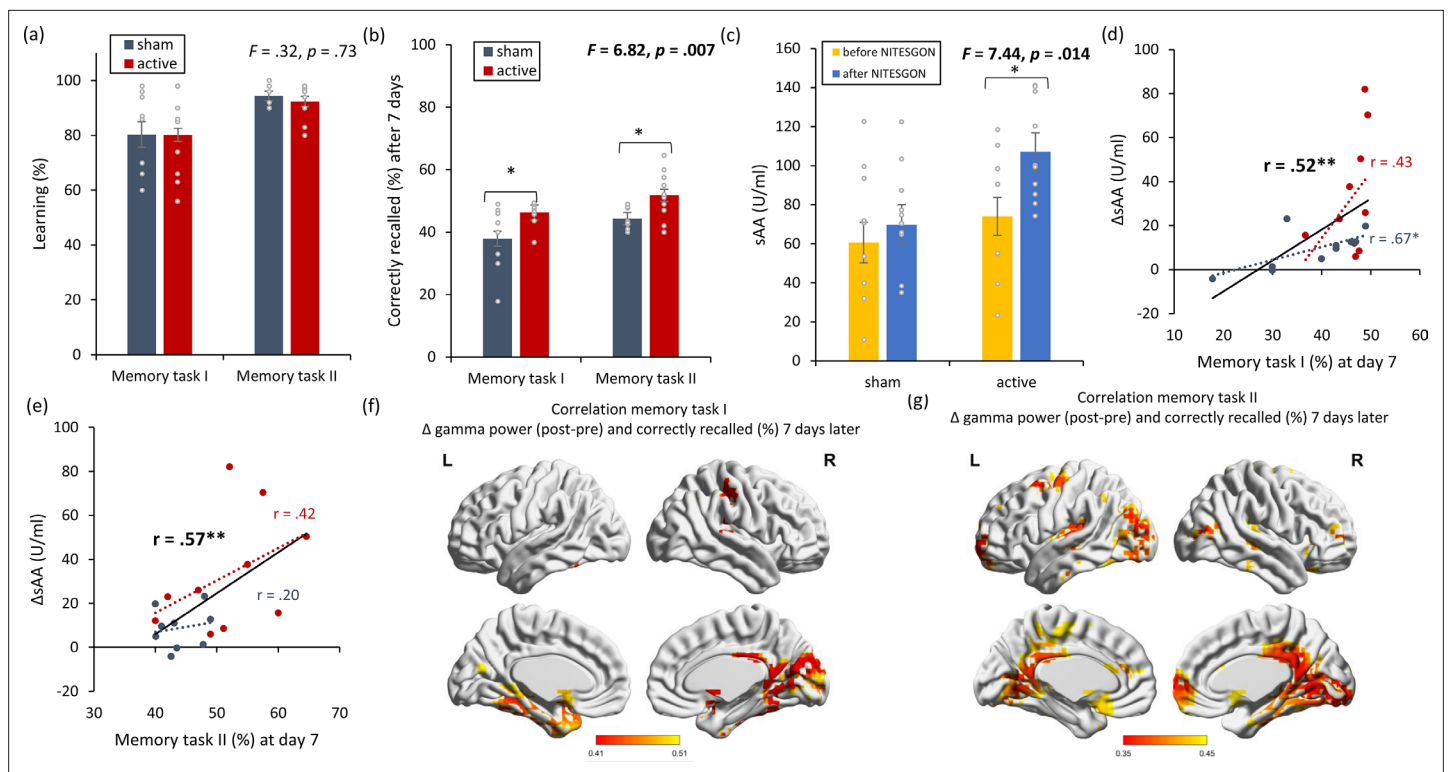


**Figure 2.** Non-invasive transcutaneous electrical stimulation of the greater occipital nerve (NITESGON) has a retroactive memory effect – NITESGON during the second task memory with **Figure 2—figure supplement 1**. (a) No difference was observed in the cumulative learning rate between active and sham NITESGON after the study phase for the first task (i.e., word-association task) or second task (i.e., object-location task). (b) NITESGON can improve memory recall 7 days after the study phase for the active relative to the sham group for both the first and second tasks. (c) After NITESGON salivary  $\alpha$ -amylase (sAA) levels increase for active group, but not for sham NITESGON. (d, e) Memory recall 7 days later correlates with the difference in sAA levels during the first visit (pre vs. post study phase) for the first and second tasks. (f, g) Improved memory recall 7 days after stimulation is associated with increased activity in the medial temporal lobe immediately after NITESGON for the gamma frequency band. Error bars, standard error of the mean (s.e.m.). Asterisks represent significant differences (\* $p < 0.05$ ; \*\* $p < 0.01$ ).  $\Delta$ sAA levels are the subtraction of sAA levels before NITESGON from sAA levels immediately after NITESGON.

The online version of this article includes the following figure supplement(s) for figure 2:

**Figure supplement 1.** To avoid the potential outliers would drive the Pearson correlation between a memory recall 7 days after learning the task and the difference in salivary  $\alpha$ -amylase (sAA) levels (difference between before and after stimulation on day 1), a Spearman rank correlation was calculated to cross validate our findings.

To test the hypothesis, Experiment 2 had participants take part in a word-association task followed by a spatial-navigation object-location task while receiving active or sham NITESGON during the second task. These two types of tasks were selected because they would not interfere with one another, seeing that both require different episodic information. rsEEG data and sAA were collected immediately before and after the two tasks on visit 1. Two memory tests were taken 7 days after learning the word-association and spatial-navigation tasks.

On visit 1, no difference in learning ( $F = 0.32$ ,  $p = 0.73$ ; see **Figure 2a**) was observed for both the first ( $F = 0.09$ ,  $p = 0.98$ ) and second ( $F = 0.64$ ,  $p = 0.43$ ) tasks between the active and sham NITESGON groups. On visit 2, 7 days after initial learning, a significant effect was obtained for recall ( $F = 0.682$ ,  $p = 0.007$ ; see **Figure 2b**) for both the first ( $F = 6.28$ ,  $p = 0.022$ ) and second tasks ( $F = 7.51$ ,  $p = 0.013$ ), revealing an increase in word recall ( $46.26 \pm 3.76\%$  vs.  $37.88 \pm 9.88\%$ ), as well as object-location recall ( $51.82 \pm 7.75\%$  vs.  $44.39 \pm 3.68\%$ ) for the active group in comparison to the sham group. Furthermore, a significant increase in sAA ( $F = 7.44$ ,  $p = 0.014$ ; see **Figure 2c**) was revealed in the active group (before:  $74.01 \pm 26.58$  vs. after:  $107.01 \pm 25.98$ ;  $p < 0.001$ ) in comparison to the sham group (before:  $60.61 \pm 37.93$  vs. after:  $69.61 \pm 35.07$ ;  $p = 0.18$ ). This increase in sAA correlated with how many items they recalled 7 days after the learning phase for both the word-association task ( $r = 0.52$ ,  $p = 0.019$ ; see **Figure 2d**;  $r_s = 0.62$ ,  $p = 0.002$ ; **Figure 2—figure supplement 1**) and the object-location task ( $r =$



0.57,  $p = 0.008$ ; see **Figure 2e**;  $r_s = 0.49$ ,  $p = 0.03$  **Figure 2—figure supplement 1**). Looking at each group separately, we found no significant correlation for the active groups (first task:  $r = 0.43$ ,  $p = 0.21$ ; second task:  $r = 0.42$ ,  $p = 0.22$ ) between memory recall 7 days later and sAA levels on visit 1 (pre vs. post). For the sham group a significant effect was obtained between memory recall 7 days later and sAA levels on visit 1 (pre vs. post) for the first task ( $r = 0.67$ ,  $p = 0.036$ ). No significant correlation was obtained for the sham group for the second task ( $r = 0.20$ ,  $p = 0.58$ ). Memory recollection 7 days after stimulation was associated with increased gamma power in the medial temporal cortex immediately after stimulation for both the first ( $r = 0.41$ ,  $p = 0.009$ ; see **Figure 2f**) and second memory tasks ( $r = 0.35$ ,  $p = 0.018$ ; see **Figure 2g**).

### Experiment 3. NITESGON during first task – proactive strengthening of memories

Experiment 2 revealed a retroactive memory effect 7 days after initial learning for the active NITESGON group compared to the sham NITESGON group, fitting well with the behavioral tagging hypothesis. In addition to a retroactive memory effect, previous research on behavioral tagging also revealed that items paired with an electric shock had a proactive memory effect, whereby items learned after the fear conditioning task were remembered (*Dunsmoor et al., 2015*). Here, we conducted the exact

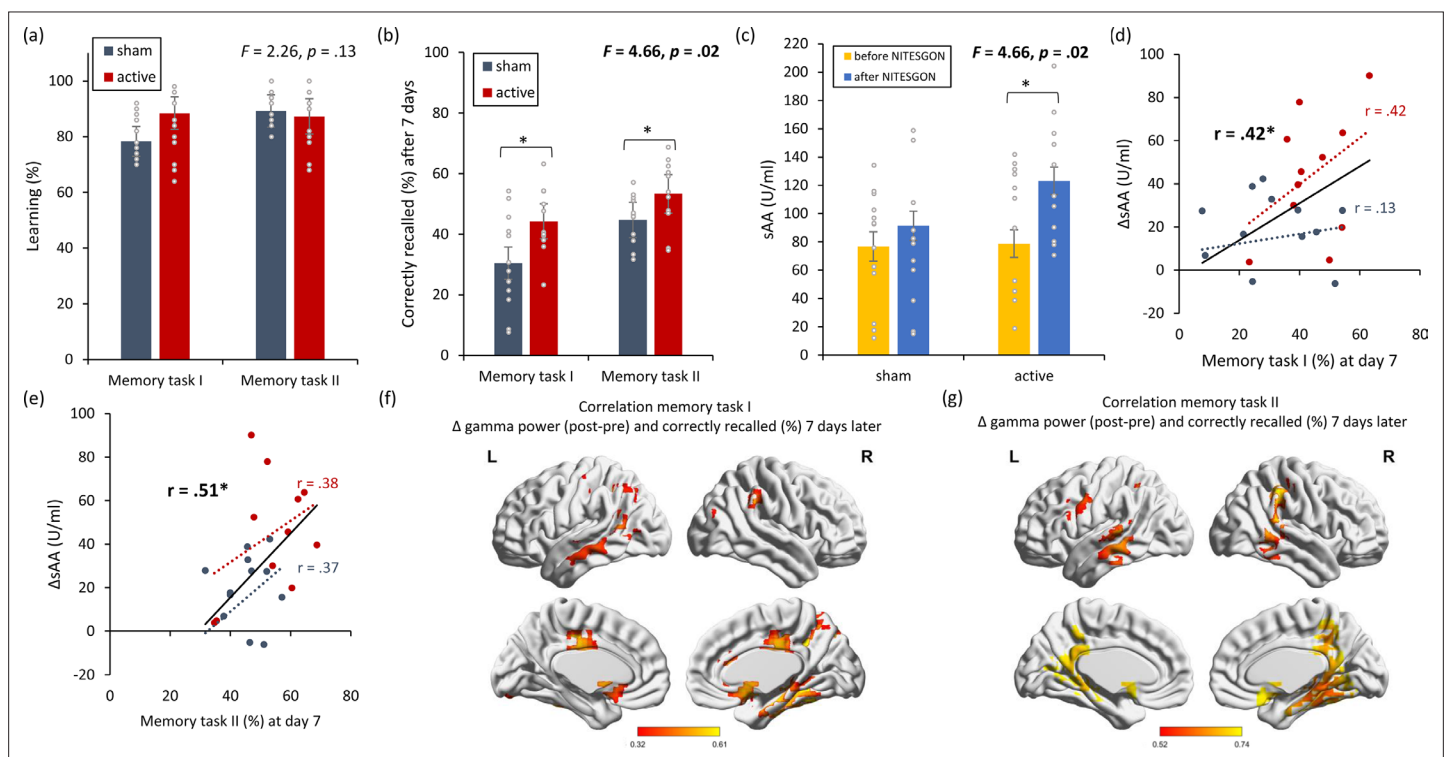


**Figure 3.** Non-invasive transcutaneous electrical stimulation of the greater occipital nerve (NITESGON) has a proactive memory effect – NITESGON during the first task memory with **Figure 3—figure supplement 1**. (a) No difference was observed in the cumulative learning rate between active and sham NITESGON after the study phase for the first task (i.e., word-association task) or second task (i.e., object-location task). (b) NITESGON can improve memory recall 7 days after the study phase for the active relative to the sham group for both the first and second tasks. (c) After NITESGON salivary  $\alpha$ -amylase (sAA) levels increase for active group, but not for sham NITESGON. (d, e) Memory recall 7 days later correlates with the difference in sAA levels during the first visit (pre vs. post study phase) for the first and second tasks. (f, g) Improved memory recall 7 days after stimulation is associated with increased activity in the medial temporal lobe immediately after NITESGON for the gamma frequency band. Error bars, standard error of the mean (s.e.m.). Asterisks represent significant differences (\* $p < 0.05$ ; \*\* $p < 0.01$ ).  $\Delta$ sAA levels are the subtraction of sAA levels before NITESGON from sAA levels immediately after NITESGON.

The online version of this article includes the following figure supplement(s) for figure 3:

**Figure supplement 1.** To avoid the potential outliers would drive the Pearson correlation between a memory recall 7 days after learning the task and the difference in salivary  $\alpha$ -amylase (sAA) levels (difference between before and after stimulation on day 1), a Spearman rank correlation was calculated to cross validate our findings.

same experiment as in Experiment 2 but applied NITESGON during the first task and not during the second task to test the hypothesis that NITESGON can induce a proactive memory effect on the second task although we stimulate during the first task. This would further support the hypothesis that NITESGON induces a long-term memory effect via the mechanism of behavioral tagging through activation of the LC pathway.

On visit 1, no significant difference ( $F = 2.26$ ,  $p = 0.13$ ; see **Figure 3a**) was found between the active and sham groups in regard to how many words or objects participants learned for both the first task (i.e., word-association task) ( $F = 1.60$ ,  $p = 0.22$ ) and the second task (i.e., object-location task) ( $F = 3.30$ ,  $p = 0.08$ ). During the second visit, 7 days after learning the tasks, participants that received active NITESGON ( $F = 4.66$ ,  $p = 0.021$ ; see **Figure 3b**) recalled more words for the first task (i.e., word-association task) ( $F = 6.32$ ,  $p = 0.020$ ) and the second task (i.e., object-location task) ( $F = 4.87$ ,  $p = 0.038$ ) than those who received sham NITESGON, indicating that the active NITESGON group ( $44.27 \pm 10.97$ ) showed significant improvement in comparison to the sham NITESGON group ( $30.46 \pm 15.13$ ) for the word-association task. For the object-location task, the active NITESGON group ( $53.33 \pm 11.29$ ) demonstrated a significant increase in the number of correctly recalled objects-locations than the sham NITESGON group ( $44.17 \pm 7.75$ ). Our data revealed that there was a significant interaction effect for sAA ( $F = 4.66$ ,  $p = 0.021$ ; see **Figure 3c**), denoted by the active group's increase in sAA ( $123.10 \pm 43.63$ ) in comparison to the sham group ( $91.38 \pm 44.67$ ) ( $F = 4.53$ ,  $p = 0.039$ ) immediately after learning. No significant difference ( $F = 0.012$ ,  $p = 0.91$ ) was obtained in sAA for the active group ( $78.72 \pm 47.67$ ) in comparison to the sham group ( $76.77 \pm 39.87$ ) before learning the association tasks. This increase in sAA seen in the active group correlated with how many items they recalled 7 days after the learning phase for both the word-association task ( $r = 0.42$ ,  $p = 0.039$ ; see **Figure 3d**;  $r_s = 0.34$ ,  $p = 0.10$  **Figure 3—figure supplement 1**; a correlation analysis for each group separately) and the object-location task ( $r = 0.51$ ,  $p = 0.012$ ; see **Figure 3e**;  $r_s = 0.54$ ,  $p = 0.007$  **Figure 3—figure supplement 1**). Looking at each group separately, we found no significant correlation for both the active (first task:  $r = 0.42$ ,  $p = 0.20$ ; second task:  $r = 0.38$ ,  $p = 0.25$ ) and sham groups (first task:  $r = 0.13$ ,  $p = 0.21$ ; second task:  $r = 0.37$ ,  $p = 0.22$ ) between memory recall 7 days later and sAA levels on visit 1 (pre vs. post). Memory recollection 7 days after stimulation was associated with increased gamma power in the medial temporal cortex immediately after stimulation for both the first ( $r = 0.32$ ,  $p = 0.037$ ; see **Figure 3f**) and second memory tasks ( $r = 0.52$ ,  $p = 0.012$ ; see **Figure 3g**).

#### Experiment 4. NITESGON during first task – reduced interference effect

Experiments 2 and 3 revealed both retroactive and proactive memory effects 7 days after initial learning of the two tasks. To further explore if NITESGON is linked to behavioral tagging and evaluate if interference impacts NITESGON as the strong stimulus, Experiment 4 removed the object-location task used in Experiments 2 and 3 and replaced it with a Japanese–English verbal associative learning task similar to the Swahili–English verbal associative task. Considering that memory formation and persistence are susceptible to interference occurring pre- and post-encoding (**Crossley et al., 2019**; **McGaugh, 1966**; **Zeithamova and Preston, 2017**) and are heavily influenced by commonality among the learned and intervening stimuli (**Varma et al., 2017**) it is believed that conducting two consecutive, like-minded word-association (i.e., Swahili–English and Japanese–English) tasks will result in one's consolidation process interfering with that of the other (**Robertson, 2012**). Furthermore, research on the synaptic tag-and-capture hypothesis suggests that memory interference is the result of synaptic competition, a proposed 'fight for proteins' that arises between tagged synapses among limited proteins that leads to one memory converting to long-term memory at the expense of the other (**Okuda et al., 2021**). Considering how our previous experiments suggest the effect obtained by NITESGON improves the consolidation of information via behavioral tagging, it is possible that NITESGON on the first task might help reduce the overall interference effect on the second task.

To test the hypothesis, participants participated in two separate word-association tasks (i.e., the Swahili–English and Japanese–English; the order of tasks was randomized across participants) while receiving either active or sham NITESGON during the first task. rsEEG data and sAA were collected immediately before and immediately after the two tasks on visit 1. Two memory tests were taken 7 days after learning both word-association tasks.



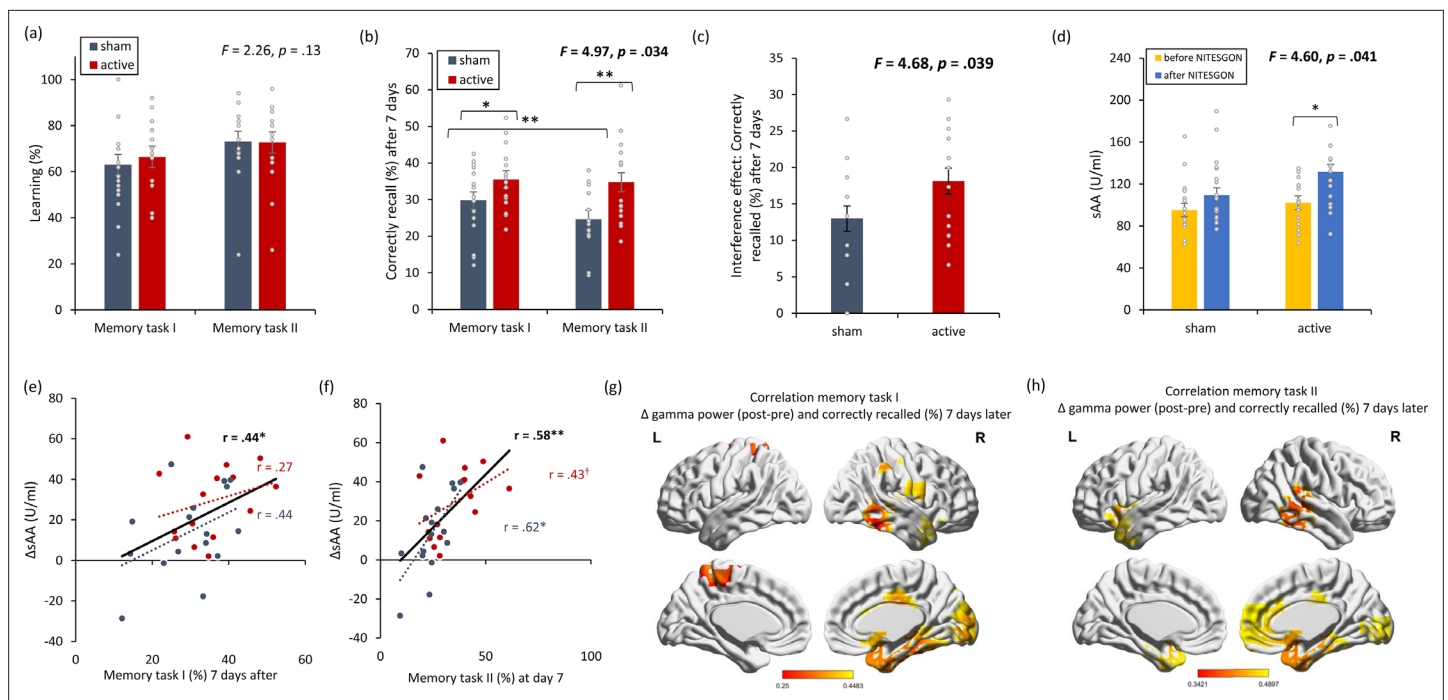


**Figure 4.** Non-invasive transcutaneous electrical stimulation of the greater occipital nerve (NITESGON) reduces the interference effect memory with **Figure 4—figure supplement 1**. (a) No difference was observed in the cumulative learning rate between active and sham NITESGON after the study phase for the first task (i.e., word-association task) or second task (i.e., word-association task). (b) NITESGON can improve memory recall 7 days after the study phase revealing improve in memory for the active relative to the sham group for both the first and second tasks. (c) The interference effect is less present for the active relative to the sham group. (d) After NITESGON salivary  $\alpha$ -amylase (sAA) levels increase for the active group, but not for sham NITESGON. (e, f) Memory recall 7 days later correlates with the difference in sAA levels during the first visit (pre vs. post study phase) for the first and second tasks. (g, h) Improved memory recall 7 days after stimulation is associated with increased activity in the medial temporal lobe immediately after NITESGON for the gamma frequency band. Error bars, standard error of the mean (s.e.m.). Asterisks represent significant differences (\* $p < 0.05$ ; \*\* $p < 0.01$ ),  $\Delta$ sAA levels are the subtraction of salivary  $\alpha$ -amylase levels before NITESGON from salivary  $\alpha$ -amylase levels immediately after NITESGON.

The online version of this article includes the following figure supplement(s) for figure 4:

**Figure supplement 1.** To avoid the potential outliers would drive the Pearson correlation between a memory recall 7 days after learning the task and the difference in salivary  $\alpha$ -amylase (sAA) levels (difference between before and after stimulation on day 1), a Spearman rank correlation was calculated to cross validate our findings.

On visit 1, no significant difference ( $F = 0.84, p = 0.37$ ; see **Figure 4a**) was detected for learning during the first ( $F = 0.27, p = 0.61$ ) and second tasks ( $F = 0.01, p = 0.94$ ) between the active and sham NITESGON groups. Seven days later, during the recall phase, we found a significant interaction effect for recall ( $F = 4.97, p = 0.034$ ; see **Figure 4b**). For both the first ( $F = 3.67, p = 0.048$ ) and the second tasks ( $F = 7.89, p = 0.009$ ), a significant increase in number of words correctly recalled was observed in the active (first task:  $35.51 \pm 8.68$ ; second task:  $34.76 \pm 11.74$ ) compared to the sham group (first task:  $29.80 \pm 9.72$ ; second task:  $24.64 \pm 8.10$ ).

Upon assessment for a potential interference effect, the active group displayed a significant difference in how many words participants were able to recall between the first and the second tasks ( $18.31 \pm 7.03\%$ ) ( $F = 4.68, p = 0.039$ ) in comparison to the sham ( $13.00 \pm 6.65\%$ ), indicating that the interference effect plays less of a role in the active group.

Our data revealed that there was a significant interaction effect for sAA ( $F = 4.60, p = 0.041$ ; see **Figure 4d**). An increase in sAA was observed for the active group ( $123.10 \pm 43.63$ ) in comparison to the sham group ( $91.38 \pm 44.67$ ) ( $F = 4.53, p = 0.039$ ) immediately after the learning. However, no significant difference ( $F = 0.012, p = 0.91$ ) was obtained in sAA for the active group ( $78.72 \pm 47.67$ ) in comparison to the sham group ( $76.77 \pm 39.87$ ) before learning the word-association tasks. This increase in sAA correlates with how many words they recalled 7 days after the learning phase for both the first word-association task ( $r = 0.44, p = 0.014$ ; see **Figure 4e**;  $r_s = 0.35, p = 0.049$  **Figure 4—figure supplement 1**) and the second word-association task ( $r = 0.58, p = 0.001$ ; see **Figure 4f**;  $r_s$

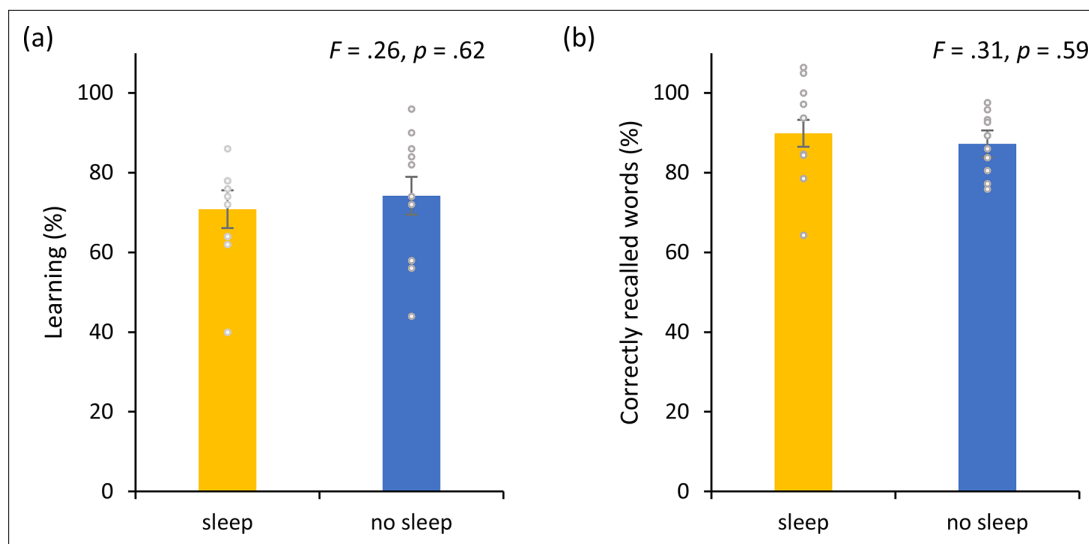


**Figure 5.** Non-invasive transcutaneous electrical stimulation of the greater occipital nerve (NITESGON) and sleep. **(a)** No difference was observed in the cumulative learning rate between participants who had slept versus those who had not slept after NITESGON applied during the study phase. **(b)** Sleep has no effect on memory recall 12 hr after the study phase. Error bars, standard error of the mean (s.e.m.). Asterisks represent significant differences (\* $p < 0.05$ ; \*\* $p < 0.01$ ).

= 0.53,  $p = 0.002$  **Figure 4—figure supplement 1**). Looking at each group separately, we found no significant correlation for either the active ( $r = 0.27$ ,  $p = 0.34$ ) or sham group ( $r = 0.42$ ,  $p = 0.11$ ) between memory recall 7 days later and sAA levels on visit 1 (pre vs. post) for the first task. For the second task, we found a significant correlation for both the active ( $r = 0.43$ ,  $p = 0.098$ ) and sham groups ( $r = 0.62$ ,  $p = 0.010$ ) was obtained between memory recall 7 days later and sAA levels on visit 1 (pre vs. post) for the first task.

Memory recollection 7 days after stimulation was also associated with increased gamma power in the medial temporal cortex immediately after stimulation for both the first ( $r = 0.25$ ,  $p = 0.042$ ; see **Figure 4g**) and second memory tasks ( $r = 0.34$ ,  $p = 0.032$ ; see **Figure 4h**).

### Experiment 5. The effect of NITESGON is not sleep dependent

Our behavioral experiments suggest that NITESGON targeting the LC is involved in synaptic consolidation via the behavioral tagging mechanism. It is assumed that synaptic consolidation occurs over a timespan of minutes to hours after encoding the information, thus this effect is time dependent (**Park, 2005**). Furthermore, prior research has revealed that retroactive memory enhancement (i.e., evidence for behavioral tagging) emerges within 6 hr and is not dependent on sleep (**Dunsmoor et al., 2015**). Based on these previous findings and the assumption that NITESGON modulates synaptic consolidation via the mechanism of behavioral tagging, we hypothesize that sleep would not mediate the memory effect induced by NITESGON.

Experiment 5 compared two groups of participants undertaking a word-association task paired with active NITESGON. One group of participants slept between the word-association task at 8 p.m. and the test phase the next day at 8 a.m., whereas the other group did not sleep between the learning phase at 8 a.m. and the test phase that took place at 8 p.m. that same day. A comparison between the two groups revealed no significant difference in the number of words learned during the learning phase ( $F = 0.26$ ,  $p = 0.62$ ; see **Figure 5a**) as well as no significant difference between the two groups when tested 12 hr later ( $F = 0.31$ ,  $p = 0.59$ ; see **Figure 5b**). Participants who slept in-between the learning and test phase correctly recalled  $89.99 \pm 13.09\%$  of word pairs and participants who did not sleep in-between the learning and test phase correctly recalled  $87.23 \pm 7.41\%$  of word pairs.

### Experiment 6. LC – hippocampus activity and connectivity

In addition to our behavioral experiments confirming the hypothesis that NITESGON targeting the LC is involved in memory consolidation via the behavioral tagging mechanism, Experiment 5 revealed that sleep does not mediate the effect generated by NITESGON. Here, in the second set of experiments,

we explored the brain network modulated by NITESGON and investigated the potential underlying neural mechanism.

The hippocampus is the key brain area that has been associated with synaptic memory consolidation. This area receives neuromodulatory input from multiple brain regions that regulate synaptic plasticity, such as the LC and the ventral tegmental area (VTA). Both brain areas enhance retention of everyday memories in the hippocampus (Takeuchi et al., 2016). Moreover, animal research identified the VTA and the LC as regulators of hippocampal-dependent long-term memory formation due to their role in regulating the synthesis of new proteins required during the behavioral tagging process, therefore allowing for the consolidation of lasting memories (Moncada, 2017). However, recent studies have shown that the VTA projections to the hippocampus are scarce, while the LC projections are abundant (Takeuchi et al., 2016; Kempadoo et al., 2016; McNamara et al., 2014). Therefore, the VTA may only play a limited role in late-phase LTP (Takeuchi et al., 2016; Kempadoo et al., 2016; McNamara et al., 2014), whereas the LC is conceivably the primary source of synaptic modulation responsible for tuning cells in the hippocampus (Kempadoo et al., 2016). Additionally, several previous observations have shown electrical and pharmacological stimulation of the LC modulated hippocampal synaptic transmission (Lemon and Manahan-Vaughan, 2012; Devoto and Flore, 2006), whilst modulation of the VTA did not significantly mediate synaptic transmission but rather suggest a greater role in salience and motivational drive underlying emotion-based learning (Kempadoo et al., 2016; Devoto and Flore, 2006).

We conducted a resting-state functional connectivity magnetic resonance imaging study to verify the relationship between changes in the LC and hippocampus as well as the VTA and hippocampus. We hypothesized that participants who received active NITESGON would show increased activity in the LC and hippocampus, but not in the VTA, and increased functional connectivity between the LC and hippocampus, but not between the VTA and hippocampus. We scanned in three consecutive blocks: immediately before, during, and immediately after stimulation. NITESGON was applied at a constant current of 1.5 mA for 20 min via electrodes placed over the left and right C2 nerve dermatome.

The regional amplitude of low-frequency fluctuations (rALFF) was inspected to verify if NITESGON evoked activity changes in the LC, VTA, and hippocampus. Our findings showed a significant effect for the LC ( $F = 4.34$ ,  $p = 0.023$ ), VTA ( $F = 3.42$ ,  $p = 0.047$ ) and hippocampus ( $F = 3.52$ ,  $p = 0.044$ ) when comparing the active and control groups (see Figure 6a–c). For both the LC and hippocampus, a significant increase was obtained during (LC:  $13.18 \pm 4.18$  vs.  $8.77 \pm 2.88$ ;  $F = 11.30$ ,  $p = 0.002$ ; hippocampus:  $6.30 \pm 3.55$  vs.  $4.50 \pm 2.88$ ;  $p = 0.045$ ) and after (LC:  $13.78 \pm 6.21$  vs.  $6.71 \pm 2.79$ ;  $p < 0.001$ ; hippocampus:  $7.17 \pm 4.61$  vs.  $4.33 \pm 1.44$ ;  $p = 0.031$ ) stimulation for the active group in comparison to the sham group. Before stimulation, no significant difference was obtained between the active and sham groups (LC:  $9.40 \pm 4.50$  vs.  $8.98 \pm 1.92$ ;  $p = 0.76$ ; hippocampus:  $5.26 \pm 2.20$  vs.  $5.50 \pm 1.64$ ;  $p = 0.75$ ). For the VTA, a significant increase was obtained during ( $20.01 \pm 5.90$  vs.  $14.12 \pm 5.34$ ;  $p = 0.008$ ) stimulation for the active group in comparison to the sham group. Before ( $14.96 \pm 4.50$  vs.  $14.96 \pm 1.92$ ;  $p = 0.99$ ) or after ( $15.33 \pm 4.98$  vs.  $15.46 \pm 13.86$ ;  $p = 0.97$ ) stimulation, no significant difference was obtained between the active and sham groups. To further confirm our data, we replicated our analysis by not including a smoothing kernel, showing similar results for the LC, VTA, and hippocampus. Furthermore, we included two control areas, the left inferior parietal cortex, where we do not expect to see any changes (see Figure 6—figure supplement 1).

Furthermore, a regions of interest (ROI)-to-ROI analysis demonstrated an effect between the right hippocampus and LC ( $F = 3.67$ ,  $p = 0.039$ ), but not between the right hippocampus and VTA ( $F = 0.27$ ,  $p = 0.76$ ) (see Figure 1d,e). Additionally, an increase in LC connectivity strength with the right hippocampus was seen for the active group relative to the sham group during ( $0.052 \pm 0.03$  vs.  $0.018 \pm 0.06$ ;  $F = 4.34$ ,  $p = 0.047$ ) and after stimulation ( $0.06 \pm 0.05$  vs.  $-0.011 \pm 0.05$ ;  $F = 15.25$ ,  $p = 0.001$ ). However, no significant effect was obtained between the LC and right hippocampus for the active group relative to the sham group before stimulation ( $0.008 \pm 0.08$  vs.  $0.015 \pm 0.03$ ;  $F = 0.09$ ,  $p = 0.76$ ).

## Experiment 7. Potential relationship between NITESGON-LC and dopamine

The previous experiment revealed activity changes in both the LC and hippocampus as well as increased connectivity between the LC and hippocampus both during and after NITESGON. Conversely, the

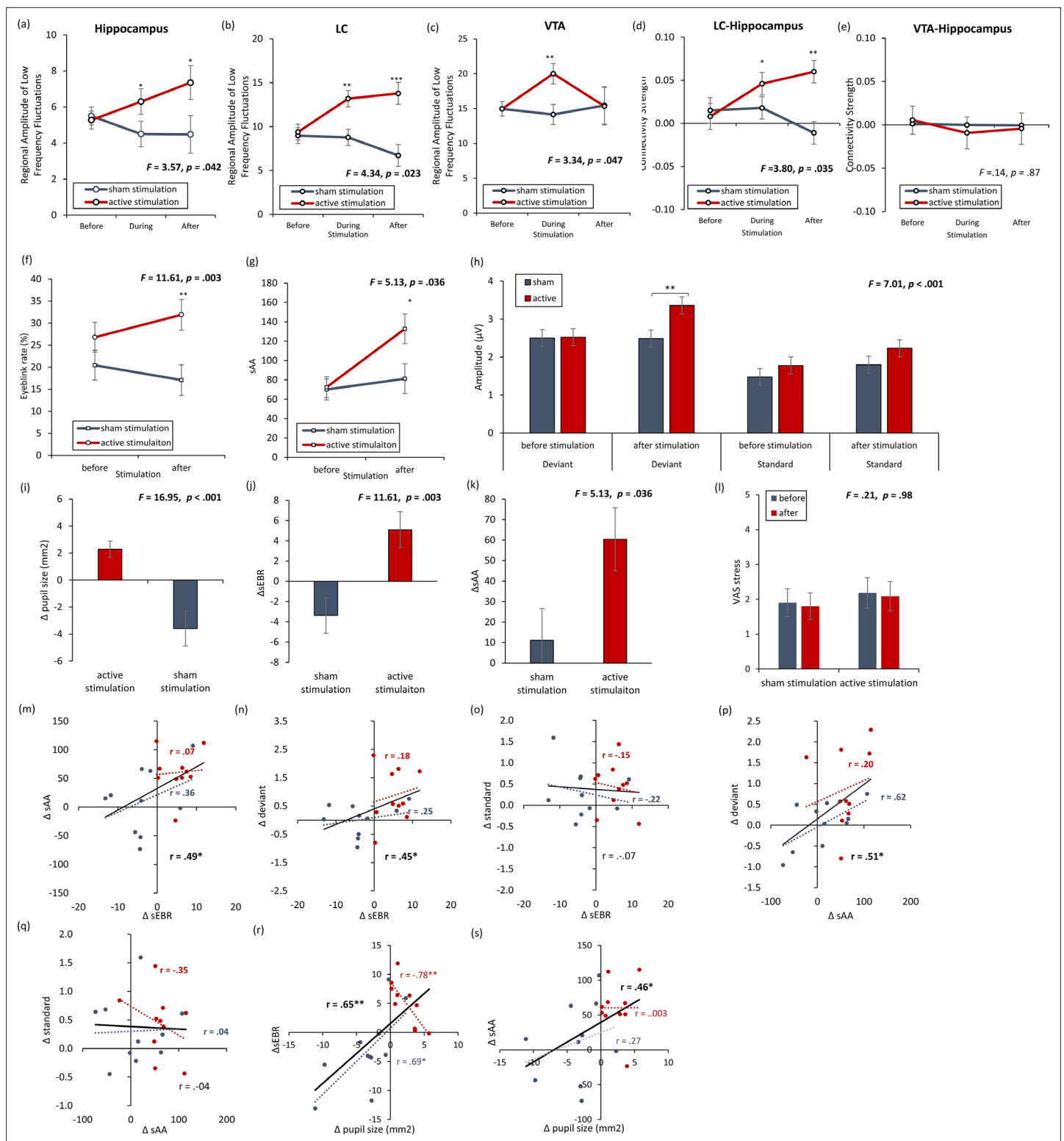


**Figure 6.** rsfMRI and physiology – locus coeruleus and dopamine with **Figure 6—figure supplement 1.** (a, b) The locus coeruleus and hippocampus revealed increased activity during stimulation as well as after stimulation for the active non-invasive transcutaneous electrical stimulation of the greater occipital nerve (NITESGON) group in comparison to the sham NITESGON group. (c) The ventral tegmental area revealed increased activity during stimulation, but not after stimulation for the active NITESGON group in comparison to the sham NITESGON group. (d) Increased connectivity between the locus coeruleus and hippocampus was observed during and after stimulation for the active NITESGON group in comparison to the sham NITESGON group. (e) No significant difference in connectivity between the ventral tegmental area and hippocampus was observed when comparing

Figure 6 continued on next page

## Figure 6 continued

the active and sham NITESGON groups during or after stimulation. **(f, g)** A significant increase in spontaneous eye blink rate and salivary  $\alpha$ -amylase (sAA) was observed after active NITESGON in comparison to sham NITESGON. **(h)** A significant increase in peak-to-peak amplitude over the left parietal electrode side was observed for the active group in comparison to the sham group for the deviant after stimulation. **(i–l)** A significant difference when subtracting pupil size, eyeblink rates,  $\alpha$ -amylase, and the visual analogues scale for stress before NITESGON from immediately after NITESGON showed a significant increase for pupil size, eyeblink rates,  $\alpha$ -amylase, but not for the VAS. **(m,n, j)** A positive correlation was observed between the difference (post–pre) in spontaneous eye blink rate and the difference in sAA as well as between the difference in spontaneous eye blink rate and the difference in peak-to-peak amplitude for the deviant. **(o)** No significant correlation was observed between the difference in spontaneous eye blink rate and the difference in peak-to-peak amplitude for the standard. **(p)** A positive correlation was observed between the difference in sAA and the difference in peak-to-peak amplitude for the deviant. **(q)** No correlation was observed between the difference in sAA and the difference in peak-to-peak amplitude for the standard. **(r, s)** A positive correlation was observed between the difference (post–pre) in spontaneous eye blink rate and the difference in pupil sizes as well as between the difference in sAA and the difference pupil size. Error bars, standard error of the mean (s.e.m.). Asterisks represent significant differences (\* $p < 0.05$ ; \*\* $p < 0.01$ ; \*\*\* $p < 0.001$ ).  $\Delta$  the subtraction of rate/levels before NITESGON from sAA levels immediately after NITESGON.

The online version of this article includes the following figure supplement(s) for figure 6:

**Figure supplement 1.** To verify if smoothing had an effect on the outcome, we recalculated the regional amplitude of low-frequency fluctuations without including a smoothing kernel was inspected to verify if non-invasive transcutaneous electrical stimulation of the greater occipital nerve (NITESGON) evoked activity changes in the locus coeruleus (LC), ventral tegmental area (VTA) and hippocampus.

VTA did not show changes in activity after stimulation or connectivity changes between the VTA and hippocampus during or after stimulation. However, activity changes in the VTA during NITESGON were detected. Previous animal research has identified selective neuronal connections between the LC and VTA, implying an interaction between the LC and VTA during NITESGON may exist (Sara, 2009).

A key neuromodulator in memory consolidation is dopamine (DA) (Takeuchi et al., 2016). DA affects plasticity, synaptic transmission, and network activity in the hippocampus, and plays a critical role for hippocampal-dependent mnemonic processes by selectively enhancing consolidation of memory information (Duszkiewicz et al., 2019). Recent literature suggests a direct link between DA and the synaptic tag-and-capture hypothesis – the mechanism underlying behavioral tagging (Redondo and Morris, 2011). The core of the synaptic tag-and-capture hypothesis indicates that memory encoding creates the potential of long-term memory by creating a tag to be captured at a later stage (i.e., during memory consolidation) by protein synthesis-dependent LTP. Suggestions are made that the signal transduction processes catalyzing this synthesis of plasticity-related proteins require DA to stabilize new memories (Morris and Frey, 1997; Frey and Morris, 1997). Previous research has identified a DA agonist's ability to chemically induce LTP specifically on synapses that are activated by test stimulation, but not those that are silent (Redondo et al., 2010), whereas a DA antagonist reduces the memory effect 24 hr after learning (Wang et al., 2010), thus indicating that DA is central to the synaptic tag-and-capture hypothesis, and hence behavioral tagging (Redondo and Morris, 2011).

To regulate synaptic plasticity, the hippocampus receives dopaminergic input from the VTA and the LC (Takeuchi et al., 2016; Sara, 2009; Kempadoo et al., 2016; Duszkiewicz et al., 2019; Rosen et al., 2015; Lisman and Grace, 2005). However, recent research revealed that mainly LC DA mediates post-encoding memory enhancement in the hippocampus, while the VTA does not respond to arousal (i.e., novelty) (Takeuchi et al., 2016; Kempadoo et al., 2016). Animal research revealed that electrical stimulation of the LC increased DA levels and modulated hippocampal synaptic transmission (Takeuchi et al., 2016; Lemon and Manahan-Vaughan, 2012; Devoto and Flore, 2006). Furthermore, animal studies identified activation of the LC via optogenetic stimulation caused more LTP-related memory consolidation 45 min after stimulation (Takeuchi et al., 2016; Lemon and Manahan-Vaughan, 2012; Devoto and Flore, 2006). This could potentially explain why NITESGON applied while learning a memory task generated a long-term memory effect but did not modify immediate learning (Luckey et al., 2020; Vanneste et al., 2020).

A proxy for DA is spontaneous eye blink rate (sEBR), or the frequency of blinks per unit of time (Jongkees and Colzato, 2016). Pharmacological studies in animals and humans have shown that DA agonists elevate sEBR, whereas DA antagonist suppresses sEBR (Jongkees and Colzato, 2016; Kleven and Koek, 1996; Karson, 1983; Cavanagh et al., 2014; Elsworth et al., 1991; Jutkiewicz and Bergman, 2004; Kaminer et al., 2011; Groman et al., 2014). Moreover, sEBR is altered in clinical conditions that are associated with dysfunctions of the dopaminergic system (Chen et al., 1996).



sAA, pupil size as well as neurophysiology (event-related potentials, ERP) are common proxies for LC-NA activity. More specifically, pupil diameter indexes LC activity in both monkeys and humans (Menétrey and Basbaum, 1987), findings confirmed by intracranial recording and pharmacological challenge studies (Kawai, 2018). Neurophysiology utilizes the P3b ERP, which peaks at 300–600 ms after a task-relevant stimulus (Sutton et al., 1965; Polich, 2007), to indirectly measure LC-NA activity, thus presenting us with a strong cortical electrophysiological correlate of the LC-NA response (Nieuwenhuis et al., 2005). Using an auditory oddball task, a standard P3b-evoking task, NITESGON increased peak and mean amplitude between 300 and 600 ms immediately after stimulation for the left parietal electrode site. Therefore, we hypothesized that NITESGON would induce an increase in DA; shown via an increase in sEBR that would correlate with pupil diameter, sAA, and amplitude of the P3b after the application of NITESGON. sAA, sEBR, and ERP were collected immediately before and immediately after 20 min of NITESGON was administered.

Results showed a significant interaction effect for sEBR by condition ( $F = 11.61$ ,  $p = 0.003$ ; see Figure 6f), indicating that the active group ( $31.90 \pm 10.90$ ) had an increase in sEBR in comparison to a sham group ( $17.08 \pm 11.07$ ;  $F = 9.10$ ,  $p = 0.007$ ) after NITESGON. Before NITESGON no significant difference ( $F = 1.77$ ,  $p = 0.20$ ) was observed in the active group ( $26.80 \pm 8.24$ ) relative to the sham group ( $20.45 \pm 12.63$ ) in sEBR. Also, a significant interaction effect for sAA by condition ( $F = 5.13$ ,  $p = 0.036$ ; see Figure 6g) was obtained, revealing a significant increase in sAA ( $F = 5.67$ ,  $p = 0.028$ ) after stimulation for the active group ( $132.82 \pm 51.23$ ) in comparison to the sham group ( $81.22 \pm 45.43$ ). No significant difference ( $F = 0.023$ ,  $p = 0.88$ ) was obtained when comparing the active group ( $72.42 \pm 43.77$ ) versus the sham group ( $70.10 \pm 19.93$ ) before stimulation. Peak-to-peak amplitude analysis for P3 electrode further showed a significant effect ( $F = 7.01$ ,  $p < 0.001$ ; see Figure 6h). An effect was revealed between active NITESGON and sham NITESGON after stimulation ( $t = 2.64$ ,  $p = 0.01$ ). In addition, a significant effect was shown for active NITESGON after stimulation in comparison to before stimulation ( $t = 2.75$ ,  $p = 0.007$ ). A positive correlation was obtained between the difference in sEBR, and sAA (overall:  $r = 0.49$ ,  $p = .029$ ; active group:  $r = 0.07$ ,  $p = 0.85$ ; sham group:  $r = 0.36$ ,  $p = 0.30$ ; see Figure 6m), peak-to-peak amplitude for deviant (overall:  $r = 0.45$ ,  $p = 0.048$ ; active group:  $r = 0.18$ ,  $p = 0.62$ ; sham group:  $r = 0.25$ ,  $p = 0.49$ ; see Figure 6n), but not peak-to-peak amplitude for standard (overall:  $r = -0.07$ ,  $p = 0.76$ ; active group:  $r = -0.15$ ,  $p = .69$ ; sham group:  $r = -0.22$ ,  $p = 0.55$ ; see Figure 6o), respectively, after NITESGON relative to before. The subtraction scores for the sEBR ( $F = 11.61$ ,  $p = 0.003$ ; Figure 6j) and sAA ( $F = 5.13$ ,  $p = 0.036$ ; Figure 6k), revealed a significant

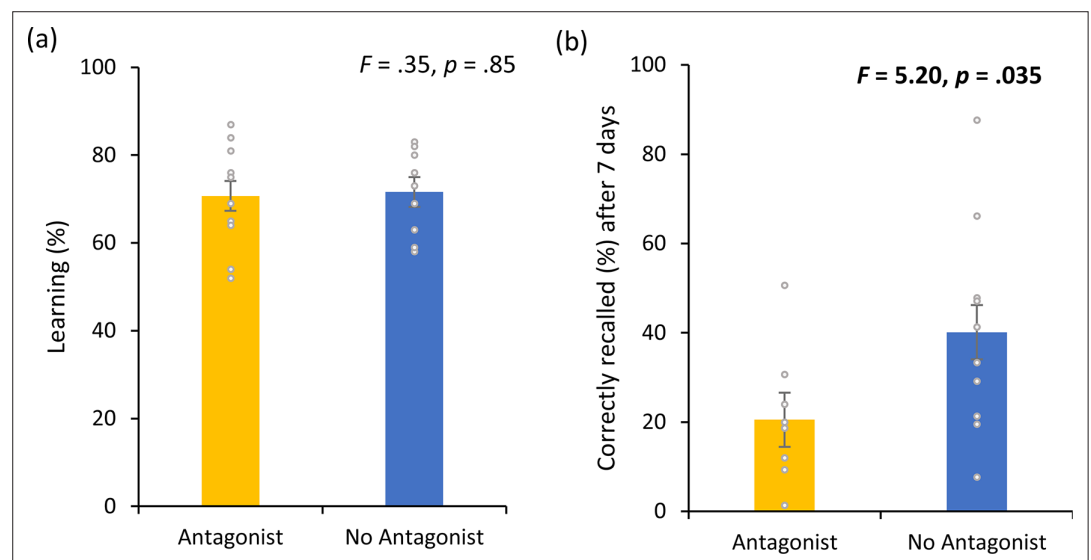


**Figure 7.** Dopamine experiment. (a) No difference was observed in the cumulative learning rate after non-invasive transcutaneous electrical stimulation of the greater occipital nerve (NITESGON) for participants who were taking a dopamine (DA) antagonist in comparison to participants who were not taking a DA antagonist. (b) A significant difference was observed in the number of recalled words after 3 or 4 days for participants who were taking a DA antagonist in comparison to participants who were not taking a DA antagonist. Error bars, standard error of the mean (s.e.m.). Asterisks represent significant differences (\* $p < 0.05$ ; \*\* $p < 0.01$ ).

difference between the active and the sham group further indicating a stimulation-induced increase in sEBR and sAA. Also, a significant correlation was obtained between sAA and peak-to-peak amplitude for deviant (overall:  $r = 0.51$ ,  $p = 0.022$ ; active group:  $r = 0.20$ ,  $p = .58$ ; sham group:  $r = 0.62$ ,  $p = .054$ ; see **Figure 6p**), but not with peak-to-peak amplitude for standard (overall:  $r = -0.04$ ,  $p = 0.87$ ; active group:  $r = -0.35$ ,  $p = 0.32$ ; sham group:  $r = 0.04$ ,  $p = 0.91$ ; see **Figure 6q**).

As previous research already showed that pupil size is an important proxy for LC mediate activity, we also look at pupil size. Our data show that a significant difference in pupil size after stimulation with baseline correction for active stimulation ( $2.28 \pm 1.90$ ) in comparison to sham ( $-3.59 \pm 4.80$ ) stimulation ( $F = 16.95$ ,  $p = 0.001$ ; see **Figure 6i**). Furthermore, a significant positive correlation was between pupil size and sEBR (overall:  $r = 0.65$ ,  $p = 0.002$ ; active group:  $r = -0.78$ ,  $p = 0.008$ ; sham group:  $r = 0.69$ ,  $p = 0.029$ ; see **Figure 6r**) and between pupil size and sAA (overall:  $r = 0.46$ ,  $p = 0.042$ ; active group:  $r = 0.003$ ,  $p = 0.99$ ; sham group:  $r = 0.27$ ,  $p = 0.45$ ; see **Figure 6s**).

## Experiment 8. Dopamine

Seeing that previous research identifies DA's vital role in memory consolidation, and NITESGON generates its effect during memory consolidation, it would be expected that blocking the DA receptor with a DA antagonist would have a direct impact on memory consolidation. To test this hypothesis, and confirm previous findings, Experiment 8 conducted the recall-only memory test 3–4 days after initial learning of the word-association task. We used the same setup as Experiment 1, whereby NITESGON was applied immediately after learning the word-association task during visit 1.

No significant effect ( $F = 0.04$ ,  $p = 0.85$ ; see **Figure 7a**) was obtained between the participants who took a DA antagonist ( $71.60 \pm 9.18$ ) and those who did not take a DA antagonist ( $70.70 \pm 12.04$ ) during the learning phase on visit 1. 7 days after learning the word associations, participants who took a DA antagonist ( $20.53 \pm 13.32$ ) performed worse on correctly recalling words in comparison to participants who did not take a DA antagonist ( $40.12 \pm 23.68$ ) ( $F = 5.20$ ,  $p = 0.035$ ; see **Figure 7b**).

## Blinding

To determine if the stimulation was well blinded, all participants in Experiments 1–7 were asked to guess if they thought they were placed in the active or control group (i.e., what stimulation participants received compared to what participants expected). Our findings demonstrated that participants

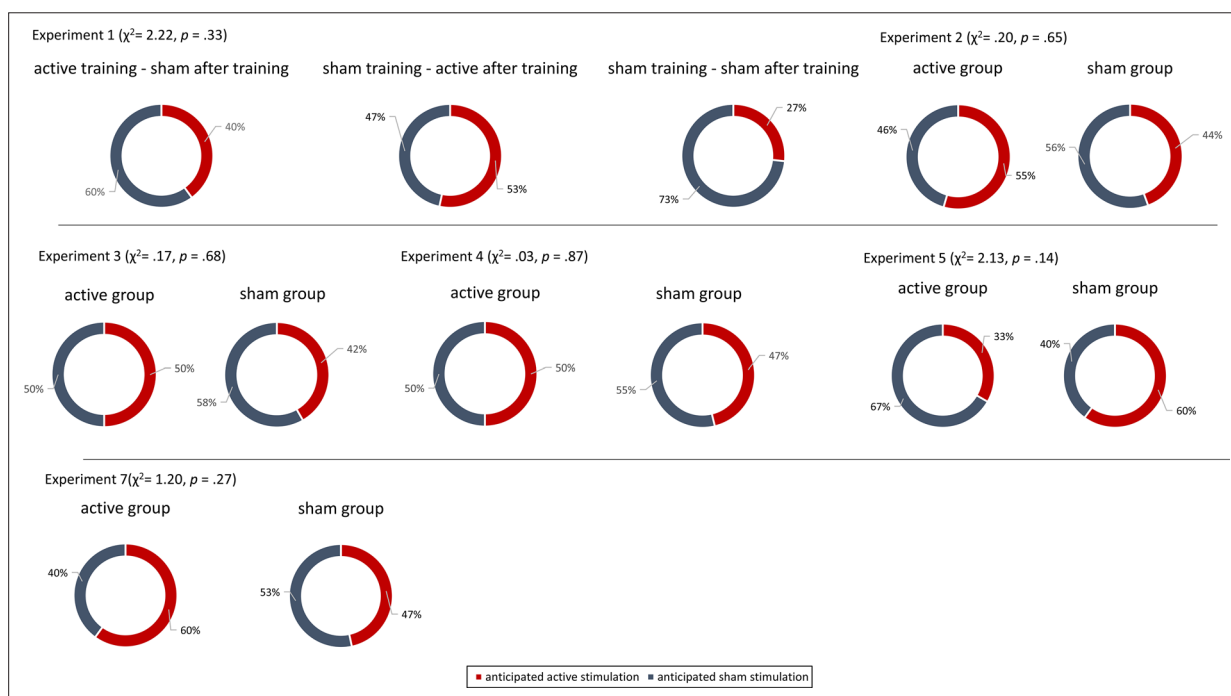


**Figure 8.** Blinding experiments. For Experiments 1–7, no difference was observed between the active and sham groups' anticipation of receiving active or sham stimulation.



could not accurately determine if they were assigned to the active or sham NITESGON group in each experiment, suggesting that our sham protocol is reliable and well blinded (see **Figure 8**).

## Discussion

Taken together, our experiments support the hypothesis that NITESGON targeting the LC strengthens hippocampal memories via the behavioral tagging mechanism. NITESGON increases activity in the LC and hippocampus during and immediately after stimulation and increases connectivity between these two areas, thus instigating initial memory consolidation and increasing the retention of memories that are formed within a window of opportunity spanning before and after LC activation. This is in accordance with the construct of behavioral tagging, which explains how memories that would normally be forgotten will endure in memory preceding, during, and following activation of the LC pathway (**Lemon and Manahan-Vaughan, 2012; McGaugh, 2004; Cahill and McGaugh, 1998**).

Notably, NITESGON does not generate an immediate memory effect during learning, however, a favorable behavioral effect is seen 7 days after initial learning. Although previous research has suggested that millisecond pairing between nerve stimulation and auditory or motor learning is essential to induce targeted plasticity (**Engineer et al., 2011; Marks et al., 2018; Conlon et al., 2020**), our data revealed that this design may not be as crucial as previously thought. This is comparable to the concept of behavioral tagging which suggests that there is a critical time window before and after training to transform a weak memory into a strong memory (**Moncada et al., 2015**). Our findings revealed that NITESGON induced a proactive and retroactive memory effect. More intriguingly, when we introduced a second word-association task (e.g., Japanese–English) that was highly anticipated to interfere with another word-association task (e.g., Swahili–English), we found that NITESGON diminished the interference effect. Interestingly, within the synaptic tag-and-capture literature, memory interference has been proposed to be the result of synaptic competition, a proposed ‘fight for proteins’ that arises between tagged synapses among limited proteins that leads to one memory converting to long-term memory at the expense of the other (**Okuda et al., 2021**). Therefore, it could be postulated that NITESGON could enable optimal availability of plasticity-related proteins, thus decreasing synaptic competition and subsequent interference. However, further investigations are needed to support this postulation. Moreover, this effect induced by NITESGON did not appear to be task specific given that we saw an advantageous effect for both spatial-navigation and word-association tasks. This suggests a generalized memory enhancement effect similar to prior studies of post-encoding increases in consolidation via the LC due to inducing stress and arousal (**McGaugh, 2004; Cahill and McGaugh, 1998; Kalbe and Schwabe, 2022**).

Previous research demonstrated that LC discharge enhances synchronization of gamma activity in the hippocampus in rats (**Hajós et al., 2003**) and that gamma oscillations play an important role in long-term memories and could potentially predict subsequent recall (**Osipova et al., 2006; Sederberg et al., 2003**). Our results confirm this by revealing that NITESGON induces gamma changes in the medial temporal lobe that correlate with successful recall.

The role of the LC–NA system in synaptic plasticity and molecular memory consolidation has been well established over the past decades (**Sara, 2009; Sara, 2015**). However, recent animal studies on enhancement of memory persistence have found that LC tyrosine-hydroxylase neurons, originally defined by their canonical NA signaling, mediate post-encoding enhancement of memory in a manner consistent with possible corelease of DA from the LC axons in the hippocampus (**Takeuchi et al., 2016; Kempadoo et al., 2016; McNamara et al., 2014**). Interestingly, electrical stimulation of the LC increases DA levels that modulate hippocampal synaptic transmission up to 30 min after encoding (**Takeuchi et al., 2016; Lemon and Manahan-Vaughan, 2012; Devoto and Flore, 2006**). Our results corroborate these findings, indicating that utilizing a DA antagonist can reduce the effect of NITESGON and that sEBR, a proxy for DA, increases after NITESGON. In addition, we demonstrated changes in sAA immediately after NITESGON that correlate with memory recall 7 days later overall (including both active and sham groups). However, if we only looked at the active group, we need to be nuanced these findings as sAA levels immediately after NITESGON did not correlate with memory recall 7 days later for every experiment. Previous research indicated that  $\alpha$ -amylase is a marker of endogenous NA activity, with human functional magnetic resonance imaging (fMRI) showing LC activity rising concomitantly with sAA levels during the viewing of emotionally arousing

slides (*van Stegeren et al., 2007*). However, original research on amylase secretion indicates that  $\alpha$ -amylase is mediated by both DA in addition to NA (*Sundström et al., 1985*).

A prevailing hypothesis is that hippocampus-dependent memory is mediated by a subiculum–accumbens–pallidum–VTA pathway via DA (*Rossato et al., 2009*). Our results indicated that the VTA was activated during NITESGON, however, the VTA activation ceased post-stimulation. No increased connectivity was revealed between the VTA and hippocampus during or after NITESGON. This corresponds with recent research that suggests hippocampal projections in the VTA are sparse (*Takeuchi et al., 2016; Kempadoo et al., 2016; McNamara et al., 2014*) and therefore may only have a limited role in late-phase LTP (*Takeuchi et al., 2016; Kempadoo et al., 2016; McNamara et al., 2014*). However, it is possible that the VTA indirectly contributes to the formation of memories via other brain areas. Recent animal research has suggested that VTA DA neurons project to the amygdala and may contribute to fear memory in addition to the LC (*Tang et al., 2020; Giustino et al., 2020*), and that the VTA may contribute to synaptic consolidation independently and complementary to the LC (*Moncada, 2017*). Additionally, it is well known that the amygdala is not the final place of memory storage, but rather has major modulatory influences on the strength of a memory (*McGaugh, 2000*). Similar to the VTA in the current study, prior research has shown that the amygdala is activated during NITESGON but ceased post-stimulation; however, NITESGON was not accompanied by a task during the experiment (*Vanneste et al., 2020*). Moreover, a recent fMRI study spotlights the dynamic behavior of the LC during arousal-related memory processing stages whereby emotionally arousing stimuli triggered engagement from the LC and the amygdala during encoding; however, during consolidation and recollection stages, activity shifted to more hippocampal involvement (*Jacobs et al., 2020*). Considering the impact of the VTA and amygdala can have on memory, future experimental investigations are needed to establish their role in the memory-enhancing effects of NITESGON. One note, is that we need to be careful with the results of the LC, as this area is notoriously difficult to image due to its small size (~1–2 mm across in humans) and susceptibility to MR signal artifacts from cardiac pulsation and partial volume effects from the fourth ventricle (*Astafiev et al., 2010*). Therefore, we re-analyzed our data using no smoothing to better approximate the size of the LC, showing similar results.

Although our results reflect the putative tag-and-capture mechanism, several emotional arousal and/or noradrenergic-related frameworks may explain advantages during the consolidation phase that lead to memory enhancement effects that were observed (*Sara, 2015; McGaugh, 2013; Aston-Jones and Cohen, 2005; Mather and Harley, 2016; Nielson et al., 2005*); therefore, future research needs to be conducted to determine whether behavioral tagging explains the behavioral effects shown here. The observation supports the theory that the effect of NITESGON generated during memory consolidation were not seen immediately, but were observed 7 days later and were not affected by sleep when observed at the 12 hr mark. This is analogous to studies showing that arousal-mediated consolidation effects are time dependent but less dependent on sleep (*Park, 2005*).

When interpreting the current findings, it must be considered that some limitations exist within the research; limitations on experimental design are noted below, followed by a discussion of utilizing indirect proxy measures. The task order for Experiment 4 was randomized during the first visit for training and the recall-only memory test 7 days later; however, the word-association and spatial-navigation task used in Experiments 2 and 3 were not counterbalanced; therefore, the findings of Experiments 2 and 3 could have been impacted by a potential order effect. Additionally, in Experiment 5, the learning and test phases for the two groups were conducted at different times of day (i.e., sleep group: training at 8 p.m. and testing at 8 a.m., sleep deprivation group: training at 8 a.m. and testing at 8 p.m.), thus introducing the potential for circadian effects between the two groups. Furthermore, the recall-only memory testing occurred at the 12 hr point rather than 7 days later, allowing us to conclude that the observed effect seen 12 hr later was not affected by sleep; however, it remains unclear whether the 7-day long-term memory effects of NITESGON are sleep dependent. Moreover, it must also be acknowledged that Experiments 5 and 8 did not include a control-sham stimulation group, thus limiting the interpretation of these two experimental findings. Control-sham stimulation groups would increase our confidence in our findings that NITESGON's memory-enhancing effects depend not on sleep but on DA receptor activity.

Although the use of indirect proxy measures, such as sAA for NA activity and sEBR for DA activity, enabled the tracking of LC–NA activity changes from baseline measurements and demonstrated the potential of an LC–DA relationship, caution must be advised when interpreting results considering

these proxy measures are affiliated with limitations, such as being substantially variable, as well as the potential of other brain regions and monoamine neurotransmitters being associated with changes seen in sAA concentration levels (Jones *et al.*, 2020), an enzyme that is provoked by both central parasympathetic and sympathetic nervous system activation, including acute stress responses (Nater and Rohleder, 2009). Additionally, although sEBR has been increasingly linked to DA, it has been defined as a more viable measure of striatal DA activity (Jongkees and Colzato, 2016; Ortega *et al.*, 2022). At the same time, our research suggests that sEBR and DA are related as well as with the peak-to-peak amplitude for deviant and pupil size suggesting a possible common underlying mechanism. Yet, these results can only be obtained at a group level including both the active and the sham group. Lastly, it must be recognized that the effects of NITESGON obtained could be explained by activating other neuromodulatory mechanisms. Previous animal research indicates that peripheral nerve stimulation, such as vagus nerve stimulation, also activates the dopaminergic (Brougher *et al.*, 2021; Perez *et al.*, 2014), serotonergic (Hulseley *et al.*, 2019), and cholinergic (Hulseley *et al.*, 2016) pathways, all of which play an essential role in inducing long-term plasticity changes related to memory consolidation (Avery and Krichmar, 2017). Further studies regarding the role of additional neuromodulators would be worthwhile.

In conclusion, our work provides evidence that NITESGON is involved in the consolidation of information rather than encoding. Our findings support an implication previously put forward in the formulation of the synaptic tag-and-capture mechanism proposing late-phase LTP of synaptic activity could explain enhanced memories. As deficits in episodic memory specifically related to memory consolidation are one of the earliest detectable cognitive abnormalities in amnesic mild cognitive impairment and AD (Yau *et al.*, 2015; Weston *et al.*, 2018; Wearn *et al.*, 2020), NITESGON might have the potential of improving memory recall by hampering the disruption of memory consolidation.

## Methods

All experiments were designed as a prospective, double-blinded, placebo-controlled, randomized parallel-group study where the researcher and the participant were blinded to the stimulation conditions. Experiment 6 was alone a single-blinded study where the participant was blinded to the stimulation condition, but not the researcher. All experiments were in accordance with the ethical standards of the Declaration of Helsinki. Experiments 1–7 were approved by the Institutional Review Board at the University of Texas at Dallas (#15-06; #17-08; #17-34; #17-84; #17-96; #18-144). All participants signed a written informed consent and consent to publish was obtained.

In all experiments, direct current was transmitted via a saline-soaked (1.3% saline) pair of synthetic sponges (5 × 7 cm) and was delivered by a specially developed, battery-driven, constant current stimulator with a maximum output of 10 mA (Eldith; <http://www.neuroconn.de>). For each participant receiving NITESGON, the anodal electrode was placed over the left C2 nerve dermatome and the cathodal electrode was placed over the right C2 dermatome. To maintain consistency across all participants, research assistants were trained to map out the placement according to the length of the participant's head.

To minimize skin sensations and to acclimate participants to the stimulation types, the current intensity was ramped-up (gradually increasing) until it reached its programmed maximum output (1.5 mA). After stimulating for the desired duration per group (active or sham), the current was ramped-down (gradually decreased) denoting the end of the stimulation. The impedance under each electrode was maintained under 10 kΩ. The ramp-up, ramp-down, and stimulation times were different depending on condition (active vs. sham) and experimental needs.

## Experiment 1. NITESGON during or immediately after training

### Participants

Participants were 48 healthy, right-handed, native-English speaking adults (24 males, 24 females; mean age was 20.02 years, standard deviation [Sd] = 1.75 years) with a similar educational background (i.e., enrolled as undergraduate students at UT Dallas) with normal to corrected vision, who all had the maximum score on the Mini Mental State Examination. Participants were screened (e.g., tES contraindications, neurological impairments, not participated in a tES study) prior to enrolling into the study. None of the participants had a history of major psychiatric or neurological disorders, or any

tES contraindications, including previous history of brain injuries or epileptic insults, cardiovascular abnormalities, implanted devices, taking neuropsychiatric medications, prescribed stimulants use, or chronic use of illicit drugs (i.e., marijuana and cocaine).

Participants were excluded from the study if screening discovered they were familiar with Swahili/Arabic language or Swahili culture due to the nature of the stimuli. Furthermore, participants received instructions advising them to abstain from the following products for the associated time window prior to their study session: dental work for 48 hr, alcohol for 24 hr, caffeine and nicotine for 16 hr, and hair styling products the day of. Participants provided written, informed consent on the day of the study session.

## Word-association task

Associative memory performance was measured using a computerized Swahili–English verbal paired-associative learning task. This task was adapted from a well-established study design published in Science by **Karpicke and Roediger, 2008**. Using an SDT<sub>N</sub> paradigm (S: study phase, D: distraction phase, T<sub>N</sub>: test phase with non-recalled word pairs), participants were instructed to read and remember 75-sequentially presented Swahili–English (e.g., Swahili: bustani, English: garden) word pairs made up of common day-to-day words. The Swahili–English word pairs were taken from the study by **Nelson and Dunlosky, 1994**. Participants had the opportunity to learn the list of 75-word pairs repetitively across a total of four alternating study and test periods each. During the study period, the word pairs were presented together on a computer screen for 5 s with the Swahili word on top and the English translation at the bottom (5 × 75 = 375 s). The study period was followed by a cued-recall test period: Swahili cue words were presented for 8 s each during which participants had to type-in the correct English translation remembered from the study period. Correctly recalled word pairs were dropped from further testing but remained to be studied in each subsequent learning period (i.e., 4 blocks of studying 75-word pairs). The order of the words being studied or tested was randomized. Previous research has demonstrated the critical role of retrieval practice in learning of a new foreign language; therefore, the paradigm ensures that all participants were well exposed to the stimuli and avoided a ceiling effect (**Karpicke and Roediger, 2008**).

## NITESGON

There were three groups – active NITESGON during learning (i.e., study phases of the word-association task) and sham NITESGON immediately after the word-association task; sham NITESGON during learning and active NITESGON immediately the word-association task in the memory consolidation period and sham NITESGON both during and after learning of the word-association task – with 16 participants each. Active NITESGON consisted of ramp-up time of 30 s followed by a constant current of 1.5 mA (current density 0.4285 A/m<sup>2</sup>) during each of the 4 study blocks, resulting in a total stimulation time of 25 min (i.e., 375 s × 4 blocks) and ramp-down time of 30 s. For the sham NITESGON group, the current intensity was ramped-up to 1.5 mA over 30 s and immediately ramped-down over 30 s. Hence, sham NITESGON only lasted 60 s per study period, resulting in a total time of 240 s (60 s × 4 blocks) of stimulation when delivered during the study phase. For the group that received active NITESGON after the word-association task, this consisted of 30 s ramp-up and ramp-down time with 25 min of constant current stimulation at 1.5 mA. The sham NITESGON delivered after the word-association task only consisted of 30 s of ramp-up and ramp-down time resulting in 60 s of stimulation. The rationale behind the sham procedure was to mimic the transient skin sensation at the beginning of active NITESGON without producing any conditioning effects on the brain.

## Resting-state EEG

Continuous EEG data were collected from each participant pre- and post-NITESGON procedures. The data were collected using a 64-channel Neuroscan Synamps2 Quick Cap configured per the International 10–20 placement system with the midline reference located at the vertex and the ground electrode located at AFZ using the Neuroscan Scan 4.5 software (Neuroscan, <http://compumed-icsneuroscan.com>). The impedance on each electrode was maintained at less than 5 kΩ. The data were sampled using the Neuroscan Synamps<sup>2</sup> amplifier at 500 Hz with online band-pass filtering at 0.1–100 Hz.

Eyes-closed recordings (sampling rate = 1 kHz, band passed DC–200 Hz) were obtained in a dark room which was dimly lit with a small lamp with each participant sitting upright in a comfortable chair; data collection lasted approximately 5 min. Participants were instructed not to drink alcohol 24 hr prior to EEG recording or caffeinated beverages 1 hr before recording to avoid alcohol- or caffeine-induced changes in the EEG stream. The alertness of participants was checked by monitoring both slowing of the alpha rhythm and appearance of spindles in the EEG stream to prevent possible enhancement of the theta power due to drowsiness during recording (*Moazami-Goudarzi et al., 2010*). No participants included in the current study showed such EEG changes during measurements.

### Saliva collection

Saliva was collected twice during each experiment: once immediately prior to NITESGON stimulation and once immediately after NITESGON stimulation. When the participants were ready to collect saliva, they were requested to gently tip their head backwards and collect saliva on the floor of their mouth and when ready, passively drool into the collection aid mouthpiece provided by Salimetrics laboratory (Salimetrics, LLC, USA; <https://salimetrics.com>). The participants were requested to collect 2 ml of saliva in one straight flow and avoid breaks between drool as much as possible. The length of time to collect 2 ml of saliva was noted and the timer was started only when participants began to passively drool into the tube. All saliva samples were stored in 2 ml cryovials, and immediately stored in an –80°C laboratory freezer. Prior to saliva collections, all participants were instructed to avoid food, sugary drinks, excess caffeine, nicotine, and acidic drinks for at least 1 hr before collecting the saliva samples. Participants were also instructed to avoid alcohol and vigorous exercise 24 hr prior to and avoid dental work 48 hr prior to their appointment. In addition, participants were instructed not to brush their teeth within 45 min of sample collection in order to avoid any risk of lowering pH levels and influencing bacterial growth. If the study was scheduled for the afternoon, participants were requested to avoid taking naps during the day. Upon completion of the collection procedures, all saliva samples were packed in dry ice and sent to the Salimetrics laboratory for analysis. We chose to use sAA as a biomarker for norepinephrine as it provided a non-invasive yet valid indicator of central sympathetic nervous system activation (*Nater and Rohleder, 2009*). sAA levels have been shown to co-vary significantly with circulating NA levels, with human fMRI showing LC activity rising simultaneously with sAA levels during viewing of emotionally arousing slides; these increases were then significantly reduced by the beta-adrenergic antagonist propranolol (*van Stegeren et al., 2007*).

### Procedure

Eligible participants were scheduled for two visits to complete the study. Visit 1 consisted of the word-association task and administration of NITESGON. Participants were randomly assigned to one of three groups during the study period. The researcher who controlled the NITESGON device was not involved in instructing the participant; this was performed by a second researcher who was blind to the stimulation protocol. rsEEG and saliva were collected twice for all participants, once immediately before and once immediately after NITESGON application. Participants were asked to refrain from studying or searching for the learned word pairs throughout the week. Participants returned 7 days after their first visit for memory testing to measure possible (long-term) effects on associative memory performance, but did not receive NITESGON, nor were they able to review word pairs. A third researcher who was not responsible for the task or NITESGON conducted the second visit.

### EEG preprocessing

For the EEG preprocessing, the data were resampled to 128 Hz, band-pass filtered (Finite Impulse Response filter) to 2–44 Hz, and re-referenced to the average reference using EEGLAB 14\_1\_1b (*Delorme and Makeig, 2004*). The EEG data were then plotted for a careful inspection for artifacts. All episodic artifacts suggestive of eye blinks, eye movements, jaw tension, teeth clenching, or body movements were manually removed from the EEG stream. In addition, an independent component analysis was conducted to further verify whether all artifacts were excluded.



## EEG source localization

Standardized low-resolution brain electromagnetic tomography (sLORETA) was used to estimate the intracerebral electrical sources that generated the scalp-recorded activity in each of the gamma frequency bands (30.5–44 Hz) (*Pascual-Marqui, 2002*). sLORETA computes neuronal activity as current density (A/m<sup>2</sup>) without assuming a predefined number of active sources. The sLORETA solution space consists of 6239 voxels (voxel size: 5 × 5 × 5 mm) and is restricted to cortical gray matter and hippocampi, as defined by the digitized Montreal Neurological Institute (MNI) 152 template (*Fuchs et al., 2002*). Scalp topographies on the MNI brain are derived from the international 10–20 system (*Jurcak et al., 2007*).

The tomography of sLORETA has received considerable validation from studies combining sLORETA with other more established spatial localization methods such as fMRI (*Mulert et al., 2004; Vitacco et al., 2002*), structural MRI (*Worrell et al., 2000*), and positron emission tomography (PET) (*Dierks et al., 2000; Pizzagalli et al., 2004; Zumsteg et al., 2005*). Further sLORETA validation is based on accepting as ground truth that the localization findings obtained from invasive, implanted depth electrodes, of which there are several studies in epilepsy (*Zumsteg et al., 2006a; Zumsteg et al., 2006b*) and cognitive ERPs (*Volpe et al., 2007*).

## Statistics task

For visit 1 learning, a one-way analysis of variance (ANOVA) was conducted with the cumulative learning rate over the different study periods as the dependent variable and three groups as the between-subjects variable. To look at the memory effect (recall) 7 days after learning, we applied a one-way ANOVA with the group as the between-subjects variable and correctly recalled words as the dependent variable.

## Statistics saliva

Using the saliva collected via the passive drool method, sAA levels were measured. We conducted a repeated measures ANOVA with groups as between-subjects variable and sAA as within-subjects variable. A simple contrast analysis was applied to compare the different conditions using a Bonferroni correction.

## Statistics EEG – whole brain analysis

A whole brain analysis was used to compare gamma activity before and after NITESGON. These activity changes were then correlated with the number of words recalled during visit 2, 7 days after the learning task, using a Pearson correlation. Non-parametric statistical analyses of functional sLORETA images (statistical non-parametric mapping) were performed for each contrast employing a t-statistic for paired groups and corrected for multiple comparisons ( $p < 0.05$ ). The significance threshold for all tests was based on a permutation test with 5000 permutations and corrected for multiple comparisons (*Nichols and Holmes, 2002*).

## Experiment 2. NITESGON during second task – retroactive strengthening of memories

### Participants

Participants were 20 healthy, right-handed, native-English speaking adults (9 males, 11 females; mean age was 21.11 years,  $Sd = 2.03$  years) with a similar educational background (i.e., enrolled as undergraduate students at UT Dallas). Participants were screened and enrolled similar to Experiment 1.

### Word-association task (task 1)

Associative memory performance was measured using the same computerized Swahili–English verbal paired-associative learning task used in Experiment 1, however, the task consisted of three study periods in which participants were asked to read and remember 50 Swahili–English word pairs in each study period ( $50 \times 5 = 250$  s).

### Object-location task (task 2)

Participants partook in a second memory performance task immediately after the word-association task. The second memory task consisted of a spatial-navigation object-location association task

that was based on previous research (Nilakantan *et al.*, 2017). Using the same SDT<sub>N</sub> paradigm, participants were instructed to view and remember 50-sequentially presented objects locations on a blue–red–gray background grid with an eye-to-screen distance of ~24 inches across three study-test blocks. The objects consisted of black and white line drawings from the Boston Naming Test; 10 objects from each of the following categories were used: animals, foods, modes of transportation, tools, and household objects. Each image appeared in a randomized order at a randomized location. Objects were presented one at a time for 5 s each (1-s interstimulus interval). Objects were presented within a white-box background (4.88 × 4.88 cm) and had a red dot superimposed at the object center to mark the precise location. Participants were instructed to study and remember the object-locations as accurately and precisely as possible. After each study phase, a cued-recall test was administered. During the test period, the studied objects were presented one at a time in the center of the screen (in a randomized order), and participants were required to recall the studied locations. At the beginning of every trial, a 2-s fixation cross at the center of the screen was presented. After this 2-s period, participants were able to use the mouse to move the object from the center of the screen to its recalled location and click a button on the mouse to indicate its final location.

The Swahili–English verbal associative task was used as task 1 and the spatial-navigation object-location task was used as task 2 for all participants.

## NITESGON

All participants received sham NITESGON during each study period of task 1 using the following parameters: a 5-s ramp-up period, followed by a constant current of 1.5 mA for 15 s, ending with a ramp-down period of 5 s, allowing for an emulated sensation of the active NITESGON. For task 2, 10 participants received active NITESGON and 10 participants received sham NITESGON. Sham stimulation parameters were the same as used in task 1 and stayed consistent in each of the three study periods of task 2. Participants given active NITESGON received a 5-s ramp-up period, followed by a constant current of 1.5 mA for 250 s, and finished with a 5-s ramp-down period during each of the three study periods of task 2 on the first day. Thus, the total stimulation time for the active group was 750 s (i.e., 250-s × 3 study periods) and the sham group was 45 s (i.e., 15-s × 3 study periods). Just before the first study period of the first task participants NITESGON was delivered for 15 s to help participants habituate to the sensation and to check if they were comfortable with the sensation.

## Resting-state EEG

Continuous EEG data were collected from each participant pre- and post-NITESGON procedures as detailed in Experiment 1.

## Saliva collection

Saliva was collected twice during each experiment: once immediately prior to NITESGON stimulation and once immediately after NITESGON stimulation as detailed in Experiment 1.

## Procedure

Eligible participants were scheduled for two visits to complete the study. Visit 1 consisted of the word-association task (i.e., task 1) paired with sham stimulation, and then were randomly assigned to either the active or sham NITESGON condition for the spatial-navigation task (i.e., task 2). The researcher who controlled the NITESGON device was not involved in instructing the participant; this was performed by a second researcher who was blind to the stimulation protocol. rsEEG and saliva were collected twice for all participants, once immediately before and once immediately after NITESGON application. Participants were asked to refrain from studying or searching for the learned word pairs throughout the week. Participants returned 7 days after their first visit for memory testing on both tasks 1 and 2 to measure possible (long-term) effects on associative memory performance, but did not receive NITESGON, nor were they able to review word pairs or objects' locations. A third researcher who was not responsible for the task or NITESGON conducted the second visit.



## EEG preprocessing and source localization

The continuous EEG data were preprocessed and the source-level gamma activity pre- and post-NITESGON procedures for the two groups was determined as detailed in Experiment 1.

## Statistics task

For visit 1 learning, a multivariate analysis of variance (MANOVA) was conducted with the cumulative learning rate over the different study periods for both tasks as the dependent variable and group as the between-subjects variable. To look at the memory effect (recall) 7 days after learning, we applied an MANOVA with groups as the between-subjects variable and correctly recalled words on both tasks as the dependent variable. For both analyses, if significant, two separate one-way ANOVAs were applied with groups as the between-subjects variable and correctly recalled words as dependent variable for task 1 or 2, respectively.

## Statistics saliva

Using the saliva collected via the passive drool method, sAA levels were measured which were compared between the groups as detailed in Experiment 1.

## Statistics EEG – whole brain analysis

A whole brain analysis was used to compare gamma activity before and after NITESGON. This activity was correlated with the number of correctly recalled items (words/locations) 7 days later as detailed in Experiment 1.

## Experiment 3. NITESGON during first task – proactive strengthening of memories

### Participants

Participants were 24 healthy, right-handed, native-English speaking adults (13 males, 11 females; mean age was 20.83 years,  $Sd = 2.21$  years) with a similar educational background (i.e., enrolled as undergraduate students at UT Dallas). Participants were screened and enrolled similar to Experiment 1.

### Word-association task (task 1)

Associative memory performance was measured using the same computerized Swahili–English verbal paired-associative learning task used in Experiment 2.

### Object-location task (task 2)

Participants partook in a second memory performance task immediately after the word-association task consisting of a spatial-navigation object-location association task used in Experiment 2.

### NITESGON

The same device, electrode placement, and active and sham NITESGON parameters described in Experiment 2 were used. Differing from Experiment 2, Experiment 3 had all participants receive active NITESGON during each study period of task 1 as opposed to task 2. Twelve participants received active NITESGON and 12 participants received sham NITESGON during the first task.

### Resting-state EEG

Continuous EEG data were collected from each participant pre- and post-NITESGON procedures as detailed in Experiment 1.

### Saliva collection

Saliva was collected twice during each experiment: once immediately prior to NITESGON stimulation and once immediately after NITESGON stimulation as detailed in Experiment 1.

## Procedure

Eligible participants were scheduled for two visits to complete the study. Visit 1 consisted of the word-association task (i.e., task 1) paired with either active or sham NITESGON, and spatial-navigation task (i.e., task 2) paired with sham NITESGON. The researcher who controlled the NITESGON device was not involved in instructing the participant; this was performed by a second researcher who was blind to the stimulation protocol. rsEEG and saliva were collected twice for all participants, once immediately before and once immediately after NITESGON application. Participants were asked to refrain from studying or searching for the learned word pairs throughout the week. Participants returned 7 days after their first visit for memory testing on both tasks 1 and 2 to measure possible (long-term) effects on associative memory performance, but did not receive NITESGON, nor were they able to review word pairs or objects' locations. A third researcher who was not responsible for the task or NITESGON conducted the second visit.

## EEG preprocessing and source localization

The continuous EEG data were preprocessed and the source-level gamma activity pre- and post-NITESGON procedures for the two groups was determined as detailed in Experiment 1.

## Statistics task

The learning in visit 1 and memory performance in visit 2 was compared between the groups as detailed in Experiment 2.

## Statistics saliva

Using the saliva collected via the passive drool method, sAA levels were measured which were compared between the groups as detailed in Experiment 1.

## Statistics EEG – whole brain analysis

A whole brain analysis was used to compare gamma activity before and after NITESGON. This activity was correlated with the number of correctly recalled items (words/locations) 7 days later as detailed in Experiment 1.

# Experiment 4. NITESGON during interference task

## Participants

Participants were 32 healthy, right-handed, native-English speaking adults (15 males, 17 females; mean age was 21.36 years,  $Sd = 2.42$  years) with a similar educational background (i.e., enrolled as undergraduate students at UT Dallas). Participants were screened and enrolled similar to Experiment 1. Experiment 4 added familiarity of Japanese language or culture to the participant screening procedure, if indicated, the participant was excluded from the study due to the nature of the stimuli.

## Word-association tasks

Associative memory performance was measured using two computerized verbal paired-associate learning tasks. Similar to Experiments 2 and 3, one task comprised of the Swahili–English vocabulary learning, and the second task consisted of a newly introduced Japanese–English (e.g., Japanese: Kumo, English: cloud) word-association task. The Japanese–English word-association task used the same Swahili–English word pairs, however, the Swahili words were replaced by Japanese words.

## NITESGON

The same device, electrode placement, and active and sham NITESGON parameters described in Experiment 2 was used. Sixteen participants received active NITESGON and 16 participants received sham NITESGON during the first task, where everyone received sham NITESGON during the second task.

## Resting-state EEG

Continuous EEG data were collected from each participant pre- and post-NITESGON procedures as detailed in Experiment 1.

## Saliva collection

Saliva was collected twice during each experiment: once immediately prior to NITESGON stimulation and once immediately after NITESGON stimulation as detailed in Experiment 1.

## Procedure

Eligible participants were scheduled for two visits to complete the study. Visit 1 consisted of two word-association tasks, whereby task 1 was paired with either active or sham NITESGON followed by a second word-association task (i.e., task 2) paired with sham NITESGON. The order of the two word-association tasks was randomized over the participants in a 1:1 ratio to remove a possible order effect. The researcher who controlled the NITESGON device was not involved in instructing the participant; this was performed by a second researcher who was blind to the stimulation protocol. rsEEG and saliva were collected twice for all participants, once immediately before and once immediately after NITESGON application. Participants were asked to refrain from studying or searching for the learned word pairs throughout the week. Participants returned 7 days after their first visit for memory testing on both tasks 1 and 2 to measure possible (long-term) effects on associative memory performance, but did not receive NITESGON, nor were they able to review word pairs. A third researcher who was not responsible for the task or NITESGON conducted the second visit. As during the first visit, the two word-association tasks were randomized over the participants in a 1:1 ratio to remove a possible order effect.

## EEG preprocessing and source localization

The continuous EEG data were preprocessed and the source-level gamma activity pre- and post-NITESGON procedures for the two groups was determined as detailed in Experiment 1.

## Statistics task

For visit 1 learning, a repeated measures ANOVA was applied with the cumulative learning rate over the different study periods for both tasks as within-subjects variable and group (active vs. sham) as between-subjects variable. A similar analysis was applied for the memory effect (recall) 7 days after learning. A simple contrast analysis was applied to compare the difference conditions using a Bonferroni correction. In addition, an interference effect was determined by calculating how many words recalled during memory task 2 had an overlap from memory task 1. The higher percentage the more overlap in remembering the English translation for both exact word in tasks 1 and 2, the lesser the interference effect. A one-way ANOVA was applied with the interference effect as dependent variable and group (active vs. sham) as between-subjects variable.

## Statistics saliva

Using the saliva collected via the passive drool method, sAA levels were measured which were compared between the groups as detailed in Experiment 1.

## Statistics EEG – whole brain analysis

A whole brain analysis was used to compare gamma activity before and after NITESGON. This activity was correlated with the number of correctly recalled items (words/locations) 7 days later as detailed in Experiment 1.

## Experiment 5. Effect of NITESGON is not sleep dependent

### Participants

Participants were 20 healthy, right-handed, native-English speaking adults (11 males, 9 females; mean age was 21.18 years,  $Sd = 1.951$  years) with a similar educational background (i.e., enrolled as undergraduate students at UT Dallas). Participants were screened and enrolled similar to Experiment 1.

## Word-association task

Associative memory performance was measured using the same computerized Swahili–English verbal paired-associative learning task used in Experiment 1.

## NITESGON

All participants received active NITESGON during each of the four study periods on visit 1 using the following parameters: a 5-s ramp-up period, followed by a constant current of 1.5 mA for 375 s (75-word pairs  $\times$  5 s), and finished with a 5-s ramp-down period. The total stimulation time was 25 min (i.e., 375 s  $\times$  4 blocks). Before the start of the first study period, an additional 15-s habituation period was added to make sure the participants got used to the sensation.

## Procedure

Eligible participants were scheduled for two visits to complete the study. Visit 1 consisted of the word-association task paired with active NITESGON. Participants were randomly assigned to one of the two groups (sleep vs. no sleep).

As Experiment 4 reveals that NITESGON is involved in synaptic consolidation that occurs over a timespan of minutes to hours after encoding the information, where sleep that has been association with systems consolidation does not play a central role. To cross validate these findings, we opted for the parallel design not including a control condition, as the aim of this study is to see if sleep mediates the memory effect induced by NITESGON, rather than the effect of NITESGON or the interaction between sleep and NITESGON on memory.

Ten participants learned the word-association task at 8:00 a.m. and were tested the same day at 8:00 p.m., while the other 10 participants learned the word-association task at 8:00 p.m. and were tested the next day at 8:00 a.m. after a night of sleep. Participants were asked to refrain from studying or searching for the learned word pairs for at least the next 12 hr. The researcher who controlled the NITESGON device was not involved in instructing the participant; this was performed by a second researcher who was blind to the stimulation protocol. A third researcher who was not responsible for the task or NITESGON conducted the second visit (12 hr later).

## Statistics task

A one-way ANOVA with group (sleep vs. no sleep) as between-subjects variable and number of words correctly recalled as dependent variable was performed.

## Experiment 6. LC – hippocampus activity and connectivity

### Participants

Participants were 32 healthy, right-handed, native-English speaking adults (16 males, 16 females; mean age was 25.32 years,  $Sd = 2.65$  years) with a similar educational background (i.e., enrolled as undergraduate students at UT Dallas). Participants were screened and enrolled similar to Experiment 1. Experiment 6 added the exclusion of those participants who had any contraindication for MRI (i.e., metallic implants, pregnancy, claustrophobia).

### Resting-state fMRI

The resting-state fMRI data were collected on a 3T MR scanner (Achieva, Philips, Netherlands) using a 32-channel SENSE phased-array head coil. The dimensions of the coil was 38 (height)  $\times$  46 (width)  $\times$  59 (length) cm<sup>3</sup>. During scanning, foam padding and earplugs were used to minimize the head movement and scanner noise. An MR-compatible, battery powered NITESGON system manufactured by MR NeuroConn Co (Germany) was applied to each participant inside the MR scanner. All the operating parts and devices that go into the scanner room were MR compatible and everything else was in the control room, connected via the waveguide. The NITESGON system was fully charged before each session and its impedance level was measured regularly to test if it was maintained at approximately 5 k $\Omega$  on each end (i.e., 10 k $\Omega$  total).

The MR session with NITESGON was divided into three consecutive blocks of scanning: before stimulation, during stimulation, and after stimulation. At the beginning of the pre-stimulation session, routine survey and T1 anatomical images were acquired for a total time of 5 min. Before acquiring the

T1 image, saline-soaked NITESGON electrodes were positioned on the subject for three consecutive blocks of rsfMRI. For each of the scanning blocks, we acquired 20-min long rsfMRI images.

For the T1 (MPRAGE) anatomical scan, parameters included a repetition time (TR) of 2300 ms, an echo time (TE) of 2.94 ms, an inversion time (TI) of 900 ms, and a flip angle of 9°. One hundred and sixty sagittal slices were taken, using a matrix size of  $256 \times 256 \text{ mm}^2$ , at a  $1 \times 1 \times 1 \text{ mm}^3$  resolution.

Resting-state fMRI sequences were acquired with the following imaging parameters (echo-planar imaging protocol): TR/TE = 3000/30 ms, field-of-view =  $220 \times 220 \text{ mm}^2$ , matrix =  $64 \times 64$ , number of slices = 53 with voxel size =  $3 \times 3 \times 4 \text{ mm}^3$  with no gap between slices. The total number of acquired volumes was 400, counting for 20 min.

MR images were preprocessed using Statistical Parametric Mapping (SPM12b, Wellcome Department of Imaging Neuroscience, University College London, UK). Images from the first five TRs in the beginning of each session were discarded. We normalized high-resolution structural images to a standard MNI template, and segmented for three structural components, which were gray matter, white matter, and cerebrospinal fluid. Functional images were realigned to the middle volume to correct for motion artifacts. Slice-timing correction was adjusted for temporal discrepancies between z-direction slices acquired in an interleaved manner. After co-registration of functional volumes to the structural image (T1), volumes that contain extreme movements were linearly regressed out as covariates using Artifact Detection Tool (Gabrieli Lab, MIT, US, [http://www.nitrc.org/projects/artifact\\_detect/](http://www.nitrc.org/projects/artifact_detect/)). Functional images were normalized to the standard template using nonlinear transformation parameters acquired by the process of normalizing structural image to the standard template. The normalized functional images were smoothed using 6 mm Gaussian kernel.

After preprocessing, the images were processed to account for motion-related and physiological noises using an independent component analysis. Confounding factors of signals from white matter and cerebrospinal fluid were linearly regressed out from the global average brain signal using CompCor. Global signal regression was performed using the grand averaged signal from the gray matter volume. When removing confounding effect, the signal was simultaneously filtered from 0.01 to 0.17 Hz, where the maximum detectable frequency of the signal is 0.167 Hz (TR = 3 s).

## NITESGON

Shielded cables connected the MR-compatible box and electrodes, and the stimulation data were transferred via the CAT.6 LAN cable that runs throughout the MR scanner room to the non-MR-compatible stimulation devices in the control room. For the active NITESGON group, the current was ramped-up for 30 s followed by a constant current of 1.5 mA for 20 min and a 10-s ramp-down period. For sham NITESGON, the current was ramped-up over 30 s to reach the intensity of 1.5 mA followed by 15-s of constant current stimulation at 1.5 mA and 10 s ramp-down. Hence, sham NITESGON only lasted 15 s (as opposed to 20 min in the active group).

## Procedure

Participants were scanned immediately before, during, and immediately after the NITESGON stimulation. The researcher who controlled the NITESGON device was not blinded to the stimulation group, but the participant was blinded to which stimulation group they were placed in. Sixteen participants received active NITESGON and 16 received sham NITESGON.

## Statistics rsfMRI

A functional connectivity analysis was performed using the CONN toolbox. The ROI considered in the analysis were the right hippocampus (based on previous findings [Vanneste et al., 2020]), LC, and VTA. Both the LC and VTA were selected using probabilistic atlas (as conducted in a study across 44 adults by localizing its peak signal level in high-resolution T1 turbo spin-echo images and verified the location using post-mortem brains) (Tona et al., 2017). The probabilistic templates were created using processing steps specifically designed to address these difficulties (Tona et al., 2017). To remove potential artifacts such as head motion, respiration, and other global imaging artifacts including potential stimulation effects, we regressed out the global average brain signal.

We conducted an rALFF analysis for the LC, VTA, and hippocampus. The time series for each voxel of each ROI was transformed to the frequency domain and the power spectrum was then obtained. Since the power of a given frequency is proportional to the square of the amplitude of this frequency

component, the square root was calculated at each frequency of the power spectrum and the averaged square root was obtained across 0.01–0.17 Hz at each voxel. This averaged square root was taken as the rALFF (Yu-Feng *et al.*, 2007). The rALFF of each voxel was divided by the individual global mean of the rALFF within a brain-mask, which was obtained by removing the tissues outside the brain using software MRIcron. Spatial smoothing was conducted on the maps with an isotropic Gaussian kernel of 8 mm of full width at half-maximum. A repeated measures ANOVA was used including group (active vs. sham) as between-subjects variable and rALFF before, during and after NITESGON as within-subjects variable for the different ROIs (ALFF for the VTA, LC, and hippocampus). A simple contrast analysis was included to compare the difference between active and sham stimulation for each ROI before, during, and after stimulation separately including a correction for multiple comparison (Bonferroni correction).

In addition, the average BOLD time series across all voxels within the ROIs were extracted from the smoothed functional images. A partial correlation analysis was performed, and the resulting *r*-value converted to Fisher's Z-transformed coefficients were used for further statistical analyses. The Z-transformed connectivity weights were compared between the active and sham groups for the LC and hippocampus, LC and VTA, and VTA and hippocampus, respectively, using a repeated measures ANOVA. A simple contrast analysis was applied to compare the difference in active and sham condition using a Bonferroni correction.

## Experiment 7. Potential relationship between NITESGON-LC and DA

### Participants

Participants were 24 healthy, right-handed, native-English speaking adults (12 males, 12 females; mean age was 23.83 years, *Sd* = 2.88 years) with a similar educational background. Participants were screened and enrolled similar to Experiment 1.

### NITESGON

Active NITESGON stimulation consisted of a ramp-up period of 5 s, followed by constant current of 1.5 mA for 20 min and ramp-down period of 5 s. Sham NITESGON only consisted of a ramp-up period of 5 s to reach the intensity of 1.5 mA and an immediate ramp-down period of 5 s. Twelve participants received active NITESGON and 12 participants received sham NITESGON.

### Electrophysiological recordings

Continuous EEG data were collected from each participant in response to the auditory oddball paradigm, before and after the application of NITESGON. The auditory oddball task is a simple and well-established paradigm for the investigation of the robust P3b component which has a predictable standard tone and an unpredictable deviant tone (Murphy *et al.*, 2011). The data were collected using a 64-channel Neuroscan Synamps<sup>2</sup> Quick Cap configured per the International 10–20 placement system with the midline reference located at the vertex and the ground electrode located at AFZ using the Neuroscan Scan 4.5 software. The impedance on each electrode was maintained at less than 5 k $\Omega$ . The data were sampled using the Neuroscan Synamps<sup>2</sup> amplifier at 500 Hz with online band-pass filtering at 0.1–100 Hz. Data were preprocessed using Matlab and EEGLAB in a manner similar to the original paper that showed a relationship between ERP and LC–noradrenergic arousal function (Murphy *et al.*, 2011).

### Peak-to-peak P3b amplitude

Peak-to-peak amplitude was defined as the amplitude difference between the N200 peak and the P300 peak for the P3 electrode. The N200 component was identified as the most negative peak between 200 and 375 ms after the stimulus onset. The P300 component was identified as the most positive peak between 250 and 600 ms after the stimulus onset.

### Spontaneous eyeblink rate

To retain the eyeblinks, the eyeblink rate was calculated using the data before cleaning the artifacts using an independent component analysis. Furthermore, the continuous dataset before epoching was used to visualize the entire temporal profile of the eyeblink potential to avoid any cutting-off of the



potential due to epoching. An eyeblink was determined to be a sharp negative peak followed immediately by a positive peak located in the frontal electrodes such as FP1, FP2, and FPz. In some cases, the negative peak was not prominent, but the positive peak was a signatory. The topography of this potential was observed to have a clear dipole covering the frontal and frontotemporal electrodes. This potential was marked manually by a researcher, who scanned the entire EEG recording manually for all the participants in the active and sham groups, in the pre- and post-stimulation conditions. The number of eyeblinks in the length of recording was obtained and the eyeblink rate was calculated as the number of eyeblinks/minute. The same procedure was performed by a second researcher who was blinded to the conditions and the inter-rater validity was calculated. The average score was calculated from both independent researchers.

### Saliva collection

Saliva was collected twice during each experiment: once immediately prior to NITESGON stimulation and once immediately after NITESGON stimulation as detailed in Experiment 1.

### Pupil dilation

The response of the pupil to three types of light stimulation (blue, 470 nm; white 8000k color temperature; and red, 624 nm) was recorded in real time using a binocular Basler Dart Near Infrared (NIR) cameras. The lenses have a fixed focal length of 8 mm with an M12x0.5 body. The images were recorded at a frame rate of 120 Hz. There is a constant NIR illumination of the eye (850 nm) and the cameras are equipped with a 'daylight cut filter' which passes NIR and blocks any wavelengths below ~800 nm. Surface-mounted LEDs were used for light stimulation and the cameras were all mounted on a single eyepiece, which communicated with a Windows laptop through a USB 3.0 cable. Each color was shown for 200 ms first in the left eye and then in the right eye with an ISI of 8 s. This left-right trial was repeated three times for each color. The average total duration of the procedure was 2 min per participant. The participant was requested to focus on a point inside the eyepiece and open their eyes as wide as possible. They were asked to avoid rapid and frequent blinking of eyes, movement of eyes, and specifically to avoid blinking during stimulus presentation. The videos were then post-processed to obtain the dilation of the pupil. The pupil was extracted as an ellipse from each frame with a segmentation algorithm and the diameter was calculated from the average of the major and minor axes of the resulting pupil ellipse. The difference between the maximum dilation and maximum constriction of both pupils in response to each color for every trial was calculated for each person immediately before and after NITESGON. The pupil size was measured as a direct response to the NITESGON and did not include a specific task.

### Procedure

Participants performed the auditory oddball task twice, once immediately before and once immediately after the NITESGON session. In addition, saliva and pupil dilation were also collected immediately before and immediately after the NITESGON session. The reason why we collected auditory oddball task and pupil size before and after NITESGON is to avoid a direct effect of the learning task or inference of the current sent to the scalp. Participants were randomly assigned to the active or sham NITESGON group. The researcher who controlled the NITESGON device was not involved in instructing the participant; this was performed by a second researcher who was blind to the stimulation protocol.

### Statistics peak-to-peak P3b amplitude

EEG data were compared using a repeated measures ANOVA with groups (active vs. sham) and condition (deviant vs. standard) as the between-subjects variable, and the peak-to-peak amplitude before and after stimulation as the within-subjects variable. A simple contrast analysis was applied to compare specific effects using a Bonferroni correction.



### Statistics sEBR

We conducted a repeated measures ANOVA with group (active vs. sham) as between-subjects variable, and the average eye blink rate before and after stimulation as within-subjects variable. A simple contrast analysis was applied to compare specific contrasts using a Bonferroni correction.

### Statistics pupil size

Using the pupil size, we conducted a one-way ANOVA with groups as group variable and difference in pupil size before and after NITESGON as the dependent variable.

### Statistics saliva

Using the saliva collected via the passive drool method, sAA levels were measured which were compared between the groups as detailed in Experiment 1.

### Statistics correlation

Pearson correlations were calculated between the difference in sAA, peak-to-peak P3b amplitude and sEBR, pupil size before and after NITESGON stimulation.

## Experiment 8. Dopamine

### Participants

Participants were 20 right-handed adults (8 males, 12 females; mean age was 35.23 years,  $Sd = 2.63$  years), half of who were selected due to their medical record indicating they were taking flupentixol (0.5 mg)/melitracen (10 mg) (Deanxit), a DA antagonist (i.e., D1 and D2) (*Hyttel, 1981*), for their tinnitus at least 2 weeks prior to the onset of the study. The remaining participants were of matching age and gender with a similar educational background. Participants were screened and enrolled similar to Experiment 1.

### Word-association task

Associative memory performance was measured using the same computerized Swahili–English verbal paired-associative learning task used in Experiment 1, however, the English words were replaced by Dutch words.

### NITESGON

All participants received active NITESGON immediately following the word-association task on visit 1 using the following parameters: a 5-s ramp-up period, followed by a constant current of 1.5 mA for 25 min, and finished with a 5-s ramp-down period.

As experiment suggests DA plays a vital role in memory consolidation, Experiment 8 is a follow-up experiment to cross validate these findings. We opted for the parallel design not including a control condition, as the aim of this study is to see if DA antagonist mediates the memory effect induced by NITESGON, rather than the effect of NITESGON or the interaction between sleep and NITESGON on memory.

### Procedure

Eligible participants were scheduled for two visits to complete the study. Visit 1 consisted of the word-association task followed by active NITESGON stimulation. Participants were asked to refrain from studying or searching for the learned word pairs throughout the week. Participants returned 3–4 days after their first visit for memory testing to measure possible (long-term) effects on associative memory performance, but did not receive NITESGON, nor were they able to review word pairs.

### Statistics task

For visit 1 learning, a one-way ANOVA was conducted with the cumulative learning rate over the different study periods as the dependent variable and two groups (antagonist or no antagonist) as between-subjects variable. To look at the memory effect (recall) 7 days after learning, we applied a

one-way ANOVA with group as the between-subjects variable and correctly recalled words as dependent variable.

## Blinding

To determine if the stimulation for all experiments was well blinded, all participants who participated in Experiments 1–7 were asked to complete a single-response questionnaire after the conclusion of the NITESGON procedure. Here, participants were asked to guess if they thought they were placed in the active or control group. A  $\chi^2$  analysis was used to determine if there was a difference between what stimulation participants received compared to what participants expected.

## Additional information

### Funding

Funder	Grant reference number	Author
Alzheimer Association	AARG-21-848486	Sven Vanneste

The funders had no role in study design, data collection, and interpretation, or the decision to submit the work for publication.

### Author contributions

Alison M Luckey, Data curation, Formal analysis, Investigation, Writing - original draft, Project administration; Lauren S McLeod, Conceptualization, Data curation, Project administration; Yuefeng Huang, Data curation, Methodology, Project administration; Anusha Mohan, Formal analysis, Writing - review and editing; Sven Vanneste, Conceptualization, Formal analysis, Supervision, Visualization, Methodology, Writing - original draft, Writing - review and editing

### Author ORCIDs

Sven Vanneste  <http://orcid.org/0000-0003-1513-5752>

### Ethics

All experiments were in accordance with the ethical standards of the Declaration of Helsinki (1964). Experiments 1–7 were approved by the Institutional Review Board at the University of Texas at Dallas. All participants signed a written informed consent and consent to publish was obtained.

### Decision letter and Author response

Decision letter <https://doi.org/10.7554/eLife.75586.sa1>

Author response <https://doi.org/10.7554/eLife.75586.sa2>

## Additional files

### Supplementary files

- Transparent reporting form

### Data availability

Data is available: <https://doi.org/10.5061/dryad.dbrv15f46>.

The following dataset was generated:

Author(s)	Year	Dataset title	Dataset URL	Database and Identifier
Vanneste V	2022	Data from: Making memories last using the peripheral effect of direct current stimulation	<a href="https://dx.doi.org/10.5061/dryad.dbrv15f46">https://dx.doi.org/10.5061/dryad.dbrv15f46</a>	Dryad Digital Repository, 10.5061/dryad.dbrv15f46

## References

- Adair D**, Truong D, Esmaeilpour Z, Gebodh N, Borges H, Ho L, Bremner JD, Badran BW, Napadow V, Clark VP, Bikson M. 2020. Electrical stimulation of cranial nerves in cognition and disease. *Brain Stimulation* **13**:717–750. DOI: <https://doi.org/10.1016/j.brs.2020.02.019>
- Asamoah B**, Khatoun A, Mc Laughlin M. 2019. tACS motor system effects can be caused by Transcutaneous stimulation of peripheral nerves. *Nature Communications* **10**:266. DOI: <https://doi.org/10.1038/s41467-018-08183-w>, PMID: 30655523
- Astafiev SV**, Snyder AZ, Shulman GL, Corbetta M. 2010. Comment on "Modafinil shifts human locus coeruleus to low-tonic, high-Phasic activity during functional MRI" and "Homeostatic sleep pressure and responses to sustained attention in the Suprachiasmatic area. *Science* **328**:309. DOI: <https://doi.org/10.1126/science.1177948>, PMID: 20395497
- Aston-Jones G**, Cohen JD. 2005. Adaptive gain and the role of the locus coeruleus-norepinephrine system in optimal performance. *The Journal of Comparative Neurology* **493**:99–110. DOI: <https://doi.org/10.1002/cne.20723>, PMID: 16254995
- Avery MC**, Krichmar JL. 2017. Neuromodulatory systems and their interactions: A review of models, theories, and experiments. *Frontiers in Neural Circuits* **11**:108. DOI: <https://doi.org/10.3389/fncir.2017.00108>, PMID: 29311844
- Bouret S**, Richmond BJ. 2009. Relation of locus coeruleus neurons in monkeys to Pavlovian and Operant behaviors. *Journal of Neurophysiology* **101**:898–911. DOI: <https://doi.org/10.1152/jn.91048.2008>, PMID: 19091919
- Brougher J**, Aziz U, Adari N, Chaturvedi M, Jules A, Shah I, Syed S, Thorn CA. 2021. Self-administration of right Vagus nerve stimulation activates Midbrain dopaminergic nuclei. *Frontiers in Neuroscience* **15**:782786. DOI: <https://doi.org/10.3389/fnins.2021.782786>
- Cahill L**, McGaugh JL. 1998. Mechanisms of emotional arousal and lasting declarative memory. *Trends in Neurosciences* **21**:294–299. DOI: [https://doi.org/10.1016/s0166-2236\(97\)01214-9](https://doi.org/10.1016/s0166-2236(97)01214-9), PMID: 9683321
- Caous CA**, Buck H, Lindsey CJ. 2001. Neuronal connections of the Paratrigeminal nucleus: a topographic analysis of neurons projecting to Bulbar, pontine and thalamic nuclei related to cardiovascular, respiratory and sensory functions. *Autonomic Neuroscience* **94**:14–24. DOI: [https://doi.org/10.1016/S1566-0702\(01\)00338-1](https://doi.org/10.1016/S1566-0702(01)00338-1)
- Cavanagh JF**, Masters SE, Bath K, Frank MJ. 2014. Conflict acts as an implicit cost in reinforcement learning. *Nature Communications* **5**:5394. DOI: <https://doi.org/10.1038/ncomms6394>, PMID: 25367437
- Chen EY**, Lam LC, Chen RY, Nguyen DG. 1996. Blink rate, Neurocognitive impairments, and symptoms in schizophrenia. *Biological Psychiatry* **40**:597–603. DOI: [https://doi.org/10.1016/0006-3223\(95\)00482-3](https://doi.org/10.1016/0006-3223(95)00482-3), PMID: 8886292
- Conlon B**, Langguth B, Hamilton C, Hughes S, Meade E, Connor CO, Schecklmann M, Hall DA, Vanneste S, Leong SL, Subramaniam T, D'Arcy S, Lim HH. 2020. Bimodal Neuromodulation combining sound and tongue stimulation reduces Tinnitus symptoms in a large randomized clinical study. *Science Translational Medicine* **12**:564. DOI: <https://doi.org/10.1126/scitranslmed.abb2830>, PMID: 33028707
- Crossley M**, Lorenzetti FD, Naskar S, O'Shea M, Kemenes G, Benjamin PR, Kemenes I. 2019. Proactive and retroactive interference with associative memory consolidation in the snail *Lymnaea* is time and circuit dependent. *Communications Biology* **2**:242. DOI: <https://doi.org/10.1038/s42003-019-0470-y>, PMID: 31263786
- Delorme A**, Makeig S. 2004. EEGLAB: an open source Toolbox for analysis of single-trial EEG Dynamics including independent component analysis. *Journal of Neuroscience Methods* **134**:9–21. DOI: <https://doi.org/10.1016/j.jneumeth.2003.10.009>, PMID: 15102499
- de Sousa Buck H**, Caous CA, Lindsey CJ. 2001. Projections of the Paratrigeminal nucleus to the ambiguous, Rostrolateral and lateral reticular nuclei, and the solitary tract. *Autonomic Neuroscience* **87**:187–200. DOI: [https://doi.org/10.1016/S1566-0702\(00\)00259-9](https://doi.org/10.1016/S1566-0702(00)00259-9)
- Devoto P**, Flore G. 2006. On the origin of cortical dopamine: is it a Co-transmitter in noradrenergic neurons. *Current Neuropharmacology* **4**:115–125. DOI: <https://doi.org/10.2174/157015906776359559>, PMID: 18615131
- Dierks T**, Jelic V, Pascual-Marqui RD, Wahlund L-O, Julin P, Linden DEJ, Maurer K, Winblad B, Nordberg A. 2000. Spatial pattern of cerebral glucose metabolism (PET) correlates with localization of intracerebral EEG-generators in Alzheimer's disease. *Clinical Neurophysiology* **111**:1817–1824. DOI: [https://doi.org/10.1016/S1388-2457\(00\)00427-2](https://doi.org/10.1016/S1388-2457(00)00427-2)
- Dunsmoor JE**, Murty VP, Davachi L, Phelps EA. 2015. Emotional learning selectively and retroactively strengthens memories for related events. *Nature* **520**:345–348. DOI: <https://doi.org/10.1038/nature14106>, PMID: 25607357
- Dunsmoor JE**, Murty VP, Clewett D, Phelps EA, Davachi L. 2022. Tag and capture: how salient experiences target and rescue nearby events in memory. *Trends in Cognitive Sciences* **26**:782–795. DOI: <https://doi.org/10.1016/j.tics.2022.06.009>, PMID: 35842373
- Duszkiewicz AJ**, McNamara CG, Takeuchi T, Genzel L. 2019. Novelty and dopaminergic modulation of memory persistence: A tale of two systems. *Trends in Neurosciences* **42**:102–114. DOI: <https://doi.org/10.1016/j.tins.2018.10.002>, PMID: 30455050
- Elsworth JD**, Lawrence MS, Roth RH, Taylor JR, Mailman RB, Nichols DE, Lewis MH, Redmond DE. 1991. D1 and D2 dopamine receptors independently regulate spontaneous blink rate in the Vervet monkey. *The Journal of Pharmacology and Experimental Therapeutics* **259**:595–600 PMID: 1682479.

- Engineer ND**, Riley JR, Seale JD, Vrana WA, Shetake JA, Sudanagunta SP, Borland MS, Kilgard MP. 2011. Reversing pathological neural activity using targeted plasticity. *Nature* **470**:101–104. DOI: <https://doi.org/10.1038/nature09656>, PMID: 21228773
- Frey U**, Morris RG. 1997. Synaptic tagging and long-term potentiation. *Nature* **385**:533–536. DOI: <https://doi.org/10.1038/385533a0>, PMID: 9020359
- Fuchs M**, Kastner J, Wagner M, Hawes S, Ebersole JS. 2002. A standardized boundary element method volume conductor model. *Clinical Neurophysiology* **113**:702–712. DOI: [https://doi.org/10.1016/s1388-2457\(02\)00030-5](https://doi.org/10.1016/s1388-2457(02)00030-5), PMID: 11976050
- Giustino TF**, Ramanathan KR, Totty MS, Miles OW, Maren S. 2020. Locus coeruleus norepinephrine drives stress-induced increases in Basolateral amygdala firing and impairs extinction learning. *The Journal of Neuroscience* **40**:907–916. DOI: <https://doi.org/10.1523/JNEUROSCI.1092-19.2019>, PMID: 31801809
- Groman SM**, James AS, Seu E, Tran S, Clark TA, Harpster SN, Crawford M, Burtner JL, Feiler K, Roth RH, Elsworth JD, London ED, Jentsch JD. 2014. In the blink of an eye: relating positive-feedback sensitivity to striatal dopamine D2-like receptors through blink rate. *The Journal of Neuroscience* **34**:14443–14454. DOI: <https://doi.org/10.1523/JNEUROSCI.3037-14.2014>, PMID: 25339755
- Hajós M**, Hoffmann WE, Robinson DD, Yu JH, Hajós-Korcsok E. 2003. Norepinephrine but not serotonin reuptake inhibitors enhance Theta and gamma activity of the Septo-hippocampal system. *Neuropsychopharmacology* **28**:857–864. DOI: <https://doi.org/10.1038/sj.npp.1300116>, PMID: 12637957
- Hulseley DR**, Hays SA, Khodaparast N, Ruiz A, Das P, Rennaker RL, Kilgard MP. 2016. Reorganization of motor cortex by Vagus nerve stimulation requires cholinergic Innervation. *Brain Stimulation* **9**:174–181. DOI: <https://doi.org/10.1016/j.brs.2015.12.007>, PMID: 26822960
- Hulseley DR**, Shedd CM, Sarker SF, Kilgard MP, Hays SA. 2019. Norepinephrine and serotonin are required for Vagus nerve stimulation directed cortical plasticity. *Experimental Neurology* **320**:112975. DOI: <https://doi.org/10.1016/j.expneurol.2019.112975>, PMID: 31181199
- Hyttel J**. 1981. Flupentixol and dopamine receptor selectivity. *Psychopharmacology* **75**:217–. DOI: <https://doi.org/10.1007/BF00432192>
- Jacobs HI**, Priovoulos N, Poser BA, Pagen LH, Ivanov D, Verhey FR, Uludağ K. 2020. Dynamic behavior of the locus coeruleus during arousal-related memory processing in a multi-modal 7t fMRI paradigm. *eLife* **9**:e52059. DOI: <https://doi.org/10.7554/eLife.52059>, PMID: 32579109
- Jones EJ**, Rohleder N, Schreier HMC. 2020. Neuroendocrine coordination and youth behavior problems: A review of studies assessing sympathetic nervous system and hypothalamic-pituitary adrenal axis activity using salivary alpha Amylase and salivary Cortisol. *Hormones and Behavior* **122**:104750. DOI: <https://doi.org/10.1016/j.yhbeh.2020.104750>, PMID: 32302595
- Jongkees BJ**, Colzato LS. 2016. Spontaneous eye blink rate as Predictor of dopamine-related cognitive function-A review. *Neuroscience & Biobehavioral Reviews* **71**:58–82. DOI: <https://doi.org/10.1016/j.neubiorev.2016.08.020>
- Jurcak V**, Tsuzuki D, Dan I. 2007. Systems Revisited: their validity as relative head-surface-based positioning systems. *NeuroImage* **34**:1600–1611. DOI: <https://doi.org/10.1016/j.neuroimage.2006.09.024>, PMID: 17207640
- Jutkiewicz EM**, Bergman J. 2004. Effects of dopamine D1 ligands on eye blinking in monkeys: efficacy, antagonism, and D1/D2 interactions. *The Journal of Pharmacology and Experimental Therapeutics* **311**:1008–1015. DOI: <https://doi.org/10.1124/jpet.104.071092>, PMID: 15292458
- Kalbe F**, Schwabe L. 2022. On the search for a selective and retroactive strengthening of memory: is there evidence for category-specific behavioral tagging *Journal of Experimental Psychology. General* **151**:263–284. DOI: <https://doi.org/10.1037/xge0001075>, PMID: 34264716
- Kaminer J**, Powers AS, Horn KG, Hui C, Evinger C. 2011. Characterizing the spontaneous blink generator: an animal model. *The Journal of Neuroscience* **31**:11256–11267. DOI: <https://doi.org/10.1523/JNEUROSCI.6218-10.2011>, PMID: 21813686
- Karpicke JD**, Roediger HL. 2008. The critical importance of retrieval for learning. *Science* **319**:966–968. DOI: <https://doi.org/10.1126/science.1152408>, PMID: 18276894
- Karson CN**. 1983. Spontaneous eye-blink rates and dopaminergic systems. *Brain* **106** (Pt 3):643–653. DOI: <https://doi.org/10.1093/brain/106.3.643>, PMID: 6640274
- Kawai Y**. 2018. Differential ascending projections from the male rat caudal nucleus of the Tractus Solitarius: an interface between local Microcircuits and global Macrocircuits. *Frontiers in Neuroanatomy* **12**:63. DOI: <https://doi.org/10.3389/fnana.2018.00063>, PMID: 30087599
- Kempadoo KA**, Mosharov EV, Choi SJ, Sulzer D, Kandel ER. 2016. Dopamine release from the locus coeruleus to the dorsal hippocampus promotes spatial learning and memory. *PNAS* **113**:14835–14840. DOI: <https://doi.org/10.1073/pnas.1616515114>, PMID: 27930324
- Kleven MS**, Koek W. 1996. Differential effects of direct and indirect dopamine agonists on eye blink rate in cynomolgus monkeys. *The Journal of Pharmacology and Experimental Therapeutics* **279**:1211–1219 PMID: 8968343.
- Lefaucheur JP**, Antal A, Ayache SS, Benninger DH, Brunelin J, Cogiamanian F, Cotelli M, De Ridder D, Ferrucci R, Langguth B, Marangolo P, Mylius V, Nitsche MA, Padberg F, Palm U, Poulet E, Priori A, Rossi S, Schecklmann M, Vanneste S, et al. 2017. Evidence-based guidelines on the therapeutic use of transcranial direct current stimulation (tDCS). *Clinical Neurophysiology* **128**:56–92. DOI: <https://doi.org/10.1016/j.clinph.2016.10.087>, PMID: 27866120

- Lemon N**, Manahan-Vaughan D. 2012. Dopamine D1/D5 receptors contribute to de novo hippocampal LTD mediated by novel spatial exploration or locus coeruleus activity. *Cerebral Cortex* **22**:2131–2138. DOI: <https://doi.org/10.1093/cercor/bhr297>, PMID: 22038910
- Lisman JE**, Grace AA. 2005. The hippocampal-VTA loop: controlling the entry of information into long-term memory. *Neuron* **46**:703–713. DOI: <https://doi.org/10.1016/j.neuron.2005.05.002>, PMID: 15924857
- Liu A**, Vöröslakos M, Kronberg G, Henin S, Krause MR, Huang Y, Opitz A, Mehta A, Pack CC, Kregelberg B, Berényi A, Parra LC, Melloni L, Devinsky O, Buzsáki G. 2018. Immediate neurophysiological effects of transcranial electrical stimulation. *Nature Communications* **9**:5092. DOI: <https://doi.org/10.1038/s41467-018-07233-7>, PMID: 30504921
- Luckey AM**, McLeod SL, Robertson IH, To WT, Vanneste S. 2020. Greater occipital nerve stimulation BOOSTS associative memory in older individuals: A randomized trial. *Neurorehabilitation and Neural Repair* **34**:1020–1029. DOI: <https://doi.org/10.1177/1545968320943573>, PMID: 32964776
- Marks KL**, Martel DT, Wu C, Basura GJ, Roberts LE, Schwartz-Leyzac KC, Shore SE. 2018. Auditory-Somatosensory Bimodal stimulation Desynchronizes brain circuitry to reduce Tinnitus in Guinea pigs and humans. *Science Translational Medicine* **10**:422. DOI: <https://doi.org/10.1126/scitranslmed.aal3175>, PMID: 29298868
- Mather M**, Harley CW. 2016. The locus coeruleus: essential for maintaining cognitive function and the aging brain. *Trends in Cognitive Sciences* **20**:214–226. DOI: <https://doi.org/10.1016/j.tics.2016.01.001>
- McGaugh JL**. 1966. Time-dependent processes in memory storage. *Science* **153**:1351–1358. DOI: <https://doi.org/10.1126/science.153.3742.1351>
- McGaugh JL**. 2000. Memory—a century of consolidation. *Science* **287**:248–251. DOI: <https://doi.org/10.1126/science.287.5451.248>, PMID: 10634773
- McGaugh JL**. 2004. The amygdala modulates the consolidation of memories of emotionally arousing experiences. *Annual Review of Neuroscience* **27**:1–28. DOI: <https://doi.org/10.1146/annurev.neuro.27.070203.144157>, PMID: 15217324
- McGaugh JL**. 2013. Making lasting memories: remembering the significant. *PNAS* **110**:10402–10407. DOI: <https://doi.org/10.1073/pnas.1301209110>
- McNamara CG**, Tejero-Cantero Á, Trouche S, Campo-Urriza N, Dupret D. 2014. Dopaminergic neurons promote hippocampal reactivation and spatial memory persistence. *Nature Neuroscience* **17**:1658–1660. DOI: <https://doi.org/10.1038/nn.3843>, PMID: 25326690
- Menétrey D**, Basbaum AI. 1987. Spinal and trigeminal projections to the nucleus of the solitary tract: a possible substrate for Somatovisceral and Viscerovisceral reflex activation. *The Journal of Comparative Neurology* **255**:439–450. DOI: <https://doi.org/10.1002/cne.902550310>, PMID: 3819024
- Moazami-Goudarzi M**, Michels L, Weisz N, Jeanmonod D. 2010. Temporo-insular enhancement of EEG low and high frequencies in patients with chronic Tinnitus. QEEG study of chronic Tinnitus patients. *BMC Neuroscience* **11**:40. DOI: <https://doi.org/10.1186/1471-2202-11-40>, PMID: 20334674
- Moncada D**, Ballarín F, Viola H. 2015. Behavioral tagging: A translation of the synaptic tagging and capture hypothesis. *Neural Plasticity* **2015**:650780. DOI: <https://doi.org/10.1155/2015/650780>, PMID: 26380117
- Moncada D**. 2017. Evidence of VTA and LC control of protein synthesis required for the behavioral tagging process. *Neurobiology of Learning and Memory* **138**:226–237. DOI: <https://doi.org/10.1016/j.nlm.2016.06.003>, PMID: 27291857
- Morris RG**, Frey U. 1997. Hippocampal synaptic plasticity: role in spatial learning or the automatic recording of attended experience. *Philosophical Transactions of the Royal Society of London. Series B, Biological Sciences* **352**:1489–1503. DOI: <https://doi.org/10.1098/rstb.1997.0136>, PMID: 9368938
- Mulert C**, Jäger L, Schmitt R, Bussfeld P, Pogarell O, Möller H-J, Juckel G, Hegerl U. 2004. Integration of fMRI and simultaneous EEG: towards a comprehensive understanding of localization and time-course of brain activity in target detection. *NeuroImage* **22**:83–94. DOI: <https://doi.org/10.1016/j.neuroimage.2003.10.051>, PMID: 15109999
- Murphy PR**, Robertson IH, Balsters JH, O’connell RG. 2011. Pupillometry and P3 index the locus coeruleus–noradrenergic arousal function in humans. *Psychophysiology* **48**:1532–1543. DOI: <https://doi.org/10.1111/j.1469-8986.2011.01226.x>, PMID: 21762458
- Nater UM**, Rohleder N. 2009. Salivary alpha-Amylase as a non-invasive biomarker for the sympathetic nervous system: Current state of research. *Psychoneuroendocrinology* **34**:486–496. DOI: <https://doi.org/10.1016/j.psyneuen.2009.01.014>
- Nelson TO**, Dunlosky J. 1994. Norms of paired-associate recall during Multitrial learning of Swahili-English translation equivalents. *Memory* **2**:325–335. DOI: <https://doi.org/10.1080/09658219408258951>, PMID: 7584298
- Nichols TE**, Holmes AP. 2002. Nonparametric Permutation tests for functional neuroimaging: a Primer with examples. *Human Brain Mapping* **15**:1–25. DOI: <https://doi.org/10.1002/hbm.1058>, PMID: 11747097
- Nielson KA**, Yee D, Erickson KI. 2005. Memory enhancement by a semantically unrelated emotional arousal source induced after learning. *Neurobiology of Learning and Memory* **84**:49–56. DOI: <https://doi.org/10.1016/j.nlm.2005.04.001>
- Nieuwenhuis S**, Aston-Jones G, Cohen JD. 2005. Decision making, the P3, and the locus coeruleus–norepinephrine system. *Psychological Bulletin* **131**:510–532. DOI: <https://doi.org/10.1037/0033-2909.131.4.510>, PMID: 16060800



- Nilakantan AS**, Bridge DJ, Gagnon EP, VanHaerents SA, Voss JL. 2017. Stimulation of the posterior cortical-hippocampal network enhances precision of memory recollection. *Current Biology* **27**:465–470. DOI: <https://doi.org/10.1016/j.cub.2016.12.042>
- Okuda K**, Højgaard K, Privitera L, Bayraktar G, Takeuchi T. 2021. Initial memory consolidation and the synaptic tagging and capture hypothesis. *The European Journal of Neuroscience* **54**:6826–6849. DOI: <https://doi.org/10.1111/ejn.14902>, PMID: 32649022
- Ortega J**, Plaska CR, Gomes BA, Ellmore TM. 2022. Spontaneous eye blink rate during the working memory delay period predicts task accuracy. *Frontiers in Psychology* **13**:788231. DOI: <https://doi.org/10.3389/fpsyg.2022.788231>, PMID: 35242077
- Osipova D**, Takashima A, Oostenveld R, Fernández G, Maris E, Jensen O. 2006. Theta and gamma Oscillations predict Encoding and retrieval of declarative memory. *The Journal of Neuroscience* **26**:7523–7531. DOI: <https://doi.org/10.1523/JNEUROSCI.1948-06.2006>, PMID: 16837600
- Park J**. 2005. Effect of arousal and retention delay on memory: a meta-analysis. *Psychological Reports* **97**:339–355. DOI: <https://doi.org/10.2466/pr0.97.2.339-355>, PMID: 16342564
- Pascual-Marqui RD**. 2002. Standardized low-resolution brain electromagnetic tomography (sLORETA): technical details. *Methods and Findings in Experimental and Clinical Pharmacology* **24 Suppl D**:5–12 PMID: 12575463.
- Perez SM**, Carreno FR, Frazer A, Lodge DJ. 2014. Vagal nerve stimulation reverses aberrant dopamine system function in the Methylazoxymethanol acetate rodent model of schizophrenia. *Journal of Neuroscience* **34**:9261–9267. DOI: <https://doi.org/10.1523/JNEUROSCI.0588-14.2014>
- Pizzagalli DA**, Oakes TR, Fox AS, Chung MK, Larson CL, Abercrombie HC, Schaefer SM, Benca RM, Davidson RJ. 2004. Functional but not structural Subgenual Prefrontal cortex abnormalities in Melancholia. *Molecular Psychiatry* **9**:325. DOI: <https://doi.org/10.1038/sj.mp.4001501>, PMID: 14699431
- Poe GR**, Foote S, Eschenko O, Johansen JP, Bouret S, Aston-Jones G, Harley CW, Manahan-Vaughan D, Weinshenker D, Valentino R, Berridge C, Chandler DJ, Waterhouse B, Sara SJ. 2020. Locus coeruleus: a new look at the blue spot. *Nature Reviews Neuroscience* **21**:644–659. DOI: <https://doi.org/10.1038/s41583-020-0360-9>
- Polich J**. 2007. Updating P300: an integrative theory of P3A and P3B. *Clinical Neurophysiology* **118**:2128–2148. DOI: <https://doi.org/10.1016/j.clinph.2007.04.019>, PMID: 17573239
- Porter BA**, Khodaparast N, Fayyaz T, Cheung RJ, Ahmed SS, Vrana WA, Rennaker RL, Kilgard MP. 2012. Repeatedly Pairing Vagus nerve stimulation with a movement Reorganizes primary motor cortex. *Cerebral Cortex* **22**:2365–2374. DOI: <https://doi.org/10.1093/cercor/bhr316>, PMID: 22079923
- Redondo RL**, Okuno H, Spooner PA, Frenguelli BG, Bito H, Morris RGM. 2010. Synaptic tagging and capture: differential role of distinct calcium/Calmodulin Kinases in protein synthesis-dependent long-term potentiation. *The Journal of Neuroscience* **30**:4981–4989. DOI: <https://doi.org/10.1523/JNEUROSCI.3140-09.2010>, PMID: 20371818
- Redondo RL**, Morris RGM. 2011. Making memories last: the synaptic tagging and capture hypothesis. *Nature Reviews Neuroscience* **12**:17–30. DOI: <https://doi.org/10.1038/nrn2963>, PMID: 21170072
- Reza-Zaldivar EE**, Hernández-Sápiens MA, Minjarez B, Gómez-Pinedo U, Sánchez-González VJ, Márquez-Aguirre AL, Canales-Aguirre AA. 2020. Dendritic spine and synaptic plasticity in Alzheimer's disease: A focus on MicroRNA. *Frontiers in Cell and Developmental Biology* **8**:255. DOI: <https://doi.org/10.3389/fcell.2020.00255>, PMID: 32432108
- Robertson EM**. 2012. New insights in human memory interference and consolidation. *Current Biology* **22**:R66–R71. DOI: <https://doi.org/10.1016/j.cub.2011.11.051>, PMID: 22280913
- Rosen ZB**, Cheung S, Siegelbaum SA. 2015. Midbrain dopamine neurons Bidirectionally regulate Ca3-Ca1 synaptic drive. *Nature Neuroscience* **18**:1763–1771. DOI: <https://doi.org/10.1038/nn.4152>, PMID: 26523642
- Rossato JI**, Bevilacqua LRM, Izquierdo I, Medina JH, Cammarota M. 2009. Dopamine controls persistence of long-term memory storage. *Science* **325**:1017–1020. DOI: <https://doi.org/10.1126/science.1172545>, PMID: 19696353
- Sara SJ**. 2009. The locus coeruleus and noradrenergic modulation of cognition. *Nature Reviews Neuroscience* **10**:211–223. DOI: <https://doi.org/10.1038/nrn2573>
- Sara SJ**. 2015. Locus coeruleus in time with the making of memories. *Current Opinion in Neurobiology* **35**:87–94. DOI: <https://doi.org/10.1016/j.conb.2015.07.004>, PMID: 26241632
- Sederberg PB**, Kahana MJ, Howard MW, Donner EJ, Madsen JR. 2003. Theta and gamma Oscillations during Encoding predict subsequent recall. *The Journal of Neuroscience* **23**:10809–10814. DOI: <https://doi.org/10.1523/JNEUROSCI.23-34-10809.2003>, PMID: 14645473
- Squire LR**. 1992. Memory and the hippocampus: a synthesis from findings with rats, monkeys, and humans. *Psychological Review* **99**:195–231. DOI: <https://doi.org/10.1037/0033-295x.99.2.195>, PMID: 1594723
- Squire LR**, Ojemann JG, Miezin FM, Petersen SE, Videen TO, Raichle ME. 1992. Activation of the hippocampus in normal humans: a functional anatomical study of memory. *PNAS* **89**:1837–1841. DOI: <https://doi.org/10.1073/pnas.89.5.1837>, PMID: 1542680
- Squire LR**, Genzel L, Wixted JT, Morris RG. 2015. Memory consolidation. *Cold Spring Harbor Perspectives in Biology* **7**:a021766. DOI: <https://doi.org/10.1101/cshperspect.a021766>, PMID: 26238360
- Sundström S**, Carlsöö B, Danielsson A, Henriksson R. 1985. Differences in Dopamine- and noradrenaline-induced Amylase release from the rat Parotid gland. *European Journal of Pharmacology* **109**:355–361. DOI: [https://doi.org/10.1016/0014-2999\(85\)90396-6](https://doi.org/10.1016/0014-2999(85)90396-6), PMID: 2580721
- Sutton S**, Braren M, Zubin J, John ER. 1965. Evoked-potential correlates of stimulus uncertainty. *Science* **150**:1187–1188. DOI: <https://doi.org/10.1126/science.150.3700.1187>, PMID: 5852977

- Takeuchi T**, Duszkiwicz AJ, Sonneborn A, Spooner PA, Yamasaki M, Watanabe M, Smith CC, Fernández G, Deisseroth K, Greene RW, Morris RGM. 2016. Locus coeruleus and dopaminergic consolidation of everyday memory. *Nature* **537**:357–362. DOI: <https://doi.org/10.1038/nature19325>, PMID: 27602521
- Tang W**, Kochubey O, Kintscher M, Schneggenburger R. 2020. A VTA to basal amygdala dopamine projection contributes to signal salient Somatosensory events during fear learning. *The Journal of Neuroscience* **40**:3969–3980. DOI: <https://doi.org/10.1523/JNEUROSCI.1796-19.2020>, PMID: 32277045
- Tona K-D**, Keuken MC, de Rover M, Lakke E, Forstmann BU, Nieuwenhuis S, van Osch MJP. 2017. In vivo visualization of the locus coeruleus in humans: Quantifying the test-retest reliability. *Brain Structure & Function* **222**:4203–4217. DOI: <https://doi.org/10.1007/s00429-017-1464-5>, PMID: 28647901
- Tonegawa S**, Morrissey MD, Kitamura T. 2018. The role of Engram cells in the systems consolidation of memory. *Nature Reviews. Neuroscience* **19**:485–498. DOI: <https://doi.org/10.1038/s41583-018-0031-2>, PMID: 29970909
- van Stegeren AH**, Wolf OT, Everaerd W, Scheltens P, Barkhof F, Rombouts SAR. 2007. Endogenous Cortisol level interacts with noradrenergic activation in the human amygdala. *Neurobiology of Learning and Memory* **87**:57–66. DOI: <https://doi.org/10.1016/j.nlm.2006.05.008>, PMID: 16884932
- Vankov A**, Hervé-Minvielle A, Sara SJ. 1995. Response to novelty and its rapid Habituation in locus coeruleus neurons of the freely exploring rat. *The European Journal of Neuroscience* **7**:1180–1187. DOI: <https://doi.org/10.1111/j.1460-9568.1995.tb01108.x>, PMID: 7582091
- Vanneste S**, Mohan A, Yoo HB, Huang Y, Luckey AM, McLeod SL, Tabet MN, Souza RR, McIntyre CK, Chapman S, Robertson IH, To WT. 2020. The peripheral effect of direct current stimulation on brain circuits involving memory. *Science Advances* **6**:eaax9538. DOI: <https://doi.org/10.1126/sciadv.aax9538>, PMID: 33148657
- Varma S**, Takashima A, Krewinkel S, van Kooten M, Fu L, Medendorp WP, Kessels RPC, Daselaar SM. 2017. Non-interfering effects of active post-Encoding tasks on episodic memory consolidation in humans. *Frontiers in Behavioral Neuroscience* **11**:54. DOI: <https://doi.org/10.3389/fnbeh.2017.00054>, PMID: 28424596
- Viola H**, Ballarín F, Martínez MC, Moncada D. 2014. The tagging and capture hypothesis from synapse to memory. *Progress in Molecular Biology and Translational Science* **122**:391–423. DOI: <https://doi.org/10.1016/B978-0-12-420170-5.00013-1>, PMID: 24484708
- Vitacco D**, Brandeis D, Pascual-Marqui R, Martin E. 2002. Correspondence of event-related potential tomography and functional magnetic resonance imaging during language processing. *Human Brain Mapping* **17**:4–12. DOI: <https://doi.org/10.1002/hbm.10038>, PMID: 12203683
- Volpe U**, Mucci A, Bucci P, Merlotti E, Galderisi S, Maj M. 2007. The cortical generators of P3A and P3B: a LORETA study. *Brain Research Bulletin* **73**:220–230. DOI: <https://doi.org/10.1016/j.brainresbull.2007.03.003>, PMID: 17562387
- Vöröslakos M**, Takeuchi Y, Brinyiczki K, Zombori T, Oliva A, Fernández-Ruiz A, Kozák G, Kincses ZT, Iványi B, Buzsáki G, Berényi A. 2018. Direct effects of transcranial electric stimulation on brain circuits in rats and humans. *Nature Communications* **9**:483. DOI: <https://doi.org/10.1038/s41467-018-02928-3>, PMID: 29396478
- Wang S-H**, Redondo RL, Morris RGM. 2010. Relevance of synaptic tagging and capture to the persistence of long-term potentiation and everyday spatial memory. *PNAS* **107**:19537–19542. DOI: <https://doi.org/10.1073/pnas.1008638107>, PMID: 20962282
- Wearn AR**, Saunders-Jennings E, Nurdal V, Hadley E, Knight MJ, Newson M, Kauppinen RA, Coulthard EJ. 2020. Accelerated long-term forgetting in healthy older adults predicts cognitive decline over 1 year. *Alzheimer's Research & Therapy* **12**:119. DOI: <https://doi.org/10.1186/s13195-020-00693-4>, PMID: 32988418
- Weston PSJ**, Nicholas JM, Henley SMD, Liang Y, Macpherson K, Donnachie E, Schott JM, Rossor MN, Crutch SJ, Butler CR, Zeman AZ, Fox NC. 2018. Accelerated long-term forgetting in Presymptomatic Autosomal dominant Alzheimer's disease: a cross-sectional study. *The Lancet. Neurology* **17**:123–132. DOI: [https://doi.org/10.1016/S1474-4422\(17\)30434-9](https://doi.org/10.1016/S1474-4422(17)30434-9), PMID: 29413314
- Worrell GA**, Lagerlund TD, Sharbrough FW, Brinkmann BH, Busacker NE, Cicora KM, O'Brien TJ. 2000. Localization of the epileptic focus by low-resolution electromagnetic tomography in patients with a lesion demonstrated by MRI. *Brain Topography* **12**:273–282. DOI: <https://doi.org/10.1023/a:1023407521772>, PMID: 10912735
- Yau W-YW**, Tudorascu DL, McDade EM, Ikonomic S, James JA, Minhas D, Mowrey W, Sheu LK, Snitz BE, Weissfeld L, Gianaros PJ, Aizenstein HJ, Price JC, Mathis CA, Lopez OL, Klunk WE. 2015. Longitudinal assessment of neuroimaging and clinical markers in Autosomal dominant Alzheimer's disease: a prospective cohort study. *The Lancet. Neurology* **14**:804–813. DOI: [https://doi.org/10.1016/S1474-4422\(15\)00135-0](https://doi.org/10.1016/S1474-4422(15)00135-0), PMID: 26139022
- Yu-Feng Z**, Yong H, Chao-Zhe Z, Qing-Jiu C, Man-Qiu S, Meng L, Li-Xia T, Tian-Zi J, Yu-Feng W. 2007. Altered baseline brain activity in children with ADHD revealed by resting-state functional MRI. *Brain and Development* **29**:89–91. DOI: <https://doi.org/10.1016/j.braindev.2006.07.002>
- Zeithamova D**, Preston AR. 2017. Temporal proximity promotes integration of overlapping events. *Journal of Cognitive Neuroscience* **29**:1311–1323. DOI: [https://doi.org/10.1162/jocn\\_a\\_01116](https://doi.org/10.1162/jocn_a_01116), PMID: 28253077
- Zumsteg D**, Wennberg RA, Treyer V, Buck A, Wieser HG. 2005. H2(15)O or 13Nh3 PET and electromagnetic tomography (LORETA) during partial status epilepticus. *Neurology* **65**:1657–1660. DOI: <https://doi.org/10.1212/01.wnl.0000184516.32369.1a>, PMID: 16301501
- Zumsteg D**, Lozano AM, Wennberg RA. 2006a. Depth electrode recorded cerebral responses with deep brain stimulation of the anterior thalamus for epilepsy. *Clinical Neurophysiology* **117**:1602–1609. DOI: <https://doi.org/10.1016/j.clinph.2006.04.008>



**Zumsteg D**, Lozano AM, Wieser HG, Wennberg RA. 2006b. Cortical activation with deep brain stimulation of the anterior thalamus for epilepsy. *Clinical Neurophysiology* **117**:192–207. DOI: <https://doi.org/10.1016/j.clinph.2005.09.015>